

**THE GENETIC AND MOLECULAR CHARACTERIZATION OF THE
POLYCYSTIC KIDNEY DISEASE-CAUSING MOUSE GENE BICC1**

by

Sarah J. Price

**Dissertation submitted to
the Graduate College
of
Marshall University
in partial fulfillment of the requirements
for the degree of**

**Doctor of Philosophy
in
Biomedical Sciences**

Approved by

**Dr. Elizabeth C. Bryda, Committee Chairperson
Dr. Beverly C. Delidow
Dr. Susan H. Jackman
Dr. Donald A. Primerano
Dr. Monica A. Valentovic**

**Department of Microbiology, Immunology, and Molecular Genetics
Joan C. Edward School of Medicine
Marshall University
Huntington, WV
April 2004**

Copyright© 2004

**Keywords Listing: genetics, polycystic kidney disease, cilia, chromosome
mapping, RNA-binding**

ABSTRACT

THE GENETIC AND MOLECULAR CHARACTERIZATION OF THE POLYCYSTIC KIDNEY DISEASE-CAUSING MOUSE GENE *BICC1*

by Sarah J. Price

Polycystic kidney disease (PKD) is one of the most common hereditary diseases and is characterized by progressive cyst formation, substantial renal enlargement, and frequently, progression to end-stage renal disease. One way to learn more about the etiology of this disease is to study mouse models that imitate the human situation. The juvenile congenital polycystic kidney disease (*jcpk*) gene on mouse Chromosome 10 has been found to cause a severe, early onset form of PKD when inherited in an autosomal recessive manner (Flaherty *et al.*, 1995). Previous genetic studies mapped the *jcpk* locus to a 1 cM region on mouse Chromosome 10 between the markers *D10Mit115* and *D10Mit173* (Bryda *et al.*, 1996). To positionally clone this gene, high resolution genetic and radiation hybrid maps were generated along with a detailed physical map of the critical region thought to contain the *jcpk* gene. Fine mapping studies allowed extensive reduction of this region to a section of mouse Chromosome 10 contained within three Bacterial Artificial Chromosomes (BACs). Nucleotide sequence analysis was performed to determine the presence of transcribed genes within this section of the chromosome. The only predicted gene was the mouse homologue of the *Drosophila* gene *Bicaudal-C* (*Bicc1*). *Bicc1* was evaluated as a disease-susceptibility gene by examining the sequence of the *Bicc1*^{*jcpk*} allele for mutations using a combination of RT-PCR and sequence analysis. A single base-pair change (G to A) was detected in the consensus splice acceptor site of exon 3. This frameshift mutation produces a premature stop codon predicted to result in a truncated protein. The function of the *Bicc1* protein is unknown; however, several functional domains have been identified: three K Homology (KH) RNA binding domains and one sterile alpha motif (SAM). Ribonucleotide homopolymer analysis determined that *Bicc1* binds RNA *in vitro*. In preliminary analyses of PKD-affected *Bicc1*^{*jcpk/jcpk*} mice, left/right patterning defects including dextrocardia and lung isomerism were identified in one animal. The present work has enabled the identification of a gene, *Bicc1*, previously unknown to be involved in PKD pathogenesis and begins to explore the role of this gene and its corresponding protein in the kidney.

DEDICATION

I would like to dedicate this dissertation to my parents.

Without their understanding, patience and love, the completion of this work would not have been possible.

ACKNOWLEDGMENTS

I would like to thank the members of my committee for their guidance and support. Their firm direction has been most appreciated. I would also like to thank the members of the Department of Microbiology, Immunology, and Molecular Genetics for their encouragement and assistance. I would like to personally thank Bryan Brubaker, Bryan O'Dell, William Ian Towler, and Jad Walters for their dedication and good humor. I would also like to acknowledge my friends and family for their undying patience.

Finally, I would like to thank my mentor and friend, Dr. Elizabeth C. Bryda. From the beginning she had confidence in my abilities to not only complete a degree, but to complete it with excellence.

TABLE OF CONTENTS

ABSTRACT	ii
DEDICATION.....	iii
ACKNOWLEDGMENTS	iv
TABLE OF CONTENTS	v
LIST OF TABLES	vi
LIST OF FIGURES	vii
CHAPTER I.....	1
INTRODUCTION.....	1
Purpose of the Research.....	1
Significance of the Research.....	2
Organization of the Dissertation	2
CHAPTER II.....	4
REVIEW OF THE LITERATURE.....	4
Polycystic Kidney Disease	4
Murine Models for Human Disease.....	14
Ciliocentric Theory of PKD Pathogenesis	22
Vertebrate Left-Right Asymmetry	27
Summary	29
CHAPTER III.....	30
MATERIALS AND METHODS.....	30
Genetic and Physical Mapping.....	30
Gene Identification	43
RNA Analysis.....	48
Protein Analysis.....	54
RNA Binding Study.....	59
Asymmetry Study	62
CHAPTER IV	63
RESULTS	63
Genetic and Physical Mapping.....	63
Gene Identification	72
RNA Analysis.....	84
Protein Analysis.....	118
RNA Binding Study.....	126
Asymmetry Study	129
CHAPTER V	132
DISCUSSION.....	132
Summary and Conclusions	132
Future Directions	149
APPENDIX A	152
APPENDIX B	155
APPENDIX C	160
APPENDIX D	162
APPENDIX E	165
APPENDIX F.....	173
APPENDIX G	174
BIBLIOGRAPHY.....	179
CURRICULUM VITAE	205

LIST OF TABLES

Table 4.1 Exon to exon comparison of the mouse and human Bicaudal-C genes.....	83
Table 4.2 Description of cell lines examined for <i>Bicc1</i> expression.....	86
Table 4.3 Real-time PCR analysis of PKD genes in <i>jcpk/jcpk</i> mice.	94
Table 4.4 Conservation of KH domains across species	123

LIST OF FIGURES

Figure 2.1 Cyst formation in PKD.	5
Figure 2.2 Pathological findings observed in cyst formation.....	6
Figure 2.3 Illustration of primary cilia.	22
Figure 2.4 Primary cilia extend into the renal tubule lumen.....	23
Figure 4.1 Genetic map of the 1-cM region containing the <i>jcpk</i> gene.	64
Figure 4.2 Physical map of the <i>jcpk</i> region on mouse Chromosome 10.	65
Figure 4.3 Minimum BAC tiling pattern covering the <i>jcpk</i> critical region.....	66
Figure 4.4 <i>EcoR</i> I restriction digestion of BACs within the physical map.	67
Figure 4.5 <i>Hind</i> III restriction digestion of selected BACs.....	68
Figure 4.6 Radiation hybrid (RH) map of mouse Chromosome 10.	71
Figure 4.7 RT-PCR analysis of exons 2-4 of the <i>Bicc1</i> gene.	74
Figure 4.8 Mutation analysis of the <i>Bicc1</i> gene.	75
Figure 4.9 Sequence analysis of the <i>Bicc1</i> transcript in <i>jcpk/jcpk</i> kidney tissue.	76
Figure 4.10 Genomic sequence analysis of <i>Bicc1</i> around exon 3.....	76
Figure 4.11 Sequence analysis of the <i>Bicc1</i> transcript.....	78
Figure 4.12 PCR analysis to determine alternative transcripts for <i>Bicc1</i>	79
Figure 4.13 Two protein isoforms are predicted for the <i>Bicc1</i> gene.	80
Figure 4.14 Predicted proteins encoded by the <i>bpk</i> and <i>jcpk</i> alleles.	82
Figure 4.15 Tissue expression of <i>Bicc1</i>	84
Figure 4.16 Expression analysis of <i>Bicc1</i> in mouse cell lines.....	86
Figure 4.17 Embryonic expression of <i>Bicc1</i>	88
Figure 4.18 RT-PCR analysis of embryonic mRNA.....	89
Figure 4.19 Northern blot analysis of <i>Bicc1</i> in normal and affected kidney.....	89
Figure 4.20 Real-time PCR analysis of <i>Bicc1</i> in <i>jcpk/jcpk</i> kidney.....	91
Figure 4.21 Real-time PCR analysis of <i>Bicc1</i> in <i>bpk/bpk</i> kidney.....	92
Figure 4.22 Real-time PCR analysis of <i>pkd1</i> mRNA expression.....	95
Figure 4.23 Real-time PCR analysis of <i>pkd2</i> mRNA expression.....	96
Figure 4.24 Real-time PCR analysis of <i>orpk</i> mRNA expression.	97
Figure 4.25 Real-time PCR analysis of <i>Invs</i> mRNA expression.	98
Figure 4.26 Real-time PCR analysis of <i>jck</i> mRNA expression.	99
Figure 4.27 Real-time PCR analysis of <i>kat</i> mRNA expression.....	100
Figure 4.28 Real-time PCR analysis of <i>cpk</i> mRNA expression.....	101
Figure 4.29 Microarray analysis of normal versus polycystic kidneys.	102
Figure 4.30 <i>Pax2</i> gene expression analysis by real-time analysis.	104

Figure 4.31 RT- PCR analysis of <i>Egfr</i> (<i>ErbB1</i>) gene expression.....	109
Figure 4.32 Real-time PCR analysis of <i>Egfr</i> mRNA expression.	110
Figure 4.33 RT-PCR analysis of <i>Tgf-α</i> gene expression.	111
Figure 4.34 Real-time PCR analysis of <i>Tgf-α</i> mRNA expression.	112
Figure 4.36 Real-time PCR analysis of <i>Egf</i> mRNA expression.	113
Figure 4.37 Breeding scheme between <i>jcpk</i> and <i>waved-2</i> mice.	114
Figure 4.38 Real-time PCR analysis of <i>ErbB2</i>	117
Figure 4.39 Western blot analysis of the Bicc1 protein.....	119
Figure 4.40 Mouse Bicc1 has two types of functional domains.	119
Figure 4.41 Sequence comparison of Bicaudal-C from 10 different species.....	121
Figure 4.42 Multiple species sequence alignment of the SAM domain of Bicaudal-C.	122
Figure 4.43 Percent sequence homology of the Bicc1 SAM domain in 7 species.	122
Figure 4.44 Percent sequence homology of all three KH domains.	124
Figure 4.45 Consensus sequence comparison in multiple species.....	125
Figure 4.46 Schematic diagram summarizing recombinant RNA binding constructs.....	127
Figure 4.47 RNA binding assay using immobilized poly(U) homoribopolymer.....	128
Figure 4.48 Summary of RNA binding analysis.	129
Figure 4.49 Comparison of the presence of L/R patterning defects in littermates.	131

CHAPTER I

INTRODUCTION

Polycystic kidney disease (PKD) represents a set of hereditary and acquired nephropathies characterized by progressive cyst formation, substantial renal enlargement, and frequently, progression to end-stage renal disease. In the mouse, several distinct recessive mutations produce PKD phenotypes that mimic the human disease (89). Genetic analysis of epithelial cyst formation in animal models has facilitated the molecular characterization of novel genes required for normal epithelial function and has contributed to the understanding of the cellular pathology observed in cystic disease. Recent evidence has suggested that the abnormal kidney development and cyst formation observed in PKD may be due to structural or functional alterations in the primary apical cilium of renal epithelial cells. Cilia, which extend from the surfaces of many cell types and are found in many species, contribute to fluid movement, chemoreception, and patterning of the left-right body axis (27, 191, 199).

The juvenile congenital polycystic kidney (*jcpk*) mutation is an autosomal recessive mouse model of PKD first identified during chlorambucil mutagenesis studies (67). The initial signs of PKD are visible as early as three days after birth and are characterized by large cysts in all areas of the nephron, enlargement of the gallbladder and abnormalities of the biliary and pancreatic ducts.

Purpose of the Research

The objective of the following body of research is to characterize the *jcpk* mouse model for polycystic kidney disease (PKD) through both genetic and molecular analyses. The *jcpk* locus was previously localized to a 1 cM region located on mouse Chromosome 10 (28). Two other mouse models, *bpk* and

67Gso, have been shown to be allelic to *jcpk* through complementation analysis (90, 206). The purpose of the following research is 1) to identify the PKD disease-causing gene shared by the *jcpk*, *bpk* and 67Gso mouse models; 2) to use current molecular analyses to evaluate the mRNA and protein expression of *jcpk*; and 3) to begin to establish a role for the *jcpk* gene in the context of current theories of PKD pathogenesis.

Significance of the Research

The rationale for the research is that once we have discerned the mechanisms involved in cystogenesis, we will be better able to design treatments for the more than 12.5 million individuals world-wide who suffer from PKD (35). Currently, the only established treatments for PKD are renal dialysis and transplantation. Slowing or eliminating cyst formation may drastically improve the quality of life for these sufferers. This research is significant in that, unlike other models for PKD, the *jcpk* mouse model has a phenotype that encompasses characteristics observed in many subtypes of PKD as well as other cystic disorders. Therefore, the information gathered is invaluable to the understanding of cystic pathogenesis regardless of the genetic cause. Elucidating the interaction of the multitude of proteins known to be involved in PKD pathogenesis will bring scientists closer to effective treatments for PKD and eventually a cure.

This dissertation contributes to the current understanding of PKD pathogenesis in that it identifies a new gene involved in PKD and begins to address the possible functional role of the corresponding protein in the kidney.

Organization of the Dissertation

The dissertation is divided into five chapters. Chapter I defines the purpose of the dissertation and provides a context for understanding the following research. Chapter II provides a precise overview of the relevant literature describing polycystic kidney disease as well as the current theories of

cyst formation and progression. Chapter III is a detailed account of the methodology and experimental design. Chapter IV provides the results of the research. Chapter V summarizes the previous chapters, discusses the conclusions that can be drawn from the dissertation research, and communicates the significance of the work in the context of current PKD research.

CHAPTER II

REVIEW OF THE LITERATURE

Polycystic Kidney Disease

Cystic diseases of the kidney are a clinically important and genetically diverse group of disorders that share in common altered tubular morphology. Of these cystic disorders, polycystic kidney disease (PKD) is a principal cause of end-stage renal failure in individuals who require chronic dialysis and transplantation (209). PKD affects over 600,000 Americans and 12.5 million individuals world-wide (35). PKD represents one of the most remarkably dynamic alterations in pathobiology, since affected renal tubules can increase in diameter from 3 μm to over 5 cm (37). Human PKD can pursue an aggressive course where renal failure can occur perinatally, or an indolent course with few symptoms developing during the course of the patient's life. Historical references to PKD can be found as early as the 15th century, and since that time there have been a multitude of publications that have contributed to our current understanding of the genetic and molecular mechanisms leading to PKD pathogenesis (258).

Pathogenesis of cyst formation

Renal cysts are abnormal, fluid-filled sacs that arise as dilatations of any portion of the nephron and collecting ducts. Cysts are lined by a single layer of continuous epithelium that has a primitive morphologic appearance characterized by the loss of the apical brush border in proximal tubular cells, cell shape alterations and an increase in the nuclear/cytoplasmic ratio (148). Independent of the cause, only a small fraction of the total nephron population undergoes cystic change in affected individuals. Cysts may occur in the medulla, in the

cortex, or in both regions of the kidney and may or may not be associated with other systemic abnormalities. Cysts seem to originate as diverticula within the walls of renal tubules (Figure 2.1). These focal areas of tubule wall enlarge progressively, until eventually, the expanding cysts lose attachment with their tubule of origin (148).

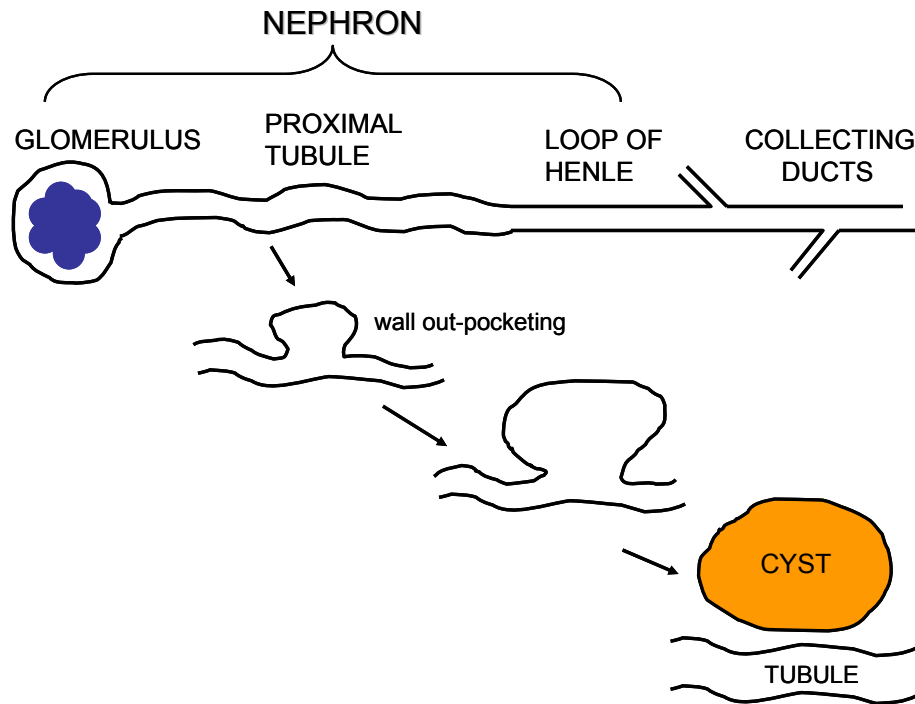


Figure 2.1 Cyst formation in PKD. Cysts arise as diverticula of any part of the nephron and collecting ducts. These out-pocketings eventually lose attachment with their tubule of origin.

Other pathological findings consistently observed in PKD include alterations in extracellular matrix composition, transepithelial fluid secretion, changes in epithelial cell polarity, an increase in cellular apoptosis, and improper epithelial differentiation and proliferation (Figure 2.2) (34). PKD can also be characterized as a systemic disorder affecting the liver, spleen, pancreas, biliary tract, heart, or brain. The extent of extra-renal involvement is dependent on the type of genetic mutation present and tissue expression of the resulting peptide products.

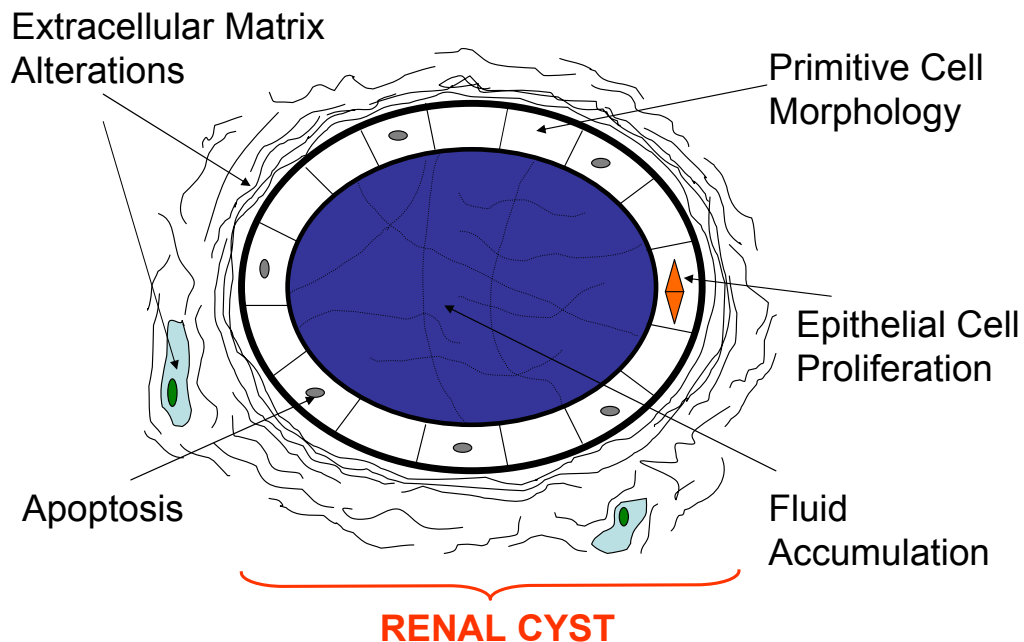


Figure 2.2 Pathological findings observed in cyst formation. A number of cellular abnormalities accompany cystogenesis and include extracellular matrix alterations, primitive cellular morphology, increased cell proliferation, fluid accumulation and cellular apoptosis.

A variety of polypeptide growth factors have been implicated in the altered cellular proliferation which accompanies renal tubular cyst formation and enlargement. Attention has particularly focused on the epidermal growth factor (EGF)/transforming growth factor α (TGF- α)/epidermal growth factor receptor (EGFR) axis in mediating tubular cyst formation. Studies in a number of laboratories have determined that 1) EGF and TGF- α are cystogenic in a variety of *in vitro* systems (13); 2) cystic renal tissue has increased expression of TGF- α and EGFR (10, 126, 136); and 3) renal cyst fluid contains bioactive and immunoreactive EGF peptides in mitogenic concentrations (159, 245).

The broad tissue distribution of the EGFR signal-transduction pathway contributes to the regulation of numerous cellular processes in the development of both the embryonic and adult kidney. EGFRs are located exclusively to the basolateral membranes of normal renal tubule epithelia. However, EGFR has been shown to become mislocalized to the apical surface on the epithelial cells

lining cystic structures (10). This mislocalization of the EGFR is known to occur in both humans and mice and is a common end point associated with several different forms of polycystic kidney disease which are initiated by mutations in different genes (184, 212, 275). Just recently, it has been observed in a number of PKD patients that certain alleles of the EGFR transcript may determine the clinical progression of cystic disease (142). How these different alleles of EGFR confer susceptibility or protection has yet to be determined. Establishing clinical treatments for PKD will be greatly facilitated by an understanding of how individual gene products participate in the disease pathway.

Genetics of PKD

Polycystic kidney disease was once considered to be a rare congenital malformation with a fate predetermined at birth. Recognition of the hereditary nature of PKD nearly a century ago has led to the understanding that cyst formation can result from a mutation in a single susceptibility gene. However, to alter the normal state of renal epithelia, it is likely that the consequence of this genetic alteration is the abnormal expression of other genes, initiating a cascade of gene expression events that ultimately results in cells that function atypically to initiate cystogenesis.

PKD can be inherited as an autosomal dominant (ADPKD) or an autosomal recessive trait (ARPKD) (118). ADPKD is a common disease that occurs in both children and adults, whereas ARPKD is relatively rare and occurs primarily in neonates and children (73, 288). ADPKD is caused by mutations in at least two genes on different chromosomes, whereas a single gene is responsible for ARPKD (200, 283).

Disease progression is quite variable among human PKD families with either ADPKD or ARPKD. Possible genetic mechanisms that may contribute to variable expressivity include: 1) mutations in different disease-susceptibility genes; 2) different alleles of the same disease gene; 3) random somatic events that disrupt the expression of the wild-type allele; or 4) modifying influences such as gene-gene or gene-environment interactions (118). Limited genotype-

phenotype analyses of human families with the same disease locus have revealed minimal correlation between mutant alleles and clinical phenotypes (16, 216). These data are consistent with observations from other single-gene disorders in human families where, despite the inheritance of the same mutant allele, phenotypic expression varies greatly. It has been proposed that in single gene disorders such as PKD, the primary mutant gene product is embedded in a highly complex system that includes other independent genetic variations and modulating environmental factors (56). Therefore, the complexity of PKD makes it difficult to quickly develop effective therapeutic interventions.

Autosomal Dominant PKD (ADPKD)

ADPKD is one of the most common genetic diseases in humans affecting all ethnic groups worldwide with an incidence of 1 in 500 to 1 in 1,000 individuals (148). ADPKD is genetically heterogeneous and can arise from mutations in two genes, *PKD1* and *PKD2*. Mutations of *PKD1* located on human chromosome 16p13.3 are responsible for 85% of cases, whereas mutations of *PKD2* on chromosome 4q21-23 are responsible for close to 15% (200). Mutations of *PKD1* and *PKD2* produce similar renal and extra-renal manifestations. However, compared with *PKD1* patients, *PKD2* patients present later in life, have longer renal survival, and have fewer complications (98). Some patients with typical features of autosomal dominant polycystic kidney disease have no mutations in *PKD1* or *PKD2*, suggesting that there may be a rare third form of the disease, although the proposed gene - *PKD3* - has not been identified (274).

The *PKD1* gene consists of 46 exons distributed over 52 kb of genomic DNA (112). The gene encodes a 14.1 kb mRNA transcript that is translated into a protein composed of 4302 amino acids. Interestingly, the region of the gene encoding exon 1 to exon 33 is duplicated at six other sites on chromosome 16p. The duplicated genes are expressed as mRNA transcripts and may represent pseudogenes (21). The existence of these duplications has hindered mutational analysis because it can be difficult to distinguish mutations of *PKD1* from sequence variations within the pseudogenes. Different types of mutations within

PKD1 include splice site mutations, in-frame and out-of-frame deletions as well as insertions, nonsense mutations, and missense mutations (198, 252). No correlations between specific mutations and specific clinical manifestations have been identified, but mutations in the 5' end of the gene appear to be associated with an earlier onset disease than mutations at the 3' end (65).

The second ADPKD gene, *PKD2*, was identified in 1996 by a positional cloning approach (155). The *PKD2* gene is located on chromosome 4q21-23 and encodes a 5.3-kb mRNA transcript that is translated into a 968 amino acid protein. *PKD2* is approximately 25% homologous to a region of the *PKD1* gene (155). Mutations have been identified throughout the transcript and mostly consist of truncating mutations (frame-shift, splicing, and nonsense mutations) that would be predicted to inactivate the gene product. Only 5% of mutations identified are missense mutations (266).

Despite the fact that almost all of the genetically caused cases of ADPKD are due to mutations in either *PKD1* or *PKD2*, a third gene, *PKD3*, has been implicated as the cause of hereditary PKD in a select number of families. A total of five families have been recognized that have an inheritable autosomal dominant form of PKD that has no linkage to either *PKD1* or *PKD2* (7, 50, 51, 150, 177). This form of ADPKD represents a much milder form than *PKD1* and *PKD2* where cysts are present in the liver or kidney or both (150). It has been suggested that this form is so mild that many families carrying mutations in *PKD3* remain undetected (7).

Polycystins

The proteins encoded by the *PKD1* and *PKD2* genes define a new protein family, the polycystins, which play important roles in a variety of biological processes including fertilization, ion translocation, and mechanosensation (18, 96, 172). Understanding the structure and function of these proteins has led to a better understanding of PKD pathogenesis.

Polycystin-1, the product of the *PKD1* gene, is an integral membrane protein that contains several different protein motifs that are involved in protein-

protein or protein-carbohydrate interactions. Polycystin-1 is expressed in a variety of tissues including kidney, heart, bone, and muscle. In the kidney, polycystin-1 has been identified in the plasma membrane of tubular epithelial cells within the nephron and collecting ducts (116). Polycystin-1 is also present in cell junctional complexes, including adherens junctions and desmosomes (225).

Polycystin-1 is thought to have several functions within the cell. The carboxyl-terminus has been shown to activate the *Wnt* signaling pathway by stabilizing β -catenin and activating T-cell factor (TCF) transcription factors during embryonic kidney development (214). Polycystin-1 has also been shown to have a direct role in the regulation of the cell cycle by inducing cell cycle arrest at the G0/G1 transition. Progression through the cell cycle is arrested by polycystin-1 through activation of the JAK-STAT signaling pathway. Activation of this pathway inhibits Cdk2 by up-regulating its inhibitor, p21^{CIP1/WAF1}. Mouse embryos lacking polycystin-1 have defective Stat1 phosphorylation and Waf1 induction (18). Polycystin-1 is also a component of the primary apical cilium on tubular epithelial cells and is thought to mediate flow response (172).

The *PKD2* gene encodes a protein, polycystin-2, that, like polycystin-1, is predicted to be an integral membrane protein. Polycystin-2 shares many structural features with transient receptor potential (TRP) channels as well as voltage-activated calcium and sodium channels (155). The carboxyl-terminal domain contains a motif known as an EF hand that can bind calcium (130). Polycystin-2 is widely expressed in many tissues, particularly the kidney, heart, ovary, testis, vascular smooth muscle and the small intestine (145). In the kidney, polycystin-2 is expressed in all areas of the nephron except the thin limbs of the loops of Henle and glomeruli. Within the cell, polycystin-2 was found to be located in the premedial Golgi compartments (224).

Several studies have shown that the polycystin-2 channel conducts divalent cations including calcium and that this activity can be stimulated by calcium on the cytosolic side (83, 96, 264). Another study further determined that polycystin-2 can amplify calcium release from intracellular stores in response

to hormone stimulation that transiently increases cytosolic calcium (130). A naturally occurring human PKD mutation altering the membrane spanning region results in complete loss of channel function without apparent loss of expression of the polycystin-2 protein (130). Taken together, these studies indicate that polycystin-2 acts to increase cytosolic calcium, and that the loss of this ability contributes to polycystic kidney disease pathogenesis.

Further *in vivo* and *in vitro* analyses have shown that polycystin-2 directly interacts with polycystin-1 (129, 172, 175). The carboxyl-terminal domain of polycystin-1 contains a coiled-coil motif that binds to the carboxyl-terminal domain of polycystin-2. A deletion in either one of these domains destroys the interaction (261). Furthermore, co-expression and co-assembly with polycystin-1 have been shown to displace polycystin-2 from the Golgi compartments and allow relocalization to the cell surface in CHO cells (96). The *in vivo* functional significance of this interaction is supported by the observation that polycystin-1 and polycystin-2 act non-redundantly in the same genetic pathway in *C. elegans* (14). The interaction between polycystin-1 and polycystin-2 in a common pathway would explain why mutations in either *PKD1* or *PKD2* produce disease with similar clinical phenotypes.

Autosomal Recessive PKD (ARPKD)

ARPKD is one of the most important childhood nephropathies. It is far less common than ADPKD with an overall frequency that is estimated to be 1 in 20,000 live births (182). The disease is characterized by a combination of renal cystic disease, biliary dysgenesis, and portal tract fibrosis (48). ARPKD typically begins *in utero* presenting with fusiform dilatation of the renal collecting ducts that radiate from the medulla to the cortex (122). During fetal development, cysts also appear transiently in the proximal tubules (171). The renal cystic disease is invariably associated with biliary dysgenesis, which is a ductal plate malformation characterized by abnormal intrahepatic bile ducts and portal fibrosis (254). Fibrosis of the pancreas has also been observed in some patients (289).

Like ADPKD, the clinical presentation of ARPKD is highly variable and can present as a perinatal, neonatal, infantile, or juvenile on-set disease (19). The variability in the age of onset is thought to be due to allelic heterogeneity of the same gene combined with the effects of modifier genes and environmental factors rather than mutations within different genes (122). Intrafamilial variability is far less common than variability between families (52). Other clinical manifestations of ARPKD in children and adults include pulmonary hypoplasia, systemic hypertension, growth retardation, urinary tract infection and hyponatremia (69).

All cases of ARPKD are due to a mutation of the *Polycystic Kidney and Hepatic Disease-1 (PKHD1)* gene on chromosome 6p21.1-p21. The *PKHD1* gene is very large and consists of 86 exons extending over 469 kb of human genomic DNA (269). The gene undergoes a complex pattern of alternative splicing to generate mRNA transcripts ranging in size from 8.5 kb to 13 kb. Consistent with the phenotype of ARPKD, *PKHD1* is expressed in the kidney, liver and pancreas (269). Different mutations of *PKHD1* have been identified in patients and include frameshift, nonsense, and out-of-frame splicing alterations that are consistent with a loss of function (269). In addition, an abundance of missense variants have been identified, the effects of which remain unclear (269). Further studies are necessary to determine if there is any relationship between the nature of the mutation and the clinical course of the disease.

Fibrocystin

The protein product of *PKHD1* has been named fibrocystin (or polyductin) and is composed of 4074 amino acids. Fibrocystin is a membrane protein consisting of an amino-terminal signal sequence, a large extracellular domain, a single transmembrane segment, and a short carboxyl-terminal tail with three potential phosphorylation sites (269). A splice variant that encodes a truncated protein lacking the transmembrane segment has also been identified and may encode a secreted form of the protein (283). Based on its predicted protein structure, fibrocystin may either be a cell surface receptor or a secreted protein.

Western blot analysis detected fibrocystin in the human kidney and liver. In tissues from ARPKD patients, fibrocystin is not expressed verifying that loss of function mutations are responsible for ARPKD (270).

Immunohistochemical analysis of developing kidneys indicates expression of fibrocystin in the branching ureteric bud and collecting ducts. This expression has been found to persist throughout adulthood (270). Extrarenal expression has been noted in the biliary duct, pancreas and developing testis. Immunofluorescence analysis of fibrocystin in Madin-Darby canine kidney (MDCK) cells has shown that it is localized to the primary cilia (270).

Treatment Prospects for PKD

Advances in molecular biology and genetics in the last three decades have made possible a greater understanding of the mechanisms responsible for the development of PKD and have laid the foundation for the development of effective therapies (162). To date, specific treatment strategies for PKD are still under investigation; but for now, patients are treated as symptoms arise. The only therapies currently available for PKD affected patients are renal dialysis and kidney transplantation. The molecular interactions of PKD-susceptibility genes and their putative genetic modifiers are likely to define critical pathways fundamental to cystogenesis and PKD progression. The characterization of these complex pathways will provide new insights into disease pathogenesis, identifying new genetic markers for prognosis, and establishing a platform from which to develop targeted therapies to halt disease progression. One way to investigate these complex pathways is to study animal models that mimic the human disease.

Murine Models for Human Disease

The contribution that animal models have made to the understanding of the etiology and pathogenesis of human kidney diseases has been invaluable. Numerous mouse models have been described with mutant phenotypes that closely resemble human PKD with respect to cyst morphology and localization, as well as disease progression. These models are the result of gene-specific targeting in murine orthologues of human PKD genes, spontaneous mutations, chemical mutagenesis, or transgenic technologies. Several models resemble human ADPKD as to cyst localization, slow disease progression and extra-renal abnormalities (86, 89, 168, 227). Other models mimic the pathological features of ARPKD with rapidly progressing disease and fusiform dilatation of the renal tubules (168).

PKD Models Arising From Gene-Specific Mutagenesis

The identification of the human ADPKD genes, *PKD1* and *PKD2*, has prompted the identification and targeted mutagenesis of their mouse orthologues, *Pkd1* and *Pkd2*. Both null and hypomorphic alleles (*Pkd1*^{del34}; *Pkd1*^L; *Pkd1*^{del17-21βgeo}; *Pkd1*^{m1Bei}) have been generated for the *Pkd1* gene (18, 25, 102, 125, 139, 140, 163, 197, 281). *Pkd2* mutant alleles have also been generated and include *Pkd2*^{WS25} and *Pkd2*^{-LacZ} (197, 281).

Mice heterozygous for the *Pkd1* mutant alleles develop renal, biliary, and pancreatic cysts between 4 and 19 months of age. In homozygous mutants, disease progression is rapid with embryonic lethality occurring in most cases. Homozygotes develop renal and pancreatic cysts by embryonic day 15.5 (E15.5). This is coincident with the initial expression of *Pkd1* and *Pkd2* in normal maturing tubular epithelium (25).

Both transgenes for *Pkd2* represent null mutations (197, 280). In particular, *Pkd2*^{-LacZ} homozygous embryos die between E12.5 and birth and are characterized by cardiac defects and renal failure (197). These data

demonstrate that the loss of either *PKD1* or *PKD2* is sufficient to cause renal cysts (89).

PKD Models Arising From Spontaneous Mutations

The *cpk* (congenital polycystic kidneys) mouse model was the first mouse model for PKD to be described and as such it is the most extensively characterized (72, 205). Inherited as an autosomal recessive trait, the mutation spontaneously arose in the C57BL/6J mouse strain at The Jackson Laboratory, Bar Harbor, Maine. Homozygous affected mutants appear normal at birth but soon develop aggressive renal cystic disease in a pattern resembling human ARPKD (46). Cysts have been observed as early as embryonic day 16 (E16) and are localized to the proximal tubules (12, 75). By post-natal day 5, cysts begin to develop in the collecting ducts and by post-natal day 21, cystic disease is primarily localized to the cortical and outer medullary collecting ducts (12). Death occurs by 3-4 weeks of age from uremia and renal failure (144).

In the *cpk* mouse model, disease expression and severity have been shown to be modulated by genetic background (92, 277). Biliary dysgenesis, an abnormality often associated with human ARPKD, is not penetrant in the C57BL/J6-*cpk/cpk* mouse (72). When the *cpk* allele is expressed on other genetic backgrounds (CAST/Ei, DBA/2J, BALB/c, or CD1), *cpk* mutants have renal collecting duct cysts as well as both biliary and pancreatic duct abnormalities (76, 78, 92, 213). C57BL/J6-*cpk* heterozygous mice do not develop cystic disease; however, aged F₁ generation heterozygotes on DBA/2J or BALB/c genetic backgrounds have been shown to develop biliary cysts (89).

The *cpk* gene, *Cys1*, maps to mouse Chromosome 12 and was identified using a positional cloning approach (108, 235). The mutation within the *cpk* allele was determined to be a deletion within the first exon. This mutation causes a frameshift which results in a premature stop in translation. The resulting truncated protein is thought to be nonfunctional (108). Cystin, the 145 amino acid protein encoded by *Cys1*, is expressed in the primary apical cilia of renal epithelial cells (108, 284).

The *inv* (inversion of embryonic turning) mutation arose in the OVE210 transgenic line due to a random insertional event of the tyrosinase minigene causing a deletion of exons 3-11 in the *Invs* gene (158). Inherited in an autosomal recessive manner, homozygous mutants are characterized by a complete reversal of embryonic left-right body axis determination (*situs inversus*), renal cysts, pancreatic islet cell dysplasia, and abnormal liver and biliary development (158). Cardiac malformations of the right ventricular outflow tract and ventricular septum have also been observed in affected homozygotes (151). Death due to renal insufficiency usually occurs within the first week of life (154).

The *Invs* gene maps to mouse Chromosome 4 (158). The syntenic interval on human chromosome 9q21-22 contains *NPHP2*, a gene locus associated with infantile nephronophthisis (NPHP) type 2 (94). NPHP is a cystic kidney disease phenotypically similar to PKD and the most frequent genetic cause of end-stage renal failure in children and adults (103). Recently, the *NPHP2* gene has been found to be orthologous to the *Invs* gene in the mouse (187). The *Invs* gene has been hypothesized to be a genetic modifier for multiple renal cystic mouse models, such as the *pcy*, *cpk* and *jck* mouse models (89, 133, 278).

Inversin, the protein encoded by *Invs*, is a novel protein containing ankyrin repeats and calmodulin-binding motifs (158). At least three isoforms of inversin exist, each localizing to different subcellular compartments, including the nucleus, cell-cell contacts complexed with N-cadherin and the catenins, the centrosomes, and in primary apical cilia of renal epithelia (158, 178).

The *bpk* (BALB/c polycystic kidneys) mutation arose as a spontaneous mutation in an inbred colony of BALB/c mice (188). The *bpk* mutation is fully penetrant and transmitted in an autosomal recessive manner (173). Affected homozygotes die within four weeks after birth from renal insufficiency caused by massively enlarged kidneys. Initially, cysts form in the proximal tubules; however, by post-natal day 21, there is a shift in the location of the cystic lesions to the collecting ducts (173). Homozygotes also exhibit liver abnormalities consisting of proliferative intrahepatic biliary tract ectasia and non-obstructive

dilation of the common bile duct (173). The *bpk* locus was mapped to mouse Chromosome 10 and through complementation testing was found to be allelic to *jcpk* (40, 90, 206).

The *jck* (juvenile cystic kidney) mutation occurred in a transgenic line of mice carrying the MMTV/*c-myc* transgene (8). Additional analyses demonstrated that the *jck* locus and the transgene segregated independently. Thus, the mutational event that occurred to produce the *jck* allele was unrelated to the transgene (8). Homozygous affected mice have palpably enlarged kidneys from 4 to 7 weeks of age and survive 5 to 6 months. However, histological analysis has shown that focal renal cysts are present as early as three days after birth. Progressive cystic changes were found with increasing age, shifting from cortical involvement to outer medullary involvement. Unlike other models for PKD, no extra-renal abnormalities have been detected (8).

The severity of the renal cystic disease in *jck* animals has been shown to be modulated by genetic background and modifier loci have been identified on mouse Chromosome 1 and mouse Chromosome 10 (114, 133). The *jck* locus has been mapped to mouse Chromosome 11 using an intercross between C57BL/6J-*jck* and DBA/2J mice (115). The gene has been cloned and the *jck* mutant allele has been found to carry a missense mutation in the *Nek8* gene which encodes NIMA (never in mitosis A)-related kinase 8 (138).

The *kat* (kidney, anemia, testes) mutation arose spontaneously in the inbred RBF/Dn mouse strain and a second mutant allele, *kat*^{2J}, occurred independently in the C57BL/6J strain (119). The *kat*^{2J} allele is associated with rapidly progressing renal cystic disease, whereas PKD associated with the *kat* allele progresses more slowly. Both *kat* and *kat*^{2J} homozygotes express a fully penetrant, pleiotropic phenotype that includes PKD, facial dysmorphism, dwarfing, male sterility, anemia, and cystic choroid plexus (119, 262, 267). Renal cystic disease is first evident at approximately two months of age, with cysts expressed primarily in the Bowman's capsule and proximal tubules. Disease severity is strongly influenced by genetic background (263).

The *kat* locus has been found to map to mouse Chromosome 8. The *kat* allele involves a 1.3 kb deletion, whereas the *kat*^{2J} allele results from a single base-pair insertion (119). The two alleles represent distinct mutations in the *Nek1* gene which encodes the NIMA (never in mitosis A)-related kinase 1. Both mutations fall within the kinase domain of the protein and are predicted to result in proteins that lack the entire C-terminal tail (262).

The *pcy* (polycystic kidney disease) mutation spontaneously occurred in the KK mouse strain and was found to be transmitted in an autosomal recessive manner (248). Due to poor reproduction of the KK-*pcy* mouse strain, a congenic *pcy* strain was developed in DBA/2J mice where the mutation was also transmitted as a fully penetrant, autosomal recessive trait (247). Cystic lesions observed in newborn pups are localized to the distal tubules. Cysts gradually extend to all areas of the nephron and death occurs between 30 and 36 weeks of age (165). Cystic disease severity has been shown to be modulated by genetic background and two modifier loci regions have been identified (166, 278). Extra-renal abnormalities are uncommon; however, a few mutants do develop cerebral vascular aneurysm in the later stages of the disease (248). Thus, considering the slow progression of renal cystic disease and the presence of vascular aneurysm, the *pcy* mouse model has long been considered a model for human ADPKD.

The *pcy* locus maps to mouse Chromosome 9 which is syntenic to human chromosome 3q21-22 (167). This region on human chromosome 3 contains the genetic locus *NPHP3*, a late onset form of nephronophthisis/medullary cystic disease (180).

PKD Models Arising From Chemical Induction or Insertional Mutagenesis

The *orp*k (Oak Ridge polycystic kidney) mutation was developed as part of a large-scale insertional mutagenesis program and is designated *TgN(lmorph)-737Rpw*, abbreviated as *TgN737Rpw* (160). The transgenic line was generated on the FVB/N inbred genetic background by pronuclear microinjection of a

construct containing the bacterial chloramphenicol acetyltransferase gene under the control of a mutated version of the polyoma early region promoter (22). In the FVB/N inbred genetic background, homozygous mutant animals have scruffy fur, pre-axial polydactyly of all limbs, polycystic kidney disease, abnormalities of the intrahepatic biliary tract, pancreatic ductal hypoplasia, and are severely growth-retarded (160, 286). Skeletal anomalies have also been observed and include craniofacial abnormalities, cleft palate, and extra teeth (290).

Most *orpk/orpk* mice on the FVB/N genetic background die within the first week of life, although a few animals live for several months. In contrast, on the C3H inbred background, affected mice display a less severe phenotype (239). These animals live longer, have polydactyly that is more variable, have renal cysts that progress at a slower rate, and have less aggressive liver disease. This difference in phenotypic expression dependent on genetic background suggests the presence of important modifier genes. This variable phenotypic severity is also seen in human ARPKD, in which the severity of the phenotype and the nature of the liver disease are quite variable (17, 239).

The mutant locus in the *TgN737Rpw* transgenic line has been mapped to mouse Chromosome 14 (247). This novel gene encodes polaris, a protein containing multiple copies of a 34-amino acid tetratricopeptide repeat (TPR) (160). The TPR motif was first described in lower eukaryotes and found to exist in proteins involved in cell cycle control, protein import, and transcription (82, 234). Protein localization studies have shown that polaris is expressed in basal bodies and the primary cilia of renal epithelium (251). The human gene has been cloned and maps to human chromosome 13 (160).

Northern blot analysis has indicated that the primary transcript of 3.2 kb is normally expressed in a number of tissues including kidney and liver but was absent in all tissues in *orpk/orpk* homozygotes. Two other larger transcripts of lower abundance have also been found. Expression of the predominant transcript as a transgene (*Tg737^{Bap}*) in *orpk* mutants rescues the renal cystic phenotype (285).

Genetic analysis has also determined that *Tg737^{orpk}* is a hypomorphic allele (160, 251, 286). An SV40 conditionally immortalized cortical collecting duct cell line has been derived from *Tg737^{orpk}* homozygous mice. These cells do not develop normal primary renal cilia, but can be corrected by the introduction and re-expression of the wild type *Tg737* gene (284).

A second targeted mutation, *Tg737^{Δ2-3βGal}*, represents a null allele (161). Homozygous *Tg737^{Δ2-3βGal}* embryos die in early to mid-gestation, with left-right axis specification defects, failure of neural tube closure, and limb patterning defects (161).

The 67Gso (t(2;10)67Gso) mutation arose during the course of large-scale mutagenesis studies (40). Animals homozygous for the 67Gso mutation express a severe form of early onset PKD characterized by renal and hepatic cysts at birth. Affected newborns are smaller and much weaker than their littermates, and develop a protruding abdomen by one day after birth. Survival is limited to three to four days after birth. Affected pups develop a yellow-orange pigmentation before death, indicating liver failure. Histological examination of the kidneys indicated many narrow, elongated cysts that extended from the cortex radially toward the medullary pyramid (40).

The phenotype expressed by 67Gso homozygotes is associated with inheritance of a t(2;10)(H1;C1) reciprocal translocation. Complementation studies with 67Gso heterozygotes and *jcpk* heterozygotes, another autosomal recessive PKD mouse mutation (see below), produced animals with disease indicating that 67Gso was allelic to *jcpk* (40, 206). Further, FISH analysis has indicated that the putative 67Gso breakpoint on mouse Chromosome 10 is within the region containing the *jcpk* gene (41).

The *jcpk* (juvenile congenital polycystic kidney) mutation was first identified during chlorambucil (CHL) mutagenesis studies (66). The disease in homozygous *jcpk/jcpk* mice is characterized by severe cystic disease in all areas of the nephron, from the glomerulus to the collecting ducts (66). Signs of the disease are visible as early as 3 days after birth, with death generally occurring by ten days of age. A number of extra-renal abnormalities have also been

observed, including enlargement of the gallbladder and abnormalities of both the biliary and the pancreatic ducts. Heterozygotes appear phenotypically normal; however, 30% of these mice exhibit cystic disease localized to the glomeruli by the age of 10 months. Bile duct abnormalities and hepatic cysts were also noted in some heterozygous animals (66).

The *jcpk* locus has been previously localized by precise genetic mapping in an intercross with *Mus musculus castaneus*, to a region of approximately 1 cM flanked by the polymorphic genetic markers *D10Mit115* and *D10Mit173* on mouse Chromosome 10 (28). Another autosomal recessive PKD mouse mutant, *bpk*, has also been localized to this same genetic region (90). Affected *bpk* homozygotes have disease that is different in terms of age of onset and phenotype compared to *jcpk* homozygotes. However, complementation testing between heterozygotes (*+/jcpk* X *+/bpk*) resulted in offspring with cystic kidney disease, indicating that *jcpk* and *bpk* are allelic. The differences in disease between *jcpk* versus *bpk* mice are likely due to the effect of the particular mutation carried by each and to differences in genetic background (C57BL/6J for *jcpk* versus BALB/c for *bpk*). As previously mentioned, similar complementation studies between *jcpk* and *67Gso* indicated that these two mutations are also allelic. Based on these data, it was predicted that all three mouse models were due to different mutations in the same gene. The genetic region containing the *jcpk/bpk/67Gso* locus overlaps with the genetic interval containing a putative PKD modifying locus, *Pkdm2*, which influences the disease phenotype of another independent PKD mouse mutant, *jck* (115). The disease-causing gene shared by the *jcpk*, *bpk*, and *67Gso* mouse models, *Bicc1*, its identification, characterization and potential role in PKD pathogenesis are the focus of this dissertation.

Ciliocentric Theory of PKD Pathogenesis

Despite the growing number of genetic mutations attributed to the formation of cysts in the kidney, the pathogenic mechanisms behind PKD still remain elusive. Recent studies in human and animal models have suggested that primary cilia of renal tubular epithelial cells may function to maintain normal tubular architecture, and that ciliary abnormalities may be a cause of cyst formation in polycystic kidney disease.

Primary cilia have an axonemal structure consisting of a circular array of nine pairs of microtubules (9+0 arrangement) (Figure 2.3). Cilia with this configuration are generally immotile, with the exception of embryonic node cilia that direct morphogen flow which is important for left-right axis (L/R) specification (176, 179).

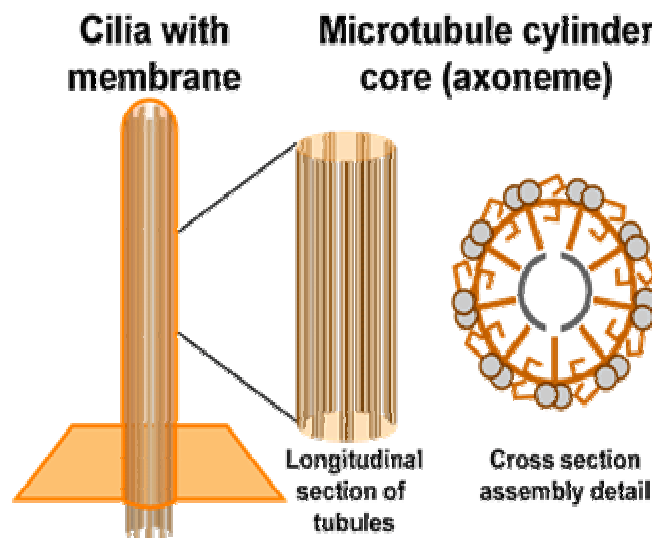


Figure 2.3 Illustration of primary cilia. Primary or monocilia are a distinct type of cilium and are responsible for the establishment of L/R asymmetry in early embryos. Primary cilia are also found in various organs, including skin, kidney (renal tubule epithelium) and blood vessels (endothelium) where their functions are largely unknown. (Illustration courtesy of Dr. Stephen Fish, Department of Anatomy, Cell and Neurobiology, Joan C. Edwards School of Medicine, Marshall University)

Primary cilia are a common feature of polarized epithelial cells in eukaryotes and are thought to serve either a chemosensory or mechanosensory function. Primary cilia often contain high concentrations of receptors and are

ideally positioned to interact with the environment, as with the odorant receptors on olfactory cilia or the highly specialized cone and rod photoreceptors that respond to light (215). In fact, cilia are thought to contain more than 200 proteins that maintain their formation and function (62).

Renal cilia project into the tubule lumen from the apical (luminal) surface of all renal tubular cells except the intercalated cells of the collecting duct (181) (Figure 2.4).

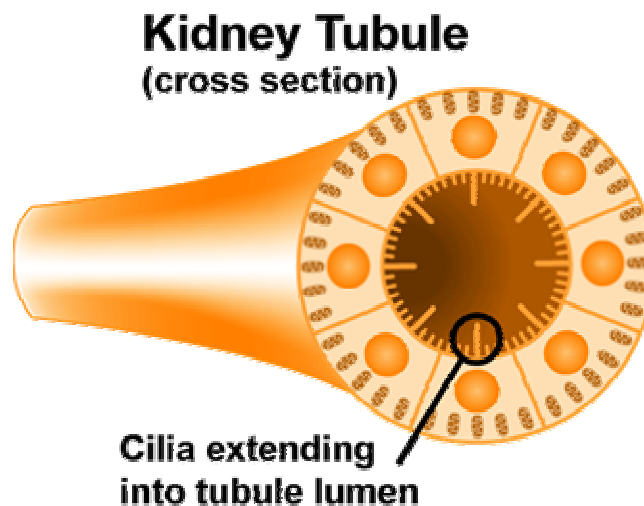


Figure 2.4 Primary cilia extend into the renal tubule lumen. In the kidney, cilia are present throughout much of the nephron and collecting duct. Cilia project from the apical surface of the epithelia into the tubule lumen, where they are optimally positioned to function in a sensory capacity. (Illustration courtesy of Dr. Stephen Fish, Department of Anatomy, Cell and Neurobiology, Joan C. Edwards School of Medicine, Marshall University)

Electron microscopy of the rat nephron has detected the presence of primary cilia on cells of the parietal wall of the renal corpuscle, the proximal tubules, the thin limb of Henle's loop, the distal tubule, and the collecting duct (68, 259). These cilia have been shown to reversibly bend in response to lateral fluid shear forces, as visualized by real-time video recorded under conditions that resemble actual tubule flow rates (203). Fluid shear-force bending of the primary cilia of Madin-Darby canine kidney (MDCK) cells has been shown to increase intracellular calcium, from both extracellular and intracellular sources, and to transmit these signals to adjacent cells through gap junctions (203). Deciliation

by chloral hydrate treatment abolishes flow-induced calcium increases but does not affect calcium mobilization in response to mechanical cell-surface stimulation, indicating that cilia are mechanosensory flow sensors (204). This flow-induced increase in intracellular calcium also caused membrane hyperpolarization and increased potassium conductance (204).

In addition to mechanosensation, it is possible that renal cilia may function in a chemosensory capacity, such as with cilia found on olfactory neurons of mammals and in *Caenorhabditis elegans* (132, 222, 228, 259). If renal cilia do act as sensors in the tubule lumen, the cilium length may be a critical factor in signaling efficacy. A few mouse mutants for PKD have shortened or absent cilium but this is not a common denominator among all mouse models for PKD that have defects in cilia proteins (161, 179, 191, 213).

The synthesis of primary cilia involves the process of intraflagellar transport (IFT) in which large particles or “rafts” containing protein cargo are transported bidirectionally along the ciliary axoneme (192). The anterograde movement of proteins along the axoneme is mediated by kinesin-II, a heterotrimeric protein composed of two motor subunits (KIF3A and KIF3B) and one non-motor subunit (KAP). Conventional knockout mice that completely lack KIF3A fail to synthesize cilia in the embryonic node and exhibit randomization of left-right symmetry and structural abnormalities of the neural tube, pericardium, branchial arches, and somites (147, 249). Tissue-specific Cre-loxP inactivation of *Kif3a* in renal tubular epithelial cells results in viable offspring with normal-appearing kidneys at birth. However, cysts begin to develop in the kidneys at postnatal day 5 and cause renal failure by postnatal day 15. The cystic epithelial cells were found to lack primary cilia and exhibit increased proliferation and apoptosis, apical mislocalization of the epidermal growth factor receptor (EGFR), and increased expression of β -catenin, c-Myc and p21^{CIP1} (137). These results demonstrate that the absence of renal cilia produces both the clinical and molecular findings associated with PKD.

A number of groups have reported the possible involvement of genes associated with PKD in either the assembly or function of cilia in mice and

Caenorhabditis elegans. The first evidence for the ciliocentric theory of PKD pathogenesis was provided by the *orpk* mouse model. The product of this gene, polaris, is localized in the axoneme and basal body of primary cilia and is required for ciliary assembly (287). Similarly, the *inv* mouse model for PKD also has a connection to primary cilia. Several isoforms of the inversin protein have been described and have been localized to primary apical cilia, cell-cell adhesion sites and the nucleus (157, 178).

The *cpk* mouse model for PKD has also been linked with cilia. The gene, *Cys1*, encodes cystin-1, has been localized in the axonemal region of primary cilia and partially overlaps with the localization of polaris (108). Interestingly, *cpk* mutants have PKD despite structurally normal cilia (89, 213).

A further link between cilia defects and PKD is provided by the *Pkd1*^{-/*LacZ*} mouse, in which a targeted deletion of exon 1 was generated using a *LacZ* “promoter trap” (197). *Pkd1* is localized to renal primary cilia and mice homozygous for *Pkd1*^{-/*Lac*} develop renal and pancreatic cysts.

Parallel work in *C. elegans* identified orthologues of *PKD1* (*lov-1*, for location of vulva) and *PKD2* (*pkd-2*), whose protein products were found specifically in the cilia or male sensory neurons co-localizing with OSM-5, an orthologue of polaris, and IFT88, the orthologue of an intraflagellar transport protein in *Chlamydomonas* (15, 99, 210). Mutations in *lov-1* or *pkd-2* seemed to affect ciliary function, whereas *osm-5* (*osm*, for osmotic avoidance) mutations affected ciliary structure. These discoveries prompted researchers to question whether the mammalian polycystins reside in the cilia of renal epithelial cells.

Studies have demonstrated that polycystin-1 and polycystin-2 co-localize to the primary cilia of cultured kidney cells and mouse kidney tubule cells *in vivo* (193). These two proteins are thought to work together to mediate mechanosensation (172, 284). This was demonstrated by showing that the calcium flux induced by fluid-flow ciliary bending did not occur in polycystin-1 null cells or when cells were treated with polycystin-1 or polycystin-2 blocking antibodies (172). Although the cellular functions of the polycystins are unknown, there is evidence suggesting that polycystin-1 (PC1) (3) is a receptor that

regulates polycystin-2 (PC2) calcium channel activity (53, 189, 190). By acting as a ciliary mechanoreceptor, PC1 may sense luminal flow rates through ciliary bending and signal morphologically relevant information through a number of cellular signaling pathways to establish and maintain appropriate luminal dimensions. Activated by signals from PC1, PC2 would then act as a tension-gated ion channel to generate an influx of calcium (33). Calculations have suggested that as few as one polycystin-2 molecule per cilium is sufficient to trigger the measured calcium influx in MDCK cells (204). Loss or dysfunction of PC1 or PC2, or cilia dysfunction in general, would impair the mechanosensing capability of epithelial cells, causing defects in cellular differentiation and tubular integrity that in turn leads to cyst formation.

The potential connection between cilia and PKD is intriguing. Elucidating the function of primary cilia and their association with PKD will require a detailed characterization of proteins involved in ciliogenesis and cilia function, as well as the development of reagents and assays to test the role of primary cilia in renal physiology.

Vertebrate Left-Right Asymmetry

The establishment of the three body axes – anterior-posterior (A/P), dorsoventral (D/V), and left-right (L/R) – is central to the organization of the vertebrate body plan. A distinctive and essential feature of the vertebrate body is a pronounced left-right asymmetry of internal organs and the central nervous system. L/R axis determination is determined last, and consequently, defects that arise from abnormal L/R patterning are less severe than A/P or D/V defects, making experimental observations much easier (95).

In the process of left-right (L/R) axis formation in the mouse, the embryonic node plays a critical role in the initial breaking of L/R symmetry (95). The current model for the establishment of left-right axis asymmetry depends upon the motility of primary cilia in the embryonic node to generate a net leftward flow of extra-embryonic fluid to ultimately create a morphogen gradient around the node. This morphogen gradient is proposed to provide a signal for subsequent asymmetric gene expression at the lateral plate mesoderm (95). These signals for "left" and "right" are ultimately interpreted by organ primordia to establish asymmetry of the visceral organs. Complex activating and inhibiting interactions involving TGF- β family members, as well as homeobox transcription factors, mediate these asymmetric patterns of gene expression (131).

The investigation of the mechanisms regulating left-right axis patterning in model organisms has resulted in the characterization of human mutations associated with left-right axis malformations. These observations indicate that the loss of primary cilia function on the embryonic node results in the randomization of visceral organs (26). This is observed in Kartagener syndrome in which loss of cilia motility can result in random laterality of heart looping where the heart is on the wrong side of the midline. This loss of motility is also responsible for *situs inversus* viscera (mirror image reversals in the orientation of internal organs), bronchiectasis, sinusitis, and infertility (2). These patients have mutations in genes encoding components of the ciliary motor, including defects in dynein intermediate chains and dynein heavy chains (246).

There is a growing body of evidence that links ciliary dysfunction, embryonic left-right patterning defects and cystic disease of the visceral organs, e.g., kidney, liver and pancreas. Polaris is one of many proteins that appear to function in ciliogenesis and L/R body axis determination (161). A targeted null mutation in *Tg737*, *Tg737^{Δ2-3βGal}*, results in complete loss of nodal cilia, left-right axis asymmetry defects, failure of the neural tube to close, limb patterning defects, and embryonic lethality (161, 251). In contrast, homozygosity for the *Tg737^{orpk}* hypomorphic allele results in renal, biliary and pancreatic cysts (251). Mice homozygous for the *Invs* gene have both reversal of L/R visceral asymmetries and renal cystic disease (158). Ultrastructural analysis of the cilia of *inv* homozygotes indicate that the nodal cilia are present and motile, but can produce only very weak leftward nodal flow (179). Recent evidence has also indicated that mice containing a knockout of the *Kif3a* gene fail to synthesize cilia in the embryonic node and exhibit randomization of left-right asymmetry and structural abnormalities of the neural tube, pericardium, branchial arches and somites (147, 249). However, tissue-specific inactivation of *Kif3a* in the kidney results in severe PKD. The cyst epithelium lack cilia and exhibit increased cell proliferation and apoptosis (137). Finally, targeted null mutations in *Pkd2* result in right pulmonary isomerism, randomization of embryonic turning, heart looping and abdominal situs (197).

Currently, the common mechanism that links cilia, L/R asymmetry, and PKD is still unknown. Further studies of cilia formation and function might yet reveal a fundamental mechanism that underlies both L/R asymmetry and PKD pathogenesis. Establishing clinical treatment for PKD will be greatly facilitated by an understanding of how individual gene products participate in the disease pathway.

Summary

Polycystic kidney disease (PKD) is a common genetic cause of chronic renal failure in children and adults, and is characterized by the accumulation of fluid-filled cysts in the kidney (118). Renal cysts originate from the epithelia of the nephrons and renal collecting system and are lined by a single layer of continuous epithelium that has higher rates of cellular proliferation and are less differentiated than normal tubular cells. Abnormalities in gene expression, cell polarity, fluid secretion, apoptosis, and extracellular matrix have also been described in PKD (117, 118). A number of genes in humans and animal models have been identified that, when mutated, cause PKD. Despite the growing number of genetic mutations attributed to the formation of cysts in the kidney, the pathogenic mechanisms behind PKD still remain elusive. In order to understand how individual gene products participate in cyst formation and disease pathogenesis, a detailed characterization of PKD-susceptibility genes and the proteins that they encode is required. The objective of the following body of research is to characterize the *jcpk* mouse model for polycystic kidney disease (PKD) through both genetic and molecular analyses. The *jcpk* locus was previously localized to a 1 cM region located on mouse Chromosome 10 (28). Two other mouse models, *bpk* and 67Gso, have been shown to be allelic to *jcpk* through complementation analysis (90, 206). The purpose of the following research is 1) to identify the PKD disease-causing gene shared by the *jcpk*, *bpk* and 67Gso mouse models; 2) to use molecular analyses to evaluate the mRNA and protein expression of *jcpk*; and 3) to begin to establish a role for the *jcpk* gene in the context of current theories of PKD pathogenesis. No specific treatments for PKD currently exist, so it is hoped that a more complete understanding of the molecular pathogenesis of this disease will identify novel therapeutic strategies.

CHAPTER III

MATERIALS AND METHODS

Genetic and Physical Mapping

Mouse Strains

Mice used for these studies were bred at the Joan C. Edwards School of Medicine, Marshall University, Huntington, WV. The *jcpk* mutation was first identified during chlorambucil mutagenesis experiments (67). Male (101/RI x C3H)F₁ mice were treated with 10 mg/kg of chlorambucil. Treated males were then mated with Tester females. The progeny of this cross were intercrossed twice so that recessive visible mutations could be recovered (67). The PKD phenotype was recognized by a grossly enlarged abdomen appearing in 3 to 10-day old mice (66). The *jcpk* mutation has been backcrossed at least 40 times to the C57BL/6 (B6) mouse strain. B6 mice were purchased from The Jackson Laboratory (Bar Harbor, Maine). The 101/RI mice were obtained from The Oak Ridge National Laboratory (Oak Ridge, Tennessee). Both B6 and 101/RI were maintained at the Marshall University Animal Resource Facility, Huntington, WV. Mice were bred for colony maintenance and as a source of tissues for DNA, RNA and protein analyses. Animals were observed from birth for signs of polycystic kidney disease and were euthanized at obvious signs of discomfort.

Heterozygous mice carrying the *waved-2* mutation (*a/a Egfr^{wa2}/J*) were purchased from The Jackson Laboratory (Bar Harbor, Maine). Mouse *waved-2* (*wa2*) was first identified as a mutation in the *Egfr* gene in an “abnormal corpus callosum” stock at the Bussey Institution (141). The *waved-2* mutation is inherited as an autosomal recessive trait. Matings between mice heterozygous for the *jcpk* mutation and homozygous for the *wa2* mutation generated compound heterozygous animals. Compound heterozygous females were backcrossed to male mice homozygous for the *wa2* mutation to produce mice that were

heterozygous for the *jcpk* allele and homozygous for the *wa2* allele. Male offspring that were heterozygous for *jcpk* and homozygous *wa2* were mated to females that were heterozygous for both alleles to generate double mutant animals. Crosses involving female *wa2/wa2* homozygotes were avoided due to impaired lactation (71). The *jcpk* mutation was determined to be present in mice using genotyping assays discussed below and the *wa2/wa2* homozygotes were recognized phenotypically by their wavy coat and curly whiskers that can be observed as early as 2-3 days after birth (71). All mice were maintained under a 17 hour light - 7 hour dark cycle and fed Purina™ Rodent Chow 5001. Pregnant and lactating mice were fed Purina™ 5K67 NIH Rat and Mouse Autoclavable Diet. Mice were given non-sterile, non-filtered water and maintained in standard rodent cages at ambient temperature. All procedures performed on the above mice were approved by the Marshall University Institutional Animal Care and Use Committee (IACUC).

Genomic DNA Extraction

Genomic DNA was extracted from tail biopsy and isolated tissues by several methods. Tail DNA was isolated based on a simplified mammalian DNA isolation procedure (135). Tail biopsies of no longer than 0.5 cm were transferred immediately to a 1.5 ml tube containing 0.5 ml of lysis buffer (100 mM Tris-HCl, pH 8.5, 5 mM EDTA, 0.2% SDS, 200 mM NaCl, and 100 µg/ml Proteinase K) immediately upon removal. The tubes were then transferred to a rotating shaker and agitated at 200 rpm at 55°C overnight. Following incubation, the tubes were vortexed and centrifuged at maximum speed for 10 minutes. The supernatants were transferred to pre-labeled 1.5 ml tubes containing 0.5 ml of isopropanol. DNA was recovered by centrifugation at maximum speed for 15 minutes at 4°C. Pellets were suspended in 50 µl of sterile dH₂O.

Genomic DNA was also extracted using the HotSHOT DNA extraction procedure (260). A small snip of mouse tail was removed using a sterile scalpel blade while mice were under anesthesia. The snip of mouse tail was then added

to 75 µl of alkaline lysis buffer (25 mM NaOH, 0.2 mM EDTA, pH 12) and incubated for 30 minutes at 94°C. After incubation, 75 µl of neutralizing buffer (40 mM Tris-HCl, pH 5) was added. Genomic DNA from mouse tissues was extracted using the Wizard® Genomic DNA Purification kit (Promega, Madison, WI).

Blood spots were also collected for DNA analysis. Freshly snipped mouse tails were touched to 3M Whatman filter paper to generate spots of blood followed by cauterization of the tail wound. The spots were allowed to air dry followed by a 15 minute wash in methanol to preserve the blood on the filter paper. The spots were allowed to air dry again and were stored at room temperature. The dried spots were then cut from the Whatman paper and used for genotyping.

Genotyping

The polymorphic marker *D10Mit42* was found to be genetically linked to the *jcpk* mutation and was used to initially genotype mice prior to gene identification (66).

The following primers were used:

F: 5'GCATTCAGAAGCTGGAAAGG3'

R: 5'TGCCCAGCATATGTTTAAAGG3'.

Primers were synthesized by the Marshall University DNA Core Facility, Huntington, WV. Tail snips or blood spots prepared as above were boiled for ten minutes in 10 µl of sterile dH₂O and used as genomic DNA sources. The forward primer of *D10Mit42* was radioactively labeled with γ-[³²P]dATP by T4 polynucleotide kinase for 30 minutes at 37°C, then 10 minutes at 65°C. A 25 µl PCR reaction containing 2X PCR buffer (3 mM MgCl₂, 20 mM Tris-HCl, pH 8.3, 100 mM KCl, 32 µg/ml BSA, 400 µM of each dNTP), 0.25 µl 10 µM reverse primer, 1µl Taq DNA polymerase (5 U/µl), and 1 µl 50 ng/µl DNA was amplified under the following conditions: 2 minutes at 97°C; 25 cycles of 95°C for 30 seconds, 56°C for 30 seconds, and 72°C for 30 seconds, with a final extension at

72°C for 7 minutes. Fifty nanograms of purified genomic DNA from C57BL/6J, 101/RI, and Tester were also labeled and amplified as controls. The PCR products were then denatured at 95°C for 5 minutes and were separated by electrophoresis in 1X TBE on 5% denaturing polyacrylamide gels at 60 watts for 1 hour. Gels were dried on a gel dryer at 80°C for 15 minutes. The bands were detected using autoradiography: the gel was exposed to X-ray film in cassettes containing an intensifying screen and stored overnight at -80°C. Mice identified as heterozygotes based on this linkage analysis were backcrossed to known heterozygotes (+/*jcpk*) of the opposite sex to confirm the presence of the *jcpk* mutant allele.

Once the *jcpk* gene was identified, an allele-specific mutation assay was developed for genotyping purposes. Genomic DNA was extracted from tail snips using the HotSHOT DNA extraction protocol as described previously. A 30 µl PCR reaction containing 2X PCR buffer (3 mM MgCl₂, 20 mM Tris-HCl, pH 8.3, 100 mM KCl, 32 µg/ml BSA, 400 µM of each dNTP), 0.25 µl 10 µM each primer, 1 µl Taq DNA polymerase (5 U/µl), and 10 µl of the tail prep DNA extracted by the HotSHOT method was amplified under the following conditions: 40 cycles of 92°C for 1 minute, 57°C for 1 minute and 72°C for 2.5 minutes.

The following primers were used for the amplification:

F: 5'CCTTTCTTGGATTAGCCCC3';

R: 5'CTCCGAGGACGATCTGGTGG3'.

Primers were synthesized by the Marshall University DNA Core Facility, Huntington, WV.

Following PCR, 15 µl of the amplification reaction was used for amplification product separation on a 1% agarose gel containing 0.5 µg/ml of ethidium bromide. A 187 bp product is visible upon separation by gel electrophoresis in 1X TAE buffer, at 100 V for 30 minutes. The *jcpk* mutation eliminates a *Ddel* restriction enzyme site in the 187 bp PCR product. Therefore, 20 µl of the previous PCR reaction mix was used in an endonuclease restriction digest reaction performed overnight with 10 units of *Ddel* at 37°C (New England BioLabs, Inc., Beverly, MA). The restriction digestion was analyzed by gel

electrophoresis on a 3% agarose gel containing 0.5 µg/ml of ethidium bromide, in 1X TAE at 100 V for 30 minutes. Homozygous normal mice (wild type) have two bands that are 115 and 72 bp in length. Homozygous affected mice (*jcpk/jcpk*) do not have the *Ddel* restriction site and have a single 187 bp band. Heterozygous animals (*+jcpk*) have three bands: a 187 bp fragment corresponding to the *jcpk* allele and two fragments of 115 and 72 bp that correspond to the wild type allele.

High Resolution Genetic Mapping

In order to significantly narrow the region on mouse Chromosome 10 thought to contain the *jcpk* gene, the polymorphic markers *393H9SP6RPT* and *282P18T7RPT* were analyzed by radioactively labeling 12 µM of one PCR primer with γ -[³²P]dATP using T4 polynucleotide kinase in a 12 µl reaction (Invitrogen, Carlsbad, CA) for 30 minutes at 37°C and then 65°C for 10 minutes. Fifty nanograms of purified genomic DNA from *jcpk* recombinant animals (28), C57BL/6J, 101/RI, C3H/HeJ, CAST/Ei, and BALB/c were used for 30 µl PCR reactions containing 2X PCR buffer (3 mM MgCl₂, 20 mM Tris-HCl, pH 8.3, 100 mM KCl, 32 µg/ml BSA, 400 µM of each dNTP), 0.25 µl 10 µM each primer, and 1 µl Taq DNA polymerase (5 U/µl) and 0.24 µl of the kinase reaction from above. PCR was performed under the following conditions: 2 minutes at 97°C; 25 cycles of 95°C for 30 seconds, 55°C for 30 seconds, 72°C for 30 seconds; with a final extension of 72°C for 7 minutes. The radioactively labeled amplification products were denatured by addition of 6 µl of Stop Buffer (80% formamide, 50 mM Tris-HCl (pH 8.3), 1 mM EDTA, 0.1% (wt/vol) xylene cyanol, and 0.1% (wt/vol) bromophenol blue) followed by incubation at 95°C for 5 minutes. Prior to separation of samples, 5-6% denaturing polyacrylamide gels in 1X TBE were pre-run at a constant of 60 watts for greater than 15 minutes. Three µl of each denatured sample was then loaded on the pre-run gels followed by gel electrophoresis at 60 watts. Gels were dried on a gel dryer at 80°C for 15 minutes and differences in control and recombinant PCR products were detected using overnight exposure to X-ray film at -80°C with an intensifying screen. Size

differences between B6 and 101/RI were used as controls and were compared to *jcpk* recombinant animals in order to determine the position of both *393H9SP6RPT* and *282P18T7RPT* relative to known markers on the genetic map representing the *jcpk* critical region on mouse Chromosome 10. Primer sequences for *393H9SP6RPT* are as follows:

F: 5'CCAGGAGGTGAAGGAGAGCA3'
R: 5'GCTGGAAACTGCCATGACC3'.

Primer sequences for *282P18T7RPT* are as follows:

F: 5'CTTGGTCTCCTAATGCCTGC3'
R: 5'TGTATTGCATAACCCCAGCA3'.

Primers were synthesized by the Marshall University DNA Core Facility, Huntington, WV.

Physical Mapping

Construction of the physical map representing the region on mouse Chromosome 10 thought to contain the *jcpk* gene was initially performed by PCR-based screening of two different mouse whole-genome BAC libraries. Analysis of the CITB BAC library (Research Genetics, Huntsville, AL) and the Mouse ES-129/SvJ BAC library (Genome Systems, St. Louis, MO) was performed according to manufacturer's protocols. Positive BAC clones were identified from either of the above libraries and subsequently analyzed by PCR for marker content. BAC end nucleotide sequences were determined by isolating and subcloning the ends of the BACs into an appropriate high copy number plasmid vector followed by sequence analysis of the subclone, or alternatively, direct sequence analysis of the BAC was performed to determine the nucleotide sequence on the ends of the BACs. Primers were designed based on these BAC end sequences and the libraries were re-screened with the new primers.

The RPCI-23 mouse whole-genome C57BL/6 BAC library (Research Genetics, Huntsville, AL) was screened using a procedure known as multiplex oligonucleotide hybridization or "overgo" (32). Overgo is a genomic library screening method that relies on the design of highly specific 3'-overlapping oligonucleotide (overgo) probes comprised of two 24 base oligonucleotides with an 8 base pair (bp) overlap. The overgo probes are labeled by adding radioactive nucleotide monophosphates to the 3'-recessed ends. These probes are multiplexed and used to quickly and efficiently screen an entire mouse whole-genome library in a single step. A large number of BACs can be identified at one time instead of using several rounds of PCR amplification as required in other screening methods.

To obtain RCPI-23 BAC end sequence information in order to design overgo primers for library screening, the BAC end sequence annotation database at http://www.tigr.org/tdb/bac_ends/mouse/bac_end_intro.html was used. Downloaded sequences were processed through the computer software RepeatMasker (<http://genome.wustl.edu/gsc/repeatmasker>) to eliminate regions

containing repetitive elements and by analysis of the non-redundant sequence database at www.ncbi.nih.gov using the Basic Local Alignment Search Tool (BLAST) (5) to insure that the regions used for overgo primer design were unique. Sequence-specific overgo primers were designed using an interactive website (<http://genome.wustl.edu>). Primer sequences for the overgo primers can be found in Appendix A. All primers were synthesized by the Marshall University DNA Core Facility, Huntington, WV.

All overgo probes were radioactively labeled and used simultaneously to screen the entire RPCI-23 library spotted on seven Hybond nylon membranes (Research Genetics, Huntsville, AL). Each membrane contained 27,648 unique BAC DNAs spotted in duplicate. Overgo probes were radioactively labeled in a reaction containing 3 μ l of overgo primer mix (10 pmol/ μ l of each primer), 1.5 μ l of BSA (2 mg/ml), 2 μ l α -[32 P]dATP (3000 Ci/mmol, 10 mCi/ml), 2 μ l α -[32 P]dCTP (3000 Ci/mmol, 10 mCi/ml), 2 μ l of Klenow fragment (2 U/ μ l), 13.5 μ l of sterile dH₂O and 6 μ l of OLB (1:2.5:1.5 ratio of solutions A:B:C). Individual solution components are as follows: Solution O (1.25 M Tris-HCl, pH 8.0, 125 mM MgCl₂), Solution A (1 ml Solution O, 18 μ l 2-mercaptoethanol, 5 μ l 0.1 M dTTP, 5 μ l 0.1 M dGTP), Solution B (2 M HEPES-NaOH, pH 6.6), and Solution C (3 mM Tris-HCl, pH 7.4, 0.2 mM EDTA) (32). The labeling reaction was incubated at room temperature for two hours. Unincorporated nucleotides were removed using Sephadex NICK™ columns (Amersham Biosciences, Piscataway, NJ). Separate overgo labeling reactions were combined into one NICK™ column to provide a single mixed reaction. The seven nylon membranes containing the spotted BACs were then separated into two hybridization bottles (30 cm x 4 cm). Membranes were wet with warmed 1X SSC and layered onto hybridization mesh. All filters were rolled together in the same direction and inserted into two hybridization bottles. With the cap on, the bottles were rotated manually to allow the membranes and mesh to unroll in the bottle. The 1X SSC was removed and replaced with 30 ml of pre-warmed sodium phosphate hybridization buffer (0.5 M sodium phosphate, 1% BSA, 1 mM EDTA, pH 8.0 and 7% SDS). Membranes were pre-hybridized for 2 hours at 60°C with constant rotation in a hybridization

oven. After pre-hybridization, 5 ml of hybridization buffer from each bottle was removed and pooled in a 25 ml conical tube. The labeled probe mixture was denatured by boiling for 10 minutes. The probe mixture was then added to the 10 ml of hybridization buffer, mixed and 5 ml of this mixture was returned to each hybridization bottle. The membranes hybridized at a temperature of 60°C for a minimum of 18 hours.

After incubation at 60°C, the hybridization solution was removed and each bottle was filled with room temperature 4X SSC, 0.1% SDS. The bottles were then returned to the hybridization oven and rotated for 30 minutes at 60°C. The membranes were transferred to a large plastic container on a rotary shaker and washed in the following manner: 1.5X SSC, 0.1% SDS at 58°C for 30 minutes where the hybridization mesh was left between the membranes; 0.75X SSC, 0.1% SDS at 58°C for 30 minutes with the mesh removed between the membranes. Both washes were rotated at a constant speed of 30 rpm. The membranes were then sealed in plastic bags and attached to individual 3M Whatman sheets. The membranes were exposed to X-ray film at -80°C without an intensifying screen for 12-16 hours. Positive clones were identified and purchased as glycerol stocks (Research Genetics, Huntsville, AL). BAC DNA used for analysis was isolated using the QIAGEN plasmid DNA extraction kit (QIAGEN, Inc., Valencia, CA).

Slot Blot Analysis

To determine which BACs contained a specific overgo probe sequence, slot blot hybridization analysis was performed. Briefly, 500 ng of each purified BAC DNA suspended in sterile dH₂O was denatured with 0.1 volume of 1 N NaOH for 5 minutes in a boiling water bath and immediately put on ice. One volume of 2 M ammonium acetate, pH 7, was then added to neutralize the denatured sample. A nylon membrane and two sheets of 3M Whatman paper for each blot were pre-wet in deionized water and then soaked in 6X SSC prior to use.

Slot blots were produced using the standard manufacturer's protocol provided with the slot blotting manifold (Schleicher and Schuell, Keene, NH). Individual slots were washed with 6X SSC on constant low vacuum (~1ml/minute). With the vacuum still on, the BAC DNA sample was applied and filtered on low vacuum. BAC DNA was immobilized on the nylon membranes by UV irradiation at 120mJ/cm².

Membranes were then pre-hybridized at 60°C in 20 ml of HyperHyb™ (Research Genetics, Huntsville, AL) for 30 minutes with constant rotation. Individual overgo probes were radioactively labeled as previously described followed by individual NICK™ column (Amersham Biosciences, Piscataway, NJ) purification. Probes were denatured by boiling for 10 minutes. The membranes were hybridized with each probe for 2 hours at 60°C with constant rotation. Membranes were then washed with 1.5X SSC, 0.1% SDS at 58°C for 10 minutes; 0.75X SSC, 0.1% SDS at 58°C for 5 minutes followed by overnight exposure with X-ray film at -80°C. Membranes were scored for the presence or absence of a specific marker in order to position BACs onto the physical map.

PCR Amplification

BAC identification by slot blot hybridization analysis was confirmed by PCR amplification using BAC end specific primers and a panel of 100 ng/ul of purified BAC DNAs as well as human, CAST/Ei, BALB/c, 101/RI, B6, 129aa and

hamster A23 genomic DNA. Primer sequences can be found in Appendix B. All primers were designed using Primer3 computer software (218) and synthesized by the Marshall University DNA Core Facility, Huntington, WV. A 30 μ l PCR reaction containing 2X PCR buffer (3 mM $MgCl_2$, 20 mM Tris-HCl, pH 8.3, 100 mM KCl, 32 μ g/ml BSA, 400 μ M of each dNTP), 1 μ l Taq DNA polymerase (5 U/ μ l), 0.25 μ l 10 μ M each primer and 1 μ l 100 ng/ μ l DNA was amplified under the following conditions: 97°C for 2 minutes; 35 cycles of 95°C for 30 seconds, the primer-specific annealing temperature for 30 seconds, and 72°C for 30 seconds; with a final extension of 72°C for ten minutes. Amplification products were resolved on 2% agarose gels containing 0.5 μ g/ml ethidium bromide, in 1X TAE at 100 V for 30 minutes. The presence or the absence of bands was noted as well as any size differences. If differences between 129aa mouse and A23 hamster DNA were present, these markers were also evaluated by radiation hybrid mapping.

Radiation Hybrid Mapping

Radiation hybrid (RH) mapping is another technique with which to order DNA markers with respect to one another on a mouse chromosome. X-ray fragmented mouse genomic DNA (129aa) is recovered in hamster (A23) cells to produce hybrid clones. Approximately 100 clones are developed that represent the whole-mouse genome. These clones are analyzed by PCR to determine the presence or absence of specific mouse DNA markers (45). DNA from each of 100 hybrid clones from the mouse T31 radiation hybrid panel (Research Genetics, Huntsville, AL) was used for construction of a radiation hybrid map of mouse Chromosome 10 (149). PCR amplification was performed under standard conditions with 2X PCR buffer (3 mM $MgCl_2$, 20 mM Tris-HCl, pH 8.3, 100 mM KCl, 32 μ g/ml BSA, 400 μ M of each dNTP), 0.25 μ l 10 μ M each primer, 1 μ l Taq DNA polymerase (5 U/ μ l), 25 ng of DNA (55). A 30 μ l PCR reaction was amplified at 97°C for 2 minutes; 35 cycles of 95°C for 30 seconds, the appropriate annealing temperature for a given primer set for 1 minute, 72°C for 1

minute; and a final extension step of 72°C for 7 minutes. Amplification products were separated on 3% agarose gels containing 0.5 µg/ml ethidium bromide, in 1X TAE at 100 V for 30 minutes.

For each locus, the 100 cell lines were typed for the presence or absence of a mouse-specific amplification product. Every locus was independently typed a minimum of three times in each cell line. Data for each locus was combined and analyzed with other loci using the computer analysis software RHMAP (20). The primer sequences for all *D10Mit* markers and *M-02039* were obtained and are available at <http://www-genome.wi.mit.edu>. The primer sequences of all other typed loci are in Appendix C. All primers used for RH analysis were synthesized by the Marshall University DNA Core Facility, Huntington, WV.

BAC Overlap Estimation

Nucleotide sequence overlap between BAC clones was assessed by determining common markers and by comparing BAC *Hind* III and *EcoR* I (New England BioLabs, Inc., Beverly, MA) restriction digestion patterns analyzed by gel electrophoresis on 1% agarose gels separated in 1X TBE overnight at 20 V. Gels were stained with 0.5 µg/ml ethidium bromide. Gel images were captured using the Gel Doc Imaging System (Bio-Rad, Hercules, CA).

DNA Sequencing

In order to identify potential gene candidates for the *jcpk* gene, six BACs between the genetic markers *D10Mit115* and *282P18T7* (RP23-310N21, RP23-395K5, RP23-337L15, RP23-440N1, RP23-348F2, and RP23-282P18) were chosen and sequenced in their entirety as part of the NHGRI BAC sequencing program. Sequences were analyzed using a number of gene identification programs including GrailEXP v3.2 (<http://compbio.ornl.gov>), GENSCAN (<http://genes.mit.edu/GENSCAN.html>) and Ensembl (www.ensembl.org). Genomic DNA and cDNA sequence analysis of the *Bicc1* gene in wild type strains B6, 101RI, and DBA/2J as well as in the mutant *jcpk* strain was performed

at Marshall University, Huntington, WV. Primers used for sequence analysis can be found in Appendix D. All primers were synthesized by the Marshall University DNA Core Facility, Huntington, WV.

Ensembl was used to obtain additional information on *Bicc1* and its intron/exon structure. Sequence homology between mouse and human sequences was determined by comparing both the mouse and human chromosome sequence databases (www.ncbi.nih.gov) using the Basic Local Alignment Search Tool (BLAST) (5).

Gene Identification

EST Candidate Analysis

A number of expressed sequence tags (ESTs) were evaluated as possible candidates for the *jcpk* gene. EST clones have been designated by GenBank accession numbers. I.M.A.G.E clones were obtained from Research Genetics, Huntsville, AL. Several ESTs were identified by BLAST analysis of BAC end sequences obtained from the TIGR annotation database (<http://www.tigr.org>). EST-specific PCR primers were designed using the available sequence information. All primers were synthesized by the Marshall University DNA Core Facility, Huntington, WV. Slot blot analysis was performed as previously described using nylon membranes containing purified BAC DNA and radioactively labeled EST-specific PCR products as probes to determine the position of the ESTs within the *jcpk* critical region.

ESTs determined to be within the *jcpk* critical region were further analyzed by Northern blot analysis. Total RNA from the kidneys and livers of normal adult B6 and 7-day old *jcpk/jcpk* animals was isolated using the RNeasy kit with on-column DNase I digestion (QIAGEN, Inc., Valencia, CA) or by using Trizol Reagent (Invitrogen, Carlsbad, CA). Briefly, 50-100 mg of frozen tissue was homogenized on ice in 1 ml of Trizol Reagent. The sample was incubated at room temperature for 5 minutes to completely dissociate nucleoprotein complexes. Two hundred microliters of chloroform was added and the tubes were vortexed for 15 seconds and incubated at room temperature again for 2-3 minutes. Samples were centrifuged at 12,000 x g for 15 minutes at 4°C.

Following centrifugation, the aqueous layer was removed and the RNA was precipitated by the addition of 500 µl isopropanol. Samples were incubated on ice for 10 minutes and the samples were centrifuged at 12,000 x g for 10 minutes at 4°C. The RNA pellet was washed with cold 75% ethanol and collected by centrifugation at 12,000 x g for 5 minutes at 4°C. The pellet was dried and resuspended in 100 µl of nuclease-free water (Ambion, Austin, TX). Genomic DNA contamination was removed using the DNA-free kit (Ambion,

Austin, TX). Northern blots were prepared with 20-30 µg of total RNA on Hybond N+ membranes (Amersham Biosciences, Piscataway, NJ) using a standard protocol for Northern analysis (70). RNA was separated on a denaturing formaldehyde 1% agarose gel in 1X MOPS/EDTA buffer at room temperature overnight at 20 V. Probes were made by isolating plasmid inserts from I.M.A.G.E. clones by restriction enzyme digestion. Products of the restriction digestions were separated on 1% agarose gels containing 0.5 µg/ml ethidium bromide, in 1X TAE at 100 V for 30 minutes. The isolated I.M.A.G.E. clone inserts were cut from the gel and purified using the Gel Extraction Purification Kit (QIAGEN, Inc., Valencia, CA). The concentration of the plasmid inserts was estimated by agarose gel electrophoresis and comparison with a low mass ladder (Invitrogen, Carlsbad, CA).

Radioactive probes were prepared by labeling 100 ng of purified insert with α -[32 P]dCTP for 2 hours using the Random Primers DNA Labeling System (Invitrogen, Carlsbad, CA). Unincorporated radionucleotides were removed using NICK™ columns (Amersham Biosciences, Piscataway, NJ). Blots were placed in hybridization buffer (50% formamide, 10% 50X Denhardt's solution, 10% 20X SSC, 10% Dextran SO₄, 0.5% SDS) and pre-hybridized at 42°C for 1 hour. Probes were boiled with 1 mg of salmon sperm DNA solution (Invitrogen, Carlsbad, CA) for 10 minutes. The denatured probes were added to the blots and hybridized at 42°C overnight with constant rotation in a hybridization oven. Northern blots were washed two times in 2X SSC, 0.1% SDS at 55°C for 15 minutes and one time in 0.1X SSC, 0.1% SDS at 55°C for 15 minutes. Blots were wrapped in clear plastic wrap and exposed to X-ray film at -80°C for 1-4 days with an intensifying screen.

ESTs localized to the region of mouse Chromosome 10 between *D10Mit115* and *D10Mit173* were also mapped in a standard PCR reaction using a panel of purified BAC DNAs covering the entire critical region. A 30 µl PCR reaction containing 2X PCR buffer (3 mM MgCl₂, 20 mM Tris-HCl, pH 8.3, 100 mM KCl, 32 µg/ml BSA, 400 µM of each dNTP), 0.25 µl 10 µM each primer, 1 µl Taq DNA polymerase (5 U/µl), and 100 ng of DNA was amplified under the

following conditions: 97°C for 2 minutes; 35 cycles of 95°C for 30 seconds, the primer-specific annealing temperature for 30 seconds, and 72°C for 30 seconds; with a final extension of 72°C for ten minutes. Amplification products were separated on 1% agarose gels containing 0.5 µg/ml ethidium bromide, in 1X TAE at 100 V for 30 minutes.

All primers were synthesized by the Marshall University DNA Core Facility, Huntington, WV. The following primers were used for PCR:

AW260721 (I.M.A.G.E. 23316553)

F: 5'CCAACTACGACAGAGGAAATGGA3'

R: 5'CCTTCTGAAACTTCTTAGTCCTGTTGA3';

BB498314

F: 5'TTGGGGTCCACATTCAGTCA3'

R: 5'TGATGCTATTGGGGAGACTGG3';

AI956350 (I.M.A.G.E. 2136285)

F: 5'TTGCCAATGACTGTTCGTGG3'

R: 5'TCCTTGATGGAAGGCTGCAT3';

AA674570 (I.M.A.G.E. 1003910)

F: 5'CTTTGGCAGAAGGGGTGAGC3'

R: 5'GCCAGGCTACAGTTACAGCTCC3'.

Southern Blot

ESTs were also mapped by Southern blot analysis. Amplification products from PCR using the above primer sets were radioactively labeled with the Random Primers Labeling System (Invitrogen, Carlsbad, CA) and used to probe nylon membranes containing purified BAC DNA digested with the restriction enzymes *Hind* III or *EcoR* I (New England BioLabs, Beverly, MA). Blots were hybridized at 42°C overnight in hybridization buffer (50% formamide, 10% 50X Denhardt's solution, 10% 20X SSC, 10% Dextran SO₄, 0.5% SDS) and washed with 2X SSC, 0.1% SDS at 55°C for 15 minutes then 0.1X SSC, 0.1% SDS at 55°C for 10 minutes. Blots were placed in plastic bags and exposed to X-ray film overnight at -80°C with an intensifying screen.

Mutation Detection

RT-PCR analysis to determine if mutations exist in the coding region of *Bicc1* was performed using the Superscript One-Step RT-PCR System (Invitrogen, Carlsbad, CA) with 0.25 µl 10 µM each primer and 500 ng of purified total RNA from 101/RI (+/+), +/*jcpk*, and *jcpk/jcpk* mouse kidneys under the following conditions: 45°C for 30 minutes, 94°C for 2 minutes; 40 cycles of 94°C for 30 sec, 64°C for 45 sec, 72°C for 1 minute; and 72°C for 10 minutes. The following primers were used:

F: 5'CTCCGAGGACGATCTGGTGG3'

R: 5'TCTGGGAAGTGGATGTGGCA3'.

Primers were synthesized by the Marshall University DNA Core Facility, Huntington, WV. Amplification products were separated on a 2% NuSieve (FMC Corporation, Philadelphia, PA) gel containing 0.5 µg/ml ethidium bromide, in 1X TAE at 80 V for 45 minutes. Images were captured on the GelDoc Imaging System (Bio-Rad, Hercules, CA).

Reverse Transcription

A 20 µl reverse transcription reaction was performed with 2.0 µg of total mouse kidney RNA extracted from 4-day old mice along and 1 µl of 100 uM random hexamers (MU DNA Core Facility, Huntington, WV), and 1 µl of 10 mM dNTP mix (Sigma-Aldrich, St. Louis, MO). The mixture was heated to 65°C for 5 minutes and then placed on ice. To the tube, 4 µl of 5X First Strand Buffer (Invitrogen, Carlsbad, CA), 2 µl of 0.1 M DTT, and 1 µl of RNaseOUT Recombinant Ribonuclease Inhibitor (40U/µl) (Invitrogen, Carlsbad, CA) were added and the reaction was incubated at 25°C for 10 minutes, and then at 37°C for 2 minutes. One microliter of M-MLV Reverse Transcriptase (200 U/µl) (Invitrogen, Carlsbad, CA) was then added and the mixture was incubated at 37°C for 50 minutes and finally 70°C for 15 minutes.

Alternative Transcripts

For the detection of alternative transcripts for *Bicc1* in mouse ESTs and mouse kidney cDNA, the following primers were used:

F: 5'GTGCCCCGAAGGAAAATGCTG3'

R: 5'GCAGGCGAGTGCAAGTGAAGA3'.

Primers were synthesized by the Marshall University DNA Core Facility. The following ESTs were used in the PCR analysis in order to determine if alternative transcripts exist: AW240366 (I.M.A.G.E. 2655954), BF785275 (I.M.A.G.E. 4236691) and AI595208 (I.M.A.G.E. 493392). A 30 μ l PCR reaction containing 2X PCR buffer (3 mM $MgCl_2$, 20 mM Tris-HCl, pH 8.3, 100 mM KCl, 32 μ g/ml BSA, 400 μ M of each dNTP), 0.25 μ l 10 μ M each primer, 1 μ l Taq DNA polymerase (5 U/ μ l), and either 50 ng of purified plasmid DNA or 5 μ l of cDNA (as described in *Reverse Transcription*) was amplified under the following conditions: 35 cycles of 97°C for 2 minutes, 97°C for 30 seconds, 60°C for 30 seconds, and 72°C for 30 seconds; with a final extension of 72°C for 10 minutes. Amplification products were separated on 2% NuSieve (FMC Corporation, Philadelphia, PA) agarose gels containing 0.5 μ g/ml ethidium bromide, in 1X TAE at 80 V for 45 minutes.

Determination of alternative transcripts for *Bicc1* was also performed by RT-PCR analysis using the above primers and the Superscript™ One-Step RT-PCR kit (Invitrogen, Carlsbad, CA). Total RNA was extracted from adult mouse brain, testis, liver, kidney and 7-day old *jcpk/jcpk* kidney, and amplified under the following conditions: 45°C for 30 minutes, 94°C for 2 minutes; 40 cycles of 94°C for 30 seconds, 60°C for 45 seconds, and 72°C for 1 minute; and a final extension of 72°C for 10 minutes. Amplification products were separated on 2-2.5% agarose gels containing 0.5 μ g/ml ethidium bromide in 1X TAE at 80 V for 45 minutes. Images were captured using the GelDoc Imaging System (Bio-Rad, Hercules, CA).

RNA Analysis

Northern Blot Analysis

To determine the size and tissue expression of *Bicc1* mRNA, prefabricated Northern blots were commercially obtained (CLONTECH, Palo Alto, CA) and hybridized with the full-length insert of AW240366 (I.M.A.G.E clone 2655954). The Northern blots contained purified poly A⁺ RNA from various mouse tissues that was separated on a denaturing formaldehyde 1.0% agarose gel, transferred to a nylon membrane and fixed with UV irradiation. The isolated cDNA insert from AW240366 was radioactively labeled using the Random Primers Labeling System (Invitrogen, Carlsbad, CA). Unincorporated nucleotides were removed using NICK™ columns (Amersham Biosciences, Piscataway, NJ). Northern blots were hybridized using ExpressHyb™ (CLONTECH, Palo Alto, CA) according to the manufacturer's instructions.

RT-PCR Analysis

Embryonic expression of *Bicc1* was determined by RT-PCR analysis using the following primers:

F: 5'CAGGAAGAACTCGAGGCCA3'

R: 5'AATGTGGCCTGGGCAGTAGA3'.

Primers were synthesized by the Marshall University DNA Core Facility, Huntington, WV. RT-PCR analysis was performed using the Superscript™ One-Step RT-PCR System (Invitrogen, Carlsbad, CA) with 0.25 µl 10 µM each primer and 100 ng of purified total RNA from adult mouse or whole embryos at embryonic days 5 and 10. Amplification proceeded under the following conditions: 45°C for 30 minutes, 94°C for 2 minutes; 40 cycles of 94°C for 15 sec, 59°C for 30 sec, 72°C for 2 minutes; and a final extension of 72°C for 10 minutes. Amplification products were separated on a 2% agarose gel containing 0.5 µg/ml ethidium bromide in 1X TAE buffer at 100 V for 30 minutes. Images were captured on the GelDoc Imaging System (Bio-Rad, Hercules, CA).

Dot Blot Analysis

Dot blot analysis for embryonic expression of *Bicc1* was also performed using a commercially available dot blot containing poly A⁺ RNA extracted from 7-day, 11-day, 15-day and 17-day mouse embryos (CLONTECH, Palo Alto, CA). The isolated insert from BF785275 (I.M.A.G.E. clone 4236691) was radioactively labeled using the Random Primers Labeling System (Invitrogen, Carlsbad, CA). Unincorporated nucleotides were removed using NICK[™] columns (Amersham Biosciences, Piscataway, CA). The slot blot was hybridized using ExpressHyb[™] (CLONTECH, Palo Alto, CA) according to the manufacturer's indications. Images were collected using the Typhoon 8600 Image Capture System (Amersham Biosciences, Piscataway, NJ). Densitometry analysis was performed using ImageQUANT software (Visual Molecular Dynamics, Urbana, IL).

Real-time PCR

Expression of *Bicc1* in 101/RI and *jcpk/jcpk* kidney tissues was determined by real-time PCR analysis with TaqMan[™] (Applied Biosystems, Foster City, CA) amplification detection. The following primers were designed for amplification:

F: 5'GTTACCGATTGCCGGGATT3'

R: 5'GTTTGTGAGATGTGCTGAATGGA3'.

Primers were synthesized by the Marshall University DNA Core Facility, Huntington, WV. A single Taqman[™] probe was designed, 5'FAM-TCCAGCCAGTCCCCGATCCCA-TAMRA3', with 6-FAM at the 5' end and TAMRA at the 3' end in order to detect amplicon quantity on the iCycler[™] Real-time PCR system (Bio-Rad, Hercules, CA). The following conditions were used in a standard 30 µl PCR reaction containing 100 nM of each primer, 200 nM of the fluorescent probe, 3.0 mM MgCl₂, 300 uM dNTP mix (Sigma-Aldrich, St. Louis, MO), 10X PCR Reaction Buffer (Applied Biosystems, Foster City, CA), 1 µl Taq DNA polymerase (5U/µl) and 2 µl of normal or *jcpk/jcpk* kidney cDNA (as described in *Reverse Transcription*): 95°C for 5 minutes; 40 cycles of 95°C for 15

seconds and 57°C for 1 minute. No extension step was included and optical data was taken at the 57°C annealing step. Four replicates of each sample were included and the entire amplification procedure was repeated in triplicate. Eight different standards were included in triplicate representing 10^2 to 10^9 DNA molecules per reaction tube. These standards were serial dilutions of a known amount of the 3 kb cDNA insert of AW240366 and were amplified along with the experimental tubes. Data was analyzed using SigmaPlot statistical software (SSPS Inc., Chicago, IL).

Real-time PCR with SYBR Green (FMC Corporation, Philadelphia, PA) was used to compare *Bicc1* mRNA expression in age-matched BALB/c and *bpk/bpk* kidneys. The following primers were used in the analysis:

F: 5'CAAGCGGCAGACGGTTGAGC3'

R: 5'GGACATATGTTGGCTGCGAGGC3'.

Primers were synthesized by the Marshall University DNA Core Facility, Huntington, WV. The following conditions were used in a 30 μ l PCR reaction containing 100 nM of each primer, 3.0 mM $MgCl_2$, 300 μ M dNTP mix (Sigma-Aldrich, St. Louis, MO), 2 μ l of cDNA (as described in *Reverse Transcription*), 1 μ l Taq DNA polymerase (5U/ μ l) and 2 μ l of SYBR Green (1:10,000 stock) at a 1:20,000 dilution: 95°C for 5 minutes; 40 cycles of 95°C for 30 seconds, 65°C for 30 seconds and 72°C for 1 minute. Optical data were taken at the 72°C extension step. Four replicates of each sample were included and the entire amplification procedure was repeated in duplicate. Eight different standards were included in duplicate representing 10^2 to 10^9 DNA molecules per reaction tube. These standards were serial dilutions of the quantified gel-extracted PCR product for the particular gene analyzed. This product was used as a template and amplified along with the experimental tubes. Data was analyzed using SigmaPlot statistical software (SSPS Inc., Chicago, IL).

Real-time PCR analysis of *Egfr*, *Egf* and *Tgf- α* mRNA expression was performed as described above with the following primers:

Egfr

F: 5' TGCCAGAAATTGACCAAAT3'

R: 5' CTTCTAGTAGTCAGGCCCA3';

Egf

F: 5'AAACCAGGCTGATGATGGTA3'

R: 5'ACCGTCCAGTGAAGAAGACA3';

Tgf-α

F: 5'TAGCGCTGGGTATCCTGTTA3'

R: 5'ACACATGCTGGCTTCTCTTC3'.

Primers were synthesized by the Marshall University DNA Core Facility, Huntington, WV. Tissues used for this analysis were age-matched progeny from *+jcpk* X *+jcpk* crosses. Real-time PCR analysis with SYBR Green (FMC Corporation, Philadelphia, PA) was used to compare gene expression of *Egfr*, *Egf*, and *Tgf-α* in age-matched *+/+*, *+jcpk* and *jcpk/jcpk* kidneys. The following conditions were used in a standard 30 µl PCR reaction containing 100 nM of each primer, 3.0 mM MgCl₂, 300 uM dNTP mix (Sigma-Aldrich, St. Louis, MO), 1 µl Taq DNA polymerase (5U/µl), 2 µl of cDNA and 2 µl of SYBR Green (1:10,000 stock) at a 1:20,000 dilution: 95°C for 5 minutes; 40 cycles of 95°C for 30 seconds, 65°C for 30 seconds and 72°C for 1 minute. Optical data were taken at the 72°C extension step. Four or five replicates of each sample were included and the entire amplification procedure was repeated in duplicate or triplicate. Eight different standards were included in duplicate or triplicate. These standards were serial dilutions of the quantified gel extracted PCR product depending on the gene analyzed and used as an indicator of DNA copy number. This product was used as a template and amplified along with the experimental tubes. Data was analyzed using SigmaPlot statistical software (SSPS Inc., Chicago, IL). For real-time characterization of expression of other PKD-causing genes, the following primers were used:

Pkd1

F: 5'TATAGCTGGACAGCGCAGCA3'

R: 5'CAGGCCAGGTGTAGCAAAGG3';

Pkd2

F: 5'CCATGAGCCAGCTCTCCACAA3'

R: 5'GGCCCCAAACTCGGTTAGC3';

cpk (Cys1)

F: 5'ACGCCTGCTGGATCAGTTGC3'
R: 5'TGCTCGCCATGAGCTCCTCT3';

Invs

F: 5'CCTGCCAGCCTGGTGTTTAG3'
R: 5'TGTGGCCTGGTCACCAAGTA3';

orpk (Tg737)

F: 5'TCCTGGTGAGACAACGAGAGC3'
R: 5'CCGATCTCCAATGGCAAAAC3';

jck (Nek8)

F: 5'GTCCCCTGAGGTTGCCAATG3'
R: 5'AATGGTGGGCTGGCTGATGT3';

kat (Nek1)

F: 5'TGGGACAGTGCAGCTTGGAGA3'
R: 5'TGAGACAGCAAGCTGCGGAGA3'.

Primers were synthesized by the Marshall University DNA Core Facility, Huntington, WV. Reaction components and amplification were the same as described previously.

Microarray

For microarray analysis, two sets of frozen kidney tissues: three 8-day old B6 kidneys and one 8-day *jcpk/jcpk* kidney were sent to CLONTECH Laboratories (Mt. View, CA) and used to identify differences in gene expression between B6 and *jcpk/jcpk* kidneys. The Atlas Mouse 1.2 Microarray used contained over 1,176 different genes (CLONTECH, Mt. View, CA).

Alterations in gene expression detected by microarray were confirmed by real-time PCR analysis using SYBR Green (Sigma-Aldrich, St. Louis, MO) as a fluorescent indicator of product amplification. The following conditions were used in a standard 30 µl PCR reaction containing 100 nM of each primer, 3.0-4.0 mM MgCl₂, 1 µl Taq DNA polymerase (5U/µl), 300 uM dNTP mix (Sigma-Aldrich, St. Louis, MO), 2 µl of cDNA and 2 µl of SYBR Green (1:10,000 stock) at a 1:20,000 dilution: 95°C for 5 minutes; 40 cycles of 95°C for 30 seconds, the appropriate

annealing temperature for 30 seconds and 72°C for 1 minute. Optical data were taken at the 72°C extension step. Four replicates of each sample were included and the entire amplification procedure was repeated in duplicate. Eight different standards were included in duplicate. These standards were serial dilutions of quantified gel extracted PCR product. This product was used as a template and amplified along with the experimental tubes and represented DNA copy number. Data was analyzed using SigmaPlot statistical software (SSPS Inc., Chicago, IL). The primers used for real-time analysis are as follows:

ErbB2 (L47239)

F: 5'ATGATGACATGGGGGAGCTG3'

R: 5'GCAGTCCTTTGGTTACCCCC3';

Pax2 (X55781)

F: 5'CTCAGGCAACCCATACAGCCR'

R: 5'CGACAGGGTGATGAGAAGGG3'.

Primers were synthesized by the Marshall University DNA Core Facility, Huntington, WV.

Protein Analysis

Protein Isoform Characterization

In silico analysis was used to structurally characterize the various isoforms of the Bicc1 protein. These tools are located at www.expasy.org and include PeptideMass (207, 273) and EMBOSS (194, 195).

Antibody Production

In order to characterize the Bicc1 protein, an anti-Bicc1 polyclonal antibody was raised in rabbit against a recombinant fusion protein containing the first 81 amino acids of the mouse Bicc1 protein. A blunt-end 247 bp PCR product of the first two exons of the *Bicc1* gene was produced in a 50 µl PCR reaction containing 1 µl of *Pfx* DNA polymerase (Invitrogen, Carlsbad, CA), 100 ng of the purified plasmid AW240366, 1 mM MgSO₄, 10X *Pfx* Amplification Buffer (Invitrogen, Carlsbad, CA), 0.3 µM each primer, and 0.3 mM each dNTP. Primers used to generate the construct from the template are as follows:

F: 5'CACCATGGCCTCGCAGAGC3'

R: 5'CTTCTGAAAAAAGTCTTCCCC3'.

Primers were synthesized by the Marshall University DNA Core Facility, Huntington, WV. PCR was performed under the following conditions: 2 minutes at 94°C and 35 cycles of 94°C for 15 s, 55°C for 30 s, and 68°C for 3 minutes. The PCR product that was produced was gel purified using the QIAGEN gel extraction kit (QIAGEN, Inc., Valencia, CA) and directionally ligated into the Champion™ pET101/D-TOPO expression vector (Invitrogen, Carlsbad, CA) containing both V5 and 6X Histidine epitopes. Plasmid ligation reactions were used to transform TOP10 chemically competent *E. coli* (Invitrogen, Carlsbad, CA) which were plated onto Luria-Bertani (LB) agarose plates containing 100 µg/ml of ampicillin (Fisher Scientific International, Hampton, NH). Isolated colonies were screened based on insert size which was determined by restriction digestion with *SacI* and *XbaI* (New England Biosystems Inc., Beverly, MA). Clones containing

the correct inserts were grown overnight and extracted with the QIAGEN Plasmid DNA extraction kit (QIAGEN, Inc., Valencia, CA). Sequence analysis of the isolated plasmid DNA was performed on an ABI 310 sequence analyzer (Applied Biosystems, Foster City, CA) using vector-specific primers to determine orientation of the insert. The following primers were used:

T7 Forward: 5'-TAATACGACTCACTATAGGG-3'
T7 Reverse: 5'-TAGTTATTGCTCAGCGGTGG-3.

Primers were synthesized by the Marshall University DNA Core Facility, Huntington, WV.

A recombinant plasmid containing an in-frame *Bicc1* insert was transformed into BL21 (DE3) chemically competent *E. coli* (Invitrogen, Carlsbad, CA) and grown overnight in 10 ml of Luria-Bertani (LB) media containing 100 µg/ml of ampicillin and 1% glucose at 37°C, 200 rpm on a rotating shaker. Three ml of the overnight culture were used to seed 250 ml of LB containing 100 µg/ml of ampicillin and 1% sterile glucose. Cultures were grown for two hours or until an A₆₀₀ of 0.4-0.6 was reached. Protein expression was induced with 1.0 M isopropyl-β-D-thiogalactoside (IPTG) (Fisher Scientific International, Hampton, NH) at a final concentration of 0.5 mM. Induced cultures were grown overnight and pelleted by centrifugation at 5,000 rpm for 15 minutes at 4°C. Cell pellets were resuspended in a volume of 5 ml/gram weight of pellet in denaturing lysis buffer (100 mM NaH₂PO₄, 10 mM Tris-Cl, 8M Urea, pH 8.0), sonicated on ice for 1 minute, and incubated on a rotating shaker at 4°C for 30 minutes. Lysates were sonicated again for 1 minute and incubated at 4°C for another 30 minutes with rotation. Lysates were then centrifuged at 4°C at 16,000 rpm for 20 minutes to produce a cleared cell lysate.

The cleared cell lysates were concentrated to a volume of approximately 5 ml using Centriprep-50 spin columns (Millipore, Billerica, MA). The cleared cell lysates were further purified by Ni⁺-NTA resin chromatography under denaturing conditions (QIAGEN, Inc., Valencia, CA). Proteins were eluted under low pH. Eluted protein was further purified using YM-10 Centricon centrifugal filter devices (Millipore, Billerica, MA). The Centricon devices were centrifuged at

5,000 rpm for 1.5 hours at 10°C in a fixed angle rotor. Complete protease inhibitor (Roche, Indianapolis, IN) was then added to the concentrated proteins at a concentration of 1 tablet per 50 ml of elution buffer.

Eluted proteins were separated on 15% SDS-PAGE gels at 200 V for 45 minutes in 10X SDS PAGE running buffer. Gels were then stained with the GelCode® E-Zinc™ Reversible Stain kit (Pierce Biotechnology, Inc., Rockford, IL) and the 18 kDa Bicc1 fusion protein was cut from the gel. Gel fragments were de-stained with GelCode® E-Zinc™ Eraser (Pierce Biotechnology, Inc., Rockford, IL) and electro-eluted in volatile elution buffer (50 mM ammonium bicarbonate, 0.1% SDS) at 15 V for 6 hours. The concentration of the eluted fusion protein was determined by the BCA assay (Sigma-Aldrich, St. Louis, MO). Purified, concentrated fusion protein was sent to a commercial facility for polyclonal Bicc1 antibody production (Covance, Inc., Princeton, NJ).

Total Protein Isolation

In order to determine the expression of the Bicc1 protein, total protein was isolated from whole organs that had been snap frozen in liquid nitrogen and stored at -80°C. Frozen organs were placed in 300 ul of ice cold RIPA buffer (150 mM NaCl, 1% NP-40, 0.5% sodium deoxycholate, 0.1% SDS, 50mM Tris, and 10mM EDTA) containing 1 µl of a complete protease inhibitor solution made by dissolving one complete protease inhibitor tablet (Roche, Indianapolis, IN) in 25 ml of RIPA buffer. Tissue was ground using a motorized homogenizer (Ultra-Turrax, Fisher Scientific International, Hampton, NH) for 30 seconds and then placed on ice. Keeping the sample on ice, the tissue sample was sonicated at intensity level six with two or three 10-15 second bursts for a total of 30 seconds using the Misonex 110VAC XL2000 Ultrasonic Cell Disruptor (Fisher Scientific International, Hampton, NH). The sample was then incubated on ice for 15 minutes. The sample was sonicated again for 30 seconds and placed on ice for another 30 minutes. The sample was then centrifuged for 10 minutes at 15,000 rpm at 4°C. The supernatant was transferred to a new tube and treated with

DNase I (10U) (QIAGEN, Inc., Valencia, CA) and RNase A with a final concentration of 40 µg/ml (Sigma-Aldrich, St. Louis, MO) for 15 minutes at room temperature. Protein concentration was determined using the BCA assay (Sigma-Aldrich, St. Louis, MO).

Western Blot (Immunoblot) Analysis

Protein-containing lysates were resolved on sodium dodecyl sulfate (SDS)-10% polyacrylamide gels and transferred to nitrocellulose membranes (Bio-Rad, Hercules, CA). Membranes were incubated in a blocking solution of 1X PBS (0.9% NaCl, 10 mM sodium phosphate, pH 7.4) and 5% nonfat milk overnight at 4°C. The membranes were then rinsed two times at room temperature for 15 minutes in blotting solution (PBS-0.5% nonfat milk), and then incubated with primary Bicc1 antibody in blotting solution overnight with continuous rotation at 4°C. The Bicc1 polyclonal primary antibody was used at a concentration of 1:40,000. Membranes were washed two times at room temperature for 15 minutes each in blotting solution. Bound antibody was detected with a horseradish peroxidase-conjugated anti-rabbit immunoglobulin G secondary antibody (Sigma-Aldrich, St. Louis, MO). The secondary antibody was used at a concentration of 1:40,000 for 1 hour in blotting solution with continuous rotation. The membranes were washed two times with blotting solution at room temperature for 15 minutes with continuous rotation. The protein bands were visualized on X-ray film by the enhanced chemiluminescence (ECL) Western blotting detection kit (Amersham Biosciences, Piscataway, NJ).

Multiple Sequence Analysis

The putative protein domains of the Bicc1 protein were identified using the web interface PROSITE (233). Protein characteristics were determined using ProtParam (134). Protein sequences for the multialignment analysis were retrieved from the NCBI protein database (208). GenBank accession numbers

for the multiple alignment analysis of Bicaudal-C are as follows: *Mus musculus* (NP_113574); *Homo sapiens* (human) (AC012168); *Rattus norvegicus* (rat) (XP342127); *Drosophila melanogaster* (fruitfly) (S55051); and *Xenopus laevis* (frog) (AAF69826); *Caenorhabditis elegans* (nematode) (NP_502067); *Caenorhabditis briggsae* (nematode) (CAE61995); *Danio rerio* (zebrafish) (ENSDDARP00000024970 at www.ensembl.org; *Fugu rubripes* (pufferfish) (Q99MQ1); and *Anopheles gambiae* (mosquito) (ENSANGP00000012257 at www.ensembl.org). Alignments were generated using the GeneStream alignment program (Multalign) (196).

RNA Binding Study

Generation of Recombinant Proteins

In order to determine the *in vitro* RNA binding ability of Bicc1, Bicc1 fusion proteins containing different combinations of Bicc1 protein structural domains were constructed as detailed in *Antibody Production*. The cDNA template used to generate the various PCR products was cDNA clone AW240366. Primers used to generate each plasmid construct containing both V5 and 6X Histidine epitopes are as follows:

Full-length (amino acids 1-934)

F: 5'CACCATGGCCTCGCAGAGC3'

R: 5'GAGATTGCCAGCAGCATTTTCCCT3';

Bicc1^{cpk} (amino acids 1-93)

F: 5'CACCATGGCCTCGCAGAGC3'

R: 5'CAGCACCAAAGGAAGCAGCTCCCG3';

KH1 (amino acids 1-132)

F: 5'CACCATGGCCTCGCAGAGC3'

R: 5'GCTTTTGTGTCTAAGACAGAC3';

KH2 (amino acids 125-209)

F: 5'CACCATGTCTGTCTTAGACACA3'

R: 5'CAGCACCAAAGGAAGCAGCTCCG3';

KH1+KH2 (amino acids 1-209)

F: 5'CACCATGGCCTCGCAGAGC3'

R: 5'CAGCACCAAAGGAAGCAGCTCCG3';

KH3 (amino acids 272-407)

F: 5'CACCATGCTGTTGGAACACCTT3'

R: 5'TAAGGCATTTGCTCAACACT3';

KH2+KH3 (amino acids 125-407)

F: 5'CACCATGTCTGTCTTAGACACA3'

R: 5'TAAGGCATTTGCTCAACACT3';

KH1+KH2+KH3 (amino acids 1-407)

F: 5'CACCATGGCCTCGCAGAGC3'

R: 5'TAAGGCATTTGCTCAACACT3'.

All primers were synthesized by the Marshall University DNA Core Facility, Huntington, WV. PCR products were gel extracted using the QIAGEN gel extraction kit (QIAGEN, Inc., Valencia, CA) and directionally cloned into the Champion™ pET101/D-TOPO expression vector, then transformed into TOP10 chemically competent *E. coli* (Invitrogen, Carlsbad, CA) as previously described in *Antibody Production*. Sequence analysis was performed on an ABI 310 sequence analyzer (Applied Biosystems, Foster City, CA) to determine orientation of the inserts. T7 forward and T7 reverse primers were used for sequence analysis. If the inserts were longer than 300 bp, nested primers were used for sequence analysis.

Recombinant Protein Expression

Isolated plasmids containing the correct in-frame insert were transformed into BL21 (DE3) chemically competent *E. coli* (Invitrogen, Carlsbad, CA) and induced with IPTG as previously described in the *Antibody Production* section with minor alterations in the methodology. Plasmids transformed in BL21 (DE3) cells were grown overnight in 20 ml of Luria-Bertani (LB) media plus 100 µg/ml ampicillin and 1% sterile glucose at 37°C, 200 rpm on a rotating shaker. Five ml of the overnight culture were used to seed 250 ml of LB containing 100 µg/ml ampicillin and 1% sterile glucose.

To determine protein expression, 10 µl of the cleared bacterial cell lysates were diluted in 10 µl of Laemmli sample buffer (Bio-Rad, Hercules, CA) and boiled for 5 minutes. The samples were then loaded onto SDS-PAGE gels (10, 12 or 15% depending on protein size) and the proteins were separated at 200 V for 45 minutes in 1X SDS PAGE running buffer. The separated proteins were immunoblotted onto nitrocellulose (Bio-Rad, Hercules, CA). Membranes were incubated in blocking solution overnight at 4°C with constant rotation. Membranes were rinsed two times at room temperature for 15 minutes in blotting solution. Membranes were then incubated in blotting solution with a horseradish peroxidase-conjugated monoclonal antibody specific to the V5 epitope present

on the fusion proteins derived from the pET101/D vector (Invitrogen, Carlsbad, CA). The anti-V5 antibody was used at a concentration of 1:5,000 with an overnight incubation at 4°C with constant rotation. Membranes were washed twice with blotting solution for 15 minutes at room temperature with continuous rotation on a Belly Dancer™ (Stovall, Greensboro, NC). Proteins were visualized on X-ray film using chemiluminescence (Amersham Biosciences, Piscataway, NJ).

RNA-binding Assays

Binding assays to determine the function of the Bicc1 protein KH domains, were performed with the concentrated cleared cell lysates for each recombinant protein. Briefly, 200 µl of cleared cell lysate was added to 40 µl of 10X RNA binding buffer (250 mM Tris-HCl, pH 7.4, 1.5 M NaCl, 10% Triton X-100, and complete protease inhibitor cocktail (Roche, Indianapolis, IN), 158 µl of nuclease-free water (Ambion, Inc., Austin, TX), 1 µl of RNaseOUT (Invitrogen, Carlsbad, CA), and 10 mg of beads. The beads that were used were either poly(U) Sepharose or Sepharose 4B (Sigma-Aldrich, St. Louis, MO). Reaction mixtures were incubated at 4°C with constant rocking. Beads were pelleted at 13,000 rpm for 2 minutes at 4°C and washed 3 times with cold 1X RNA binding buffer. Between each rinse, the beads were briefly vortexed and centrifuged at 13,000 rpm for 2 minutes. The proteins were separated from the beads by adding 25 µl of Laemmli sample buffer (Bio-Rad, Hercules, CA) and boiling for 5 minutes. Samples were then loaded onto SDS-PAGE gels (10, 12 or 15% depending on protein size) and the proteins were separated at 200 V for 45 minutes. The separated proteins were transferred onto nitrocellulose and immunoblotted with a horseradish peroxidase-tagged monoclonal primary antibody specific to the V5 epitope tag on the pET101/D-TOPO vector system (Invitrogen, Carlsbad, CA). The V5 antibody was used at a concentration of 1:5,000 with an overnight incubation at 4°C. Proteins were visualized using chemiluminescence (Amersham Biosciences, Piscataway, NJ).

Asymmetry Study

Anatomical Analysis

In order to determine whether left/right specification defects exist in *jcpk* homozygotes, mouse litters from *jcpk* heterozygous crosses were dissected 4-5 days after birth and observed for the presence of any anatomical defects in the major organ systems. Only litters containing a polycystic pup(s) were included in the study. A total of 149 mice were observed for the presence of L/R patterning defects. If patterning defects were present, the visceral organs were removed and preserved in 10% buffered formalin (Fisher Scientific International, Hampton, NH). If defects were found, the organs of the remaining littermates were also preserved in 10% buffered formalin for comparison. Defects were noted and catalogued. Many litters without defects were saved for later tissue analysis. These organs were snap frozen in liquid nitrogen and stored at -80°C.

CHAPTER IV

RESULTS

Genetic and Physical Mapping

High Resolution Genetic Mapping

Previously, a high resolution genetic map was generated by the integration of simple sequence length polymorphism (SSLP) markers and other genetic markers to localize the *jcpk* gene to a 1 cM region on mouse Chromosome 10 defined by the microsatellite markers *D10Mit115* and *D10Mit173* (28). During the course of the work described here, two different polymorphic markers within this region, *393H9SP6RPT* and *282P18T7RPT*, were identified by sequence analysis and were used in fine mapping studies to significantly narrow the original critical region (Figure 4.1). Both markers were found to contain a variable number of tandem repeats among different mouse strains. These markers were derived from the SP6 end of BAC RP23-393H9 and the T7 end of BAC RP23-282P18. Fine genetic mapping of these two loci was accomplished by genotyping using a mapping panel containing genomic DNA from *jcpk* intercross recombinant animals (28). Allele segregation of *393H9SP6RPT* and *282P18T7RPT* was compared to the strain distribution pattern of the known recombinants from the mapping panel in order to position these genetic markers within the genetic map. These two markers were found to be genetically informative and were thereafter used to define the boundaries of the minimal region thought to contain the *jcpk* gene (Figure 4.1).

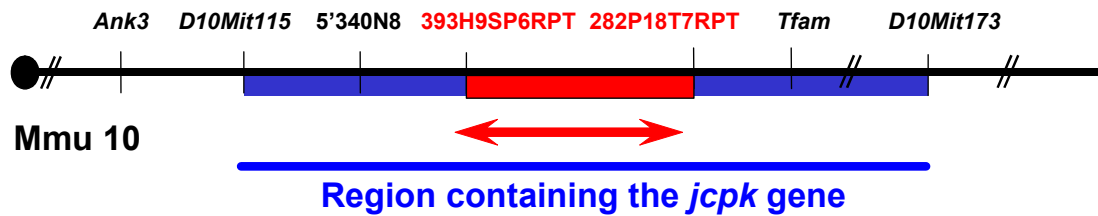
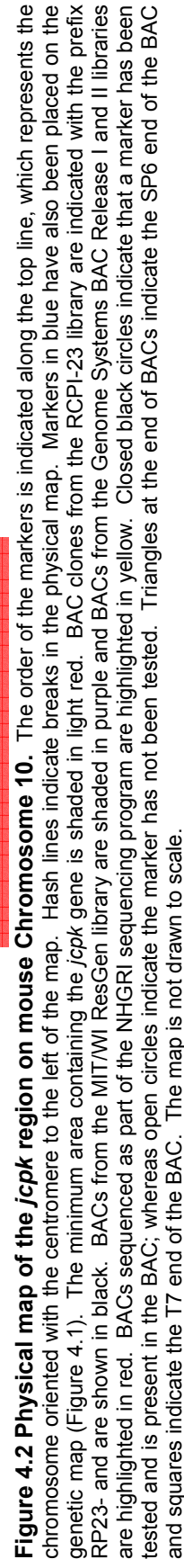


Figure 4.1 Genetic map of the 1-cM region containing the *jcpk* gene. This schematic represents mouse Chromosome (Mmu) 10 with the centromere (circle) on the left. Previously, the *jcpk* critical region was defined by the markers *D10Mit115* and *D10Mit173* (shown in blue) (28). SSLP analysis significantly narrowed this region to an area defined by the markers *393H9SP6RPT* and *282P18T7RPT* (shown in red). Other genetic markers are shown for reference. Hash marks indicate regions of the chromosome not shown.

Physical Mapping

A physical map representing the *jcpk* critical region on mouse Chromosome 10 defined by the genetic markers *D10Mit115* proximally and *D10Mit173* distally was constructed with 72 overlapping BACs (Figure 4.2). A majority of the BACs used to construct the physical map were isolated from the RCPI-23 (RP23) Mouse BAC Library which contains cloned genomic DNA from an adult B6 mouse. BACs from this library were isolated using a mapping approach known as multiplex oligonucleotide hybridization or “overgo” (32). The minimum tiling pattern covering the critical region defined by genetic marker *393H9SP6RPT* proximally and *282P18T7RPT* distally consists of four overlapping BACs (RP23-393H9, RP23-200D18, and RP23-282P18) (Figure 4.2). Six BACs between *D10Mit115* and *282P18T7RPT* (RP23-310N21, RP23-395K5, RP23-337L15, RP23-440N1, RP23-348F2, and RP23-282P18) (Figure 4.3) were sequenced in their entirety as part of the NHGRI BAC sequencing program. Restriction endonuclease digestion with either *EcoR* I or *Hind* III has indicated that the BACs in this region share considerable overlap (Figure 4.4 and Figure 4.5). This overlap is determined qualitatively by observing the number of restriction fragments that each BAC shares with another BAC. If two BACs contain a number of shared restriction fragments it is likely that these two BACs overlap and therefore contain identical sequence within that region.



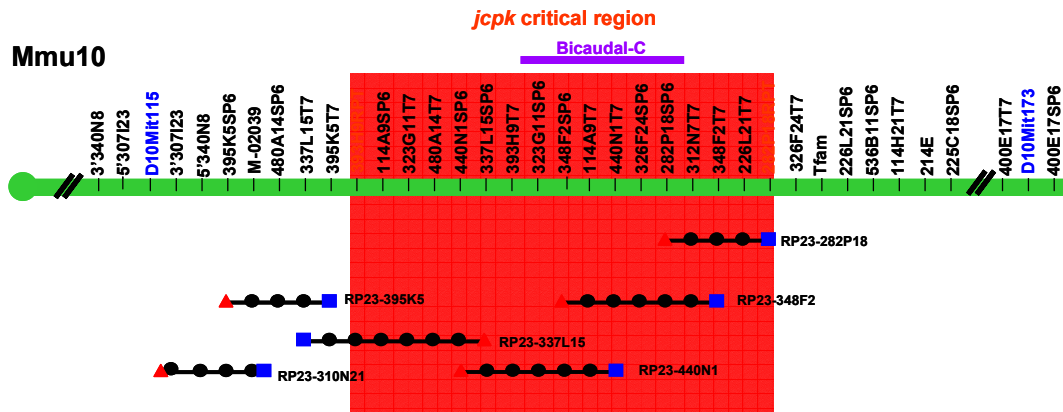


Figure 4.3 Minimum BAC tiling pattern covering the *jcpk* critical region. The order of the markers is indicated along the top line, which represents the chromosome oriented with the centromere to the left of the map. Hash lines indicate breaks in the physical map. Markers in blue have also been placed on the genetic map (Figure 4.1). The minimum area containing the *jcpk* gene is shaded in red. Six BACs were selected for sequence analysis as shown above.

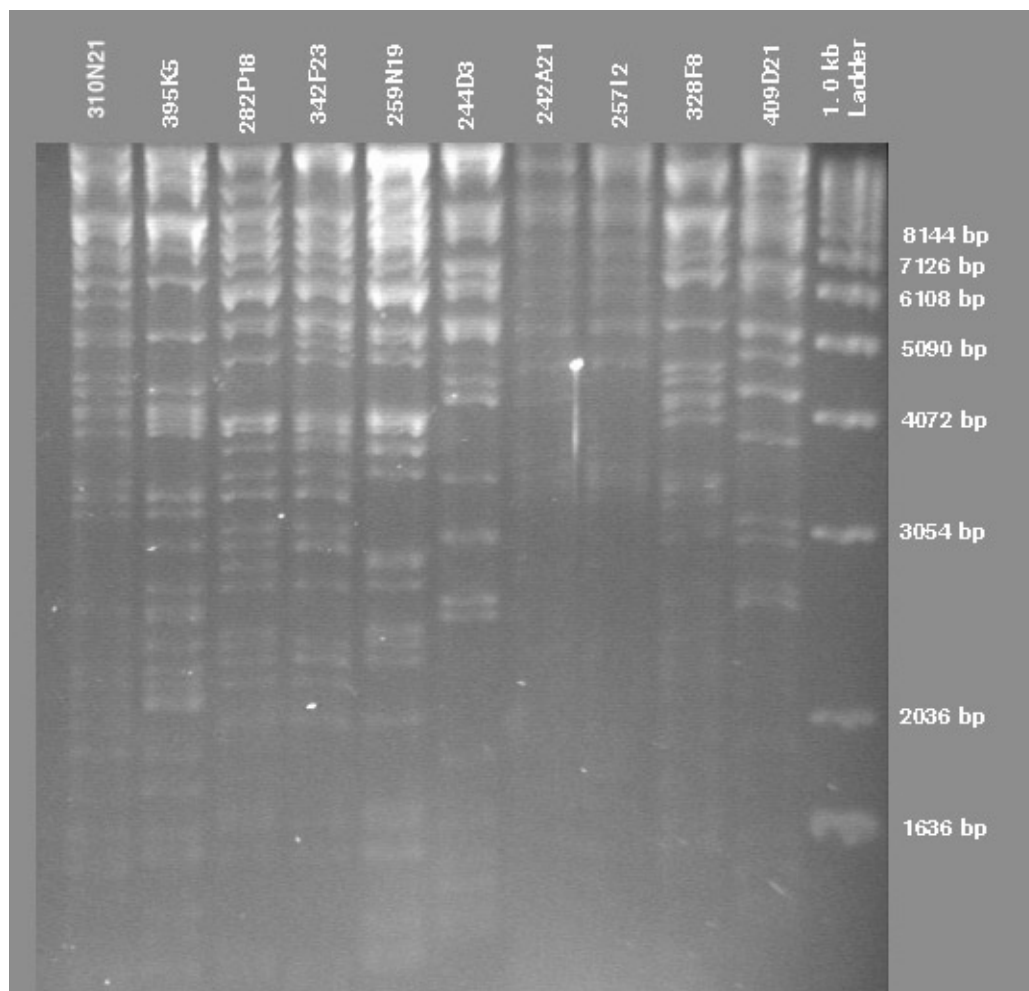


Figure 4.4 *EcoR* I restriction digestion of BACs within the physical map. *EcoR* I digestion of selected BACs within the physical map. Note the number of restriction fragments each BAC shares in common with other BACs within the physical map. A molecular size standard is present in the last lane on the right with the sizes of each fragment indicated in base pairs (bp).

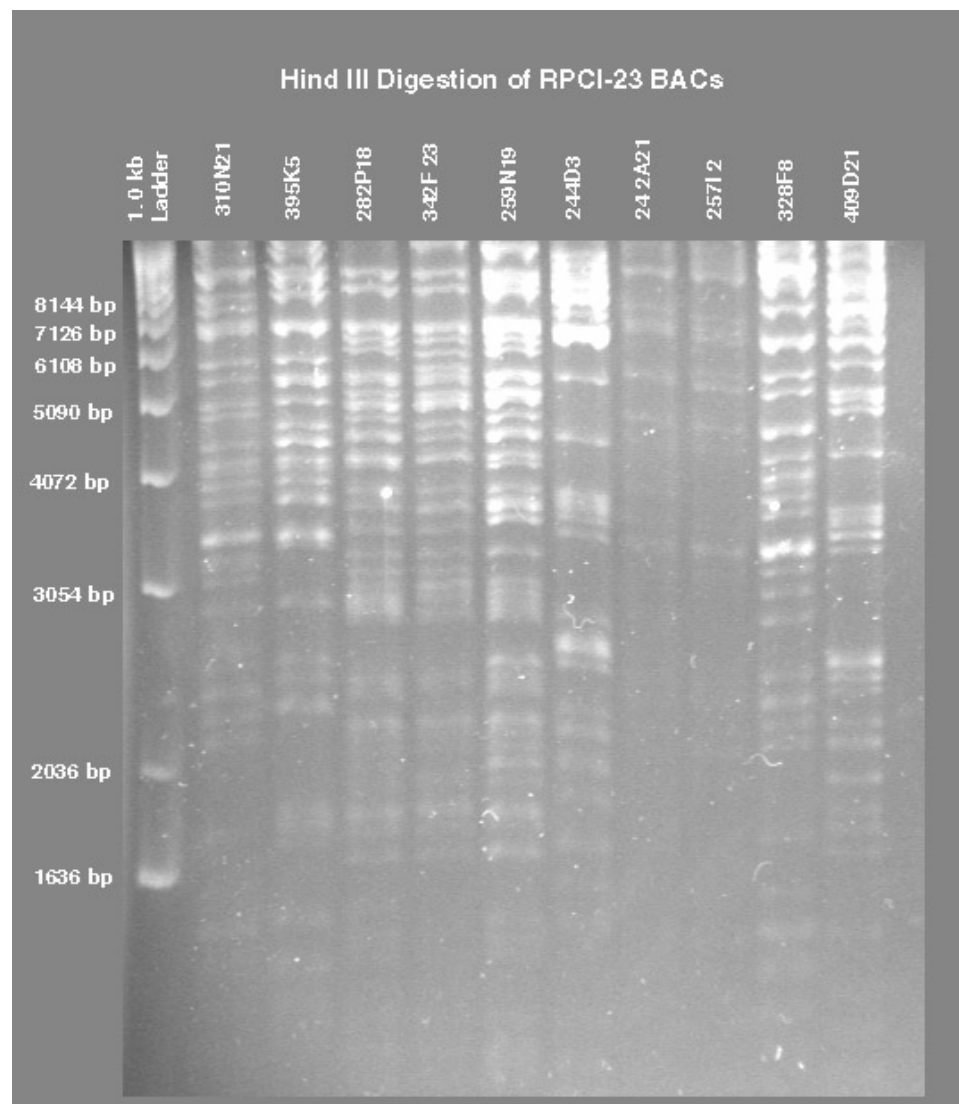


Figure 4.5 *Hind* III restriction digestion of selected BACs. Restriction digestion of *Hind* III of selected BACs within the physical map. Note the number of genomic DNA fragments that each shares in common with the other BACs. A molecular size standard is included in the first lane on the left with the sizes indicated in base pairs (bp) for each fragment.

Radiation Hybrid Mapping

To complement physical mapping strategies to positionally clone the *jcpk* gene, radiation hybrid (RH) mapping was employed to quickly order genetic markers along mouse Chromosome 10. The commercially available radiation hybrid panel (T31) used in our study was created by exposure of mouse cells to a high dose of X-ray irradiation in order to break mouse (strain 129aa) chromosomes into several fragments. These broken chromosomal fragments were recovered in hamster (strain A23) cells, and the resulting 100 mouse-hamster hybrid clones are available for analysis by a standard PCR assay to determine the presence or absence of specific mouse DNA markers. The whole genome mouse T31 radiation hybrid panel was used in this study because it offers high resolution in that it has roughly 20-fold as many chromosomal breaks as there would be crossovers in a similar number of mice (221). By estimating the frequency of breakage, and thus the distance between markers, it is possible to determine marker order in a manner analogous to meiotic mapping (45).

RH mapping data were submitted to the interactive auto RHMAPPER v1.22 software program available at <http://www.genome.wi.mit.edu/ftp/pub/software/rhmapper/> (241). This computer program compares the generated data with data from over 14,163 loci that has served as the basis of an RH map of the entire mouse genome. Multipoint analysis was performed using the software program RHMAP (20). This software program not only evaluates the linkage of a particular marker to its nearest neighbor but its linkage to all other markers within the data set.

Twenty-two *D10Mit* markers were used to construct the initial framework RH map of mouse Chromosome 10. Additional mapped markers were derived from nine BAC sequences, six expressed sequence tags (ESTs), six genes and one anonymous marker (Figure 4.6). Sixteen of the *D10Mit* markers have also been mapped by others and appear in The Jackson Laboratory T31 Mouse Radiation Hybrid Database (<http://www.jax.org/resources/documents/cmdata/rhmap>) which includes all publicly available RH data. All markers used to

construct the mouse Chromosome 10 RH map (Figure 4.6) had a LOD score (logarithm of the likelihood ratio for linkage) greater than 5 when these markers were mapped relative to the *jcpk* locus.

Radiation hybrid mapping has proven to be a valuable tool in evaluating possible gene candidates for *jcpk*. For example, the expressed sequence tag (EST) *D10Ertd214e* had previously been mapped to mouse Chromosome 10 near the region thought to contain the *jcpk* gene (127). However, based on RH mapping data, this EST was placed distal to *jcpk* thus eliminating it as a possible candidate for the *jcpk* gene. This placement is confirmed by physical localization of *D10Ertd214e* within BACs that fall outside the *jcpk* critical region (Figure 4.2). Together, these two maps give a detailed representation of the region containing the *jcpk* gene.

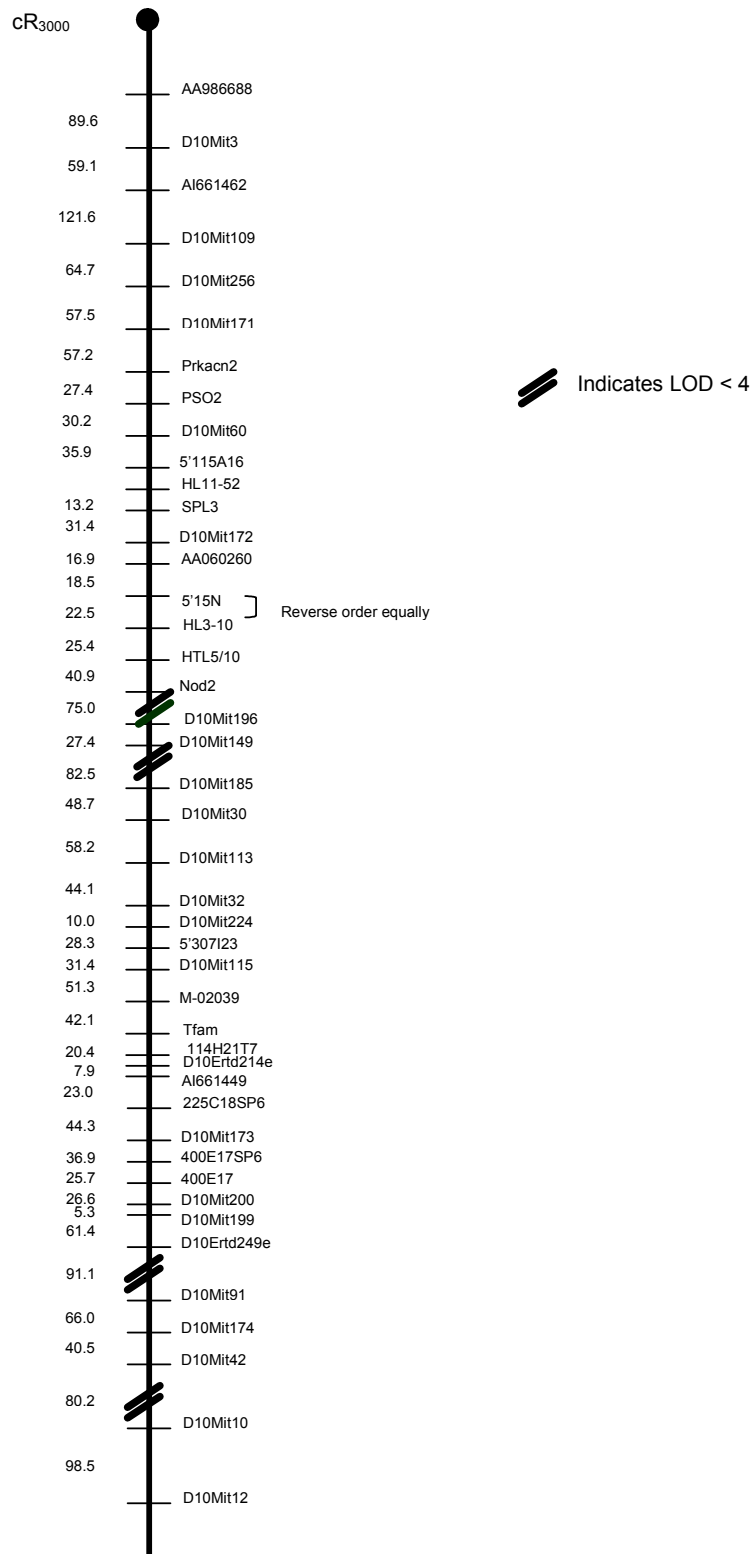


Figure 4.6 Radiation hybrid (RH) map of mouse Chromosome 10. The mouse chromosome is oriented with the centromere at the top (black dot). The distance between loci is given in cR₃₀₀₀. Hash marks indicate regions where the LOD score (logarithm of the likelihood ratio for linkage) between markers is less than <4.0. Map order was generated using the software programs RHMAPPER (241) and RHMAP (20).

Gene Identification

Gene Candidate Analysis

Three expressed sequence tags (ESTs), AW260721, BB498314, and AI956350, were identified between markers *D10Mit173* and *D10Mit115* by Basic Local Alignment Search Tool (BLAST) analysis (5) of BAC end sequences found in the TIGR BAC end annotation database (www.tigr.org). The ESTs were physically mapped using a combination of slot blot hybridization analysis and PCR of a panel of purified BAC DNAs selected from all areas of the contig. Northern blot analysis was also performed with wild type kidney and *jcpk/jcpk* kidney mRNA to determine if any transcript differences were present.

AW260721 was originally discovered on the end sequence of BAC RP23-430F6 and was found to map between markers *395K5T7* and *393H9SP6RPT*. This position places AW260721 outside the *jcpk* critical region defined by *393H9SP6RPT* and *282P18T7RPT*. As expected, Northern blot analysis showed no differences in transcript size or expression in wild type versus *jcpk/jcpk* kidneys. Therefore, AW260721 was eliminated as a candidate for *jcpk*.

AI956350 was originally discovered on the end sequence of BAC RP23-337L15T7. Slot blot and southern blot analysis placed AI956350 at the T7 end of RP23-337L15 proximal to *393H9SP6RPT*, thus eliminating it as a candidate for *jcpk*. Northern blot analysis confirmed that there were no differences in expression in wild type versus *jcpk/jcpk* kidneys.

The EST BB498314 was identified from nucleotide sequence from the SP6 end of BAC RP23-307C12. Slot blot analysis determined that this EST mapped between the markers *395K5T7* and *393H9SP6*. Thus, BB498314 is outside of the region thought to contain the *jcpk* gene. Northern blot analysis showed no transcript or expression differences between wild type and *jcpk/jcpk* kidneys.

Gene Identification

Sequence analysis was performed on six BACs (RP23-310N21, RP23-395K5, RP23-337L15, RP23-440N1, RP23-348F2, and RP23-282P18) (Figure 4.3) representing the region of mouse Chromosome 10 between markers *D10Mit115* and *282P18T7*. Using BLAST analysis (5) and the Ensembl database (110), considerable overlap was found between the BAC sequences within the region between markers *393H9SP6RPT* and *282P18T7RPT*.

Four of the above BACs (RP23-282P18, RP23-348F2, RP23-440N1 and RP23-337L15) (Figure 4.3) that minimally cover the *jcpk* critical region between markers *393H9SP6RPT* and *282P18T7RPT* were analyzed for the presence of transcribed genes using a number of gene prediction programs including GrailEXP v3.2 and GENESCAN. Within this region, only two partial transcripts were identified by *in silico* analyses. These corresponded to two known ESTs, BG062853 and BF785275, which were later determined to be part of a single mouse gene, *Bicc1*. This gene is the mouse orthologue of the *Drosophila melanogaster* *Bicaudal-C* (*Bic-C*) gene (272).

Alignment of the *Bicc1* Genbank mRNA sequence AF319464 with BAC genomic DNA that had undergone sequence analysis revealed 21 separate exons spanning three of the BAC genomic DNA inserts. Exons 1 and 2 were found on RP23-282P18. Exon 1 contains an ATG start site and was determined to be located approximately 80 kb upstream of exon 2. RP23-348F2 contained exons 2 through 16. Exon 2 was found to be present on both RP23-282P18 and RP23-348F2 and is approximately 51 kb away from exon 3. RP23-440N1 contained nucleotide sequence for exons 10 through 21. The entire *Bicc1* gene, including exons and introns, spans a physical distance of over 234 kb as estimated from nucleotide sequence data from both the Ensembl and TIGR databases.

Mutational Analysis

To evaluate *Bicc1* as the disease-susceptibility gene in the *jcpk* mouse model for PKD, RT-PCR analysis using total RNA from 101/RI (+/+), *+jcpk*, and *jcpk/jcpk* kidneys was performed on the coding region of the *Bicc1* gene. Primers were designed to evaluate each exon of the *Bicc1* transcript. When a RT-PCR primer set which generates a PCR product containing a portion of exon 1, all of exons 2-4 and a portion of exon 5 was used (Figure 4.7), a 70 bp deletion was present when comparing +/+ and *jcpk/jcpk* RT-PCR products (Figure 4.8). Both a wild type and *jcpk/jcpk* band were present in heterozygous kidney.

```

EXON 1
GTCGGACCCCGGCTCCAACAGCGAGCGCAGCACCGACTCGCCGGTGGCCGGCTCCGAGGACGATCTG
Forward primer

GTGGCCGCGGCGCCCTCTTGACAGCCCGAGTGGAGCGAGGAGCGCTTCCGCGTGACAGGAAG

EXON 2
AAACTCGAGGCCATGCTCCAAG| CTGCAGCTGAAGGAAAAGGCCGAAGTGGGAAGACTTTTTTCAGAA

EXON 3
G| ATCATGGAGGAGACAAACACGCAGATTGCATGGCCGTCCAACTGAAGATCGGGGCTAAATCCAAGA

EXON 4
AAG| ATCCCCACATCAAGGTTTCTGGGAAGAAAGAGGATGTGAAGGAAGCCAAAGAAATGATCATGTCTG

EXON 5
TCTTAGACACAAAA| AGCAACCGCGTCACATTGAAGATGGATGTCTCGCACACGGAGCACTCCACGTC

TCGGCAAGGGTGGTAACAACATTAATAAGGTCATGGAAGACACGGGCTGCCACATCCACTTCCCAGACT
Reverse primer

CCAA

```

Figure 4.7 RT-PCR analysis of exons 2-4 of the *Bicc1* gene. Different exons are distinguished by a green vertical line within the sequence. The forward primer used to evaluate the exons is shown in red and the reverse primer is shown in blue. RT-PCR analysis in +/+ mice produces a product that is 423 bp in length.

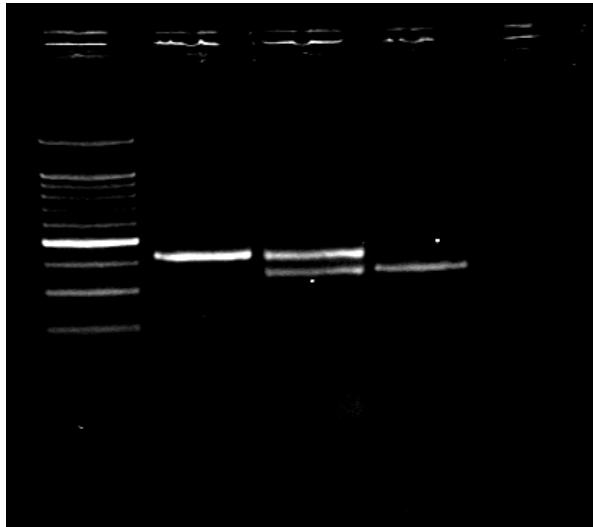


Figure 4.8 Mutation analysis of the *Bicc1* gene. RT-PCR of *Bicc1* transcripts using primers that evaluate exons 2-4 (Figure 4.6) in 3-day old *+/+* (Lane 2), *+/jcpk* (Lane 3), and *jcpk/jcpk* (Lane 4) kidneys. A 100 bp ladder is shown in Lane 1. Lane 5 is a no-template control. A 70 bp deletion was detected upon comparison of *jcpk/jcpk* versus *+/+* tissues. The band in *+/+* kidney has a size of 423 bp, whereas the band in *jcpk/jcpk* tissue is 353 bp. Both bands are observed in the heterozygous (*+/jcpk*) sample.

Nucleotide sequence analysis of the amplification products showed a complete deletion of exon 3 in the mutant mRNA transcript (Figure 4.9). The noncoding regions around exon 3 were then sequenced in 101/RI wild type and *jcpk/jcpk* kidney genomic DNA and a single base-pair change (G to A) in the splice acceptor site of exon 3 was discovered (Figure 4.10). This mutation is predicted to cause abnormal splicing, eliminating exon 3, and thereby joining exon 2 to the acceptor site of exon 4. The resulting reading frameshift introduces a premature stop codon in exon 4. Exon 3 is 70 nucleotides in size and accounts for the differences seen by RT-PCR and sequencing analysis.

EXON 1
CTCCGAGGACGATCTGGTGGCCGCGGCGCCCTCTTGACAGCCCGAGTGGAGCGAGGAGCGCTTCCG
 Forward primer
 CGTGGACAGGAAGAACTCGAGGCCATGCTCCAAG; CTGCAGCTGAAGGAAAAGGCCGAAGTGGGGAAG
 EXON 2
 ACTTTTTTCAGAAG; ATCCCCACATCAAGTTTCTGGGAAGAAAGAGGATGTGAAGGAAGCCAAAGAAATG
 EXON 4
 ATCATGTCTGTCTTAGACACAAAA; AGCAACCGCGTCACATTGAAGATGGATGTCTCGCACACGGAGCACT
 EXON 5
 CCCACGTCATCGGCAAGGGTGGTAACAACATTA AAAAGGTCATGGAAGACACGGGCTGCCACATCCACTTC
 Reverse primer
CCAGACTCAA

Figure 4.9 Sequence analysis of the *Bicc1* transcript in *jcpk/jcpk* kidney tissue. Different exons are distinguished by a green vertical line within the sequence. The forward primer used to evaluate the exons is shown in red and the reverse primer is shown in blue. Sequence analysis indicates a complete loss of exon 3 in the mRNA transcript. This deletion is 70 bp in length and corresponds to that shown in Figure 4.7.

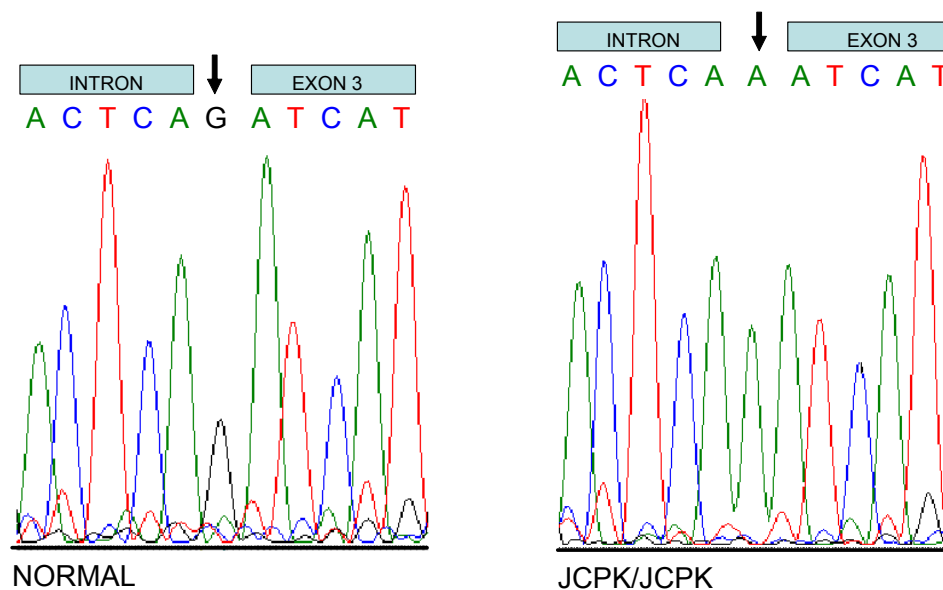


Figure 4.10 Genomic sequence analysis of *Bicc1* around exon 3. Both normal (+/+) and *jcpk/jcpk* kidney tissues were used. Comparing +/+ (left) and *jcpk/jcpk* (right), a single point mutation (G to A) was observed at the splice acceptor site of exon 3. This mutation produces a frameshift that results in a premature stop codon.

Additional confirmation that *Bicc1* is the disease-causing gene comes from observations in the *bpk* and 67Gso PKD mouse models, both of which had been demonstrated previously to be allelic to *jcpk* by complementation analyses (90).

In collaboration with Dr. Lisa Guay-Woodford (University of Alabama-Birmingham), RT-PCR analysis identified an insertion in the *bpk* allele of *Bicc1* that is predicted to alter the terminal portion of the Bicc1 protein (41). Through fluorescent *in situ* hybridization (FISH) analysis done in collaboration with Dr. Lisa Stubbs (Lawrence Livermore Laboratory, Livermore, CA), it was determined that the translocation breakpoint on Chromosome 10 in 67Gso falls within a region defined by two overlapping BACs RP23-348F2 and RP23-200D18 (40, 206). Since, both of these BACs are within the *jcpk* critical region and *Bicc1* is the only gene within that region, it is highly probable that the PKD phenotype in 67Gso mutant mice is due to disruption of the *Bicc1* gene by the translocation breakpoint.

Thus, it seems that three different mutations in the *Bicc1* gene cause PKD in three mouse models, *jcpk*, *bpk*, and 67Gso.

Alternative Transcripts

During sequence analysis of the EST BF785275, a previously unknown exon in the *Bicc1* transcript was discovered between exons 20 and 21 as defined by Wessely *et al.* (272) (Figure 4.11). BLAST analysis was used to compare the extra exon to the mouse EST database. At least five ESTs (AW240366, BF785375, AV170850, AA275580, and BY7635542) were found to contain this extra exon.

```

EXON 20
| ATCGATCTTCAGACATTCCCTCACCCCTCACAGATCAGGATCTGAAGGAGCTGGGAATCACAACCTTTGGTGCCCGAAGGA
                                                    Forward primer

EXON 21
AAATGCTGCTGGCAATCTCAG|TTTGTGACTCTGTTTCAGATCCGCAACAAGATCCTGAGAGCTGCCAGGATTCTGTGAAC

EXON 22
CTTGGAATGTCAAAGAAAAAAG|AGCTAAGTAAAAACCGAAGAAAACCTTTTGAACCACCAAACGCATCATGCACCTCCT

TCCTGGAAGGCGGAGCCAGTGGGAGGCTGCCTCGCCAGTATCATTTCAGACATTGCGAGCGTCAGTGGCCGCTGGTAGCGG

TACCTTCTGGACACGCACCTGCTATCTTGCAAAGGTGGACACGATCCGTGGACAGTCTTCACTCACTCGCCTGCCTTGG
                                                    Reverse primer

CACTCGGAGTGTCTGGTATCAGGACCAAAGTGTTGATTTCGTACCTGTACTTCATGGCCAAAAAAAAAAAAAAAAA

```

Figure 4.11 Sequence analysis of the *Bicc1* transcript. Different exons are distinguished by a green vertical line within the sequence. The forward primer used to evaluate the exons is shown in red and the reverse primer is shown in blue. Sequence analysis allowed identification of an extra exon (designated exon 21).

This exon was also found in a *Bicaudal-C* human transcript (BF325944). However, other mouse *Bicc1* ESTs were found that did not contain this exon. These ESTs included BI101203, AI595208, BM217996, AW488477, BY434239, and AA276596. From these data it can be concluded that the original report by Wessley *et al.* (272) indicating that mouse *Bicc1* gene contains only 21 exons is incomplete. *Bicc1* has instead 22 exons.

Using primers within exons 20 and 22 designed to bridge exon 21, PCR analysis confirmed that the extra exon is not only present in a number of these ESTs, but is also present in +/+ and *jcpk/jcpk* kidney. As seen in Figure 4.12, there are two amplification products differing by 80 nucleotides. Sequence analysis of both transcripts confirmed that it was exon 21 that was the only difference between these transcripts.

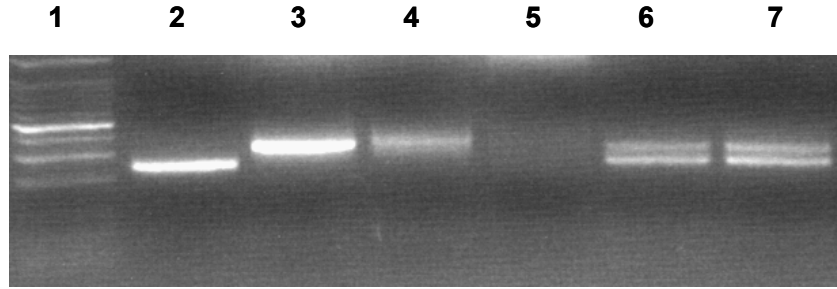


Figure 4.12 PCR analysis to determine alternative transcripts for *Bicc1*. PCR analysis of ESTs and tissues with primers spanning exons 20-22 of the *Bicc1* gene. Lane 1: 100 bp ladder, Lane 2: AI595208, Lane 3: AW340366, Lane 4: BF785275, Lane 5: No-template control, Lane 6: 101/RI kidney cDNA (wild type), Lane 7: *jcpk/jcpk* kidney cDNA. Note that both wild type and *jcpk/jcpk* kidney tissue contain the two transcripts.

Thus, data indicates that the *Bicc1* gene has at least two alternatively spliced transcripts: transcript A which contains exons 1-20 and 22, and transcript B which contains exons 1-22. It is predicted that transcript A encodes a protein with 977 amino acids, while transcript B has a premature stop codon in exon 21 and encodes a shorter protein of only 951 amino acids (Figure 4.13).

PANEL A: Bicc1 protein from transcript A

MASQSEPGYLAAAQSDPGSNSERSTDSPVAGSEDDLVAAPLLHSP EWSEERFRVDRK
KLEAMLQAAAEGKGRSGEDFFQKIMEETNTQIAWPSKLGAKSKKDPHIKVS GKKED
VKEAKEMIMSVLDTKSNRVTLKMDVSHTEHSHVIGKGGNNIKKVMEDTGCHIHF PDSN
RNNQAEKSNQVSIAGQPAGVESARARIRELLPLVLMFELPIAGILQPVPDPNTPSIQH
ISQTYSVSVSFKQSRMYGATVTVRGSQNNNTNAVKEGTAMLL EHLAGSLASAI PVSTQ
LDIAAQHHLFMMGRNGSNVKHIMQRTGAQIHFPDPSNPQKKSTVYLQGTIESVCLARQ
YLMGCLPLVLMFDMKEDIEVDPQVIAQLMEQLDVFISIKPKPKQPSKSVIVKSVERNA
LNMYEARCKLLGLESSGVS IATSLSPASCPAGLACPSLDILASAGLGLTGLGLLGPTT
LSLNTSATPNSLLNALNTSVSPLQSSSSGTPSPTLWAPPIANTASATGFSTIPHLMLP
STAQATLTNILLSGVPTYGHTAPSPPPGLTPVDVHINSMQTEGKNISASINGHVQPAN
MKYGPLSTSSLGEKVLSSNHGDPSMQTAGPEQASPKSNSVEGCNDAFVEVGMPRSPSH
SGNAGDLKQMLGASKVSCAKRQTVELLQGTKNSHLHGTDRLLSDPELSATESPLADKK
APGSERAAERAAAQ QKSERARLASQPTYVHMQAFDYEQKKLLATKAMLKKPVVTEVR
TPTNTWSGLGFSKSM PAETIKELRRANHVSYKPTMTTAYEGSSLSLSRSSSREHLASG
SESDNWRDRNGIGPMGHSEFSAPIGSPKRKQNK SREHYLSSSNYMDCISSLTGSNGCN
LNSCFKGSDLP ELF SKLGLGKYTDVFQQQEIDLQTFLTLTDQDLKELGITTFGARRKM
LLAIS **ELSKNRKLFEPNASCTSFLEGGASGR LPRQYHSDIASVSGRW**

PANEL B: Bicc1 protein from transcript B

MASQSEPGYLAAAQSDPGSNSERSTDSPVAGSEDDLVAAPLLHSP EWSEERFRVDRK
KLEAMLQAAAEGKGRSGEDFFQKIMEETNTQIAWPSKLGAKSKKDPHIKVS GKKED
VKEAKEMIMSVLDTKSNRVTLKMDVSHTEHSHVIGKGGNNIKKVMEDTGCHIHF PDSN
RNNQAEKSNQVSIAGQPAGVESARARIRELLPLVLMFELPIAGILQPVPDPNTPSIQH
ISQTYSVSVSFKQSRMYGATVTVRGSQNNNTNAVKEGTAMLL EHLAGSLASAI PVSTQ
LDIAAQHHLFMMGRNGSNVKHIMQRTGAQIHFPDPSNPQKKSTVYLQGTIESVCLARQ
YLMGCLPLVLMFDMKEDIEVDPQVIAQLMEQLDVFISIKPKPKQPSKSVIVKSVERNA
LNMYEARCKLLGLESSGVS IATSLSPASCPAGLACPSLDILASAGLGLTGLGLLGPTT
LSLNTSATPNSLLNALNTSVSPLQSSSSGTPSPTLWAPPIANTASATGFSTIPHLMLP
STAQATLTNILLSGVPTYGHTAPSPPPGLTPVDVHINSMQTEGKNISASINGHVQPAN
MKYGPLSTSSLGEKVLSSNHGDPSMQTAGPEQASPKSNSVEGCNDAFVEVGMPRSPSH
SGNAGDLKQMLGASKVSCAKRQTVELLQGTKNSHLHGTDRLLSDPELSATESPLADKK
APGSERAAERAAAQ QKSERARLASQPTYVHMQAFDYEQKKLLATKAMLKKPVVTEVR
TPTNTWSGLGFSKSM PAETIKELRRANHVSYKPTMTTAYEGSSLSLSRSSSREHLASG
SESDNWRDRNGIGPMGHSEFSAPIGSPKRKQNK SREHYLSSSNYMDCISSLTGSNGCN
LNSCFKGSDLP ELF SKLGLGKYTDVFQQQEIDLQTFLTLTDQDLKELGITTFGARRKM
LLAIS **VCD SVQIRNKILRAARIL**

Figure 4.13 Two protein isoforms are predicted for the *Bicc1* gene. **PANEL A:** Putative protein product from *Bicc1* transcript A which does not contain exon 21. This protein contains 977 amino acids. **PANEL B:** Putative protein product of *Bicc1* transcript B which contains exons 1-22. This protein contains only 951 amino acids. Differences between the two transcripts are shown in red.

RT-PCR and nucleotide sequence analysis of the *bpk* mutation identified a two-base pair insertion in exon 22 of *Bicc1* (41). This mutation is predicted to extend the amino acid sequence of transcript A by 149 amino acids. The predicted amino acid sequence of transcript B would be unaffected by this mutation, since the predicted stop codon in transcript B occurs in exon 21 prior to the insertion mutation (Figure 4.14). This is different from the mutation in *jcpk* which is predicted to truncate both protein isoforms (Figure 4.14). The observation that the *jcpk* mutation affects both transcripts A and B; whereas *bpk* affects only transcript A, may explain why affected *jcpk* animals have a more severe phenotype and have an earlier onset of disease compared to affected *bpk* mice. Future transcript-specific analyses are needed to explore this phenotypic difference.

PANEL A: Protein product from *bpk* mutation

MASQSEPGYLAAAQSDPGNSERSTDSPVAGSEDDLVAAPLLHSPWESEERFRVDRK
KLEAMLQAAAEGKGRSGEDFFQKIMEETNTQIAWPSKLGAKSKKDPHIKVSGKKED
VKEAKEMIMSVLDTKSNRVTLKMDVSHTEHSHVIGKGGNNIKVMEDTGCHIHFPDSN
RNNQAEKSNQVSIAGQPAGVESARARIRELLPLVLMFELPIAGILQPVDPNTPSIQH
ISQTYSVSVSFKQSRMYGATVTVRGSQNNNAVKEGTAMLLEHLAGSLASAI PVSTQ
LDIAAQHHLFMMGRNGSNVKHIMQRTGAQIHFPDPSNPQKKSTVYLQGTIESVCLARQ
YLMGCLPLVLMFDMKEDIEVDPQVIAQLMEQLDVFISIKPKPKQPSKSVIVKSVERNA
LNMYEARCCLLGLESSGVSIAATSLSPASCPAGLACPSLDILASAGLGLTGLGLLGPTT
LSLNTSATPNLLNALNTSVSPLQSSSSGTPSPTLWAPP IANTASATGFSTI PHLMLP
STAQATLTNILLSGVPTYGHTAPSPPPGLTPVDVHINSMQTEGKNISASINGHVQPAN
MKYGPLSTSSLGEKVLSSNHGDPSMQTAGPEQASPKSNSVEGCNDAFVEVGMPSRPSH
SGNAGDLKQMLGASKVSCAKRQTVELLQGTKNSHLHGTDRLLSDPELSATESPLADKK
APGSERAAERAAAAQKSERARLASQPTYVHMQAFDYEQKKLLATKAMLKKPVVTEVR
TPTNTWSGLGFSKSMPAETIKELRRANHVSYKPTMTTAYEGSSLSLSRSSSREHLASG
SESDNWRDRNGIGPMGHSEFSAPIGSPKRKQNK SREHYLSSSNYMDCISSLTG SNGCN
LNSCFKGS DLPFLFSKLGLGKYTDVFQQQEIDLQTF LTLTDQDLKELGITTFGARRKM
LLAISELSKNRRKLFEPNASCTSFLEGAEPVGGCLASIIQTLRASVAAGSGTFWTRT
CYLAKVD TIRGQSSSLHSPALGTRSVWYQDQSVDFVPVLHGQKKKKKKKEREK RQEKCL
MFSCCHKSTKGRNAFINWQLDRICKMRVGLCFFLFYITYALIFFFMVPMKENFDIW
DARKLRSYFCWLELSWCLGIWKKK

PANEL B: Protein product from *jcpk* mutation

MASQSEPGYLAAAQSDPGNSERSTDSPVAGSEDDLVAAPLLHSPWESEERFRVDRK
KLEAMLQAAAEGKGRSGEDFFQKI P T S R F L G R K R M

Figure 4.14 Predicted proteins encoded by the *bpk* and *jcpk* alleles. **PANEL A:** Predicted protein encoded as a result of the *bpk* mutation. The mutation results in 170 novel amino acids (shown in red) at the C-terminus and lengthens the protein by 149 amino acids. This mutation affects only *Bicc1* transcript A. **PANEL B:** Predicted protein encoded as a result of the *jcpk* mutation. The mutation causes a frameshift resulting in a premature stop codon that produces a protein that is only 93 amino acids in length. The amino acids that differ from the normal *Bicc1* protein are shown in red. The *jcpk* mutation is expected to affect proteins translated from both transcripts A and B.

Mouse-Human Homology

The human orthologue of *Bicc1* was previously mapped to human 10q21 (272). Considerable homology exists between mouse and human sequences, ranging from 80-96% in exon to exon comparisons (Table 4.1). The *Bicc1* gene is highly conserved in at least 9 different species. Ensembl database analysis indicates that *Bicc1* orthologues exist in human, *Xenopus* (frog), rat, *Danio rerio*

(zebrafish), *Drosophila* (fruitfly), *Anopheles* (mosquito), *Caenorhabditis* (nematode) and *Fugu* (pufferfish). Such high conservation would suggest that *Bicc1* plays an important function in development or cell regulation across many species.

Table 4.1 Exon to exon comparison of the mouse and human Bicaudal-C genes.

EXON	% HOMOLOGY
1	89
2	90
3	90
4	91
5	82
6	87
7	84
8	86
9	89
10	96
11	83
12	89
13	81
14	83
15	80
16	88
17	80
18	92
19	84
20	92
21	84
22	85

RNA Analysis

Tissue Expression of Bicc1

Previous work has indicated that mouse *Bicc1* is predominantly expressed in the adult kidney and heart, with low levels of expression evident in the testis (272). This expression was confirmed by Northern blot analysis using the radioactively labeled EST AW240366 as a probe. *Bicc1* expression is the strongest in the kidney with weak expression in the heart, lung, and liver (Figure 4.15). Faint bands were also present in the brain and testis. Interestingly, experiments done by others did not observe expression in the brain, lung, or liver (272). Northern blots in both experiments were probed with the cDNA insert from AW240366.

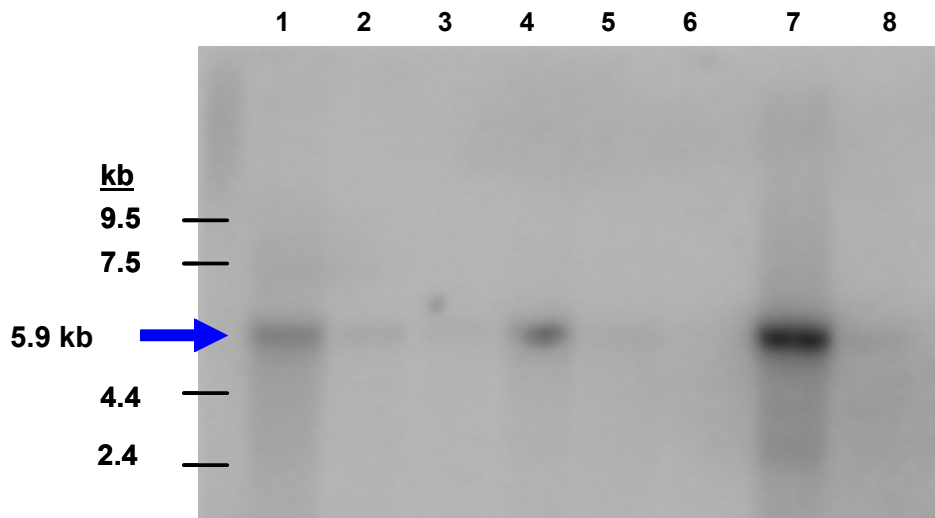


Figure 4.15 Tissue expression of *Bicc1*. Northern blot containing approximately 2 μ g of poly A+ RNA per lane from eight different mouse tissues. Blot was hybridized with a 3 kb cDNA probe (AW240366). The probe detects an approximately 5.9 kb transcript (arrow). To the left is a size marker indicating the size of bands in kilobases (kb). Lane 1: heart, Lane 2: brain, Lane 3: spleen, Lane 4: lung, Lane 5: liver, Lane 6: skeletal muscle, Lane 7: kidney, Lane 8: testis.

By Northern blot analysis, a *Bicc1* transcript of approximately 5.9 kb in length is detected. While the *Bicc1* coding region itself is only 3.0 kb in length, the size of the *Bicc1* transcript is larger due to a relatively short 5' untranslated region and a long 3' untranslated region. Because transcript A and transcript B differ by only 80 nucleotides, they could not be individually distinguished by Northern blot analysis.

Several other cell lines were examined for *Bicc1* expression using EST AW240366 as a probe (Table 4.2). Of the twelve cell lines analyzed, the *Bicc1* gene was detected in two cell lines K-BALB (K-234) and Hepa 1-6 (Figure 4.16). A low level of expression was also detected in the P19 cell line. P19 and K-BALB are both embryonic cell lines, whereas Hepa 1-6 is a liver carcinoma cell line. No detectable expression was found in the other cell lines which were mostly of hematopoietic lineage. This is consistent with the previous tissue expression data. Comparing cell lines, *Bicc1* is highly expressed in Hepa 1-6, a liver carcinoma cell line. In *Bicc1*^{icpk} heterozygous mice, cysts are present in the liver (41).

Table 4.2 Description of cell lines examined for *Bicc1* expression

Cell Line	ATCC #	Strain	Tissue
PU5-1.8 (PU5-1R)	TIB61	BALB/c	Lymphoid Tumor, Macrophage, Monocyte
RAW264.7	TIB71	BALB/c	Monocyte, Macrophage
K-BALB (K-234)	CCL163.3	BALB/c	Embryo, Fibroblast
M-MSV-BALB/3T3	CCL163.2	BALB/c	Embryo, Fibroblast
L-M	CCL1.2	C3H/An	Normal: Subcutaneous connective tissue, Areolar and Adipose
P19	CRL1825	C3H/He	Teracarcinoma, Embryonal Carcinoma, Embryo
Hepa 1-6	CRL1830	C57L	Hepatoma, Liver
R1.1	TIB42	C58/J	Lymphoma, Thymus, T lymphocyte
L1210	CCL219	DBA Subline212	Lymphocytic, Leukemia
P388D1	CCL46	DBA/2	Lymphoma, Macrophage, Monocyte
P815	TIB64	DBA/2	Mastocytoma, Mast Cell
NB41A3	CCL147		Neuroblastoma, Brain, Neuroblast

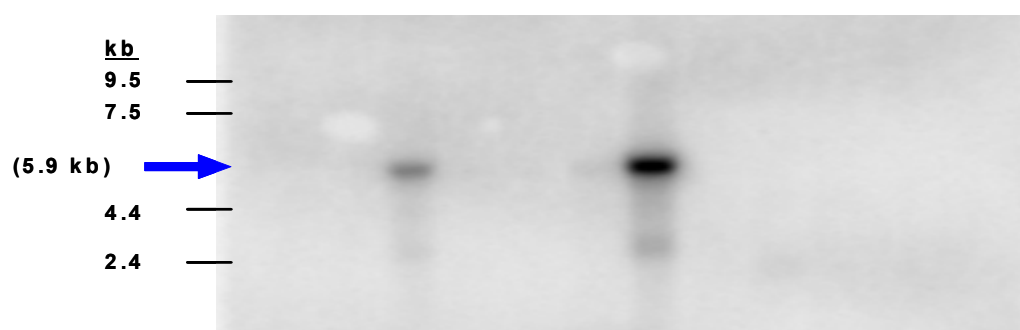


Figure 4.16 Expression analysis of *Bicc1* in mouse cell lines. Northern blot containing approximately 1 µg of poly A+ RNA per lane from twelve different mouse cell lines (see Table 4.2). Lane 1: PU5-1.8, Lane 2: RAW264.7, Lane 3: K-BALB, Lane 4: M-MSV-BALB/3T3, Lane 5: L-M, Lane 6: P19, Lane 7: Hepa1-6, Lane 8: R1.1, Lane 9: L1210, Lane 10: P388D1, Lane 11: P815, Lane 12: NB41A3.

It has been previously demonstrated by hybridization studies that expression of *Bicc1* appears early in development and can first be detected in the embryonic node at the rostral tip of the primitive streak (272). It was also shown that by embryonic day 13 (E13), *Bicc1* mRNA is evident in the metanephros, the limbs, and the mesenchyme of the lung (272). Dot blot analysis using the EST BF785275 as a probe was consistent with the above data showing increasing embryonic expression starting at E7 (earliest time point examined) through E15 with a leveling off of expression beyond this time point (Figure 4.17). Similar results were seen by Northern blot analysis using the EST probe AW240366 (Figure 4.17). RT-PCR analysis was performed on RNA from staged whole mouse embryos and *Bicc1* was detected as early as E5 (Figure 4.18).

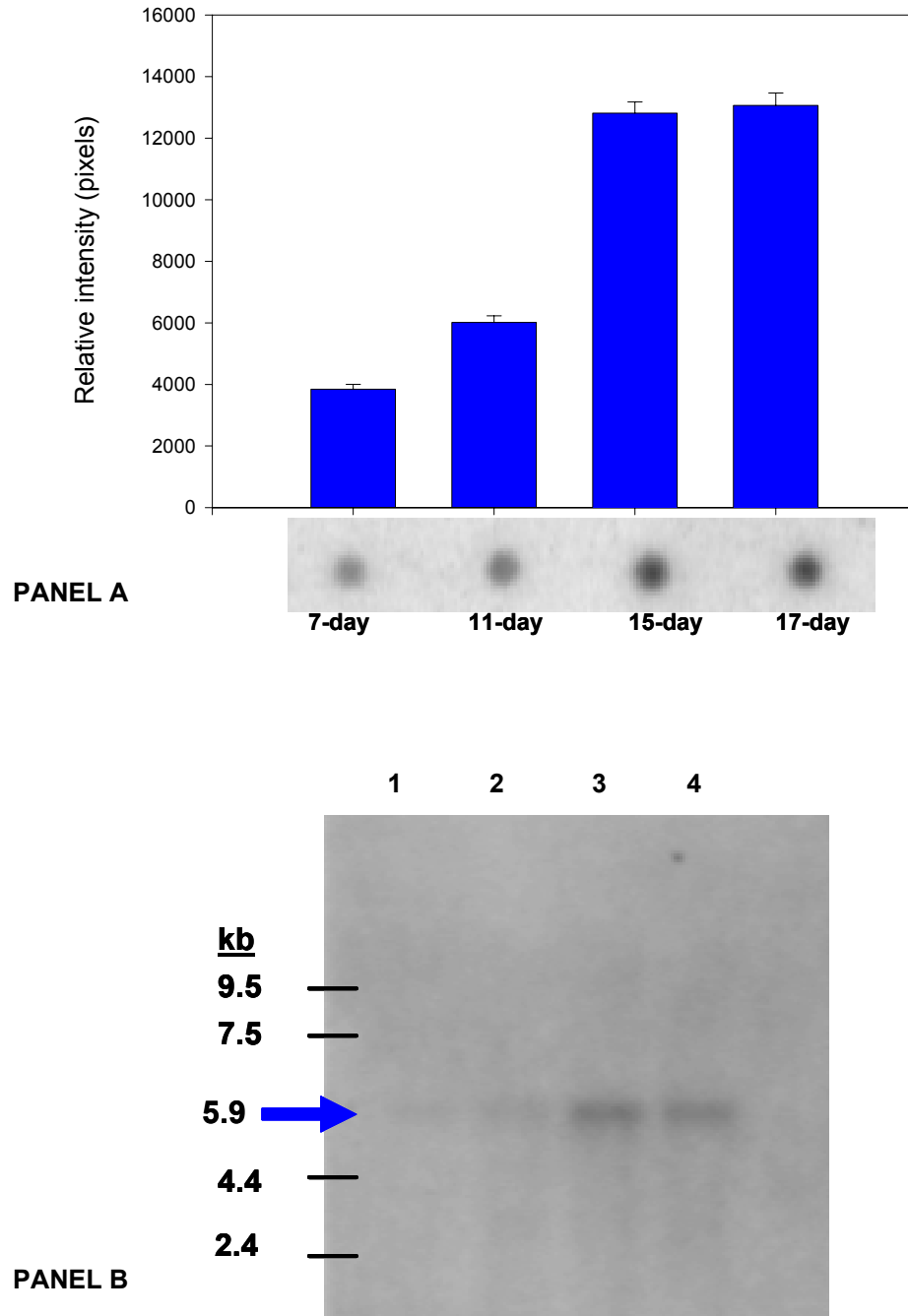


Figure 4.17 Embryonic expression of *Bicc1*. **PANEL A:** Slot blot analysis of embryonic mRNA using the radioactively labeled EST BF785275 as a probe. Stages analyzed were E7, E11, E15, and E17. *Bicc1* expression increases as the embryo matures. Densitometry was performed using the Typhoon Imaging System (Applied Biosystems, Foster City, CA). **PANEL B:** Northern blot analysis of 2 ug embryonic mRNA using EST AW240366 as a probe. Lane 1: E7, Lane 2: E11, Lane 3: E15, and Lane 4: E17.

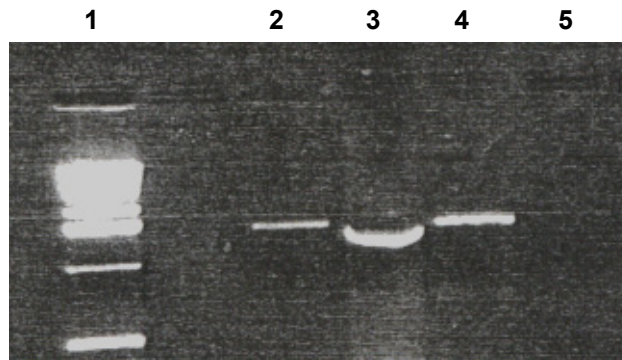


Figure 4.18 RT-PCR analysis of embryonic mRNA. Analysis was performed using mRNA from staged embryos and primers specific for the *Bicc1* gene. Lane 1: 100 bp ladder, Lane 2: E5 mRNA, Lane 3: E10 mRNA, Lane 4: Adult B6 kidney, Lane 5: no template control.

Northern blot analysis using different *Bicc1* ESTs as probes was performed to determine the expression of *Bicc1* in *jcpk/jcpk* affected kidneys compared to normal controls (B6 or 101/RI kidney). It was found that *Bicc1* was expressed in *jcpk/jcpk* kidney at a level that was indistinguishable from that of controls (Figure 4.19). This situation is unusual, especially when considering that

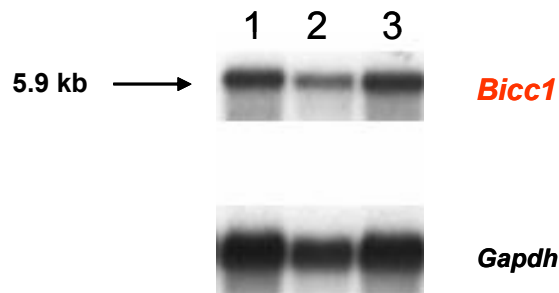


Figure 4.19 Northern blot analysis of *Bicc1* in normal and affected kidney. The blot was analyzed with a radioactively labeled probe for *Bicc1*. The blot was also probed for expression of *Gapdh* as a loading control. Other blots with similar results were probed with ESTs BF785275, AI595208, and AA086944. Lane 1: B6 (+/+) kidney, Lane 2: +/*jcpk* kidney, Lane 3: *jcpk/jcpk* kidney. Similar bands are present in normal and affected kidney. The image is captured on the Typhoon Image System (Applied Biosystems, Foster City, CA).

the *jcpk* mutation produces a premature termination codon (PTC) which should make the transcript susceptible to nonsense-mediated mRNA decay (NMD). NMD has been shown to be a quality control mechanism developed by cells to maintain homeostasis by destroying mRNA species which contain PTCs so that only full-length proteins are produced (31). This is important since many times mRNAs containing PTCs can be translated and have deleterious dominant negative effects on the cell (226). Most mRNAs containing PTCs in their 5' regions are degraded by NMD and are expressed at lower levels compared to the normal transcript (47). Exon-skipping resulting in a PTC, as seen in the *jcpk* mutation, is a common target for NMD. It is an unexpected observation that *Bicc1* would be expressed at normal levels in homozygous *jcpk* kidneys compared to wild type controls given the presence of a PTC in the homozygous *jcpk* transcripts. It is difficult to speculate why the *Bicc1*^{*jcpk*} mRNA transcript is not degraded by NMD. Sequence and Northern blot analysis alone are not enough to determine this mechanism, thus further study is required.

Real-time PCR Analysis of Bicc1 Gene Expression

A commonly used and more sensitive strategy for monitoring gene expression is real-time PCR analysis. This method monitors product amplification by the use of fluorescently labeled probes or fluorescent dyes. Specifically, Taqman™ PCR analysis was used to determine differences in *Bicc1* gene expression in 3-day old +/+ and *jcpk/jcpk* littermates. Real-time analysis determined that the *Bicc1* gene is expressed at similar levels in *jcpk/jcpk* kidneys as compared to the age-matched control (+/+) (Figure 4.20). This data is consistent with that seen in Northern blot analysis. *Bicc1* gene expression was also evaluated in *bpk/bpk* mice using real-time PCR analysis with SYBR Green as a reporter (Figure 4.21). No difference in gene expression was seen when comparing *bpk/bpk* and BALB/c age-matched mice. This data was confirmed by Northern blot analysis in collaboration with Dr. Lisa Guay-Woodford (41).

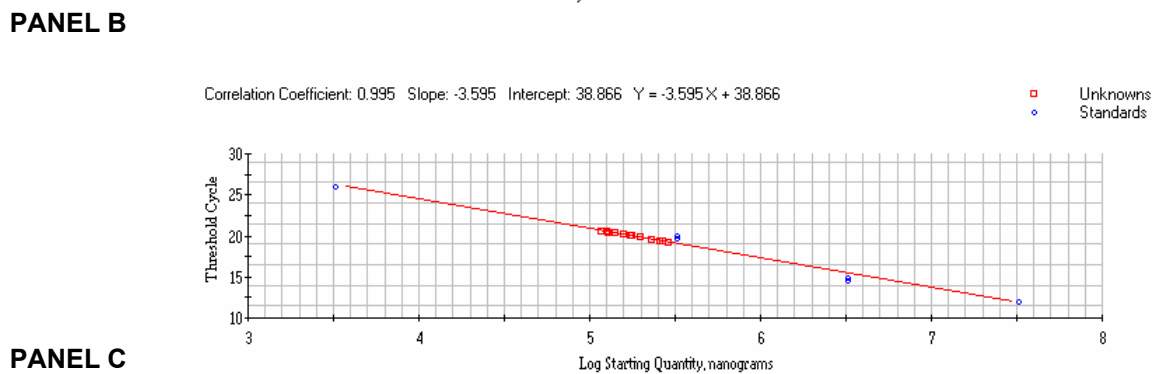
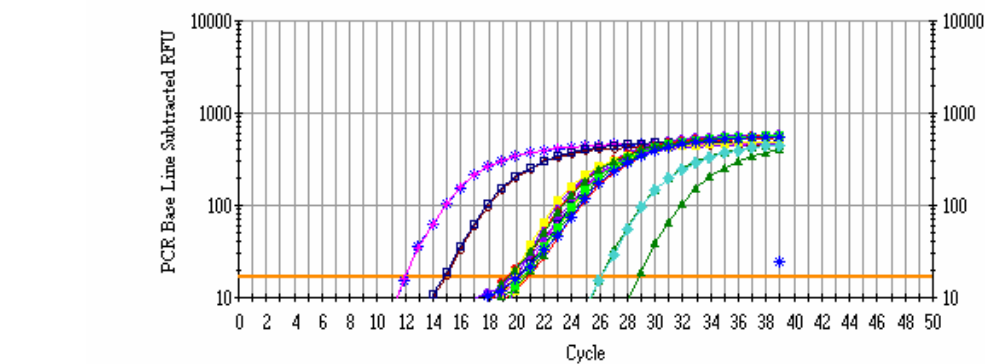
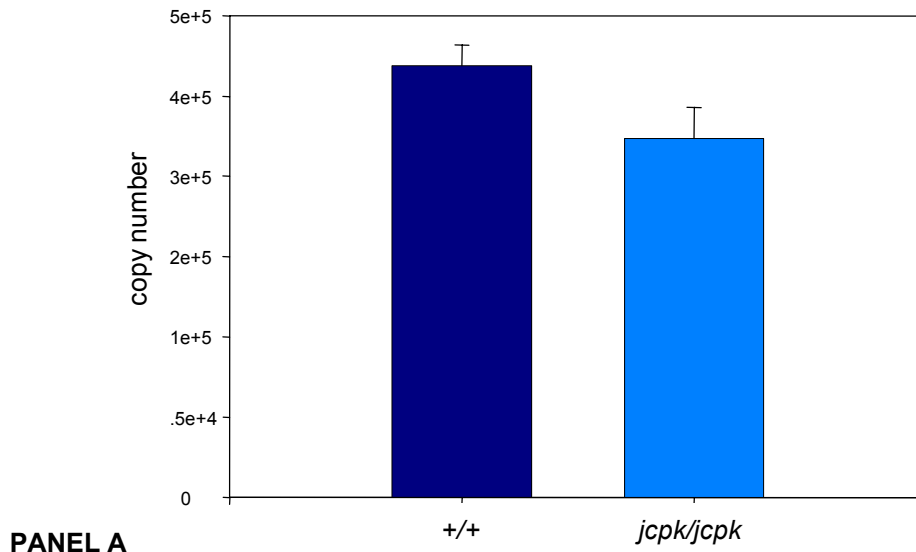


Figure 4.20 Real-time PCR analysis of *Bicc1* in *jcpk/jcpk* kidney. Taqman probes with either FAM or VIC fluorophores were used to measure product amplification. **PANEL A:** A mean quantity for each littermate was determined and those means were grouped as either normal (*+/+*, N=2) or PKD affected (*jcpk/jcpk*, N=2) mice. An unpaired two-tailed t-test was performed on the above groups. There was no significant difference between groups ($P=0.101$). **PANEL B:** Amplification profile plotting Δ RFU (relative fluorescence units) versus cycle number. All sample groups and standard groups are plotted on the same graph. **PANEL C:** Standard curve generated from the BioRad iCycler software. Blue dots indicate standards and red squares indicate unknown samples.

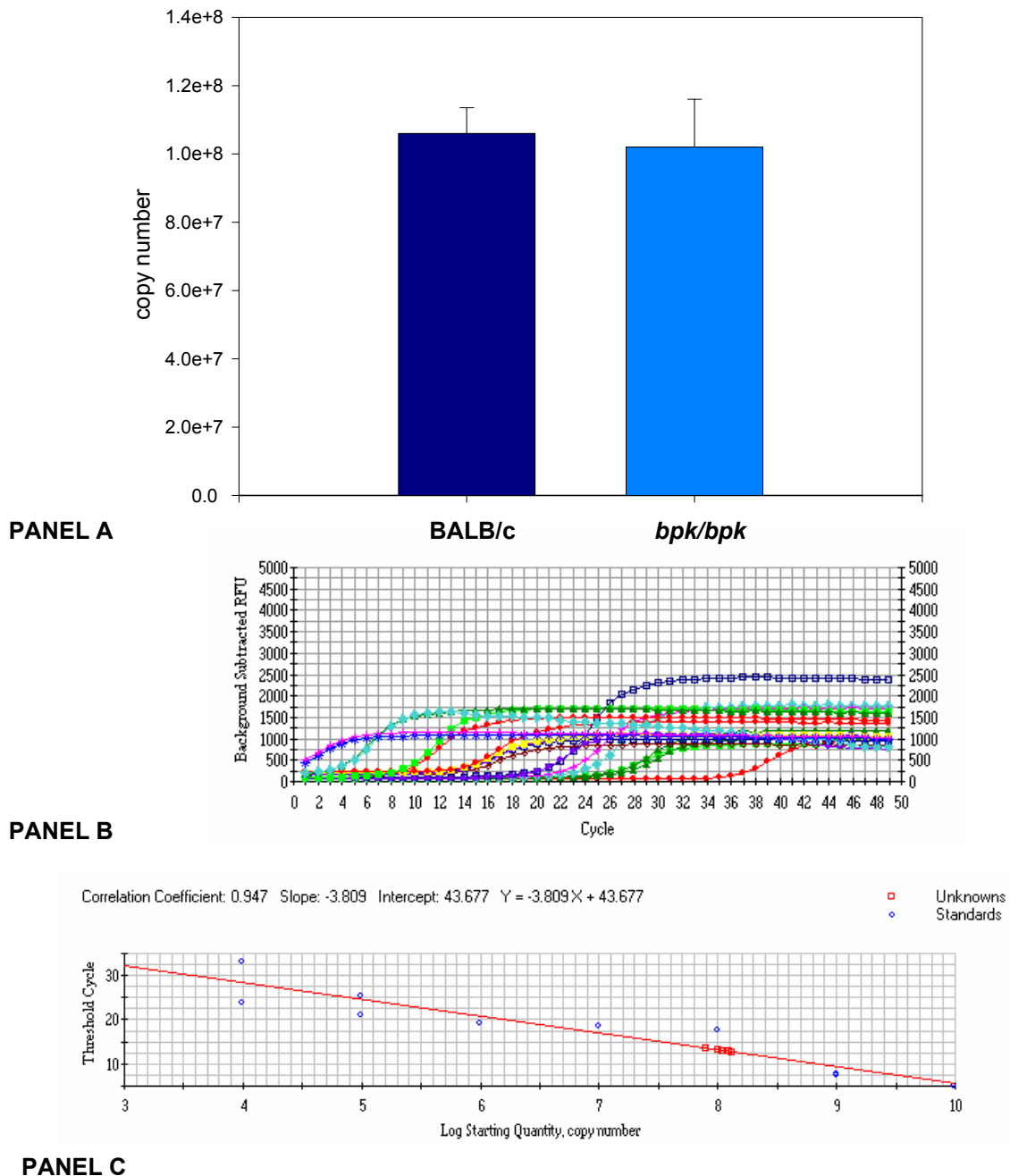


Figure 4.21 Real-time PCR analysis of *Bicc1* in *bpk/bpk* kidney. **PANEL A:** A mean quantity for each littermate was determined and those means were grouped as either normal (+/+, N=2) or PKD (*jcpk/jcpk*, N=2) affected mice. An unpaired two-tailed t-test was performed on the above groups. There was no significant difference between groups (P=0.826). **PANEL B:** Amplification profile plotting Δ RFU (relative fluorescence units) versus cycle number. All sample groups and standard groups are plotted on the same graph. **PANEL C:** Standard curve generated from the BioRad iCycler software. Blue dots indicate standards and red squares indicate unknown samples.

Real-time PCR Gene Expression Analysis of Other PKD Genes

A single, non-motile cilium is expressed on the apical surface of the epithelium lining much of the nephron, the biliary tract, and the pancreatic ducts. The proteins encoded by *orpk* (*Tg737*), *Invs*, *Pkd1*, *Pkd2*, and *cpk* (*Cys1*) have been shown to be part of this primary cilia (99, 108, 172, 197). Mutations in some of these genes result in shortened or nonfunctional cilia. Moreover, mutations in all of these genes result in PKD. Both *jck* and *kat* genes encode NIMA (never in mitosis-A) kinases and when mutated, are also known to cause PKD (Table 4.3). Interestingly, the protein encoded by *jck*, Nek8, has been shown to be associated with the developmental patterning protein, Bicaudal-D (BicD), in the mouse (104). Using real-time PCR analysis, the expression of these seven genes was evaluated in the *jcpk* mouse model for PKD to determine if the mRNA expression of any of these genes is altered as a result of the *jcpk* mutation.

Of the seven genes evaluated, only two were found to have altered expression in *jcpk/jcpk* animals. These results are summarized in Table 4.3. The genes *Pkd1*, *Pkd2*, *orpk* (*Tg737*), *Invs*, and *jck* (*Nek8*) showed no difference in expression when comparing homozygous normal and homozygous affected kidneys (Figures 4.22 through 4.26). The cystic gene *kat* was found to have a 6-fold decrease in gene expression in *jcpk/jcpk* mice when compared to control mice (Figure 4.27). The expression of *cpk* was increased 3-fold in polycystic mice versus control mice (Figure 4.28). It has not been determined whether there are associations between the products of these genes and *Bicc1*. *In vivo* analysis to test whether *Bicc1* affects the expression of *cpk* and *kat* are needed in order to determine the possible relationship between *Bicc1* and these other genes.

Table 4.3 Real-time PCR analysis of PKD genes in *jcpk/jcpk* mice.

Gene	Mouse Chromosome	Protein	Change in Expression *
<i>Pkd1</i>	17	polycystin-1	none
<i>Pkd2</i>	5	polycystin-2	none
<i>cpk (Cys1)</i>	12	cystin	increased (3X)
<i>Invs</i>	4	inversin	none
<i>orpk(Tg737)</i>	14	polaris	none
<i>jck (Nek8)</i>	11	nek-8	none
<i>kat (Nek1)</i>	8	nek-1	decreased (6X)

*Represents change in gene expression in the kidneys of polycystic *jcpk/jcpk* mice versus normal mice

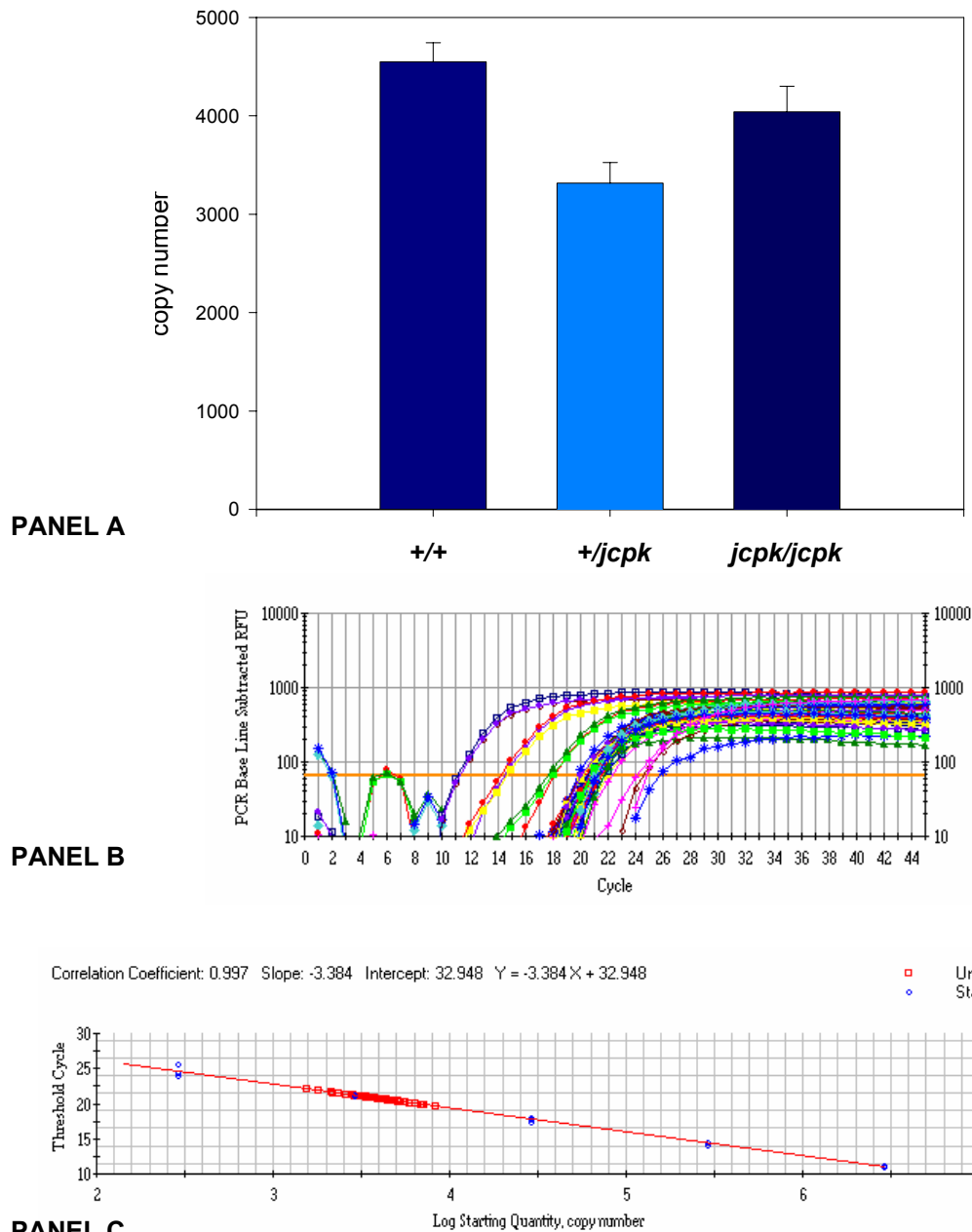
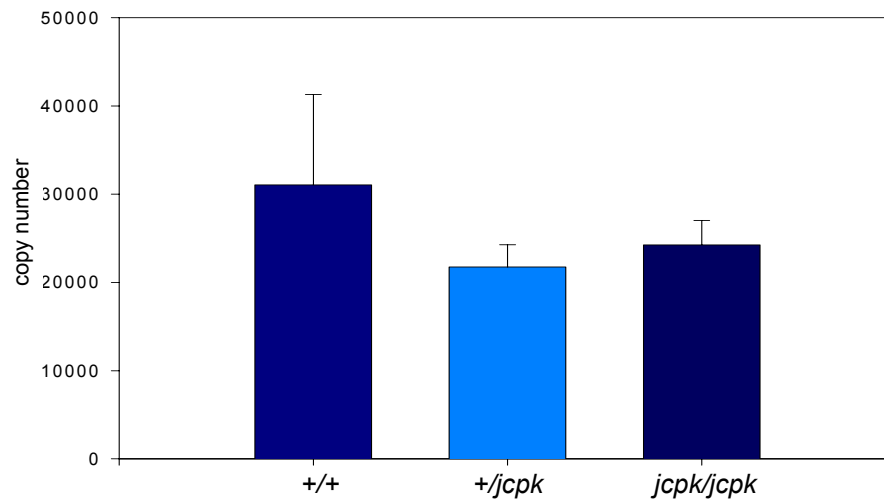
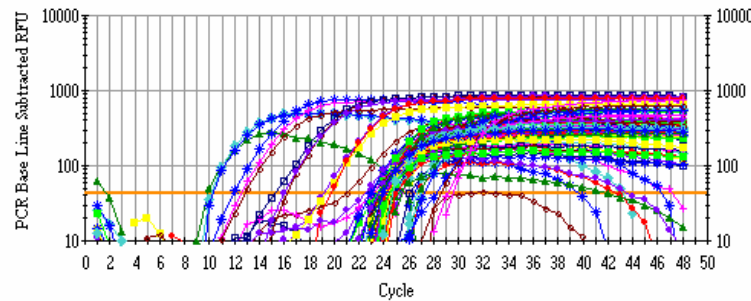


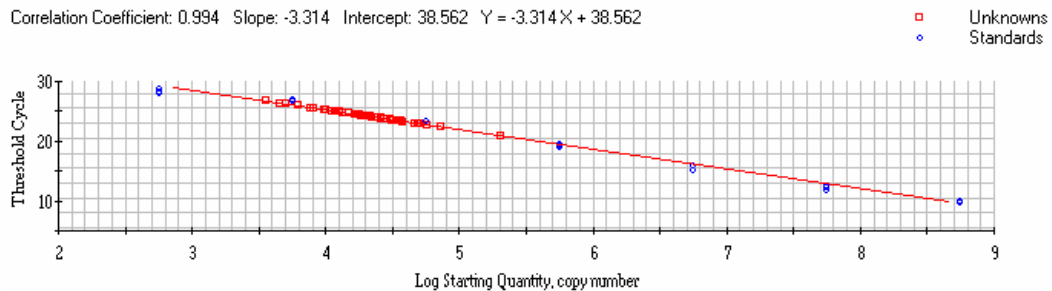
Figure 4.22 Real-time PCR analysis of *pkd1* mRNA expression. Equal volumes of cDNA from each of fifteen 4-day old mice were subjected to PCR using primers homologous to a specific region of the mouse *pkd1* gene. **PANEL A:** Template quantity analysis. Means were grouped as (+/+), (+/jcpk), or (jcpk/jcpk) mice. The values shown represent the mean \pm standard error for each groups (+/+ N = 5, +/jcpk N = 5, jcpk/jcpk N = 5) with 4 replicates for each animal. A one-way ANOVA was performed on the above groups. No significant difference between genotypic groups was found ($P = 0.681$). **PANEL B:** Amplification profile plotting Δ RFU (relative fluorescence units) versus cycle number. All sample groups were plotted on the same graph. **PANEL C:** Standard curve generated from the iCycler software (BioRad, Hercules, CA). Blue dots indicate standards and red squares indicate experimental samples.



PANEL A



PANEL B



PANEL C

Figure 4.23 Real-time PCR analysis of *pkd2* mRNA expression. Equal volumes of cDNA from 4-day old mice were subjected to PCR using primers homologous to a specific region of the mouse *pkd2* gene. The reporter used to detect product formation was SYBR Green (1:20,000 dilution). Four replicates of each cDNA sample were compared to amplification standards. **PANEL A:** Template quantity analysis. Means were grouped as (+/+), (+/*jcpk*), or (*jcpk/jcpk*) mice. The values shown represent the mean + standard error for each groups (+/+ N = 5, +/-cpk N = 5, *jcpk/jcpk* N = 5). A one-way ANOVA was performed on the above groups. There was no significant difference between genotypic groups ($P = 0.313$). **PANEL B:** Amplification profile plotting Δ RFU (relative fluorescence units) versus cycle number. All sample groups are plotted on the same graph. **PANEL C:** Standard curve generated from the iCycler software (BioRad, Hercules, CA). Blue dots indicate standards and red squares indicate experimental samples.

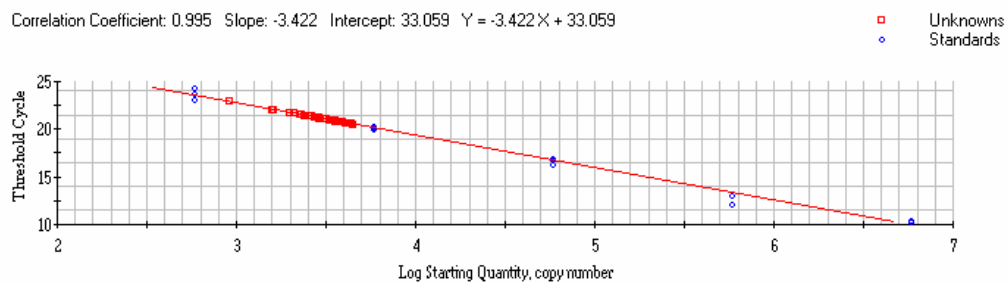
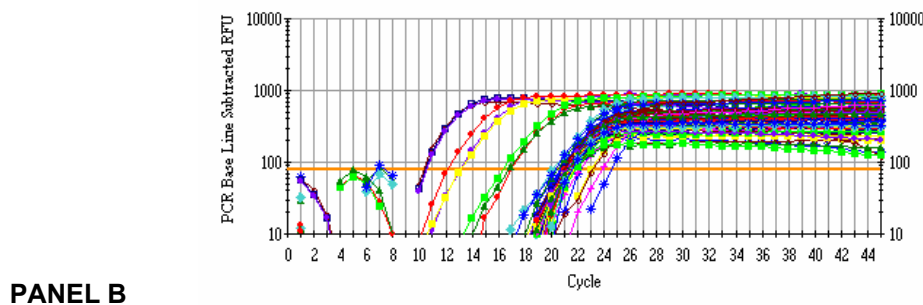
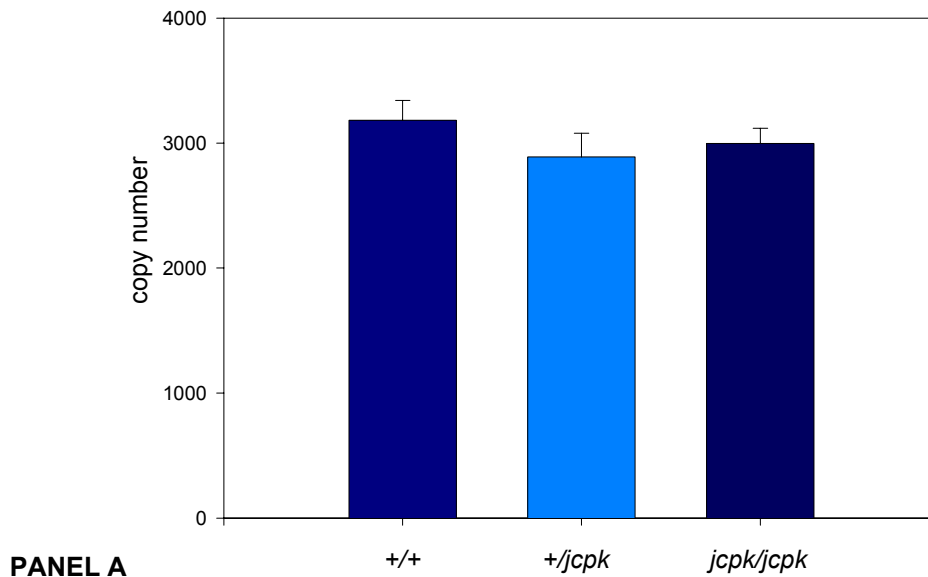
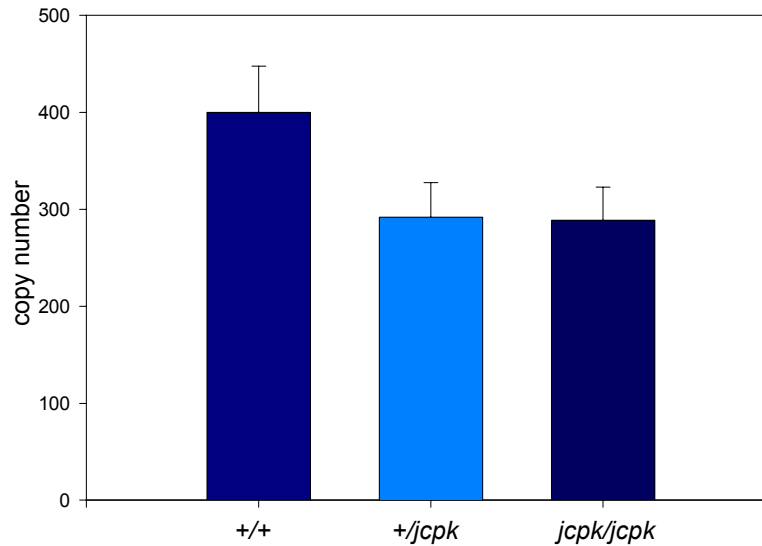
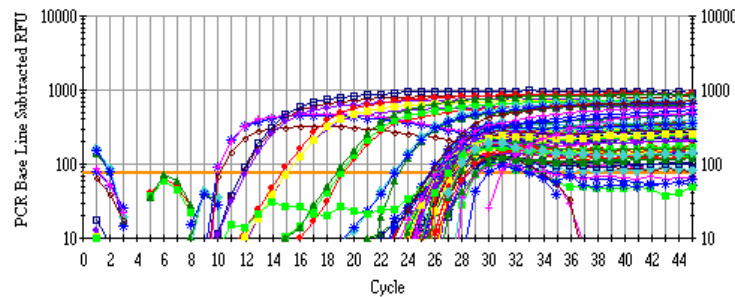


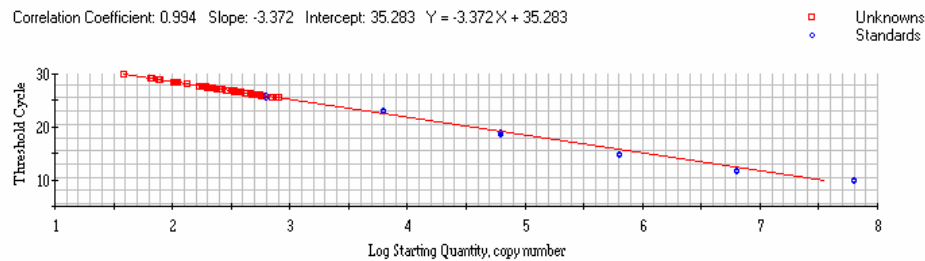
Figure 4.24 Real-time PCR analysis of *orpk* mRNA expression. Equal volumes of cDNA from each of fifteen 4-day old mice were subjected to PCR using primers homologous to a specific region of the mouse *orpk* gene. The reporter used to detect product formation was SYBR Green (1:20,000 dilution). Four replicates of each cDNA sample were compared to amplification standards. **PANEL C:** Template quantity analysis. Means were grouped as (+/+), (+/*jcpk*), or (*jcpk/jcpk*) mice. The values shown represent the mean \pm standard error for each groups (+/+ N = 5, +/*jcpk* N = 5, *jcpk/jcpk* N = 5). A one-way ANOVA was performed on the above groups. There was no significant difference between genotypic groups ($P = 0.865$). **PANEL B:** Amplification profile plotting Δ RFU (relative fluorescence units) versus cycle number. All sample groups were plotted on the same graph. **PANEL C:** Standard curve generated from the iCycler software (BioRad, Hercules, CA). Blue dots indicate standards and red squares indicate experimental samples.



PANEL A

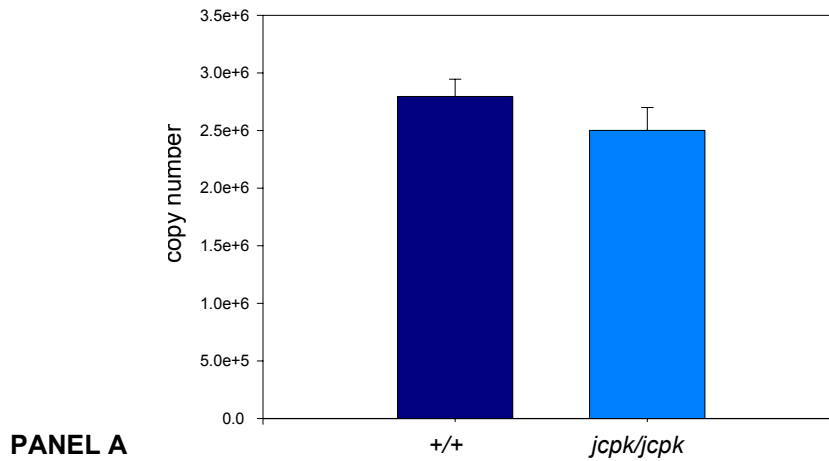


PANEL B

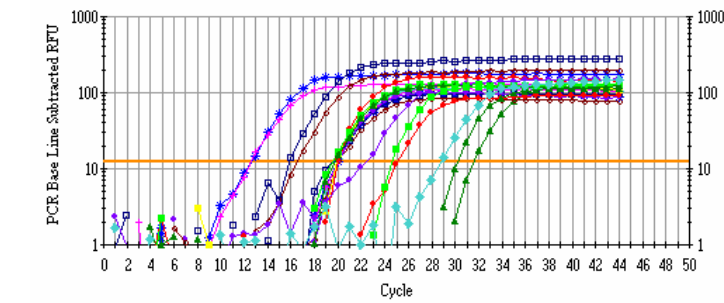


PANEL C

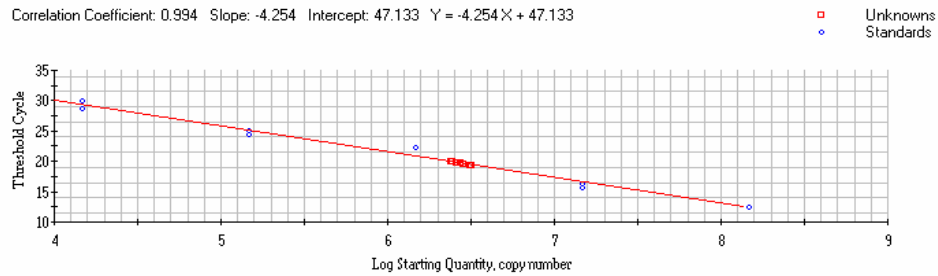
Figure 4.25 Real-time PCR analysis of *Invs* mRNA expression. Equal volumes of cDNA from 4-day old mice were subjected to PCR using primers homologous to a specific region of the mouse *Invs* gene. The reporter used to detect product formation was SYBR Green (1:20,000 dilution). Four replicates of each cDNA sample were compared to amplification standards. **PANEL A:** Template quantity analysis. Means were grouped as (+/+), (+/jcpk), or (jcpk/jcpk) mice. The values shown represent the mean \pm standard error for each groups (+/+ N = 5, +/jcpk N = 5, jcpk/jcpk N = 5). A one-way ANOVA was performed on the above groups. There was no significant difference between genotypic groups ($P = 0.654$). **PANEL B:** Amplification profile plotting Δ RFU (relative fluorescence units) versus cycle number. All sample groups were plotted on the same graph. **PANEL C:** Standard curve generated from the iCycler software (BioRad, Hercules, CA). Blue dots indicate standards and red squares indicate experimental samples.



PANEL A

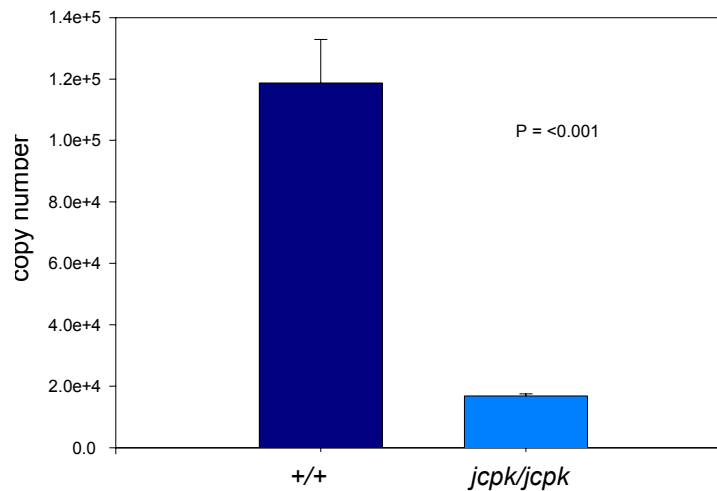


PANEL B

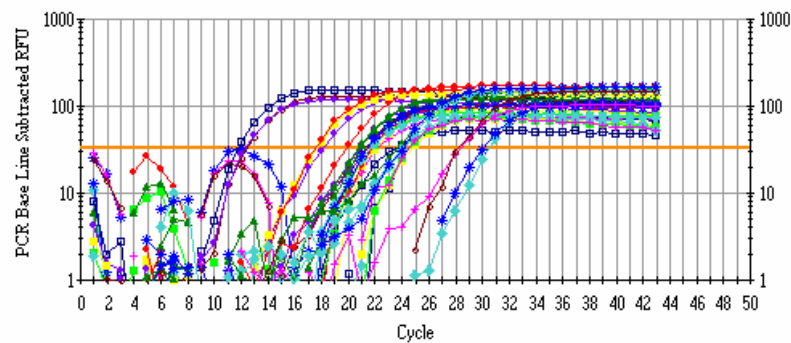


PANEL C

Figure 4.26 Real-time PCR analysis of *jck* mRNA expression. Equal volumes of cDNA from 4-day old mice were subjected to PCR using primers homologous to a specific region of the mouse *jck* gene. The reporter used to detect product formation was SYBR Green (1:20,000 dilution). Four replicates of each cDNA sample were compared to amplification standards. **PANEL A:** Template quantity analysis. Means were grouped as *+/+* or *jcpk/jcpk* mice. The values shown represent the mean \pm standard error for each groups (*+/+* N = 5, *jcpk/jcpk* N = 5). A one-way ANOVA was performed on the two groups. There was no significant difference between genotypic groups ($P = 0.127$). **PANEL B:** Amplification profile plotting Δ RFU (relative fluorescence units) versus cycle number. All sample groups were plotted on the same graph. **PANEL C:** Standard curve generated from the iCycler software (BioRad, Hercules, CA). Blue dots indicate standards and red squares indicate experimental samples.



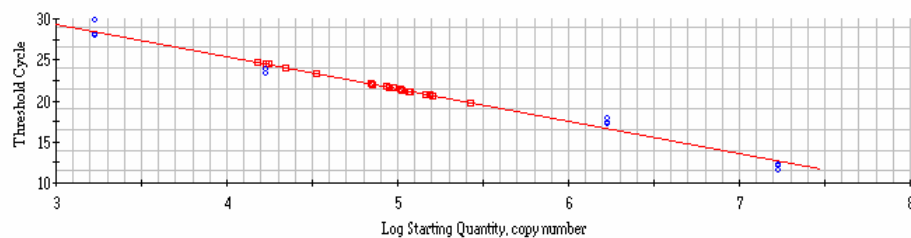
PANEL A



PANEL B

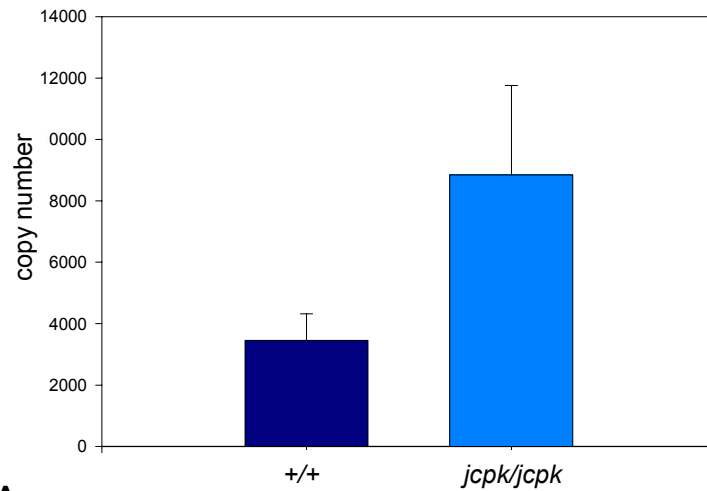
Correlation Coefficient: 0.991 Slope: -3.963 Intercept: 41.278 $Y = -3.963X + 41.278$

□ Unknowns
○ Standards

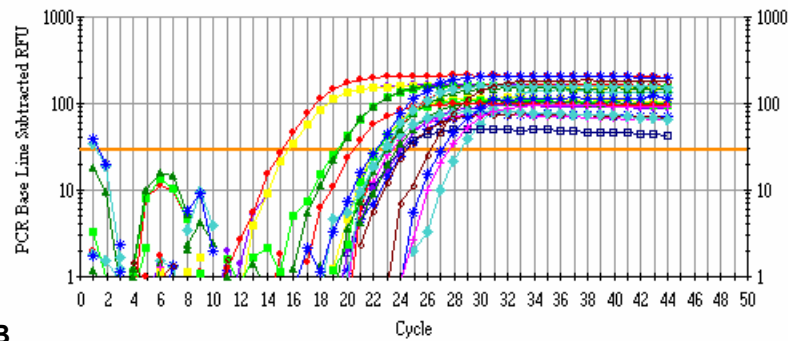


PANEL C

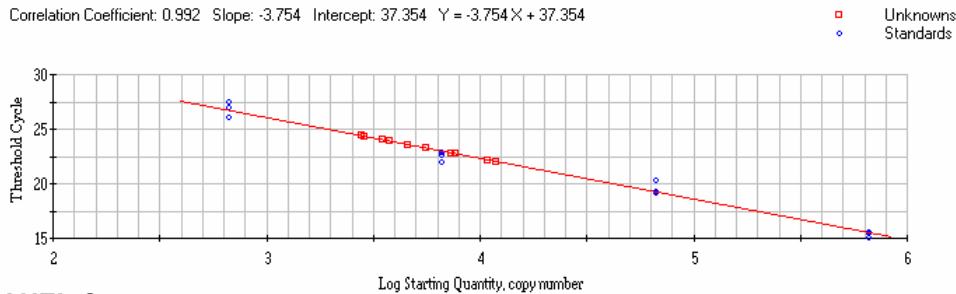
Figure 4.27 Real-time PCR analysis of *kat* mRNA expression. Equal volumes of cDNA from each of four 4-day old mice were subjected to PCR using primers homologous to a specific region of the mouse *kat* gene. The reporter used to detect product formation was SYBR Green (1:20,000 dilution). Four replicates of each cDNA sample were compared to amplification standards. **PANEL A:** Template quantity analysis. Means were grouped as (+/+) or (*jcpk/jcpk*) mice. The values shown represent the mean \pm standard error for each groups (+/+ N = 2, *jcpk/jcpk* N = 2). A one-way ANOVA was performed on the two groups. There was a significant difference between genotypic groups ($P = <0.001$). **PANEL B:** Amplification profile plotting Δ RFU (relative fluorescence units) versus cycle number. All sample groups were plotted on the same graph. **PANEL C:** Standard curve generated from the iCycler software (BioRad, Hercules, CA). Blue dots indicate standards and red squares indicate experimental samples.



PANEL A



PANEL B



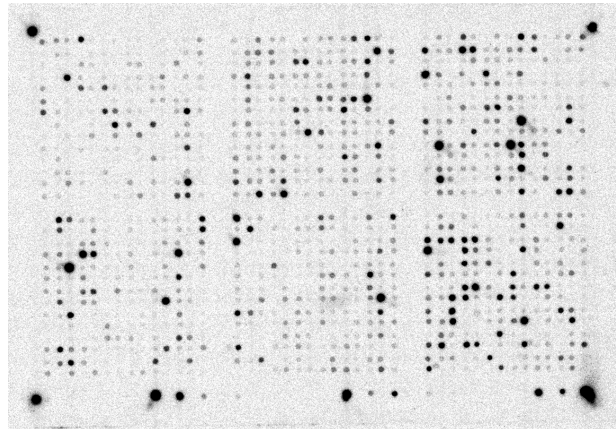
PANEL C

Figure 4.28 Real-time PCR analysis of *cpk* mRNA expression. Equal volumes of cDNA from each of four 4-day old mice were subjected to PCR using primers homologous to a specific region of the mouse *cpk* gene. The reporter used to detect product formation was SYBR Green (1:20,000 dilution). Four replicates of each cDNA sample were compared to amplification standards. **PANEL A:** Template quantity analysis. Means were grouped as *+/+* or *jcpk/jcpk* mice. The values shown represent the mean \pm standard error for each group (*+/+* N = 2, *jcpk/jcpk* N = 2). A one-way ANOVA was performed on the two groups. There was a significant difference between genotypic groups (P = 0.012). **PANEL B:** Amplification profile plotting Δ RFU (relative fluorescence units) versus cycle number. All sample groups were plotted on the same graph. **PANEL C:** Standard curve generated from the iCycler software (BioRad, Hercules, CA). Blue dots indicate standards and red squares indicate experimental samples.

Microarray Analysis

Renal gene misexpression is a feature of polycystic kidney disease in rodents and is reflective of changes in cell proliferation, apoptosis, differentiation and morphogenesis. In order to better understand the mechanism(s) involved in the pathogenesis of renal cystic disease in the *jcpk* mouse model for polycystic kidney disease, gene expression profiling by microarray analysis was performed using 8-day old littermates from a *+jcpk* X *+jcpk* genetic cross (Figure 4.29).

PANEL A



PANEL B

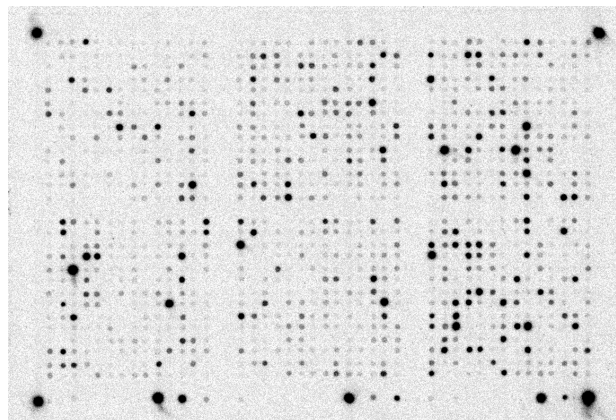


Figure 4.29 Microarray analysis of normal versus polycystic kidneys. The Atlas Mouse 1.2 Microarray used for this analysis contains over 1,176 different genes (CLONTECH, Mt. View, CA). These genes were profiled for differences in expression between normal (+/+) and affected (*jcpk/jcpk*) kidney. PANEL A: Normal kidney microarray panel. PANEL B: *jcpk/jcpk* kidney microarray panel.

Expression differences in the *jcpk/jcpk* kidney were only considered significant if they represented a two-fold difference (plus or minus) when compared to the normal control. Of the more than 1100 genes profiled on the mouse microarray, 50 genes were found to have higher expression values (> 2-fold difference) and 152 genes were found to have lower expression values (< 2-fold difference) in *jcpk/jcpk* kidneys when compared to normal kidneys. In the cystic kidney, alterations in the expression levels of mRNAs were found, for the most part, in one of four general groups: proliferation/cell growth, apoptosis, extracellular matrix, or cellular junction components.

Several genes were abnormally expressed that exert an effect on cellular growth and proliferation. Two *Pax* genes, *Pax2* and *Pax8*, were found to be elevated in *jcpk/jcpk* kidneys. *Pax2* was elevated almost 3-fold in mutant kidney compared to wild type, whereas *Pax8* was elevated 2-fold. Normally, both *Pax2* and *Pax8* are expressed in the mesenchymal/epithelial conversion during nephron formation and decrease as the kidney completes nephrogenesis (279). These genes are down-regulated as the kidney matures. Transgenic overexpression of *Pax2* has been shown to cause epithelial hyperproliferation and cyst formation (58-60, 201). Overexpression of both *Pax2* and *Pax8* in *jcpk/jcpk* kidney is indicative of a hyperproliferative state. The overexpression of *Pax2* was confirmed by real-time PCR analysis which indicated an over five-fold increase of *Pax2* in *jcpk/jcpk* kidney compared to wild type kidney (Figure 4.30).

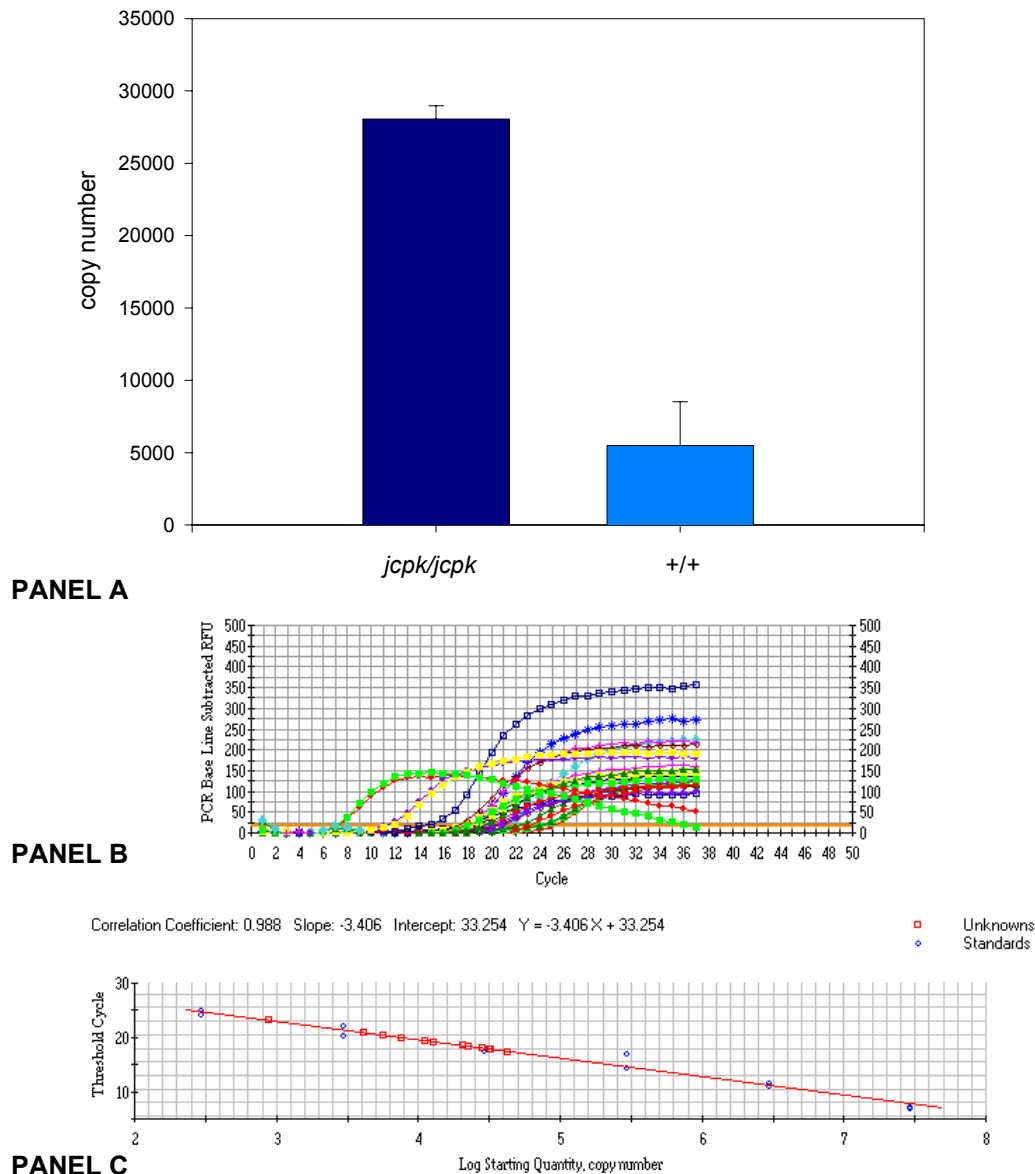


Figure 4.30 *Pax2* gene expression analysis by real-time analysis. Equal volumes of cDNA from 4-day old mice were subjected to PCR using primers homologous to a specific region of the mouse *Pax2* gene. The reporter used to detect product formation was SYBR Green (1:20,000 dilution). Four replicates of each cDNA sample were compared to amplification standards from 10^2 to 10^{10} molecules per reaction. **PANEL A:** Template quantity analysis. Means were grouped as *(+/+)* or *(jcpk/jcpk)* mice. The values shown represent the mean \pm standard error for each group (*+/+* N = 5, *jcpk/jcpk* N = 5) with 4 replicates for each animal. A one-way ANOVA was performed on the above groups. There was a significant difference between genotypic groups ($P = <0.001$) **PANEL B:** Amplification profile plotting Δ RFU (relative fluorescence units) versus cycle number. All sample groups were plotted on the same graph. **PANEL C:** Standard curve generated from the iCycler software (BioRad, Hercules, CA). Blue dots indicate standards and red squares indicate experimental samples.

A study in the *cpk* mouse model for PKD demonstrated that nuclear expression of *Pax2*, which is normally down-regulated in normal mature epithelial cells, is persistent in many epithelial cells in the *cpk* mutant (186). However, reducing the *Pax2* gene dose in the *cpk* mouse model by breeding *cpk/cpk* mice to *Pax2* homozygotes and heterozygotes led to an increase in apoptosis and less severe cystic disease (117). In addition, the high rate of apoptosis in polycystic kidneys may exert counter-proliferative or counter-proto-oncogenic effects which may explain the low incidence of renal cell carcinoma in ADPKD (152, 185).

Proliferation and apoptosis are tightly regulated during nephrogenesis. In normal mature kidneys and in the majority of kidneys with noncystic diseases, there is a very low rate of epithelial proliferation, and apoptotic DNA fragmentation is undetectable. The exact role of apoptosis with respect to cystogenesis is uncertain. However, microarray analysis identified several genes that are known to function in apoptosis that had altered expression in the *jcpk/jcpk* kidney. Expression of the apoptosis regulator *Bax* was elevated 2-fold in the *jcpk/jcpk* kidney compared with the normal kidney. The expression of interleukin-converting enzyme (*Ice*) was also increased 2-fold in the PKD affected kidney. However, the expression of the anti-apoptotic gene *Bcl-2* was found to be down-regulated 2-fold in the affected kidney. It has been established that the ratio of *Bcl-2* to *Bax* determines the relative cellular sensitivity or resistance to apoptotic stimuli (211). This data has not been confirmed by real-time PCR. A decrease in the ratio of *Bcl-2/Bax* favors apoptosis. As a side note, in BALB/c-*cpk* mice, both the expression of *Bax* and *Bcl-2* were elevated (4). This is contradictory to what is seen in the *jcpk* mouse model. However, it has been shown that transgenic knockouts of *bcl-2* develop renal cysts and renal failure (240). Our microarray data suggest an expression pattern in which survival and apoptotic factors are altered thus favoring apoptosis. This seems to suggest that, at least in the *jcpk* mouse model, a decrease in anti-apoptotic factors may exert a cystogenic effect (209). Further studies are needed to define the role of apoptosis in cystic disease progression (209, 231).

A number of cytoskeletal proteins were altered in their gene expression when comparing wild type and affected kidneys. *Fibronectin* had over a 5-fold increase in expression compared to wild type. *Fibronectin* has also been shown to be overexpressed in other mouse models including C57BL/J6-*cpk* and BALB/c-*bpk* (63, 64). Extracellular matrix genes that were also found to be up-regulated greater than 2-fold were *tubulin*, *keratin*, *entactin*, *syndecan*, *nidogen* and *laminin*. The products of all of these genes are required for the function and maintenance of the cytoskeleton within the epithelial cell.

Microarray analysis also indicated that there was a decline in the expression of genes encoding junctional proteins in the *jcpk/jcpk* kidney compared to the normal control. These genes include *alpha-1-catenin*, *occludin*, *integrins* and *cadherin-6*. All of these genes encode proteins that are important in the function and maintenance of cell-cell and cell-matrix contacts including tight junctions, desmosomes and focal adhesions (1, 111, 164, 223).

Other genes found to have putative protein interactions with *jcpk* were also found to be altered in the microarray analysis. Yeast two-hybrid analysis was performed and using *Bicc1* as bait, several putative interactions were identified (E. Bryda, unpublished data). Two of these proteins were the 40S ribosomal subunit and ubiquitin conjugating enzyme E2. Genes for both of these were found to be down-regulated in cystic kidneys. Whether these are true interactions and their decreased expression is a direct result of the *Bicc1* mutation has yet to be determined.

Analysis of the EGFR Receptor and Ligands

A number of elegant studies during the last decade have provided evidence for a major role for the epidermal growth factor (EGF)-transforming growth factor- α (TGF- α)-EGF receptor (EGFR) axis in promoting epithelial hyperplasia, cyst formation and enlargement, and for its potential as a target for treatment in PKD. It has been previously demonstrated that the expression of *Egf* mRNA and protein is markedly down-regulated in the kidneys of *cpk* and *pcy*

mice and of Han:SPRD-Cy rats (44, 74, 136, 275). The expression of *Tgf- α* mRNA and protein in human ADPKD kidneys was found to be increased (136). Both *Egf* and *Tgf- α* utilize the same receptor, *Egfr*, and have been shown to induce abnormal epithelial hyperplasia and solute transport in both murine metanephric organ culture and in normal human kidney cell in culture, leading to cyst formation (184). Further, this ligand-induced cyst formation is mediated by *Egfr* tyrosine kinase activity (184). *Egfr* (*ErbB1*) is overexpressed and mislocated to the apical surface of cystic epithelial cells in human ADPKD and ARPKD, as well as in the *cpk*, *bpk*, and *orpk* mouse models of PKD (61, 244).

In order to determine the mRNA expression of *Egfr*, *Egf*, and *Tgf- α* , both relative RT-PCR and real-time PCR were employed to identify differences in age-matched +/+ and *jcpk/jcpk* kidneys. Relative RT-PCR is a commonly used method for the quantitative analysis of gene expression. The assumption behind this method is simple: start with equal amounts of RNA from multiple samples, use identical RT-PCR conditions on each, and amplify the same target from each sample. Relative RT-PCR requires an optimized internal control, such as β -actin, and can sometimes take more time than real-time PCR to obtain reproducible results. This is because real-time PCR is a technique allowing the quantification of starting amounts of nucleic acid during the PCR reaction without the need for post-PCR analysis. Amplification is measured directly, as discussed earlier, using a fluorescent reporter to monitor the PCR reaction as it occurs in real time. This eliminates the need for both post-run electrophoresis and densitometry analysis. The starting amount for each unknown template can be determined immediately following the PCR reaction.

Both relative and real-time PCR analyses show that *Egfr* mRNA is expressed in higher levels in *jcpk* homozygous mice compared to unaffected littermates (+/+) (Figure 4.31 and 4.32). Both analyses indicate a two to three-fold difference in expression between wild type and *jcpk* homozygous samples. Both analyses indicated no difference in *Tgf- α* mRNA expression in normal versus affected mice (Figure 4.33 and Figure 4.34). This is different than what is seen in human ADPKD and other mouse models where *Tgf- α* was found to be

up-regulated (136). Also, relative RT-PCR showed no difference in *Egf* expression, but it was found to be down-regulated (1.5-fold decrease) using real-time analysis in *jcpk/jcpk* mice (Figure 4.35 and 4.36). Real-time PCR is considered to be a much more sensitive quantitative method than relative PCR. This could account for the difference in expression found between the two methods.

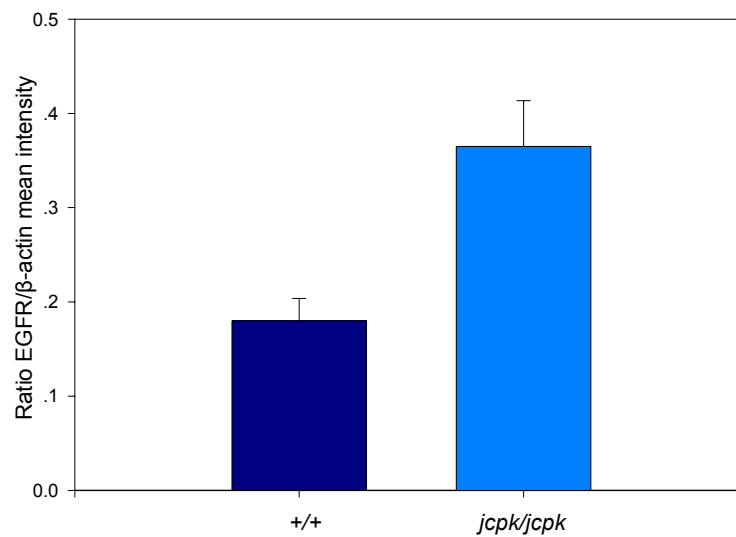
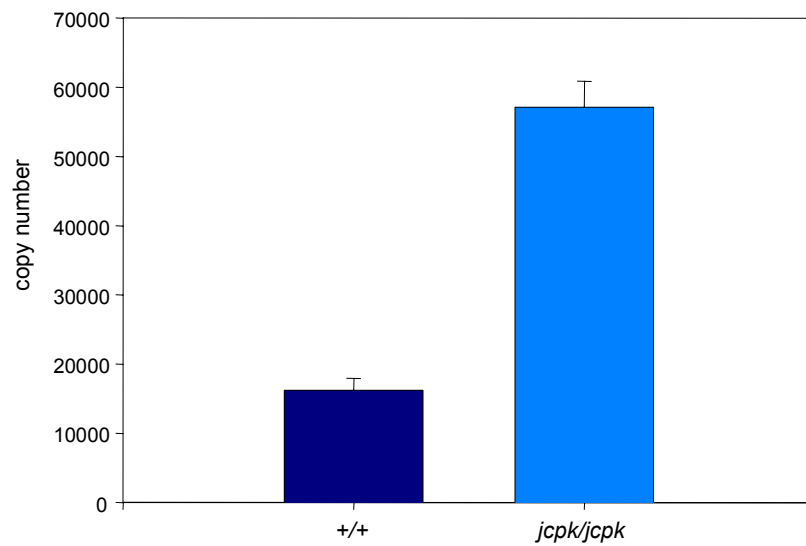
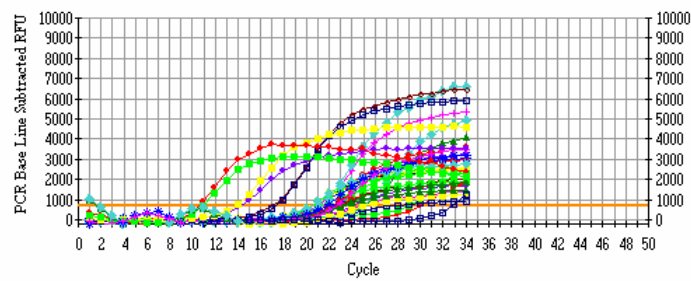


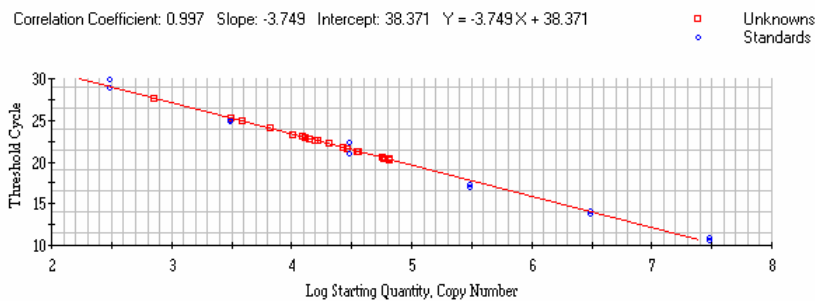
Figure 4.31 RT-PCR analysis of *Egfr* (*ErbB1*) gene expression. Relative RT-PCR analysis of *Egfr* mRNA expression in 4-day old mouse kidney. An unpaired two-tailed t-test revealed a difference in the mean values of the two groups (wild type N=4, *jcpk/jcpk* N=4) that is greater than would be expected by chance. Thus, there is a statistically significant difference between affected and normal groups ($P = 0.011$). EGFR is expressed at higher levels in affected mice. *B-actin* was used as an internal control. The y-axis was determined by dividing the mean band intensity of *Egfr* by the mean band intensity of β -actin.



PANEL A



PANEL B



PANEL C

Figure 4.32 Real-time PCR analysis of *Egfr* mRNA expression. PANEL A: Template quantity analysis of 4-day old normal (+/+ N=4) and affected littermates (*jcpk/jcpk* N=4). An unpaired two-tailed t-test showed a significant difference between groups. ($P = < 0.001$). **PANEL B:** Amplification profile of EGFR amplification up to 35 cycles. **PANEL C:** Standard curve generated from standards ranging from 300 to 3×10^9 product molecules per reaction.

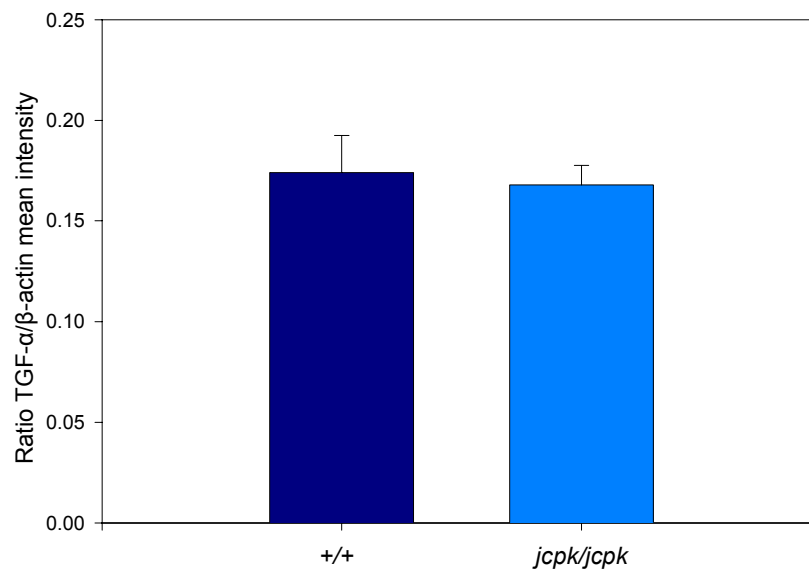
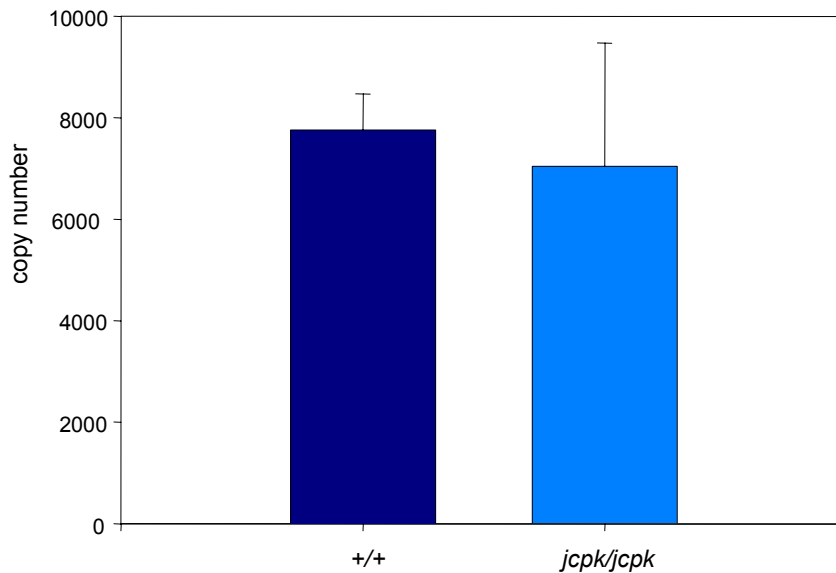
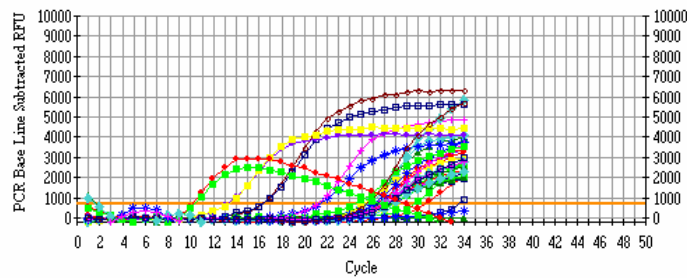


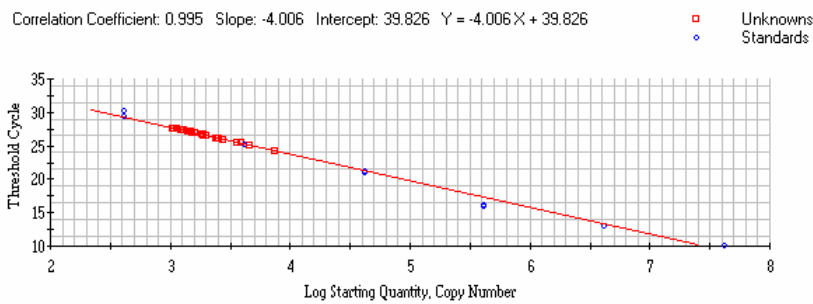
Figure 4.33 RT-PCR analysis of *Tgf-α* gene expression. Relative RT-PCR analysis of *Tgf-α* mRNA expression in four day-old mice (wild type N=4, *jcpk/jcpk* N=4). Analysis performed as in Figure 4.31. An unpaired two-tailed t-test revealed no difference between affected and non-affected groups ($P = 0.863$).



PANEL A

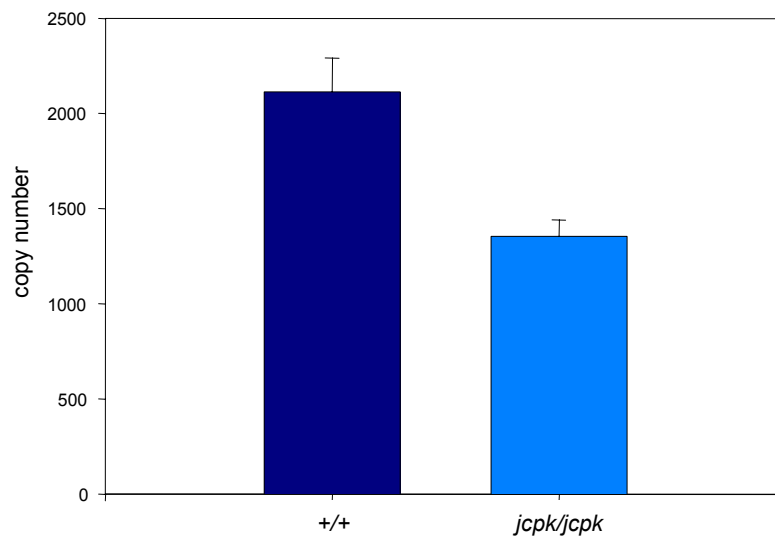


PANEL B

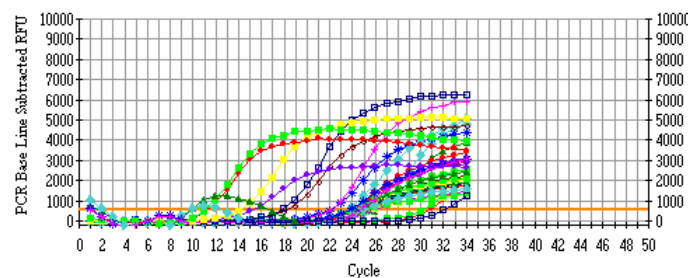


PANEL C

Figure 4.34 Real-time PCR analysis of *Tgf-α* mRNA expression. **PANEL A:** Quantity analysis of 4-day old normal (wild type N=4) and affected 4-day old littermates (*jcpk/jcpk* N=4). An unpaired two-tailed t-test showed no significant difference between groups ($P = 0.696$). **PANEL B:** Amplification profile of *Tgf-α* amplification up to 35 cycles. **PANEL C:** Standard curve generated from standards ranging from 300 to 3×10^9 product molecules.

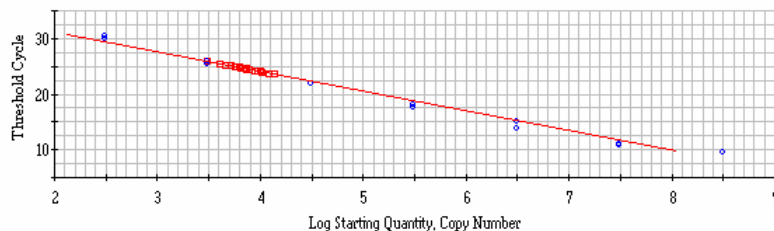


PANEL A



PANEL B

Correlation Coefficient: 0.992 Slope: -3.520 Intercept: 38.144 $Y = -3.520X + 38.144$



PANEL C

Figure 4.36 Real-time PCR analysis of *Egf* mRNA expression. The reporter used to detect product formation was SYBR Green. Three replicates of each 4-day old littermate were compared to amplification standards ranging from 400 to 4×10^9 molecules per reaction. **PANEL A:** A mean quantity for each littermate was determined and those means were grouped as either normal or PKD affected mice. The values shown represent the mean \pm standard error for each group (normal $N = 4$, PKD $N = 2$). An unpaired two-tailed t-test was performed on the above groups. There was a significant difference between groups ($P = 0.048$). **PANEL B:** Amplification profile plotting Δ RFU (relative fluorescence units) versus cycle number. All sample groups and standard groups are plotted on the same graph. **PANEL C:** Standard curve generated from the BioRad iCycler software. Blue dots indicate standards and red squares indicate unknown samples.

To begin to explore the possible relationship between the *jcpk* mutation and *Egfr*, a genetic approach was taken. Mice heterozygous for the *jcpk* allele were bred with mice carrying the *waved-2* mutation, a point mutation that decreases EGFR tyrosine kinase activity. Mice that carry two mutant *waved-2* alleles are recognized phenotypically by the presence of a wavy coat and curly whiskers (Figure 4.37).

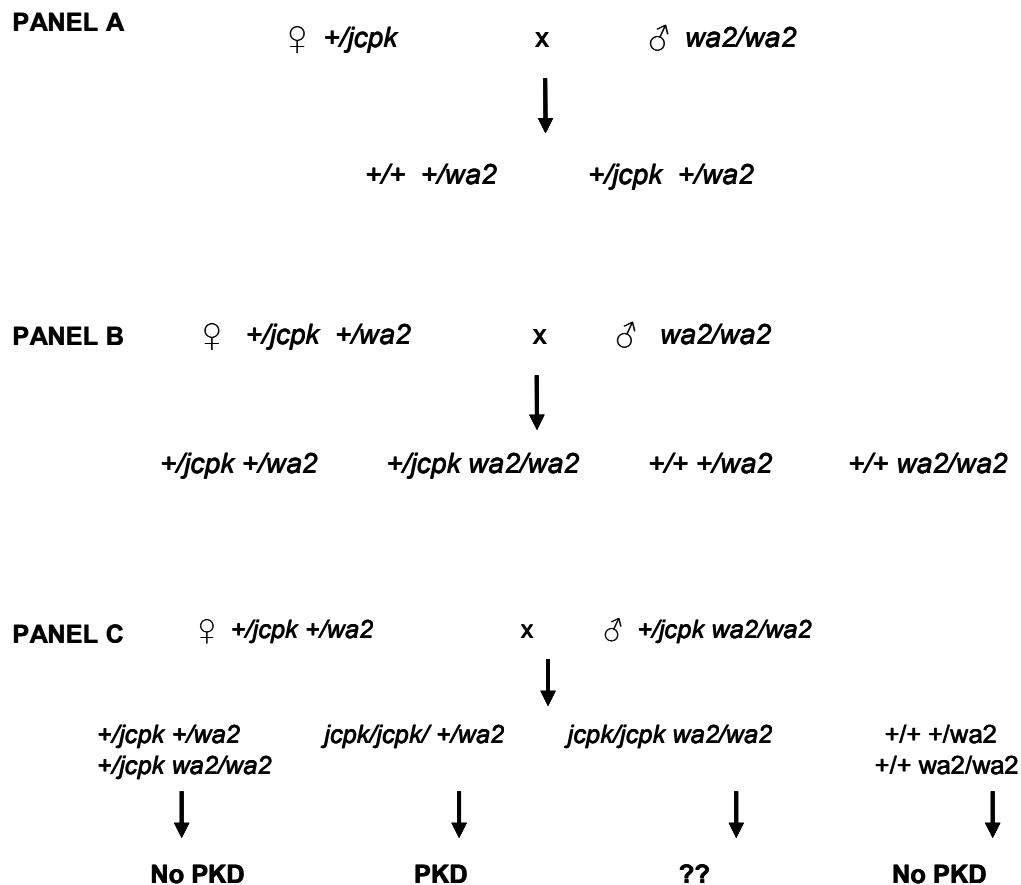


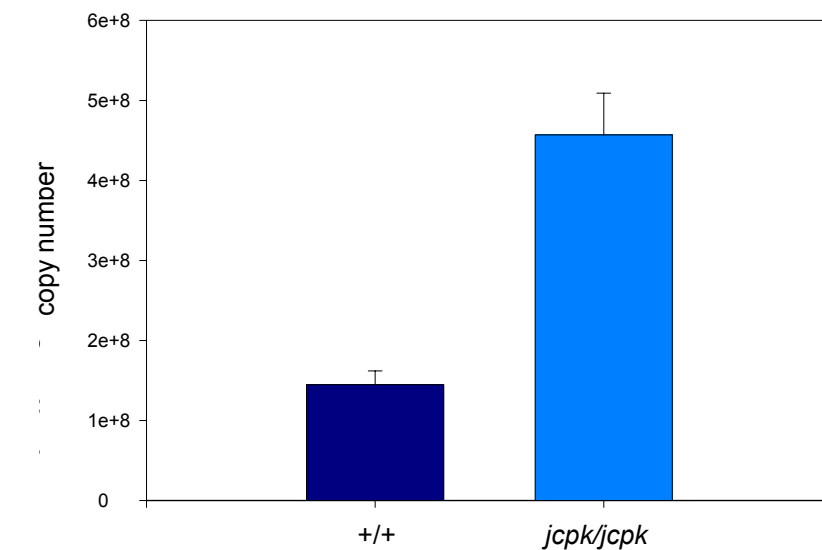
Figure 4.37 Breeding scheme between *jcpk* and *waved-2* mice. A three-part breeding scheme was used to produce double homozygous mice to determine if the *wa2* mutation has an effect on PKD progression in *jcpk* homozygotes. **PANEL A:** Cross 1: *+/jcpk* females and *wa2/wa2* males were mated to produce mice that were heterozygous for both the *jcpk* and *waved-2* mutations. **PANEL B:** Cross 2: double heterozygous females generated in Cross 1 were mated to *wa2/wa2* males to produce offspring for use in Cross 3. **PANEL C:** Cross 3: double heterozygous females were mated to males that were heterozygous for the *jcpk* mutation and homozygous for the *wa2* mutation. The genotypes and expected phenotypes of the offspring are indicated.

The rationale for undertaking this approach was based on a previous study in the *orpk* mouse model for PKD where animals homozygous for both *orpk* and *waved-2* showed a marked decrease in the formation of collecting tubule cysts and an improvement in renal function. This study served as the basis for clinical trials in which PKD patients were treated with EGFR tyrosine kinase inhibitors (244).

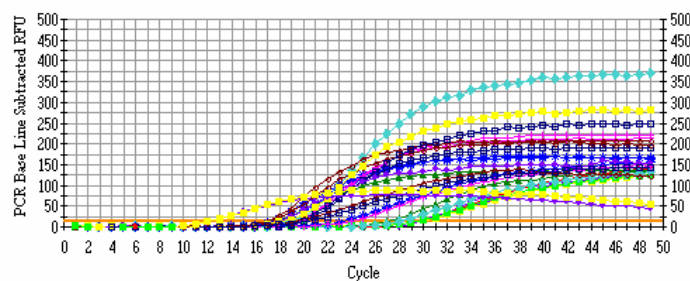
If the higher levels of EGFR detected in *jcpk/jcpk* kidneys by RT-PCR and real-time PCR analysis (Figures 4.31 and 4.32) contribute to cyst formation, it seemed reasonable to hypothesize that decreasing levels of EGFR kinase activity by introducing the *waved-2* mutation might slow cyst progression in *jcpk/jcpk wa2/wa2* animals. Using the crosses described in Figure 4.37, mice homozygous for both mutations were generated and were observed for changes in the progression of the disease, changes in cyst size and time of death. Double homozygotes were extremely rare in this study with fewer than ten double homozygotes detected during a three year period. All double homozygotes that were allowed to live until PKD caused death survived no longer than 10 days after birth. This is similar to the death rate found in *jcpk* homozygous mice. Histological analysis showed no difference in cyst size or disease progression in the kidneys of double homozygous animals when compared to littermates that were homozygous for *jcpk* and either wild type or heterozygous at the *wa2* locus (data not shown). Based on this preliminary data, a decrease in tyrosine kinase activity of *Egfr* does not make a difference in disease progression in the *jcpk* model.

While it has been shown in a number of studies that there is up-regulation of *ErbB1* (*Egfr*) in cystic kidneys, overexpression of *ErbB2* has also been detected in a small number of patients with ADPKD as well as patients with ARPKD (101, 170). *ErbB2* (also referred to as Neu or HER2), is a transmembrane glycoprotein with intrinsic tyrosine kinase activity and is structurally related to epidermal growth factor receptor (EGFR). EGFR often forms active heterodimers with *ErbB2* as well as other members of the EGFR family. *ErbB2* is reported to mediate differentiation and proliferation in epithelial

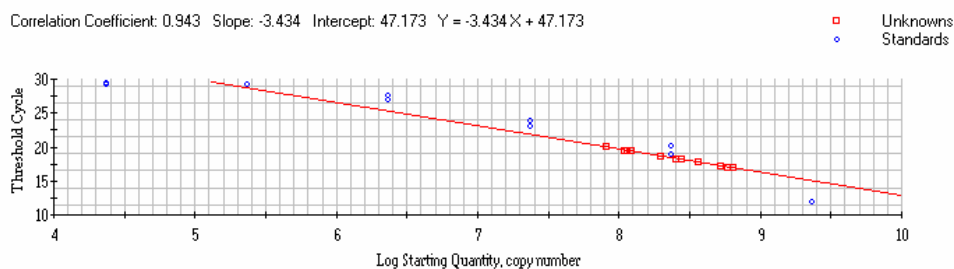
cells and is expressed in a tissue-specific and developmental stage-specific manner (101). Further, the expression of *ErbB2* as a mouse transgene causes multifocal hyperplasia of renal tubular epithelium and cyst formation (242). *ErbB2* was shown to be up-regulated in *jcpk* kidneys in the microarray analysis. Therefore, in order to determine the expression of *ErbB2* in *jcpk/jcpk* versus normal mouse kidney, real-time PCR analysis was performed using primers specific to mouse *ErbB2*. Template quantity analysis showed a 3-fold increase in the expression of *ErbB2* in cystic kidneys (Figure 4.38). Altered expression of *ErbB2* has not been examined in other mouse models for PKD.



PANEL A



PANEL B



PANEL C

Figure 4.38 Real-time PCR analysis of *ErbB2*. The reporter used to detect product formation was SYBR Green. **PANEL A:** A mean quantity for each 4-day old littermate was determined and those means were grouped as either normal (*+/+*) or affected (*jcpk/jcpk*) mice (N=5 (*+/+*), N=5 (*jcpk/jcpk*)). It was determined that there was a statistical difference between groups (P = 0.029). **PANEL B:** Amplification profile plotting Δ RFU (relative fluorescence units) versus cycle number. All sample groups and standard groups are plotted on the same graph. **PANEL C:** Standard curve generated from the BioRad iCycler software. Blue dots indicate standards and red squares indicate unknown samples.

Protein Analysis

Western Blot Analysis

Two distinct mRNA transcripts for mouse *Bicc1* have been previously described (41). These two transcripts differ by one exon at the 3' end of the transcript. The two transcripts were designated transcript A which does not contain the extra exon and is 21 exons in length, and transcript B which contains 22 exons. *In silico* translational analyses of the full-length mRNA transcripts of mouse *Bicc1* has predicted two putative isoforms of the Bicc1 protein. The first isoform derived from mRNA transcript A is 977 amino acids in length with a predicted mass of 105 kDa (Figure 4.13). The second putative isoform derived from mRNA transcript B is 951 amino acids length with a mass of 102 kDa (Figure 4.13). The proteins are predicted to have similar isoelectric points of 8.79 and 8.80, respectively. Western blot analysis using a polyclonal antibody raised in rabbit against amino acids 1-81 of the mouse Bicc1 protein identifies a single protein band in kidney between 75 and 100 kDa (Figure 4.39). This band may represent both putative isoforms of Bicc1 since the resolving power of the polyacrylamide gel was not great enough to separate two proteins so close in size. A smaller band of less than 75 kDa was found to be expressed only in heart. The significance of this unique band as a potential third Bicc1 protein isoform has yet to be determined.

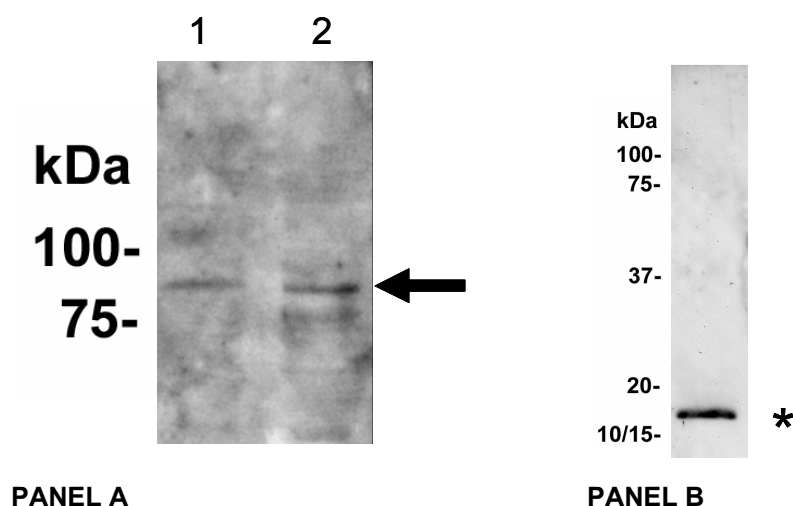


Figure 4.39 Western blot analysis of the Bicc1 protein. **PANEL A:** Western blot containing total protein from +/- mouse kidney (Lane 1) and +/- mouse heart (Lane 2). The blot was probed with a polyclonal antibody raised in rabbit against the first 81 amino acids of the mouse Bicc1 protein. Arrow indicates the Bicc1 protein between 75 and 100 kDa. **PANEL B:** Western blot analysis demonstrating the specificity of the Bicc1 antibody. Asterisk indicates band representing the fusion protein (AB101) which includes the N-terminal 81 amino acids of Bicc1. AB101 was the antigen used to generate the Bicc1 antibody.

Functional Domains

The Bicc1 protein is predicted to contain several putative functional domains (Figure 4.40). Three K homology (KH) domains are located in tandem near the N-terminus. One sterile alpha motif (SAM) is located near the C-terminus of the protein. A descriptive nucleotide to amino acid comparison map with highlighted functional domains can be found in Appendix E.



Figure 4.40 Mouse Bicc1 has two types of functional domains. Based on *in silico* motif analysis, the Bicc1 protein contains three KH domains thought to bind RNA and one SAM domain thought to be involved in protein-protein interactions. The specific intercellular functional partners of Bicc1 are currently unknown.

Bicaudal-C Species Conservation

Currently, the function of mammalian Bicaudal-C is unknown; however, previous investigations of the *Drosophila* orthologue, Bic-C, have shown that it is required for a number of processes in oogenesis, including the establishment of anterior-posterior polarity of the oocyte (143, 156). Specifically, Bic-C is a maternally expressed protein that is thought to regulate the translation of *oskar* mRNA during oogenesis (220). Mutations in *Bic-C* in *Drosophila* result in mislocalization of *oskar* mRNA and severe defects in anterior-posterior patterning of the developing embryo (220).

Database mining utilizing pBLAST and multiple sequence alignment carried out with the full-length protein sequence corresponding to mouse Bicaudal-C, determined that the Bicaudal-C protein was present in at least 10 different species. Based on current nucleotide and protein sequence databases containing information from a variety of organisms, the Bicc1 protein is found to be present in *Homo sapiens*, *Mus musculus*, *Rattus norvegicus*, *Xenopus*, *Fugu*, *Caenorhabditis elegans*, *Caenorhabditis briggsae*, *Danio rerio*, *Anopheles gambiae*, and *Drosophila melanogaster*.

The presence of Bicc1 throughout such diverse phyla may indicate an important and highly conserved function. Bicaudal-C protein sequences from all ten species listed above were compared for amino acid conservation (Figure 4.41). Mouse and rat Bicaudal-C shared the most residues in common as did both species of *Caenorhabditis*. However, both species of *Caenorhabditis* share only about 23% of amino acid residues with mouse. When comparing protein sequences of mouse and human, 77% of amino acid residues are conserved between the two species.

%	Mouse	Human	Rat	Xenopus	Fugu	Danio	Drosophila	Anopheles	C.elegans
Mouse									
Human	77								
Rat	85	73							
Xenopus	76	65	67						
Fugu	33	31	33	36					
Danio	53	48	56	51	32				
Drosophila	31	27	27	31	21	21			
Anopheles	33	28	29	32	23	23	44		
C.elegans	24	21	22	23	20	19	21	23	
C.briggsae	23	21	21	24	21	20	22	23	81

Figure 4.41 Sequence comparison of Bicaudal-C from 10 different species. All protein sequences were retrieved from GenBank or Ensembl databases. Amino acids were compared using GeneStream alignment software (www.expasy.org). Values represent the percentage of identical amino acid residues.

SAM Domain

The sterile alpha motif (SAM) domain is a novel protein module of approximately 70 amino acids originally found in a number of developmental proteins (230). It is proposed that SAM domains may mediate protein-protein contacts, yet the molecular mechanisms employed *in vivo* remain unclear (238).

The SAM domain of Bicc1 was examined independently of the whole protein sequence in several species including mouse, rat, human, *Xenopus*, *Drosophila*, *Danio*, and *Anopheles*. Over 95% of all amino acid residues were conserved in 4 of the species examined (Figure 4.42 and Figure 4.43). *Danio rerio* shares close to 60% of its amino acid residues with mouse, rat, human, and *Xenopus*. All organisms examined except for *Danio* contained a conserved tyrosine at position 19 of the SAM domain. This tyrosine is conserved in other SAM domain containing proteins (230). When this tyrosine is phosphorylated within the SAM domain, these proteins bind to SH2 domain-containing proteins in order to mediate cell-cell initiated signal transduction (39).

```

RAT      -FKGSDLPELFSKLGLGKYT--DVFQQQEIDLQTFLLTDQDLKELGITTFGARRKMLLAISELSKN 64
MOUSE    -FKGSDLPELFSKLGLGKYT--DVFQQQEIDLQTFLLTDQDLKELGITTFGARRKMLLAISELSKN 64
HUMAN    -FKGSDLPELFSKLGLGKYT--DVFQQQEIDLQTFLLTDQDLKELGITTFGARRKMLLAISELSKN 64
XENOPUS  -FKGSDLPELFSKLGLGKYT--DIFQQQEIDLQTFLLTDQDLKELGISTFGARRKMLLAISELNKN 64
DANIO    -----HLWSYISTLSLKKIQTKNIIISVCQIDLQTFLLTDQDLKELGITTFGARRKMLLAISEMNKN 62
DROSOPHILA LAKHKDIQTLLTSLGLEHYI--KIFVLNEIDLEVFTLLEENLMELGIAAFGARKKLLTAIHTLLAN 65
ANOPHELES MSQYNDVTILTGLGLEHYI--KNFINGEIDMTVFQTLTDQDLNLDIKPLGARRRILMAIHDLVR 65

```

Figure 4.42 Multiple species sequence alignment of the SAM domain of Bicaudal-C. The SAM domains of mouse, rat, human, *Xenopus*, *Danio*, *Drosophila* and *Anopheles* were compared using Multialign and CLUSTAL W software (www.expasy.org) Amino acid residues conserved in all species are highlighted in red. Residues present in four or more species are shown in blue. The conserved tyrosine is positioned at residue 19. *Fugu* and *C.elegans* were not included because their relative amino acid conservation compared to other species was less than 10%.

%	Mouse	Human	Rat	Xenopus	Danio	Drosophila
Mouse						
Human	98					
Rat	100	98				
Xenopus	95	96	95			
Danio	58	59	58	59		
Drosophila	48	48	48	50	35	
Anopheles	43	42	43	42	30	49

Figure 4.43 Percent sequence homology of the Bicc1 SAM domain in 7 species. The SAM domain is highly conserved among mouse, human, rat, and *Xenopus*. Sequences were aligned and compared using Multialign and CLUSTAL W analysis software. The sequence homology between species is given as a percentage.

KH Domains

The K homology (KH) domain was first identified in the human heterogeneous nuclear ribonucleoprotein (hnRNP) K (236, 237). It is an evolutionarily conserved sequence of approximately 70 amino acids that is present in a wide variety of quite diverse nucleic acid-binding proteins (81). While a detailed picture of the KH domain-nucleic acid interaction is not yet available, a number of proteins containing KH domains have been shown to bind RNA (81). KH motifs are found in one or multiple copies, suggesting that they may function cooperatively or, in the case of single KH motif proteins, independently. Significant sequence similarity in the KH motifs of proteins from

different species reflects descent from a common ancestor and a high degree of functional conservation.

The KH domains of Bicaudal-C in 10 phyla were examined using the computer program MotifScan (www.expasy.com) to determine their conservation and amino acid identity. MotifScan compares the protein of interest to current protein databases to determine if and what protein motifs are present and utilizes a statistical algorithm to score whether these matches are true or false positives based on amino acid identity. All three of the KH domains are present in all species examined except for *Danio rerio* which only contains KH3 (Table 4.4).

Table 4.4 Conservation of KH domains across species

Species	KH Domains	Domains Conserved
Mouse	3	KH1, KH2, KH3
Human	3	KH1, KH2, KH3
Rat	3	KH1, KH2, KH3
<i>Xenopus</i>	3	KH1, KH2, KH3
<i>Fugu</i>	3	KH1, KH2, KH3
<i>Danio rerio</i>	1	KH3
<i>Drosophila</i>	3	KH1, KH2, KH3
<i>Anopheles</i>	3	KH1, KH2, KH3
<i>C. elegans</i>	3	KH1, KH2, KH3
<i>C. briggsae</i>	3	KH1, KH2, KH3

Multi-sequence alignment of all three KH domains in 9 species indicates a high degree of amino acid conservation. Mouse and human share 88% of the residues within their KH domains (Figure 4.44). Interestingly, *Danio rerio* only contains KH3 but this domain is over 80% similar to mouse, human, rat, and *Xenopus*. *C. elegans* is the most divergent sharing only 20-30% of its amino acid residues with other species.

Next, individual KH domains were compared among different species. Over 98% of amino acids are conserved in KH2 and KH3 when comparing mouse and human sequences (Appendix F). However, only 72% of residues are conserved when comparing the residues within KH1. Even the sequence between the KH domains seems to be conserved. When comparing mouse and human sequences, there is 100% conservation of the amino acids located between the KH1 and KH2 domains and over 94% conservation of the amino acids located between the KH2 and KH3 domains.

%	Mouse	Human	Rat	Xenopus	Fugu	C.elegans	Danio	Drosophila
Mouse								
Human	88							
Rat	98	95						
Xenopus	92	81	91					
Fugu	75	67	65	76				
C. elegans	28	22	26	27	20			
Danio	80	83	80	80	77	8		
Drosophila	49	41	47	47	44	24	38	
Anopheles	50	44	49	48	46	25	40	69

Figure 4.44 Percent sequence homology of all three KH domains. The KH domain is highly conserved among mouse, human, rat, and *Xenopus*. Sequences were aligned and compared using Multalign and CLUSTAL W analysis software.

GXXG Consensus Conservation

The most conserved sequence within the KH domain is the consensus VIGXXGXXI where X is any amino acid. This conserved sequence most often maps within the middle of the KH domain and is thought to mediate the function of the motif (87). Further, the conformations of residues in and around the KH consensus are very similar among different KH-containing proteins. The importance of this sequence is that it is where the protein chain is thought to fold into two alpha helices at an angle of 100°-120° to each other. This folding is vital to the function of the KH domain. A variable residue turn (GXXGXX) is the “hinge” that connects these two helices. The two largely invariant glycines separated by two variable residues in the turn (GXX) serve as C- and N-caps of the two alpha helices. KH2 and KH3 of mouse Bicc1 protein have the conserved consensus motif (Figure 4.45). KH1 is observed by *in silico* analysis in almost all of the species considered; however, this domain does not fit the amino acid

pattern (GXXGXX) commonly seen in other KH domains (or KH2 and KH3 for that matter). Based solely on conservation analysis, KH1 would not be expected to function in a similar way as KH2 and KH3 domains despite its species conservation. Perhaps this domain has a function in stabilizing the folding of the Bicc1 protein for RNA or protein binding. More studies need to be performed to evaluate this function. Both KH2 and KH3 have been preserved throughout a number of phyla (Figure 4.45). The exceptions are *Drosophila*, *Anopheles*, and *C. elegans*.

	KH2	KH3
CONSENSUS	VIGXXGXXI	VIGXXGXXI
MOUSE	VIGKGGNNI	MMGRNGSNV
HUMAN	VIGKGGNNI	MMGRNGSNI
RAT	VIGKGGNNI	MMGRNGSNV
XENOPUS	VIGKGGNNI	MMGRNGCNI
FUGU	VIGKGGNNI	MKGRNGSNI
DANIO		MMGRNGSNI
DROSOPHILIA	IIGRGGNNI	VKGKNNVNL
ANOPHELES	IIGRGGNNI	VLGRSSSNL
C.ELEGANS	IIGKGGRGI	GLLRTESNL

Figure 4.45 Consensus sequence comparison in multiple species. KH domains two and three were compared to the VIGXXGXXI consensus sequence present in functional KH motifs. Sequences were aligned using CLUSTAL W on www.expasy.org. *Danio rerio* only contains the third KH domain. Blue highlight indicates amino acid is conserved in five or more species examined. Red highlight indicates amino acid is conserved in all species examined.

Structural analysis of the mouse Bicc1 KH domains indicates that the domains fall into the category of type-1 KH motifs. Type-1 KH motifs contain a beta-alpha-alpha-beta-beta-alpha folding structure where the VIGXXGXXI consensus motif is located between helices 1 and 2. Other KH domain containing proteins that fall within this category are FMR1, Vigilin (Vg1), and Nova-1 (100, 237), (29).

RNA Binding Study

In vitro RNA-binding properties of His-V5-Bicc1

Many KH proteins can bind either RNA or single-stranded DNA *in vitro* (29). Currently, the physiological targets of mouse Bicc1 are unknown. An accepted methodology to test whether a protein has affinity for RNA is its *in vitro* ability to bind to synthetic homoribopolymers. In order to determine the RNA binding ability of mouse Bicc1, a full-length *Bicc1* construct and a number of constructs containing only portions of the *Bicc1* gene were designed and used in binding assays with poly(U)-Sepharose beads. The PCR-derived constructs encoding the full-length recombinant histidine-V5-mouse Bicc1 or partial forms were directionally inserted into pET101/D-TOPO (Figure 4.46 and Appendix G).

Recombinant proteins were expressed in BL21 (DE3) chemically competent *E. coli*. Cell lysates for each recombinant construct were incubated with either poly(U)-Sepharose or Sepharose 4B agarose beads. Proteins retained on the beads were separated by SDS-PAGE and analyzed by immunoblotting using a horseradish peroxidase-conjugated monoclonal antibody specific to the V5 epitope on each recombinant protein. The results of the RNA binding assays are summarized in Figure 4.47.

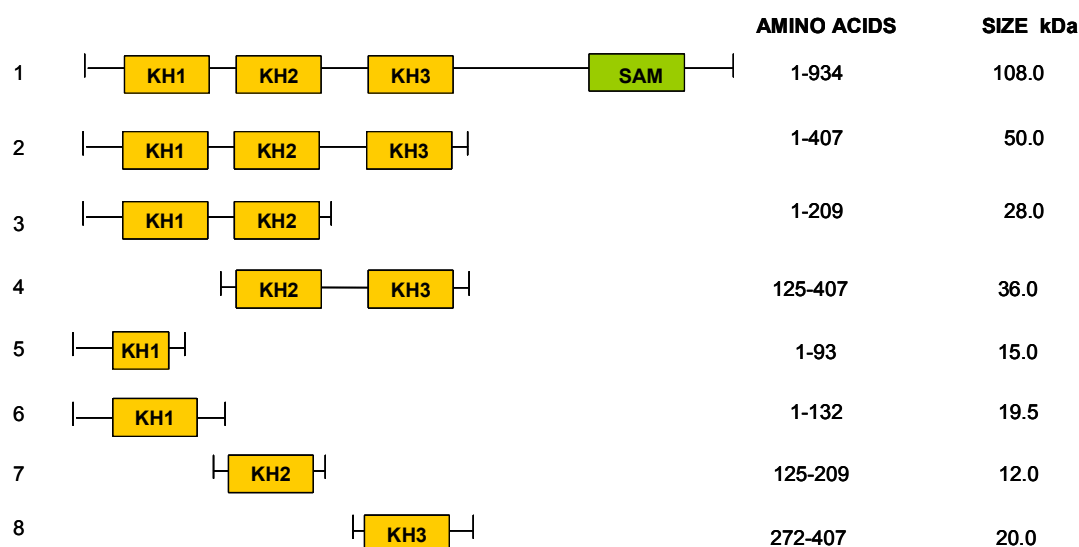


Figure 4.46 Schematic diagram summarizing recombinant RNA binding constructs. RT-PCR products were directionally cloned into the pET101/D-TOPO vector and expressed in BL21(DE3) cells. The relative sizes for each expressed recombinant protein and the amino acids of Bicc1 encoded by each construct are listed to the right of the construct.

The full-length Bicc1 construct (#1, Figure 4.47) as well as the recombinant construct containing only three KH domains (#2, Figure 4.47) bound to poly(U) in the presence of 150 mM NaCl concentration. The construct representing the putative protein produced due to the *Bicc1*^{jcpk} mutation (#5, Figure 4.47) did not bind poly(U). This indicates that the mutation eliminates the RNA binding function of the protein. When the constructs were assayed with Sepharose 4B agarose beads alone, no signal was detected.

To more precisely determine which domain(s) is required for mouse Bicc1 to bind RNA, recombinant constructs were designed that contained either two domains or a single isolated KH domain. The construct containing KH domains two and three (#4, Figure 4.47) was retained on the homoribopolymers; however, the construct containing only KH domains one and two (#3, Figure 4.47) was not retained. Further, of the single KH domain constructs, only the construct containing KH3 (#8, Figure 4.47) bound to RNA. This suggests that KH domain three is responsible for RNA binding. Data is summarized in Figure 4.48.

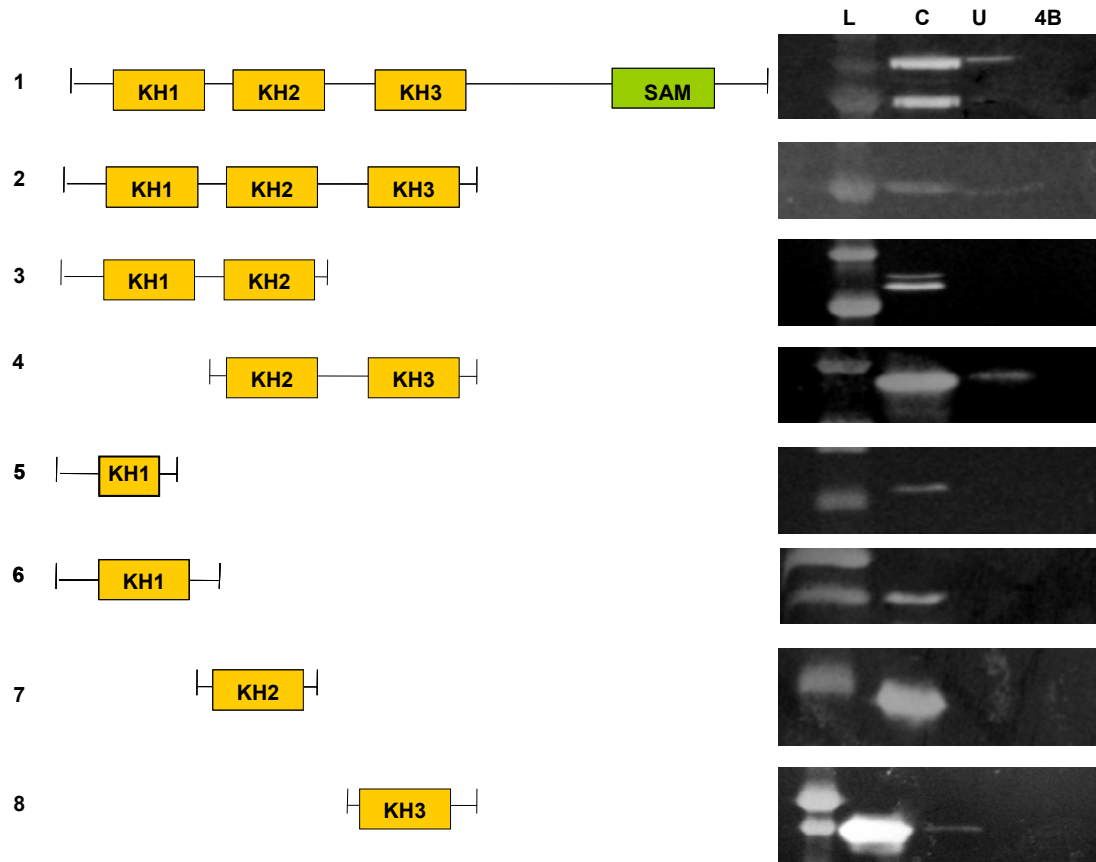


Figure 4.47 RNA binding assay using immobilized poly(U) homoribopolymer. Recombinant constructs are numbered on the left and the corresponding binding results are shown to the right of each construct. Lane L is a protein molecular weight ladder, Lane C is the isolated cell lysate (a positive control indicating the expression of each recombinant protein). Lane U contains the lysate exposed to poly(U) Sepharose. Presence of the recombinant protein in this lane indicates successful binding. Lane 4B is the lysate plus Sepharose 4B (negative control). Pictures are a summary of at least two independent observations.

The data indicating that KH3 is important for binding correlates well with previous experiments in *Drosophila* involving a strong mutant allele in *Bic-C*, *Bic-C^{RU35}*, which carries a point mutation leading to a substitution of arginine for glycine (amino acid 295). This mutation is just prior to KH3 and was found to completely abolish Bic-C binding to *oskar* mRNA during oogenesis (143, 220). This substitution is predicted to destabilize KH domain three by placing a charged residue into a hydrophobic core. This would suggest that KH3 is important for Bic-C protein function.

<u>RECOMBINANT CONSTRUCT</u>	<u>BINDING</u>
Full Length	YES
KH1+KH2+KH3	YES
KH1 + KH2	NO
KH2 + KH3	YES
KH1 only	NO
<i>jcpk</i> mutation	NO
KH2 only	NO
KH3 only	YES

Figure 4.48 Summary of RNA binding analysis. All constructs containing KH3 were found to bind poly(U) Sepharose.

Asymmetry Study

L/R Patterning Defects in *jcpk/jcpk* Mice

The establishment of the three body axes – anteroposterior (A/P), dorsoventral (D/V) and left-right (L/R) – is central to the organization of the vertebrate body plan. Nearly all visceral organs of the thorax and abdomen are L/R asymmetrical with respect to the midline. The L/R axis is established last and defects that arise from abnormal L/R patterning are less severe than aberrant A/P or D/V patterning. Some anomalies in humans associated with L/R patterning include *situs inversus*, organ isomerism, or single organ inversions. These anomalies have been shown to occur in approximately 1 in 10,000 patients (95). The process in which L/R asymmetry is established involves the biased transfer of signaling molecules via rapidly beating cilia (153).

Cilia and flagella are complex organelles with more than 200 peptides involved in their formation, maintenance, and function (99). Mutations in the genes that code for these proteins have been implicated in disorders such as retinal degeneration, *situs inversus*, and polycystic kidney disease (PKD). There is a growing body of evidence that links ciliary dysfunction, embryonic L/R

patterning defects and cystic disease of the visceral organs (e.g., kidney, liver and pancreas) (99, 108, 172, 197). In order to determine if L/R patterning defects were present in the *jcpk* mouse model of PKD, an anatomical survey of litters was performed. Mating between *+jcpk* heterozygous mice were performed and litters from these matings that contained at least one polycystic pup were sacrificed at 4 or 5 days after birth. Internal organs were evaluated for patterning defects visible by gross examination. Any defects present were recorded and tail snips were taken for genotype analysis. Individual characteristics were recorded in a searchable database to determine the statistical occurrence of any defects.

Genotype analysis indicated that of the 129 mice used in the study, 35 were *+/+*, 57 were *+jcpk* mice and 37 were *jcpk/jcpk*. Twenty-five litters were examined where six was the average litter size with a range of 2-11 pups/litter. Of the 37 homozygous *jcpk/jcpk* mice dissected, one mouse was found to have multiple patterning defects. These abnormalities include altered heart situs and right pulmonary isomerism (Figure 4.49). Normally, the apex of the heart is pointed toward the left (levocardia). However, in dextrocardia, the apex of the heart is abnormally pointing toward the right. A normal set of mouse lungs contains five individual lobes with four lobes on the right and a single lobe on the left. This is often referred to as a 4 + 1 arrangement. When right pulmonary isomerism occurs, the four right lung lobes are mirrored on the left, where the lung lobes are present in a 4 + 4 arrangement. Similar asymmetry defects were also observed in transgenic *pkd-2* mutant embryos (197). Since only 37 *jcpk/jcpk* mice were examined, more mice are needed to establish a solid link between the *jcpk* mutation and L/R patterning abnormalities.

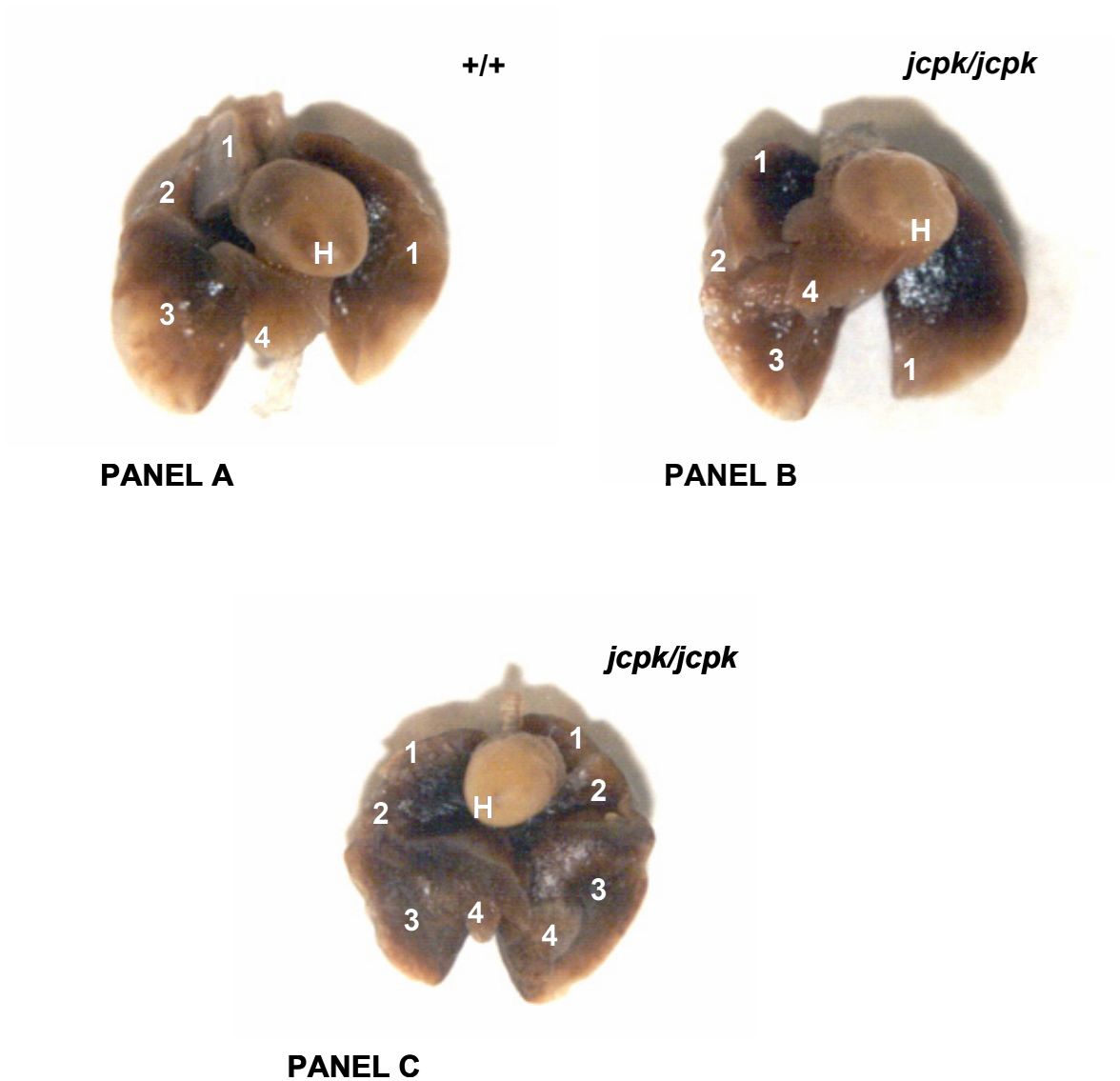


Figure 4.49 Comparison of the presence of L/R patterning defects in littermates. Three animals from the same litter were examined for patterning defects. H = heart, lung lobes are designated by numbers. **PANEL A:** In homozygous normal (+/+) mice, the lungs display normal 4+1 asymmetry and the heart is pointed to the left (levocardia). **PANEL B:** A *jcpk/jcpk* littermate that is asymmetrically normal. **PANEL C:** Another *jcpk/jcpk* littermate. The heart is abnormally positioned to the right (dextrocardia) and the lungs display 4+4 symmetry.

CHAPTER V

DISCUSSION

Summary and Conclusions

Cystic diseases of the kidney are a clinically important and genetically diverse group of disorders that share a common altered regulation of tubular morphology. Despite their clinical and pathological heterogeneity, the fact that the disease results in a similar outcome, cyst formation, has led to extensive investigation into the mechanisms of cystogenesis and disease progression. Renal pathologies found in essentially all forms of polycystic kidney disease include increased fluid secretion, matrix remodeling, increased cellular proliferation, increased apoptosis, and altered differentiation of the epithelial cells lining the renal cysts (257).

Genetic and molecular analysis in a number of animal models has facilitated the characterization of novel genes required for normal epithelial function and maintenance. Ultimately, these discoveries have contributed to the understanding of the cellular pathology of cystic disease. Numerous mouse models have been described with mutant phenotypes that closely resemble human PKD with respect to cyst morphology and localization, as well as disease progression. Among these models, the *juvenile congenital polycystic kidney (jcpk)* model for PKD is distinct from other mouse models for PKD based on its early age of onset and histological appearance.

The objective of the preceding body of research was to characterize the *jcpk* mouse model for polycystic kidney disease (PKD) through both genetic and molecular analyses. The *jcpk* locus was previously localized to a 1 cM region

located on mouse Chromosome 10 (28). Two other mouse models, *bpk* and *67Gso*, were shown to be allelic to *jcpk* through complementation and FISH analyses (90, 206). The purpose of the research was to identify the PKD-susceptibility gene shared by the *jcpk*, *bpk* and *67Gso* mouse models as well as to use current molecular analyses to evaluate the mRNA and protein expression of *jcpk*. These investigations will lay the groundwork for establishing a role for the *jcpk* gene in the context of current theories of PKD pathogenesis.

With the use of genetic and physical mapping strategies, it was determined that the mouse gene, *Bicaudal-C (Bicc1)*, is the disease-susceptibility gene responsible for PKD in the *jcpk* mouse model. The *jcpk* mutation was chemically induced by the mutagen, chlorambucil, and was originally predicted to consist of a large sequence alteration such as a deletion or chromosomal rearrangement (66). This hypothesis was based on previous observations of the predominant mutations produced by this drug (67). However, it was determined that the mutation in the *jcpk* mouse model is a single base-pair change (G to A) in the consensus splice acceptor site prior to exon three (41). Though unexpected that a point mutation would be caused by chlorambucil mutagenesis, it has recently been shown that at least one other chlorambucil-induced mutation is due to a single base pair change in a donor splice site (54). Thus, chlorambucil may induce this type of mutation more frequently than originally thought.

Interestingly, different mutations in the *Bicc1* gene have also been found to be responsible for PKD in the *bpk* and *67Gso* mouse models. All three mutations (*jcpk*, *bpk*, and *67Gso*) produce PKD phenotypes that differ in both the age of onset and disease severity (40, 66, 90). Unlike *jcpk*, the *bpk* allele is an insertional mutation at the 3' end of *Bicc1*, whereas *67Gso* is a translocation mutation involving Chromosomes 10 and 2. The phenotypic differences observed in the three models may be due to the type of mutation carried in each case. However, differences in the genetic background that each mutation is carried on (*jcpk*-B6, *bpk*-BALB/c, and *67Gso*-BLH) are also likely to influence phenotypic outcome.

In many mammalian systems, the phenotypic expression of mutations can be greatly influenced by genetic background. For example, the age of onset and the progression of PKD caused by mutations in the *PKD1* locus can be markedly variable (232). In ARPKD, the phenotypic variation is even more dramatic. In this disorder, the presentation can range from a neonate with the classic oligohydramnios sequence (Potter's facies, pulmonary hypoplasia, and joint contractures), to infants with oliguria or anuria, to older children who have symptoms relating primarily to hepatic fibrosis, such as portal hypertension. Although some of the variability in these disorders is likely due to different mutations in the same gene, the observation that the apparent phenotype of ARPKD can be quite variable within a kindred population, despite the fact that the affected members have presumably all inherited the same mutation, suggests that genetic background plays an important role in the expression of PKD (113, 123). The identification of modifying loci that affect expression of human diseases represents an area of considerable importance because their characterization might provide insight into fundamental biological processes. In addition, these genes may provide useful targets for therapeutic intervention that could significantly ameliorate disease-related morbidity (113).

Mouse models have represented an attractive system for characterizing modifying loci that are responsible for affecting the expression of mutant phenotypes. The existence of inbred strains allows the generation of progeny in which the parental origin of alleles is known (113). The development of maps of highly polymorphic markers and the ease with which these markers can be tested has made the localization of modifier loci possible. However, the influence of these loci has been difficult to assess since modifying loci many times do not have simple additive effects but display complex epistatic interactions. Even when these loci can be localized by genetic mapping, they may be obscured when isolated in a different genetic background by congenic analysis (113). This again reiterates the importance of the use of animal models for studying complex traits, as it is likely that the influence of modifier loci would be obscured in humans with highly heterogeneous genetic backgrounds.

A number of mouse PKD-susceptibility genes have been shown to have modifying effects on other mouse cystic genes. The region containing *Invs* on mouse Chromosome 4 has been suggested to contain a putative genetic modifier that modulates PKD phenotype in multiple renal cystic mouse models, such as the *pcy*, *cpk*, and *jck* mouse models (133, 278). In the *pcy* mouse, this locus (*MOP1*) modifies 36.7% of the variance for the renal cystic *pcy* phenotype (278). Another modifier, *MOP2*, has also been shown to influence 48.6% of the variance for *pcy* (278). Both of these modifiers (*MOP1* and *MOP2*) have been shown to influence PKD progression in *pcy/pcy* homozygotes in a complex additive manner (278).

The genetic region containing the *Bicc1* gene overlaps with the genetic interval thought to contain a putative PKD modifying locus, *Pkdm2*, which influences the disease severity of another mouse PKD gene, *Nek8* (*jck*) (115). Now that the *jcpk* gene has been identified, it will be possible to design experiments to determine whether *Bicc1* is in fact a modifier for *Nek8* and, if so, characterize the nature of the relationship between *Bicc1* and *Nek8*. Understanding the interaction between PKD-susceptibility genes and their putative genetic modifiers will help to define critical pathways fundamental to cystogenesis and PKD pathogenesis.

Bicaudal-C is highly conserved throughout many species. Multi-species analysis indicates that orthologues exist in human, frog, rat, zebrafish, fruitfly, mosquito, nematode and pufferfish. Such high conservation suggests a critical function in development or cellular regulation. It has been shown that the *Drosophila* orthologue of *Bicaudal-C* (*Bic-C*) plays an important role in anterior-posterior patterning of the developing oocyte (220). At least 12 dominant patterning *Bic-C* alleles have been identified that produce different phenotypic consequences (143, 220). It has been determined that gene lesions that truncate the protein or mutate the functional domains in *Drosophila* *Bic-C* lead to defects in oogenesis and anterior-posterior patterning. Severe mutations in *Bic-C* result in anterior cells of the embryo or oocyte adopting posterior cell fates producing profound developmental abnormalities (79). Thus, *Bic-C* is thought to

be finely regulated in normal development, such that small changes in dosage result in relatively large phenotypic consequences (143).

Northern blot and RT-PCR analysis has indicated that mouse *Bicc1* is expressed in a number of tissues including kidney, heart, lung, and liver. The *Bicc1* gene was also found to be expressed in both embryonic and liver cell lines but not in any of the hematopoietic cell lines examined. The *Bicc1* mRNA transcript in all tissues examined by Northern blot analysis was approximately 5.9 kb in length. Analysis of *Bicc1* expression in embryos indicated that the *Bicc1* gene is expressed as early as embryonic day 5 (E5). Increased expression is observed from E7 to E15. This data correlates with previous studies using *in situ* hybridization which indicated that *Bicc1* is expressed in the mouse embryo at E13 in the derivatives of the pleuroperitoneal membrane, the diaphragm and the pericardium, as well as the mesenchyme of the developing lung, the mesonephros and the metanephros (272).

Both real-time PCR and Northern blot analysis indicated that there was no difference in the expression of *Bicc1* in *Bicc1*^{jcpk} homozygotes compared to age-matched controls. There was also no difference in the expression of *Bicc1* when comparing *Bicc1*^{bpk} homozygotes to age-matched controls. This situation is unusual, especially when considering that the *Bicc1*^{jcpk} mutation produces a premature termination codon (PTC) which should make the transcript susceptible to nonsense-mediated mRNA decay (NMD)(31). The mRNA transcript produced by the *Bicc1*^{bpk} mutation would also be a target for NMD due to its extended 3'UTR (93).

NMD has been shown to be a mechanism developed by cells to maintain homeostasis by destroying mRNA species which contain PTCs or extended 3'UTRs so that only proteins of the correct length are produced (31). This is important since many times mutants mRNAs can be translated and have deleterious dominant negative effects on the cell (226). Given the type of mutation and the observation that *Bicc1*^{jcpk} and *Bicc1*^{bpk} are expressed at a normal level compared to controls, it is difficult to speculate why these abnormal

mRNA transcripts are not degraded by NMD. Sequence analysis alone is not enough to determine this mechanism, thus further investigation is required.

Expression analysis by RT-PCR demonstrates that *Bicc1* encodes two splice variants, transcript A and transcript B. Both transcripts are expressed in a number of normal tissues as well as *Bicc1*^{jcpk/jcpk} kidneys. It has also been shown that both of these transcripts exist in human kidney (E. Bryda, unpublished data). Transcripts A and B were shown to differ by only 80 nucleotides and sequence analysis indicated that the only difference between the two transcripts was either inclusion or exclusion of exon 21. Transcript A contains exons 1-20 and exon 22 and is predicted to encode a protein that is 977 amino acids in length. Transcript B contains exons 1-22 and is expected to encode a protein that is 951 amino acids in length. The predicted protein encoded by Transcript B is shorter due to a termination codon in exon 21 of the coding region.

Western blot analysis using a polyclonal antibody raised in rabbit against amino acids 1-81 of the mouse *Bicc1* protein identified a single protein band in kidney between 75 and 100 kDa. This band most likely represents both putative isoforms of *Bicc1* since the resolving power of the polyacrylamide gel was not great enough to separate two proteins so close in size. A smaller band of less than 75 kDa was found to be expressed only in heart. The significance of this unique band as a potential third *Bicc1* protein isoform has yet to be determined. Analysis by mass spectrometry would be a valuable tool for determining the identity of this unique protein band.

Through *in silico* motif analysis, it was determined that the two putative protein isoforms of *Bicc1* contain several functional motifs. Three K homology (KH) domains are located in tandem near the N-terminus. One sterile alpha motif (SAM) is located near the C-terminus of the protein. The particular mechanics involved in the specific the function of the KH domain-nucleic acid interaction are not yet available; however, a number of proteins containing KH domains have been shown to bind RNA (80). The function of the SAM domain is more elusive, but is thought to play a role in protein-protein interactions (230).

SAM domains have been shown to be able to self-associate as well as oligomerize and bind to other SAM domains (238). By phosphorylation of a conserved tyrosine within the SAM domain, the motif also has the ability to interact with SH2 domain-containing proteins (230). Src Homology 2 (SH2) domains are protein modules of about 100 amino acids in size which are found in a large number of proteins involved in signal transduction. The function of SH2 domains is to specifically recognize the phosphorylated state of tyrosine residues, thereby allowing SH2 domain-containing proteins to localize to tyrosine-phosphorylated sites (128, 219). SH2 domains function as regulatory modules of intracellular signaling cascades by interacting with high affinity to phosphotyrosine-containing target peptides in a sequence-specific manner (229). Determining the specific signaling partners of Bicc1 will hopefully elucidate its role in cell signaling.

More recent research has revealed a completely unanticipated function for some SAM domains: binding RNA (9). The Nanos protein gradient in *Drosophila*, required for proper abdominal segmentation, is generated in part via translational repression of its mRNA by Smaug. Smaug functions in the proper establishment of the anterior-posterior axis of the developing embryo. A combination of structural and genetic analyses have indicated that the SAM domain of Smaug interacts specifically with *nanos* mRNA. It is the localization of *nanos* that specifies the posterior pole of the embryo (268). Disrupting Smaug function leads to the translation of unlocalized *nanos* mRNA and ectopic Nanos protein resulting in lethal body patterning defects (49).

The K homology (KH) domain is an evolutionarily conserved sequence of around 70 amino acids that is present in a number of quite diverse nucleic acid-binding proteins (81). Significant sequence similarity in the KH motifs of proteins from different species reflects descent from a common ancestor and a high degree of functional conservation. All species examined contained all three KH domains except for *Danio rerio* which contained only KH domain 3. The conservation of this domain among all species suggests that perhaps KH domain 3 is important to the RNA binding ability of the Bicc1 protein.

In the *jcpk* mouse model, the mutant Bicc1 protein is altered immediately after amino acid 48 and terminates shortly thereafter. Therefore, the putative truncated protein that is produced does not contain any intact functional domains and is predicted to be nonfunctional. In the *bpk* mutant, the insertion responsible for the mutation occurs within the terminal exon. The consequence of this insertion is that the *Bicc1* gene would encode intact KH and SAM domains, but result in a protein that is elongated by 149 amino acids. Both the *jcpk* and *bpk* alleles would be predicted to have a dramatic effect on any phenotype dependent on the expression of *Bicc1*. The current hypothesis is that the *jcpk* mutation affects both proteins encoded by transcripts A and B, whereas the *bpk* mutation only affects the protein encoded by transcript A. This in part may explain why the *Bicc1*^{*jcpk*} allele produces a more severe phenotype with an earlier age of onset compared to that conferred by the *Bicc1*^{*bpk*} allele. However, future transcript or isoform-specific analyses using transcript-specific RNA interference or transcript-specific antibodies are needed to explore this phenotypic difference.

It has previously been determined that KH domain containing proteins can bind either RNA or single-stranded DNA *in vitro* (29). Using recombinant protein constructs encoding the full-length mouse Bicc1 protein or truncated forms, the *in vitro* ability of Bicc1 to bind RNA using synthetic homoribopolymers was explored. It was determined that the full-length Bicc1 protein binds RNA and that KH domain three is responsible for that binding. This is not entirely surprising considering that KH domain 3 is the only domain conserved in all 10 species examined in this study. It was also determined that the *Bicc1*^{*jcpk*} mutation causes the complete loss of RNA binding. This data confirms previous observations in *Drosophila melanogaster* where a strong mutant allele, *Bic-C*^{*RU35*}, lacks RNA binding activity. The mutation present in this allele is a point mutation resulting in a single amino acid change just prior to the third KH domain (143).

Microarray analysis was used to examine multiple gene expression alterations in *Bicc1*^{*jcpk*} homozygotes. Changes in expression seen in *jcpk/jcpk* kidneys when compared to normal control kidneys included: altered expression of extracellular matrix (ECM) constituents, increased expression of epithelial

proliferative factors such as *Pax2* and *Pax8*, an increase in factors favoring apoptosis, and alterations in the expression of cell junction components. Even though microarray analysis was performed on samples collected late in the pathological progression in the *jcpk* mouse model (postnatal day 8), valuable phenotypic information was gathered. The microarray data for *jcpk/jcpk* kidney from animals with advanced PKD showed a gene expression profile that is consistent with that seen in both human ARPKD and ADPKD and many other mouse models for PKD.

Several studies on human and animal models for PKD have demonstrated a number of ECM abnormalities, suggesting that an abnormal cellular matrix plays a key role in the development of tubular cysts. The ECM consists of a meshwork of collagens, proteoglycans, and other high molecular weight glycoproteins such as laminin, entactin, nidogen, syndecans and fibronectin (36). Cell adhesion is central to the interaction of cells with the ECM and is mediated by specific cell membrane adhesion receptors, the integrins. Integrins are linked to the ECM via both talin and vinculin. Interactions of ECM proteins with cell surface receptors induces organization of the cytoskeletal network which modulates differentiation and development of cell membrane domains (36). The formation of cell-cell contacts and expression of specialized adhesion molecules integrates the epithelial cells into a polarized monolayer and maintains the separation of the cell membrane domains (106, 107). Precise coordination of ECM and cell adhesion factors in the kidney tubule results in a continuous layer of polarized epithelial cells that interact with their environment to control both the concentration and flow of renal filtrate (106). Alterations in either or both of these factors (as seen in *jcpk* homozygotes) would result in a disease state favoring cyst formation.

A characteristic observed among many animal models and some human forms of PKD are alterations in the EGFR/EGF/TGF- α axis. Studies in a number of laboratories have determined that 1) EGF and TGF- α are cystogenic *in vitro*; 2) cystic renal tissue has decreased preproEGF and EGF concentrations but increased expression of TGF- α and EGFR; and 3) renal cyst fluid contains

bioactive and immunoreactive EGF peptides in mitogenic concentrations (184).

Using real-time PCR analysis, the levels of gene expression for each component of this receptor pathway were examined. It was determined that *Egf* mRNA expression in *Bicc1^{jcpk/jcpk}* kidneys was reduced while the expression of *Egfr* was elevated compared to normal (+/+) littermates. This pattern of expression has also been observed in other rodent PKD models and human ADPKD (43, 75, 78, 105). EGF has been shown to be produced by the kidney and appears to be a regulator of renal function by enhancing cellular proliferation, migration, and differentiation in the normal kidney (78). However, the relative decrease in renal EGF expression may serve to up-regulate the expression of EGFR in the cystic kidney. This data is consistent with data gathered from microarray analysis that suggests an increase in markers of epithelial cell proliferation. This altered expression of proliferation and growth factor-related mRNAs also confirms data from other models suggesting that cell proliferation is a component in the pathogenesis of cystic disease (77, 169, 213).

Unlike other human and other mouse models for PKD, *Tgf- α* expression did not change when comparing wild type and affected kidneys. In number of animal and cell systems for PKD, *Tgf- α* has been shown to be overexpressed when compared to wild type controls (126, 136). A transgenic mouse model over-expressing *Tgf- α* develop renal cysts (276). Normally, *Tgf- α* is thought to play several important roles in the kidney, such as modulation of glomerular hemodynamics, renal metabolism, tubular transport functions, and eicosanoid synthesis (97, 250). It is expressed at similar levels as the EGFR and was originally thought to be the fetal ligand for the EGFR (84, 85). It is currently not understood why *Tgf- α* expression is not altered in the *jcpk* mouse model. Perhaps this ligand does not play a major role in cyst formation in this model for PKD.

A common feature of the development of ARPKD in human and mice is mislocalization of the EGFR from the basolateral surface of normal collecting tubule epithelium to the apical surface on the cells lining cystic structures (11). This mislocalization is accompanied by an increase in the mRNA, protein, and

tyrosine kinase activity of the EGFR in the cystic kidneys (184). It is possible that the increased EGFR tyrosine kinase activity in the collecting tubules is part of an autocrine/paracrine cycle that drives the cellular proliferation which is required for cyst formation and enlargement (183). In order to determine whether the activity of the EGFR axis was directly part of cystogenesis in the *jcpk* mouse model, a genetic approach was used in which a mutant *Egfr* gene (*waved-2*) was introduced into the *jcpk* model. In the *waved-2* mutation, a T to G point mutation results in reduced tyrosine kinase activity of the EGFR (71). Double homozygotes for *Bicc1^{jcpk}* and *waved-2* were observed for changes in disease progression. Interestingly, double homozygotes do not show any obvious signs of altered disease progression. This contrasts with the results observed in *orpk* and *waved-2* (*wa2*) double homozygous mice (212). There, a substantial decrease in cyst formation was observed accompanied with an improvement of overall kidney function in *orpk;wa2* double mutants. In the case of the *jcpk* mouse model, the few double homozygotes recovered in our studies never lived past ten days of age. Histological analysis did not reveal any significant differences in cyst pathogenesis between *jcpk* homozygotes and *jcpk;wa2* double homozygotes. Therefore, it seems that altering the activity of the EGFR in *Bicc1^{jcpk/jcpk}* mice does not notably alter the progression of PKD. It is likely that *jcpk* and *orpk* are genes that belong to two different signal transduction pathways. The *orpk* gene is more likely to be involved in a pathway in which EGFR mediates cyst formation, whereas *Bicc1* likely belongs to a yet undiscovered regulatory pathway.

Controlled apoptosis is also a key player in cellular differentiation and epithelial cell maturation (152). The mature mammalian kidney is a quiescent organ with little or no mitotic activity, and little or no apoptosis. Large-scale apoptosis occurs during metanephric development, which may serve to match the number of collecting ducts developed from the metanephric mesenchyme (152, 185). As a result, after all the differentiated nephrons are formed, the mature kidney can no longer generate new nephrons. In polycystic kidneys, uncompensated apoptosis and the inability to regenerate new nephrons results in

the progressive loss of renal tissue (277). EGF expression has been shown to inhibit developmentally-regulated apoptosis in the kidney (42). Therefore, in the normal kidney, the early expression of growth factors, such as EGF, may inhibit apoptosis as well as inhibit epithelial cell progression into a mature differentiated state. However, the increased expression of pro-apoptotic factors and a decline in normal EGF expression early in nephrogenesis in PKD-affected animals would therefore contribute to the progression of PKD pathogenesis. Further, apoptosis must be important in cyst formation since *Bcl-2* knockout mice develop PKD (121, 240). However, the specific role of apoptosis in the pathogenesis of PKD is still unclear (256).

Another interesting observation uncovered in both real-time PCR and microarray analysis is the increased expression of *ErbB2* in *Bicc1^{jcpk/jcpk}* kidneys. Human epidermal growth factor receptor-2 (HER2/neu; *ErbB2*) belongs to a family of four transmembrane receptor tyrosine kinases involved in signal transduction pathways that regulate cell growth and proliferation. Amplification or overexpression of HER2/neu occurs in about 30% of human breast and ovarian cancers and is associated with a poor clinical outcome, including short survival time and short time to relapse (291). In humans, *ErbB2* has been shown to be overexpressed in a small number of patients with either ADPKD or ARPKD (101, 170). Until now, the gene expression of *ErbB2* has not been evaluated in any other mouse models for PKD. Further, the expression of *ErbB2* as a mouse transgene has been shown to cause multifocal hyperplasia of renal tubular epithelium and cyst formation (242). It is difficult to speculate why *ErbB2* is increased in PKD considering the low frequency of renal carcinoma associated with human and animal models of PKD (6). This finding may define a new role for *ErbB2* in cystic disease.

The present study has identified a number of misexpressed genes in the cystic kidneys of *Bicc1^{jcpk}* homozygotes. One gene that was found to have increased mRNA expression in *Bicc1^{jcpk/jcpk}* kidneys compared to normal was *Pax2*. *Pax* genes encode a family of transcriptional regulators specifically expressed during the development of a wide range of structures and organs (88,

255). As indicated by both human and mouse mutations, at least eight *Pax* genes have critical morphogenetic functions during the develop of complex tissues (38, 243).

During embryonic development, the *Pax2* gene is essential for the differentiation and proliferation of the renal epithelium in both mouse and human (124, 217). Genetic evidence in mice and humans indicates that *Pax2* plays a critical role in normal renal development and may sit atop a molecular cascade which unfolds during the transition from undifferentiated mesenchyme to the early stages of nephrogenesis (253). During the normal course of kidney development, *Pax2* is expressed in the nephric duct, the ureteric bud, and the induced mesenchyme which ultimately generates much of the glomerular, proximal tubular, and distal tubular epithelium (59).

It has also been shown that *Pax2* is required for the specification and differentiation of the renal epithelium (186). *Pax2* is down-regulated as the kidney matures and transgenic overexpression of *Pax2* has been shown to cause increased cellular proliferation, and cyst formation (60, 186). Persistent expression of *Pax2* in *cpk* mice is correlated with cyst formation and progression (186). Thus, the results found in *Bicc1^{jcpk/jcpk}* kidney are consistent with data from both human and other mouse models that suggest that renal cysts consist of dedifferentiated epithelial cells that require embryonic factors, such as *Pax2*, for continued growth and expansion.

Another developmental gene found to be increased in *Bicc1^{jcpk/jcpk}* kidneys was *Pax8*. Less is known about the role of *Pax8* in kidney development; however, it has been suggested that *Pax8* is a critical regulator in the initial phases of kidney development (24). *Pax8* is expressed in the S-shaped body and early proximal tubule and preliminary data suggest that renal morphogenesis is unaffected by its absence (201). This may be due to the overlapping embryonic expression patterns between *Pax8* and that of *Pax2* (253). Most likely, *Pax8*, like *Pax2*, is a mediator of epithelia maturation and increased expression helps to maintain the dedifferentiated state seen in cystic epithelium.

These numerous abnormalities in the expression of genes involved in kidney development and cell proliferation suggest that the kidney epithelial cells in *Bicc1* mutants are unable to complete the terminal phases of tubuloepithelial differentiation and therefore maintain a dedifferentiated state. This, along with the abnormal expression of growth factors and their receptors increases epithelial cell proliferation, producing a disease state favoring cyst formation. Treatments aimed to regulate common pathways in kidney development and epithelial maturation may lead to the development of clinically relevant treatments to slow or halt the progression of PKD. However, caution needs to be taken in that some treatments, as in the case of EGFR tyrosine kinase inhibitors, may not work for all forms of cystic disease.

Because signaling from cell-cell and cell-matrix adhesion complexes regulate cell proliferation and polarity, it is not surprising to observe alterations in the expression of these genes in *Bicc1*^{*jcpk/jcpk*} mutant mice. It has previously been shown that polycystin-1 is part of a cellular complex containing both E-cadherin and the catenins (109). The catenins have effects on such diverse cellular functions as the polarization of the cytoskeleton (174), regulation of gene transcription (30), and the formation of desmosomes (146), all of which are altered in PKD. *Inversin* is another PKD-susceptibility genes that encodes a protein that is complexed with the catenins and cadherins (178). In *Bicc1*^{*jcpk/jcpk*} mutants, both K-cadherin and α -catenin are each down-regulated more than five-fold compared to wild type. Like polycystin-1 and inversin, perhaps *Bicc1* is part of a protein complex that is critical for the stabilization of adherens junctions and the maintenance of a fully differentiated polarized renal epithelium. Mutations in the *Bicc1* gene would therefore result in the phenotype observed in the *jcpk* mouse model.

There is a growing body of evidence that links ciliary dysfunction and cystic disease of the visceral organs, e.g. kidney, liver, and pancreas. Primary cilia are most commonly thought to be only associated with the embryonic node; however, primary cilia are a common feature of polarized epithelial cells in eukaryotes and are thought to serve either a chemosensory or mechanosensory

function (181). The proteins encoded by *Kif3a*, *cpk*, *orpk*, *Invs*, *Pkd1*, and *Pkd2* have been shown to be either structural components of cilia or cilia formation (181). A few mouse mutants for PKD have shortened or absent cilium but this is not a common denominator among all mouse model for PKD that have defects in cilia proteins (161, 179, 191, 213).

A number of groups have reported the possible involvement of genes associated with PKD in either the assembly or function of cilia in mice and *Caenorhabditis elegans*. The first evidence observed for the ciliocentric theory of PKD pathogenesis was provided in the *orpk* mouse model, where a null mutation was found to cause embryonic lethality and an absence (or severe stunting) of cilia on embryonic node epithelium, disrupting early morphological left-right axis determination (161). The product of this gene, polaris, is localized in the axoneme and basal body of primary cilia and is required for ciliary assembly (287).

Similarly, the *inv* mouse model for PKD has a connection to primary cilia. Several isoforms of the inversin protein have been described and have been localized to primary apical cilia, cell-cell adhesion sites and the nucleus (157, 178). The human gene, *INVS*, when mutated, has been shown to cause NPHP2, an infantile form of nephronophthisis with clinical manifestations that include renal cysts (187).

The *cpk* mouse model for PKD has also been linked with cilia. The gene, *Cys1*, encodes cystin-1, which has been localized within the axonemal region of primary cilia, partially overlapping with polaris (108). Interestingly, *cpk* mutants have PKD despite structurally normal cilia (89, 213).

In preliminary confocal microscopy studies, it has been observed in cell culture that the Bicc1 protein is present in the apical cilium of renal epithelial cells as well as having diffuse expression in the cytoplasm (L. Guay-Woodford, unpublished data). It has not been determined whether or not mouse Bicc1 is associated with specific cytoplasmic organelles; however, previous work has shown that in mouse primary oocytes, *Bicc1* mRNA is associated with the Golgi complex (272).

Previous work has demonstrated that the *Bicc1* orthologues in *Drosophila* and *Xenopus* play critical roles in regulating embryonic patterning (220, 271). In the mouse, *Bicc1* is expressed in the embryonic node at E7.5 (271). At the late headfold stage, *Bicc1* expression specifically demarcates the layer of the node from which definitive endoderm and midline mesoderm arises. In contrast to many other genes expressed in the node at this stage, *Bicc1* is never detected in the primitive streak suggesting that it marks the undifferentiated cells of this organizing center (272). Perhaps the single epithelial cilium is important in the functional differentiation of polarized lumen-forming epithelia and it is ciliary dysfunction that underlies the PKD phenotype in *Bicc1*^{jcpk}.

Based on the putative functional domains of mouse *Bicc1*, it is unlikely that the protein plays a structural role in maintenance or formation of the cilia. However, it may serve to localize specific mRNAs that are involved in ciliogenesis or perhaps play a role in the translational repression of cilia proteins. Abnormalities in both of these mechanisms would cause defects in cilia formation or lead to cyst formation. It may also be possible that *Bicc1* is part of a yet undefined molecular pathway that may also be responsible for epithelial cell homeostasis.

The potential connection between cilia and PKD is intriguing in light of the knowledge of the role of primary cilium found on epithelial cells lining the nephron and collecting duct. Whether renal cilia perform a similar function as embryonic node cilia with regard to fluid movement, or the act as organelles responsible for sensing local environments, remains to be explored. Elucidating the function of primary cilia and their association with PKD will require a detailed characterization of proteins involved in ciliogenesis and cilia function, plus the development of reagents and assays to test their role in renal physiology.

Bicc1 may also be among the several PKD-causing proteins that appear to be expressed in apical cilia and are also associated with L/R axis determination. Based on the finding of a single *Bicc1*^{jcpk} homozygote with lung isomerism and abnormal heart situs, it is tempting to speculate that *Bicc1* plays a role in L/R patterning defects. However, more mice are needed to provide a solid

link between mutations in *Bicc1* and L/R patterning defects. Patterning defects have not been observed in *Bicc1^{bpc}* homozygous mice (91). The majority of *Bicc1^{jcpk}* homozygotes that are born do not seem to have L/R patterning defects. It is essential to investigate patterning abnormalities in *Bicc1^{jcpk}* embryos to determine the extent of those defects, considering that the majority of similar types of defects in other mouse models are lethal and only seen at the embryonic stage. Determining whether or not mutations in *Bicc1* affect both renal and node cilia would provide important clues to the role that the *Bicc1* protein has, if any, in the function of primary cilia.

L/R patterning defects have not been associated with all genes encoding cystoproteins. For example, ultrastructural studies have demonstrated that cilia in *cpk* mutants are morphologically normal yet functionally defective (108). Cystin has also been shown to only be present in chordates and not in primitive ciliated eukaryotes such as *C. elegans* (108). Researchers have predicted that cystin has a later phylogenetic origin than proteins associated with intraflagellar transport, such as polaris, inversin, polycystin-2 and Kif3a (137, 172, 187). Cystin more likely has a specialized function in ciliated epithelium of higher vertebrates rather than a key role in ciliogenesis (108).

Extrapolating from the observations in other mouse models, *Bicc1* may be directly involved in the process of ciliogenesis, a process that is both critical in embryonic patterning and organogenesis. The high level of species conservation of *Bicc1* indicates that it is likely a key player in both embryonic and organ development in a wide range of organisms. However, further research needs to be performed in order to elucidate the exact role of the *Bicc1* gene in both normal development as well as cystogenesis.

Future Directions

Positional cloning and preliminary molecular characterization are only the first steps in elucidating the pathogenesis of PKD in the *jcpk* mouse model. More information is needed to understand the role of the Bicc1 protein in normal mammalian development and organogenesis. Bicc1 is a protein that contains two distinct types of relatively uncharacterized functional motifs, KH and SAM domains. A number of approaches exist to evaluate their function.

Determining the particular mRNAs that bind to the KH domains is of considerable importance. A technique known as SELEX (Selective Evolution of Ligands for Exponential enrichment) provides one potential approach for the identification of RNA binding motifs that are recognized by the Bicc1 protein. This technique involves serial enrichment of a synthetic nucleic acid population in order to select a specific consensus sequence that has affinity for the protein being examined (120, 202, 265). Discovery of these consensus elements will provide important information for evaluating the *in vivo* RNA targets of Bicc1. At that point, specific RNA-Bicc1 interactions can be identified and a putative functional model for Bicc1 can emerge.

A second area of research that needs to be explored is the importance and function of the SAM domain at the C-terminus of the Bicc1 protein. Previous studies involving other proteins that contain SAM domains have shown that SAM domains often facilitate homo- or heterodimerization. Additionally, these SAM domain-containing proteins sometimes interact with proteins that contain SH2 and SH3 domains (128, 238). More recent studies have shown that the SAM domain in the *Drosophila* protein Smaug plays a role in RNA-binding (9). The SAM domain in the Bicc1 protein was not examined for its independent ability to bind RNA. However, based on the RNA binding analysis of the recombinant full-length protein and the recombinant containing only the three KH domains, the SAM domain is not essential for RNA binding. This domain should now be included in future RNA binding analyses to determine if the SAM domain in Bicc1

does interact with RNA and if the SAM domain alters the affinity of RNA binding in the Bicc1 protein.

Additional studies are needed to determine the functional relevance of the alternative transcripts identified for *Bicc1*. As previously noted, the *Bicc1*^{jcpk} mutation alters both *Bicc1* transcripts A and B resulting in the truncation of both encoded proteins, whereas *Bicc1*^{bpk} affects only the protein product of transcript A. Specific antibody analyses and allele-specific expression studies are needed to determine the novel importance of each transcript and its corresponding protein. Employing specific antibodies to block the function of a specific Bicc1 isoform will provide insight into which particular isoform is important in cyst formation. It is interesting to consider whether these different transcripts encode proteins with distinct functions that may or may not act in the same signaling pathway. For example, one protein isoform could be localized in or near the cilia, whereas the other protein isoform could be available in the cytoplasm for cell signaling. At the present date, a model for Bicc1 function is purely speculative.

Left-right patterning defects have been observed in one *Bicc1*^{jcpk} homozygous animal. Examination of additional animals is necessary to confirm this preliminary observation and determine the relative frequency of these defects in homozygous affected animals. In addition, studies using timed matings to recover embryos at defined stages of development will test the hypothesis that L/R patterning defects occur at a greater frequency but due to prenatal lethality, these animals have not been detected in our post-natal studies. Also, detailed heart-specific histological studies need to be performed to determine if structural defects exist in the heart. These types of abnormalities would include septation defects, pericardial effusion, and valve defects. These defects were first observed in the *Pkd2* mouse model for PKD (197, 282). Further study of the heart is also warranted in light of the possible presence of the unique heart-specific Bicc1 protein isoform as suggested by Western blot analysis. Bicc1 may have a novel function in the heart that has yet to be determined.

A challenge for the ciliocentric model of PKD pathogenesis is to establish a definitive causal connection between cilia and cyst formation. A possible approach to study this would be to selectively inhibit the ciliary function of cystoproteins and then assess the effect on cyst formation. Unfortunately, it is still not known how proteins are targeted and transported to the basal bodies and cilium. Considering that Bicc1 is an RNA-binding protein, it is possible that it may play a role in this cilia-specific targeting.

Another challenge is trying to explain how ciliary dysfunction results in such disparate renal phenotypes among a large number of PKD mouse models and human cystic diseases. In the case of ADPKD, macroscopic cystic disease is the principal finding, even in the end-stage kidney, whereas in NPHP, kidneys are small and fibrous. The localization of most cystoproteins is not limited to the cilia. Proteins such as polycystin-1, nephrocystin, and inversin, have been detected not only in cilia but also within other structures involved in cell-cell and cell-matrix interactions such as adherens junctions and desmosomes (23, 57, 154, 178). Dysfunction of any of these structures could independently result in altered tubular morphology leading to a cyst-inducing environment. This observation suggests that many cystoproteins are multifunctional and it is uncertain which of their activities are directly related to cyst formation. Also, like Bicc1, many of these cystoproteins have multiple isoforms and little research has been performed to determine the significance of these independent protein forms.

A theory including both possibilities is that ciliary dysfunction initiates cyst formation but the loss of functional cystoproteins at extraciliary sites determines the final phenotypic outcome. The identification of a variety of cystoproteins has laid the ground work for arriving at a model that encompasses all forms of cystic disease. The characterization of the many complex pathways that lead to cyst formation will not only provide new insights into PKD pathogenesis, but will serve to identify new genetic markers for prognosis and ultimately establish a platform from which to develop targeted therapeutic interventions to halt disease progression.

APPENDIX A

The following “overgo” primers were designed for multiplex oligonucleotide hybridization as discussed in *Physical and Genetic Mapping* in Chapter III of Materials and Methods:

282P18T7

F: 5'ATCAGGTTTCAGAGTGGGCATGTTG3'

R: 5'CATCCTCATATTGGCCCAACATGC3';

282P18SP6

F: 5'GCTTTTGACGTGAACATAGAAGGG3'

R: 5'TTCCCTCTCGTTATGCCCCTTCTA3';

393H9T7

F: 5'TGGAAGAGTCCATGGATTTGAAAG3'

R: 5'TATCCTACCATGCTTTCTTTCAA3';

393H9SP6

F: 5'ATGGCAGTTTTCCAGCGATGAGGA3'

R: 5'AAAGCTCATCCCTGCTTCCTCATC3';

323G11T7

F: 5'ATGACACTATGCCACCCACCTTGA3'

R: 5'TAGCTCTAAGGCCAACTCAAGGTG3';

323G11SP6

F: 5'TGTGCCTTCCTGTTTGGTTCCGTA3'

R: 5'GATTTTCACATGGCGGTACGGAAC3';

440N1SP6

F: 5'ACGCTCATTGACAGCAATCAGGAG3'

R: 5'TGCGCAGTAAAGAGAACTCCT3';

440N1T7

F: 5'AAAGGGTTGAGGGTTGGAACAGTG3'

R: 5'GACATGTGCAGTGAACCACTGTTC3';

480A14SP6

F: 5'GCAAATATTCTATGCCAGGAAAGC3'

R: 5'TCTTCTGTGGGAAGAGGCTTTCCT3';

480A14T7

F: 5'CAGCACATTTCTCAGGACAGTCTG3'

R: 5'CAGCATCCAGAAGCCCCAGACTGT3';

348F2T7

F: 5'TTCGGTGCAACGCAGAACTCAAAC3'

R: 5'GCCACGGTTCTGAATAGTTTGAGT3';

348F2SP6

F: 5'AGCCACCACGAACATTTAAGCCAC3'

R: 5'AGTCGATGACAACCGTGTGGCTTA3';

337L15T7

F: 5'AGAGCTGGGAACGAATAAAGGGAG3'

R: 5'CCTGCCCTATTTGTTCTCCCTTT3';

337L15SP6

F: 5'GTGATCAGGTGTCACCTTTGGTGTG3'

R: 5'AAACCATGGCACCTAGCACACCAA3';

395K6SP6

F: 5'AATTCCTACGAGGAGGGTGGCACAA3'

R: 5'GTTTCTGAGGCTTACCTGTGCCAC3';

395K5T7

F: 5'TTAAGAGCAGCAGCTCCTGTGGAT3'

R: 5'GTTCTCTGATAGCGTCATCCACAG3';

326F24T7

F: 5'GCACACTTGACCTGTATTCTGTCC3'

R: 5'TTCCATGACAACCGCAGGACAGAA3';

326F24SP6

F: 5'TGAGGTGGGCTTTCAAGAACATTG3'

R: 5'CACACTTGGCACAAATGCAATGTTC3';

3'307I23

F: 5'CTTATCAGAGCAGAGGTTTCAGCTC3'

R: 5'GGAAATGCACACCATCGAGCTGAA3';

5'340N8

F: 5'GGTGCATCAGGAATGATGAATCTG3'

R: 5'ACCAGGGATTTATGTCCAGATTCA3';

D10Ert214E

F: 5'GCACCACATGTTTCAGTAGCAAGG3'
R: 5'ATATCCATGGCATCGGCCTTGCTA3';

226L21T7

F: 5'GAGAAGCCACTGCATTTCCAGAGA3'
R: 5'GGGAGCAAGTTATTCCTCTCTGGA3';

225C18SP6

F: 5'CAGCTGGTATAGAAGGGCAATGAC3'
R: 5'GGAATGAGGGGTTTCAGTCATTGC3';

M-02039

F: 5'TCTCAGAAGCCCTTCTGTCCCCAC3'
R: 5'AATGGAGTGGCACGTGGTGGGGAC3';

312N7T7

F: 5'GTTCCCTCTGAGCTTTAACACCAG3'
R: 5'TCCCACTTCTTCAGTCCTGGTGTT3';

114H21SP6

F: 5'GACAGCTTGACATGCTGTCCTATG3'
R: 5'TGTGAACCCACATGTCATAGGAC3'

337G9SP6

F: 5'GTAACACAGTTCCTGCTGCTGGTA3'
R: 5'TCACACCAGGGCCCTGTACCAGCA3';

536B11T7

F: 5'GATTGCTTGGTCTACGTAGGAAGC3'
R: 5'ATGTGGTATCCCTCTCGCTTCCTA3';

536B11SP6

F: 5'CATGAGCCATAGAACCGTGTCATG3'
R: 5'TGTGCATTTGTGTGCGCATGACAC3'.

APPENDIX B

The following primers were used for PCR amplification as described in *Physical and Genetic Mapping* in Chapter III.

33E18T7

F: 5'CTTTGGCAGAAGGGGTGAGC3'

R: 5'GCCAGGCTACAGTTACAGCTCC3';

536B11

F: 5'GCAGGAAAGAGAAAGCGCAA3'

R: 5'AACATTGGCTGCTGGGCTAA3';

400E17T7

F: 5'TCAAAAAGATTGGGGCAAAG3'

R: 5'GCTCTCCGTAGTCCACTCCA3';

5'400E17

F: 5'GTAATGGAACCTACCCACCTGCTCTG3'

R: 5'CGTCCTTCATACACTCCTGTGAACC3';

3'400E17

F: 5'AATACTCAAGCTTTGATCTGCGGT3'

R: 5'ATTAAGTTGGTTACCCCCAGGGTT3';

114H21T7

F: 5'TCTCCTGATGGATGGCTTCT3'

R: 5'GTTGTACCCATTTTCCTGCC3';

114H21SP6

F: 5'AAGAAATGGCAGGCAGAGAA3'

R: 5'CAATGCCCACCTTTACGTCT3';

17205SP6

F: 5'TCCTTACCTACCTGGCATGG3'

R: 5'AGAGCGGCACTCCGTAGATA3';

226L21T7

F: 5'CCAGCTACCTCATCTCTGCC3'

R: 5'GATCGGAAGCAAATGCTGAT3';

226L21SP6

F: 5'GGATCTGCCAGAGTGGACAT3'

R: 5'CAGGCCTGAGAGGTAAGTGC3';

536B11T7

F: 5'TACGTAGGAAGCGAGAGGGA3'

R: 5'GCATCTCAGCCACAACAGAA3';

536B11SP6

F: 5'TTTGGCACAGAGAAGCACAC3'

R: 5'GAGCCCTGAGACATAGCTGG3';

172O5T7

F: 5'GCCATCTCTGCATCTCTGAA3'

R: 5'AGAGACCCTGGAAGGAAGGT3';

400E17SP6

F: 5'GGGTGACCAGCATCACACTG3';

R: 5'TGTGATATCTTGGGGGTGGC3';

114H21T7

F: 5'TTAAAGGACTGGCCACCAAG3'

R: 5'AGTCCAATTCACATTCCCCA3';

400E17T7

F: 5'TGGCTTGCACACTCAGGTTG3'

R: 5'ATTCCCTGGACAGATGGCCT3';

50A5T7

F: 5'GAAGGCTCGGCTATGCAA3'

R: 5'GTTGTAGCGCAAGATTTCTGG3';

50A5SP6

F: 5'CATGGCAGTGGAGAAAGTGA3'

R: 5'AAATTCCCGGGATAATGGG3';

115L9T7

F: 5'CTTGGTATTCCACTGGCGAT3'

R: 5'CAAAAAGACGGTGCTGACAA3';

115L9SP6

F: 5'AGCAATACCCTACCCCTCGT3'

R: 5'TAAGCTCTCAGTCCCTCCCA3';

Tfam

F: 5'TGCTGAGTTCTGCCTTTTGC3'
R: 5'AGCCTGGCAGCTTCTTTGAA3';

225C18T7

F: 5'GAGCCCTGAGACATAGCTGG3'
R: 5'TTTGGCACAGAGAAGCACAC3';

295N22T7

F: 5'TGCAGCAAGATTTCTGATGG3'
R: 5'AGGCAAGTGGAGAACTGGAA3';

225C18SP6

F: 5'AAGACAGACAACCGCTGCTT3'
R: 5'GCTGGGGCTTACGTAATTGA3';

M-02039

F: 5'TGCCACTCCATTCCCTGTCA3'
R: 5'AGTGTCCACGGGGCTTCTTG3';

59E15T7

F: 5'CCTTGGGCAGAAATGGAAGG3'
R: 5'GCAAAATGGGTCGCCAAGGT3';

337G9T7

F: 5'GGCCACCTGCAACTCTGCTT3'
R: 5'GAGGGAAAAGGCTTGGCTCC3';

337G9SP6

F: 5'GGCATTATGGGCACACCGAT3'
R: 5'TGGGGCTGAAGAGATGGCTC3';

59E15SP6

F: 5'TCACAAAGCCCTCACACAACG3'
R: 5'TCCATGCTGTGCCATGTGTTT3';

312N7T7

F: 5'TCAAAGGCTCTTGGCCTTGC3'
R: 5'GCAAGGTGTGGGAAATTGGG3';

312N7SP6

F: 5'AGTTCAGCCCTGGCATCAGC3'
R: 5'AGAGATGGCAAGGGCAGTGG3';

226L21SP6

F: 5'ACGTGGACAAACCCAAAAAG3'

R: 5'GTTCTTTGCGTGTGGATTT3';

337G9T7

F: 5'TGCCGTGAACTACATACCCA3'

R: 5'GGATGATTCGGCTCAGGTAA3';

310N21T7

F: 5'AAACAGCCGTCCCTAGGATT3'

R: 5'TGGTTAGCTCTGGGCTCATT3';

310N21SP6

F: 5'ATTCAGGCTACTCCGCT3'

R: 5'AGATGGAGACTCTGCCAGGA3';

282P18T7

F: 5'TCTTGGTAGCTGGCAGGAGT3'

R: 5'TTTCATCCTTTCAGGGCATC3';

282P18SP6

F: 5'TTTCATCCTTTCAGGGCATC3'

R: 5'AGTATAGCAGGCCCTCCTCC3';

244D3T7

F: 5'GAAGAGGGAGGGTGATGGAT3'

R: 5'GCTGTGGTTGCATATTCCCT3'

244D3SP6

F: 5'AGTGAGCACAGTGCAAGCTC3'

R: 5'AACAGTTGTTTTTCTTATTGCAGC3';

395K5SP6

F: 5'AAACCATCAGAACCACAGCC3'

R: 5'AAACCATCAGAACCACAGCC3';

395K5T7

F: 5'CCAAGTAACCCAAACATCCG3'

R: 5'GTGGGCTGGTGTTTCTGAAT3';

328F8SP6

F: 5'GGGTCATGTTTTGCAATGAA3'

R: 5'GCACCTGCAAACCTGACACAT3';

259N19T7

F: 5'TCGGTGGGTACCTGAGGTTACTG3'

R: 5'TGGCTAAGAGCATGAGAAGAAAGGA3';

259N19SP6

F: 5'CTTTGGCACAGAGAAGCACACAC3'

R: 5'CAGCCAAGCTGAGCAGGATCTAA3';

326F24T7

F: 5'AGTCCCCGCAATTGGCTGTA3'

R: 5'ACCCCTCACCTGGGGAATGA3';

326F24SP6

F: 5'GGATGCTGGAGACCCAGAGC3'

R: 5'CAGCCTCCTGAATGCTGGGT3'.

APPENDIX C

The following primers were used for RH Mapping as described in *Physical and Genetic Mapping* in Chapter III.

HTL5/10

F: 5'CGGGCTGGACAAGAGCCTGG3'

R: 5'CCTCCAGAAGCAGAAGCACCACTC3';

5'400E17

F: 5'GTAATGGAACTCACCACTGCTCTG3'

R: 5'CGTCCTTCATACACTCCTGTGAACC3'

400E17SP6

F: 5'GGGTGACCAGCATCACACTG3'

R: 5'TGTGATATCTTGGGGGTGGC3';

225C18SP6

F: 5'AAGACAGACAACCGCTGCTT3'

R: 5'GCTGGGGCTTACGTAATTGA3';

114H21T7

F: 5'TCTCCTGATGGATGGCTTCT3'

R: 5'AGTCCAATTCACATTCCCCA3';

Tfam

F: 5'GAAGTGATCTCATCCGTCGAAGGT3'

R: 5'TAAGCAAAAGGCAGAACTCAGCATC3';

5'307I23

F: 5'GGAAATGCACACCATCGAGCTGAA3'

R: 5'GGAAATGCACACCATCGAGCTGAA3';

5'115A16

F: 5'GGGTGCAGACTGTGATCTTCTCAAT3'

R: 5'ATTCGTTCTTAGCACTCTCCAGCCT3';

PSO2

F: 5'GCAAGGGTAGATCAGGTTAAG3'

R: 5'GCCAGTCTGTAAGAAGTGCT3';

SPL3

F: 5'ACCCTTGTGAAGTTCCTTGG3'

R: 5'ATTGTGCTCTACGGAGCCAG3';

APPENDIX D

The following primers were used for DNA and/or cDNA sequencing analysis of the *Bicc1* gene as described in Chapter III, *DNA Sequencing*:

RT-PCR Primers

BG062853

F: 5'AATCCGGCAAGGGTGGTAAC3'

R: 5'CAATGGTGCCCTGGAGGTAG3';

BF785275

F: 5'CATGCAGACAGAAGGCGAAA3'

R: 5'AGGAGCCCTCATAGCCGTGT3';

KHDOMAIN

F: 5'CAGGAAGAACTCGAGGCCA3'

R: 5'AATGTGGCCTGGGCAGTAGA3';

JCPK20-22

F: 5'GTGCCCCGAAGGAAAATGCTG3'

R: 5'GCAGGCGAGTGCAAGTGAAGA3';

BIC-C

F: 5'ACCATGGCCTCGCAGAGC3'

R: 5'TGGCCATGAAGTACAGGTACGA3';

SP3

F: 5'AAAACAGCTCAAGGGCAGGG3'

R: 5'GCCCTGACTGCCTCTCCTTT3';

493392E3-4

F: 5'GAGAGCACTATCTAAGCAGCAGCA3'

R: 5'GAGAGCACTATCTAAGCAGCAGCA3';

AI26426RT

F: 5'CCAAACATGTTCACTGGGCA3'

R: 5'ATGTGCAGTGGGTTCACACC3';

RIKEN48334

F: 5'AGGGAAGCTTACGCACCTCG3'

R: 5'CAGCCTGACATTTTAACAGCCAC3';

Genomic Primers

EXON1

F: 5'GCAAGCTGACAAAGTTGGGG3'

R: 5'AAGCAAGCTTGTACGCCTGG3';

EXON2

F: 5'CCTGGGTGTGAGAAACCAGC3'

R: 5'AGGGCAGCTTCCATCTAGCA3';

EXON3

F: 5'CACACCCCCTCTTCTCCCTC3'

F: 5'TTGACAAGCACTTGAGGCCA3';

EXON4

F: 5'GCAGACTCCCATGCACCTTT3'

R: 5'TCGCAGTGGTGTGATTGCT3';

EXON5

F: 5'GGTGGTGGTAACACATCGGG3'

R: 5'TCCAGTGATATCTGGCCATTGA3';

EXON6 (Genomic2)

F: 5'CAAAAGGGAGAAATGCTGTGG3'

R: 5'TGACGTCTGCAGAGAGGCAC3';

EXON7 (Genomic3)

F: 5'GCCTGAAGGCAGTTCAAGTCTC3'

R: 5'CAACTGTTCCCACACAGGCA3';

EXON8 (Genomic4)

F: 5'CCATGACCACACCCAGAACA3'

R: 5'GCCTACAGCGACACAATAACCC3';

EXON9

F: 5'CCCCAGATAGTCTCCTGCCC3'

R: 5'ATAACGGAGGGGGCACTGTT3';

EXON10

F: 5'TGGTATCCAGCCTCCTGTGG3'

R: 5'TCATGCGTGCATCCTACCAG3';

EXON11

F: 5'GCTTGAGCTGAGGTTCGTCC3'

R: 5'GGGAGAGCATAGAGACCGGG3';

EXON12

F: 5'GGAACCCAGCTTCTTGGAGG3'

R: 5'AGCCACAAGCCAGTCTGAGG3';

EXON14

F: 5'CTCTCTCCCCCAACGTCCTC3'

R: 5'TTCAAGAGGCAGCAGGAAGC3';

EXON15

F: 5'GGCAGGTGATAGCTGAAGCA3'

R: 5'AATTCATTAGCAGGCGGGTG3';

EXON16

F: 5'TTTGTGGTCCCATGATGCAG3'

R: 5'TCCCCTCTGGTGGCTTGATA3';

EXON18

F: 5'TTCCTGAGAATGGGTGTGCC3'

R: 5'GCCAATGGTCACTGGGGAAA3';

EXON19

F: 5'GGCTCATCCGAACAACGAAA3'

R: 5'CCTGATGAGGAAGAAGGGCA3';

EXON20

F: 5'TGTCCCCTGGACAGATCCAT3'

R: 5'GGCAGGAGGAACTACTCCCC3';

EXON22

F: 5'CAAACACCATTTGCCCTGGT3'

R: 5'CCCTTTGGTGCTTTTATGGC3'.

APPENDIX E

Mouse Bicaudal-C Transcripts

TRANSCRIPT A

```
1  M A S Q S E P G Y L A A A Q S D P G S N
1  ATGGCCTCGCAGAGCGAGCCGGGCTACCTGGCGGCGGCGCAGTCGGACCCCGGCTCCAAC

21  S E R S T D S P V A G S E D D L V A A A
61  AGCGAGCGCAGCACC GACTCGCCGGTGGCCGGCTCCGAGGACGATCTGGTGGCCGCGGCG

41  P L L H S P E W S E E R F R V D R K K L
121 CCCCTCTTGCACAGCCCGGAGTGGAGCGAGGAGCGCTTCCGCGTGGACAGGAAGAAACTC

1  2
61  E A M L Q | A A A E G K G R S G E D F F Q KH1
181 GAGGCCATGCTCCAAGCTGCAGCTGAAGGAAAAGGCCGAAGTGGGAAGACTTTTTTTCAG

2  3
81  K | I M E E T N T Q I A W P S K L K I G A
241 AAGATCATGGAGGAGACAAACACGCAGATTGCATGGCCGTCCAAACTGAAGATCGGGGCT

3  4
101 K S K K | D P H I K V S G K K E D V K E A
301 AAATCCAAGAAAGATCCCCACATCAAGGTTTCTGGGAAGAAAGAGGATGTGAAGGAAGCC

4  5
121 K E M I M S V L D T K | S N R V T L K M D KH2
361 AAAGAAATGATCATGTCTGTCTTAGACACAAAAAGCAACCGCGTCACATTGAAGATGGAT

141 V S H T E H S H V I G K G G N N I K K V
421 GTCTCGCACACGGAGCACTCCCACGTCATCGGCAAGGGTGGTAACAACATTAAAAAGGTC

161 M E D T G C H I H F P D S N R N N Q A E
481 ATGGAAGACACGGGCTGCCACATCCACTTCCCAGACTCCAACAGGAACAACCAGGCAGAG

5  6
181 K S N Q | V S I A G Q P A G V E S A R A R
541 AAGAGTAACCAGGTGTCTATAGCAGGACAGCCAGCAGGAGTAGAATCGGCCCCGAGCAAGG

6  7
201 I R | E L L P L V L M F E L P I A G I L Q
601 ATTCGGGAGCTGCTTCCTTTGGTGCTGATGTTTGAGTTACCGATTGCCGGGATTCTCCAG

221 P V P D P N T P S I Q H I S Q T Y S V S
661 CCAGTCCCCGATCCCAACACCCCGTCCATTTCAGCACATCTCACAAACCTACAGCGTTTCT

241 V S F K Q R S R M Y G A T V T V R G S Q
721 GTGTCCTTTAAGCAGAGGTCTCGAATGTATGGTGCTACAGTCACAGTACGAGGCTCTCAG
```

⁷ ⁸
261 N N T N A V K | E G T A M L L E H L A G S
781 AATAACACTAATGCTGTGAAGGAAGGAACAGCCATGCTGTTGGAACACCTTGCGGGAAGC
KH3
281 L A S A I **P V S T Q L D I A A Q H H L F**
841 TTGGCCTCCGCCATCCCCGTGAGCACACAACCTGGACATAGCAGCCCAGCATCACCTCTTC

301 **M M G R N G S N V K H I M Q R T G A Q I**
901 ATGATGGGCCGGAACGGGAGCAACGTCAAACACATCATGCAGAGGACAGGGGCGCAGATT

321 **H F P D P S N P Q K K S T V Y L Q G T I**
961 CACTTTCCCGACCCCAGCAATCCACAGAAGAAATCCACCGTCTACCTCCAGGGCACCATT

⁸ ⁹
341 **E S V C L A R Q Y L M** | G C L P L V L M F
1021 GAGTCTGTCTGCCTAGCAAGGCAGTATCTCATGSGGTGTCTTCCTCTGGTGTGTGATGTTT

361 D M K E D I E V D P Q V I A Q L M E Q L
1081 GATATGAAGGAAGACATTGAAGTGGACCCACAGGTCATCGCACAGCTGATGGAACAGCTG

⁹ ¹⁰
381 D V F I S I K P K P K Q P S K | S V I V K
1141 GACGTCTTTATCAGTATTAAACCAAAGCCCCAAACAGCCGAGCAAGTCTGTGATTGTGAAA

401 S V E R N A L N M Y E A R K C L L G L E
1201 AGTGTTGAGCGAAATGCCTTAAATATGTATGAAGCAAGGAAGTGTCTCCTCGGACTTGAA

421 S S G V S I A T S L S P A S C P A G L A
1261 AGCAGTGGGGTTTCCATAGCAACCAGTCTATCCCCAGCATCGTGCCCTGCCGGCCTGGCC

¹⁰ ¹¹
441 C P S L D I L A S A G L G L T G L | G L L
1321 TGTCCCAGCCTGGATATCTTAGCTTCGGCAGGCCTCGGACTCACTGGACTAGGTTTATTG

461 G P T T L S L N T S A T P N S L L N A L
1381 GGGCCCACCACATTGTGCTAAATACGTGAGCCACCCCAAACCTCACTCCTGAATGCTCTC

481 N T S V S P L Q S S S S G T P S P T L W
1441 AACACTTCGGTCAGTCCTTTGCAAAGTTCAAGTTCTGGTACTCCAGTCCTACACTGTGG

¹¹ ¹²
501 A P P I A N T A S A T | G F S T I P H L M
1501 GCACCCCCAATCGCTAACACTGCAAGCGCCACAGGTTTCTCTACGATACCACACCTTATG

521 L P S T A Q A T L T N I L L S G V P T Y
1561 CTTCCCTCTACTGCCAGGCCACATTAACCAATATTTTGCTGTCTGGAGTGCCACATAC

541 G H T A P S P P P G L T P V D V H I N S
1621 GGGCACACGGCTCCATCTCCCCACCTGGCTTGACTCCTGTTGATGTTACATCAACAGC

561 M Q T E G K N I S A S I N G H V Q P A N
1681 ATGCAGACAGAAGGCAAAAACATCTCTGCGTCTATAAATGGACATGTGCAGCCTGCAAAC

581 M K Y G P L S T S S L G E K V L S S N H
1741 ATGAAATACGGTCCGCTGTCCACTTCATCGCTTGGGGAAAAAGTGCTGAGTTCGAATCAT

601 G D P S M Q T A G P E Q A S P K S N S V
1801 GGTGACCCATCCATGCAGACAGCTGGGCCCGAACAGGCTTCTCCTAAATCAAACCTCGGTG

621 E G C N D A F V E V G M P R S P S H S G
1861 GAAGGCTGCAATGATGCCTTTGTTGAAGTGGGCATGCCTCGAAGTCCCTCCCATTCTGGA

641 N A G D L K Q M L G A S K V S C A K R Q
1921 AACGCTGGCGACTTGAAGCAGATGCTGGGTGCCTCCAAGGTCTCCTGTGCCAAGCGGCAG

661 T V E L L Q G T K N S H L H G T D R L L
1981 ACGGTTGAGCTACTGCAGGGCACGAAGAACTCGCACCTCCACGGCACTGACAGACTACTC

681 S D P E L S A T E S P L A D K K A P G S
2041 TCAGACCCTGAACTGAGCGCCACAGAAAGTCCGCTTGCTGACAAGAAGGCCCCGGGGAGC

701 E R A A E R A A A A Q Q K S E R A R L A
2101 GAACGTGCAGCTGAGAGGGCAGCAGCTGCCCAGCAGAAATCGGAGAGGGCCCGCCTGGCC

721 S Q P T Y V H M Q A F D Y E Q K K L L A
2161 TCGCAGCCAACATATGTCCACATGCAGGSCATTTGATTATGAGCAGAAGAACTATTAGCC

741 T K A M L K K P V V T E V R T P T N T W
2221 ACCAAAGCGATGTTAAAGAAGCCAGTGGTGACTGAGGTCAGAACACCTACGAATACGTGG

761 S G L G F S K S M P A E T I K E L R R A
2281 AGTGGCCTGGGATTCTCAAAGTCCATGCCGGCAGAAACCATTAAGGAACTGAGGAGAGCC

781 N H V S Y K P T M T T A Y E G S S L S L
2341 AACCACGTATCCTATAAGCCCACGATGACCACCGCCTATGAGGGCTCCTCATTGTCCCTC

801 S R S S S R E H L A S G S E S D N W R D
2401 TCAAGGTCCAGCAGTCGTGAGCACCTGGCAAGTGGAAGCGAGTCAGACAACCTGGAGAGAC

821 R N G I G P M G H S E F S A P I G S P K
 2461 CGGAATGGAATAGGCCCATGGGTCACAGTGAATTCTCAGCACCAATCGGCAGCCCCAAG

841 R K Q N K S R E H Y L S S S N Y M D C I
 2521 CGCAAGCAGAACAAATCAAGAGAGCACTATCTAAGCAGCAGCAACTACATGGACTGCATT

861 S S L T G S N G C N L N S C F K G S D L
 2581 TCCTCGCTGACGGAAGCAATGGCTGTAACTGAACAGCTGCTTCAAAGGCTCCGACCTC

881 P E L F S K L G L G K Y T D V F Q Q Q E
 2641 CCCGAGCTTTTCAGCAAGCTGGGCCTAGGCAAATACACGGATGTCTTCCAGCAGCAAGAG

901 I D L Q T F L T L T D Q D L K E L G I T
 2701 ATCGATCTTCAGACATTCCTCACCTCACAGATCAGGATCTGAAGGAGCTGGGAATCACA

921 T F G A R R K M L L A I S E L S K N R R
 2761 ACCTTTGGTGCCGAAGGAAAATGCTGCTGGCAATCTCAGAGCTAAGTAAAAACCGAAGA

941 K L F E P P N A S C T S F L E G G A S G
 2821 AAACCTTTTGAACCAACAAACGCATCATGCACCTCCTTCCTGGAAGGC▼GGAGCCAGTGGG

R L P R Q Y H S D I A S V S G R W -
 2881 AGGCTGCCTCGCCAGTATCATTCAGACATTGCGAGCGTCAGTGGCCGCTGGTAGCGGTAC

2941 GCTTCTGGACACGCACCTGCTATCTTGCAAAGGTGGACACGATCCGTGGACAGTCTTCAC

3001 TCACTCGCCTGCCCTTGGCACTCGGAGTGTCTGGTATCAGGACCAAAGTGTTGATTTTCGT

3061 ACCTGTACTTCATGGCCAAAAAAAAAAAAAAAA

I

TRANSCRIPT B

```

1   M A S Q S E P G Y L A A A Q S D P G S N
1   ATGGCCTCGCAGAGCGAGCCGGGCTACCTGGCGGCGGCAGTCGGACCCCGGCTCCAAC

21  S E R S T D S P V A G S E D D L V A A A
61  AGCGAGCGCAGCACC GACTCGCCGGTGGCCGGCTCCGAGGACGATCTGGTGGCCGCGGGC

41  P L L H S P E W S E E R F R V D R K K L
121 CCCCTCTTGCACAGCCCGGAGTGGAGCGAGGAGCGCTTCCGCGTGGACAGGAAGAAACTC

      1 2
61  E A M L Q | A A A E G K G R S G E D F F Q KH1
181 GAGGCCATGCTCCAAGCTGCAGCTGAAGGAAAAGGCCGAAGTGGGGAAGACTTTTTTTCAG

      2 3
81  K | I M E E T N T Q I A W P S K L K I G A
241 AAGATCATGGAGGAGACAAACACGCAGATTGCATGGCCGTCCAAACTGAAGATCGGGGCT

      3 4
101 K S K K | D P H I K V S G K K E D V K E A
301 AAATCCAAGAAAGATCCCCACATCAAGGTTTCTGGGAAGAAAGAGGATGTGAAGGAAGCC

      4 5
121 K E M I M S V L D T K | S N R V T L K M D KH2
361 AAAGAAATGATCATGTCTGTCTTAGACACAAAAAGCAACCGCGTCACATTGAAGATGGAT

141 V S H T E H S H V I G K G G N N I K K V
421 GTCTCGCACACGGAGCACTCCCACGTCATCGGCAAGGGTGGTAACAACATTAAAAAGGTC

161 M E D T G C H I H F P D S N R N N Q A E
481 ATGGAAGACACGGGCTGCCACATCCAATTCCCAGACTCCAACAGGAACAACCAGGCAGAG

      5 6
181 K S N Q | V S I A G Q P A G V E S A R A R
541 AAGAGTAACCAGGTGTCTATAGCAGGACAGCCAGCAGGAGTAGAATCGGCCCCGAGCAAGG

      6 7
201 I R | E L L P L V L M F E L P I A G I L Q
601 ATTCGGGAGCTGCTTCCTTTGGTGCTGATGTTTGAGTTACCGATTGCCGGGATTCTCCAG

221 P V P D P N T P S I Q H I S Q T Y S V S
661 CCAGTCCCCGATCCCAACACCCCGTCCATTCAGCACATCTCACAAACCTACAGCGTTTCT

241 V S F K Q R S R M Y G A T V T V R G S Q
721 GTGTCCTTTAAGCAGAGGTCTCGAATGTATGGTGCTACAGTCACAGTACGAGGCTCTCAG

```

261 N N T N A V K ⁷ | ⁸ E G T A M L L E H L A G S
 781 AATAACACTAATGCTGTGAAGSAAGGAACAGCCATGCTGTTGGAACACCTTGCGGGAAGC

KH3

281 L A S A I P V S T Q L D I A A Q H H L F
 841 TTGGCCTCCGCCATCCCCGTGAGCACACAACCTGGACATAGCAGCCCAGCATCACCTCTTC

301 M M G R N G S N V K H I M Q R T G A Q I
 901 ATGATGGGCCGGAACGGGAGCAACGTCAAACACATCATGCAGAGGACAGGGGCGCAGATT

321 H F P D P S N P Q K K S T V Y L Q G T I
 961 CACTTTCCCGACCCCAGCAATCCACAGAAGAAATCCACCGTCTACCTCCAGGGCACCATT

341 E S V C L A R Q Y L ⁸ | ⁹ C L P L V L M F
 1021 GAGTCTGTCTGCCTAGCAAGGCAGTATCTCATGSGGTGTCTTCCTCTGGTGTGTGATGTTT

361 D M K E D I E V D P Q V I A Q L M E Q L
 1081 GATATGAAGGAAGACATTGAAGTGGACCCACAGGTCATCGCACAGCTGATGGAACAGCTG

381 D V F I S I K P K P K Q P S K ⁹ | ¹⁰ S V I V K
 1141 GACGTCTTTATCAGTATTAAACCAAAGCCCCAAACAGCCGAGCAAGTCTGTGATTGTGAAA

401 S V E R N A L N M Y E A R K C L L G L E
 1201 AGTGTGAGCGAAATGCCTTAAATATGTATGAAGCAAGGAAGTGTCTCCTCGGACTTGAA

421 S S G V S I A T S L S P A S C P A G L A
 1261 AGCAGTGGGGTTTCCATAGCAACCAGTCTATCCCCAGCATCGTGCCCTGCCGGCCTGGCC

441 C P S L D I L A S A G L G L T G L ¹⁰ | ¹¹ G L L
 1321 TGTCCCAGCCTGGATATCTTAGCTTCGGCAGGCCTCGGACTCACTGGACTAGGTTTATTG

461 G P T T L S L N T S A T P N S L L N A L
 1381 GGGCCCACCACATTGTCGCTAAATACGTGAGCCACCCCAAACCTCACTCCTGAATGCTCTC

481 N T S V S P L Q S S S S G T P S P T L W
 1441 AACACTTCGGTCAGTCCTTTGCAAAGTTCAAGTTCTGGTACTCCCAGTCCTACACTGTGG

501 A P P I A N T A S A T ¹¹ | ¹² G F S T I P H L M
 1501 GCACCCCCAATCGCTAACACTGCAAGCGCCACAGGTTTCTCTACGATACCACACCTTATG

521 L P S T A Q A T L T N I L L S G V P T Y
 1561 CTTCCCTCTACTGCCCAGGCCACATTAACCAATATTTTGCTGTCTGGAGTGCCACATAC

541 G H T A P S P P P G L T P V D V H I N S
1621 GGGCACACGGCTCCATCTCCCCACCTGGCTTGACTCCTGTTGATGTTACATCAACAGC

561 M Q T E G K N I S A S I N G H V Q¹²₁₃ P A N
1681 ATGCAGACAGAAGGCAAAAACATCTCTGCGTCTATAAATGGACATGTGCAGCCTGCAAAC

581 M K Y G P L S T S S L G E K V L S S N H
1741 ATGAAATACGGTCCGCTGTCCACTTCATCGCTTGGGGAAAAAGTGCTGAGTTCGAATCAT

601 G D P S M Q T A G P E Q A S P K S N S V
1801 GGTGACCCATCCATGCAGACAGCTGGGCCCCAACAGGCTTCTCCTAAATCAAACCTCGGTG

621 E¹³₁₄ G C N D A F V E V G M P R S P S H S G
1861 GAAGGCTGCAATGATGCCTTTGTTGAAGTGGGCATGCCTCGAAGTCCCTCCCATTCTGGA

641 N A G D L K Q M L G A S K V S C A K R Q
1921 AACGCTGGCGACTTGAAGCAGATGCTGGGTGCCTCCAAGGTCTCCTGTGCCAAGCGGCAG

661 T V E L L Q G T K N S H L H¹⁴₁₅ G T D R L L
1981 ACGGTTGAGCTACTGCAGGGCACGAAGAACTCGCACCTCCACGGGCACTGACAGACTACTC

681 S D P E L S A T E S P L A D K K A P G S
2041 TCAGACCCTGAACTGAGCGCCACAGAAAGTCCGCTTGCTGACAAGAAGGCCCCGGGGAGC

701 E R A A E R A A A A Q Q K S E R A R L A
2101 GAACGTGCAGCTGAGAGGGCAGCAGCTGCCCAGCAGAAATCGGAGAGGGCCCGCCTGGCC

721 S Q P T Y V H M Q¹⁵₁₆ A F D Y E Q K K L L A
2161 TCGCAGCCAACATATGTCCACATGCAGGSCATTTGATTATGAGCAGAAGAACTATTAGCC

741 T K A M L K K P V V T E V R T P T N T W
2221 ACCAAAGCGATGTTAAAGAAGCCAGTGGTGACTGAGGTCAGAACACCTACGAATACGTGG

761 S G L G F S K S M P A E T I K E L R R A
2281 AGTGGCCTGGGATTCTCAAAGTCCATGCCGGCAGAAACCATTAAGGAAGTGGAGAGAGCC

781 N H V S Y K P T M T T A Y E¹⁷₁₈ G S S L S L
2341 AACCACGTATCCTATAAGCCCACGATGACCACCGCCTATGAGGGCTCCTCATTGTCCCTC

801 S R S S S R E H L A S G S E S D N W R D
2401 TCAAGGTCCAGCAGTCGTGAGCACCTGGCAAGTGGAAGCGAGTCAGACAACCTGGAGAGAC

821 R N G I G P M G H S E F S A P I G S P K
 2461 CGGAATGGAATAGGCCCATGGGTCACAGTGAATTCTCAGCACCAATCGGCAGCCCCAAG

841 R K Q N K S R E H Y L S S S N Y M D C I
 2521 CGCAAGCAGAACAATCAAGAGAGCACTATCTAAGCAGCAGCAACTACATGGACTGCATT

861 S S L T G S N G C N L N S C F K G S D L
 2581 TCCTCGCTGACGGGAAGCAATGGCTGTAACCTGAACAGCTGCTTCAAAGGCTCCGACCTC

881 P E L F S K L G L G K Y T D V F Q Q Q E
 2641 CCCGAGCTTTTCAGCAAGCTGGGCCTAGGCAAATACACGGATGTCTTCCAGCAGCAAGAG

901 I D L Q T F L T L T D Q D L K E L G I T
 2701 ATCGATCTTCAGACATTCTCACCCTCACAGATCAGGATCTGAAGGAGCTGGGAATCACA

921 T F G A R R K M L L A I S V C D S V Q I
 2761 ACCTTTGGTGCCCGAAGGAAAATGCTGCTGGCAATCTCAGTTTGTGACTCTGTTTCAGATC

941 R N K I L R A A R I L -
 2821 CGCAACAAGATCCTGAGAGCTGCCAGGATTCTGTGAACCTTGAATGTCAAAGAAAAAAG

2882 AGCTAAGTAAAAACCGAAGAAAACTTTTTGAACCACCAAACGCATCATGCACCTCCTTCC

2941 TGGAAGG▼CGGAGCCAGTGGGAGGCTGCCTCGCCAGTATCATTAGACATTGCGAGCGTCA
 GC (bpk) insertion

3001 GTGGCCGCTGGTAGCGGTACCTTCTGGACACGCACCTGCTATCTTGCAAAGGTGGACACG

3061 ATCCGTGGACAGTCTTCACTGCACTCGCCTGCCCTTGGCACTCGGAGTGTCTGGTATCAG

3121 GACCAAAGTGTTGATTTTCGTACCTGTACTTCATGGCCAAAAAAAAAAAAAAAAA

I

APPENDIX F

KH Domain Multialignment

KH1

MOUSE	-----KIMEETNTQIAWPSKLKIGAKSKK-----DPHIKVS	31
HUMAN	-----HRVVGQPDQPYKYITGFKQFHRNTKEAQYILQCQSQSTCVDPHIKVS	47
RAT	-----DPHIKVS	7
XENOPUS	AAEGKGKSGEDFFQKIMEETNTQIAWPSKLKIGAKSKK-----DPHIKVS	45
FUGU	-----QIMDETQTQIAWPSKLKIGAKSKK-----GDC	27
DANIO	-----	
DROSOPHILA	-----HDIMNTTDTYVSWPCRLKIGAKSKK-----DPHVRIV	32
ANOPHELES	-----TNIMKETTTYVSWPCRLKIGAKTKK-----DPHIRIV	32

KH2

MOUSE	GKKEDVKEAKEMIMSVLDTKSNRVTLKMDVSHTEHSHVIGKGGNNIKKVMEDTGCHIHF	91
HUMAN	GKKEDVKEAKEMIMSVLDTKSNRVTLKMDVSHTEHSHVIGKGGNNIKKVMEDTGCHIHF	107
RAT	GKKEAVKEAKEMIMAVLDTKSNRVTLKMDVSHTEHSHVIGKGGNNIKKVMEDTGCHIHF	67
XENOPUS	GKKENVKEAKERIMSVLDTKSNRVTLKMDVLTHTHSHVIGKGGNNIKKVMEDTGCHIHF	105
FUGU	ILKGQMSITSITFSASFHPLVSNRVTLKMDVSHTEHSHVIGKGGNNIKKVMEDTGCHIHF	87
DANIO	-----	
DROSOPHILA	GKVDQVQRAKERILSSLDGRGT RVIMKMDVSYTDHSYII GRGGNNIKRIMDDTHTHIHF	92
ANOPHELES	GKMADVLRADKVMARLDSRGS RVIMKMDVSYTDHSFI GRGGNNIKKIMEETATHIHF	92

MOUSE	DSNRNNQAEKSNQVS IAGQPAGVESARARIRELLPLVLMFELPIAGILQPVDPNTPSIQ	151
HUMAN	DSNRNNQAEKSNQVS IAGQPAGVESARVRIRELLPLVLMFELPIAGILQPVDPNTPSIQ	167
RAT	DSNRNNQVEKSNQVS IAGQPAGVESARARIRELLPLVLMFELPIAGILQPVDPNTPSIQ	127
XENOPUS	DSNRNNQAEKSNQVS IAGQPAGVESARVRIRELLPLVLMFELPIAGILQPIPDNTPSIQ	165
FUGU	DSNRNNQAEKSN-----QELLPLVLSFELP--AIMQ--SDPSSPTVQ	125
DANIO	-----QELLPLVLMFELPVIGQLN--PDSPSPAIQ	28
DROSOPHILA	DSNRSNPTEKSNQVSLCGSLEGVERARALVRLSTPLLISFEMPMGPNKQPDHETPYIK	152
ANOPHELES	DSNRSNPTEKSNQVSMCGSIEGVERARSLVRNSTPLLISFELPILAPGKTPDNNDTPYVK	152

KH3

MOUSE	HISQTYSVSVSFKQSRMYGATVTVRGSQNNTNAVKEGTAMLEHLAGSLASAI PVSTQL	211
HUMAN	HISQTYNISVSFKQSRMYGATVIVRGSQNNTSAVKEGTAMLEHLAGSLASAI PVSTQL	227
RAT	HISQTYSVSVSFKQSRMYGATVIVRGSQNNTNAVKEGTAMLEHLAGSLASAI PVSTQL	187
XENOPUS	QISQTYNLTVSFKQSRVYGATVIVRGSQNNTSAVKEGTAMLEHLAGSLATAI PVSTQL	225
FUGU	HISQTYNLTVSFKPPTRLYRASGVVRGSQNNTNAVKRGTALLLEHLVGLASTISVSTHL	185
DANIO	HISQTYNISVAFKQSRRLYGATGVVRGSQNNAAVKRGTAVLLEHLAGNLSAIIISTQL	88
DROSOPHILA	MIETKFNQVIFSTRPKLHTSLVLVKGSEKESAQVRDATQLLINFACESIASQILVNVQM	212
ANOPHELES	EIEAEYGVQVIFSTRPKLHSSLVLVKGSEKEERMVKEATRRLMDLMCENMASQIPVHMQL	212

MOUSE	DIAAQHHLFMMGRNGSNV KHIMQRTGAQIHFPDPS----NPQKKSTVYLQGTIESVCLAR	267
HUMAN	DIAAQHHLFMMGRNGSNIKHIMQRTGAQIHFPDPS----NPQKKSTVYLQGTIESVCLAR	283
RAT	DIAAQHHLFMMGRNGSNV KHIMQRTGAQIHFPDPS----NPQKKSTVYLQGTIESVCLAR	243
XENOPUS	DIAAQHHLFMMGRNGCNIKHIMQRTGAQIHFPDPN----NPLKKSTVYLQGTIDSVCLAR	281
FUGU	DIAAPQHHLFMKGRNGSNIKHITQRTGAQIHFPDPN----SPQKKSTVYIQGTIESVCLAR	241
DANIO	DIALQHHLFMFGRNGSNIKHIMQRTGAQVHFPDPN----CPQKKSTVYVQGTIDSVCLAR	144
DROSOPHILA	EISFQHHIEIVKGKNNVNLLSIMERTQTKIIFPDLSDMNVKPLKKSQVTISGPIDDVYLAR	272
ANOPHELES	EISTQHHPIVLGRSSSNLREIMNRTGTQIMFPDANDVNIKPIKRSQVTTIGSINGVYLAR	272

MOUSE	QYL	270
HUMAN	QYL	286
RAT	QYL	246
XENOPUS	QYL	284
FUGU	QYL	244
DANIO	QYL	147
DROSOPHILA	QQL	275
ANOPHELES	QQL	275
	* *	

Red = conserved in all species
Blue = conserved in four or more species

APPENDIX G

PRIMER MAP FOR RECOMBINANT PROTEINS

Primers used are indicated in purple.

Biccl/pET.f

1 M A S Q S E P G Y L A A A Q S D P G S N
 1 **ATG**GCCTCGCAGAGCGAGCCGGGCTACCTGGCGGCGGCGCAGTCGGACCCCGGCTCCAAC

21 S E R S T D S P V A G S E D D L V A A A
 61 AGCGAGCGCAGCACCGACTCGCCGGTGGCCGGCTCCGAGGACGATCTGGTGGCCGCGGCG

41 P L L H S P E W S E E R F R V D R K K L
 121 CCCCTCTTGCACAGCCCGGAGTGGAGCGAGGAGCGCTTCCGCGTGGACAGGAAGAACTC

61 E A M L Q ¹ ² A A A E G K G R S G E D F F **Q** **KH1**
 181 GAGGCCATGCTCCAAGCTGCAGCTGAAGGAAAAGCCGAAGTGGGGAAGACTTTTTTTCAG

² ³

81 **K I M E E T N T Q I A W P S K L K I G A**
 241 AAGATCATGGAGGAGACAAACACGCAGATTGCATGGCCGTCCAAACTGAAGATCGGGGCT

³ ⁴

101 **K S K K D P H I K V S G K K E D V K E A**
 301 AAATCCAAGAAAGATCCCCACATCAAGGTTTCTGGGAAGAAAGAGGATGTGAAGGAAGCC

KH2.f ⁴ ⁵ **KH2**

121 **K E M I M** S V L D T K S N **R V T L K M D**
 361 AAAGAAATGATCATGTCTGTCTTAGACACAAAAAGCAACCGCGTCACATTGAAGATGGAT

KH1.r

141 **V S H T E H S H V I G K G G N N I K K V**
 421 GTCTCGCACACGGAGCACTCCCACGTCATCGGCAAGGGTGGTAACAACATTAAAAAGGTC

161 **M E D T G C H I H F P D S N R N N Q A E**
 481 ATGGAAGACACGGGCTGCCACATCCACTTCCCAGACTCCAACAGGAACAACCAGGCAGAG

181 **K S N Q** | **V S I A G Q P A G V E S A R A** R
 541 AAGAGTAACCAGGTGTCTATAGCAGGACAGCCAGCAGGAGTAGAATCGGCCCCGAGCAAGG

201 I R | ⁶7 **KH1+KH2.r** E L L P L V L M F E L P I A G I L Q
 601 ATTCGGGAGCTGCTTCCTTTGGTGCTGATGTTTGAGTTACCGATTGCCGGGATTCTCCAG

221 P V P D P N T P S I Q H I S Q T Y S V S
 661 CCAGTCCCCGATCCCAACACCCCGTCCATTGAGCACATCTCACAAACCTACAGCGTTTCT

241 V S F K Q R S R M Y G A T V T V R G S Q
 721 GTGTCCTTTAAGCAGAGGTCTCGAATGTATGGTGCTACAGTCACAGTACGAGGCTCTCAG

261 N N T N A V K | ⁷8 **KH3.f** E G T A M L L E H L A G S
 781 AATAACACTAATGCTGTGAAGGAAGGAACAGCCATGCTGTTGGAACACCTTGCGGGAAGC

281 L A S A I **KH3** **P V S T Q L D I A A Q H H L F**
 841 TTGGCCTCCGCCATCCCCGTGAGCACACAACCTGGACATAGCAGCCCAGCATCACCTCTTC

301 **M M G R N G S N V K H I M Q R T G A Q I**
 901 ATGATGGGCCGGAACGGGAGCAACGTCAAACACATCATGCAGAGGACAGGGGCGCAGATT

321 **H F P D P S N P Q K K S T V Y L Q G T I**
 961 CACTTTCCCGACCCAGCAATCCACAGAAGAAATCCACCGTCTACCTCCAGGGCACCATT

341 **E S V C L A R Q Y L** M | ⁸9 G C L P L V L M F
 1021 GAGTCTGTCTGCCTAGCAAGGCAGTATCTCATGSGGTGTCTTCCTCTGGTGTTGATGTTT

361 D M K E D I E V D P Q V I A Q L M E Q L
 1081 GATATGAAGGAAGACATTGAAGTGGACCCACAGGTCATCGCACAGCTGATGGAACAGCTG

381 D V F I S I K P K P K Q P S K | ⁹10 S V I V K
 1141 GACGTCTTTATCAGTATTAAACCAAAGCCCAAACAGCCGAGCAAGTCTGTGATTGTGAAA

KH1+KH2+KH3.r

```

401   S V E R N A L N M Y E A R K C L L G L E
1201  AGTGTGAGCGAAATGCCTTAAATATGTATGAAGCAAGGAAGTGTCTCCTCGGACTTGAA

421   S S G V S I A T S L S P A S C P A G L A
1261  AGCAGTGGGGTTTCCATAGCAACCAGTCTATCCCCAGCATCGTGCCCTGCCGGCCTGGCC

441   C P S L D I L A S A G L G L T G L
1321  TGTCCCAGCCTGGATATCTTAGCTTCGGCAGGCCTCGGACTCACTGGACTAG10G11TTTATTG

461   G P T T L S L N T S A T P N S L L N A L
1381  GGGCCCACCACATTGTCGCTAAATACGTCAGCCACCCCAAACCTCACTCCTGAATGCTCTC

481   N T S V S P L Q S S S S G T P S P T L W
1441  AACACTTCGGTCAGTCCTTTGCAAAGTTCAAGTTCTGGTACTCCCAGTCCTACACTGTGG

501   A P P I A N T A S A T
1501  GCACCCCCAATCGCTAACACTGCAAGCGCCACAG11G12TTTCTCTACGATAACCACACCTTATG

521   L P S T A Q A T L T N I L L S G V P T Y
1561  CTTCCCTCTACTGCCCAGGCCACATTAACCAATATTTTGCTGTCTGGAGTGCCCACATAC

541   G H T A P S P P P G L T P V D V H I N S
1621  GGGCACACGGCTCCATCTCCCCACCTGGCTTGACTCCTGTTGATGTTACATCAACAGC

561   M Q T E G K N I S A S I N G H V Q
1681  ATGCAGACAGAAGGCAAAAACATCTCTGCGTCTATAAATGGACATGTGCAG12C13CCTGCAAAC

581   M K Y G P L S T S S L G E K V L S S N H
1741  ATGAAATACGGTCCGCTGTCCACTTCATCGCTTGGGGAAAAAGTGCTGAGTTCAATCAT

601   G D P S M Q T A G P E Q A S P K S N S V
1801  GGTGACCCATCCATGCAGACAGCTGGGCCCCGAACAGGCTTCTCCTAAATCAAACCTCGGTG

```


¹³ ¹⁴
621 E G C N D A F V E V G M P R S P S H S G
1861 GAAGGCTGCAATGATGCCTTTGTTGAAGTGGGCATGCCTCGAAGTCCCTCCCATTCTGGA

641 N A G D L K Q M L G A S K V S C A K R Q
1921 AACGCTGGCGACTTGAAGCAGATGCTGGGTGCCTCCAAGGTCTCCTGTGCCAAGCGGCAG

¹⁴ ¹⁵
661 T V E L L Q G T K N S H L H G T D R L L
1981 ACGGTTGAGCTACTGCAGGGCACGAAGAACTCGCACCTCCACGGGCACTGACAGACTACTC

681 S D P E L S A T E S P L A D K K A P G S
2041 TCAGACCCTGAACTGAGCGCCACAGAAAGTCCGCTTGCTGACAAGAAGGCCCCGGGGAGC

701 E R A A E R A A A A Q Q K S E R A R L A
2101 GAACGTGCAGCTGAGAGGGCAGCAGCTGCCCAGCAGAAATCGGAGAGGGCCCGCCTGGCC

¹⁵ ¹⁶
721 S Q P T Y V H M Q A F D Y E Q K K L L A
2161 TCGCAGCCAACATATGTCCACATGCAGSCATTTGATTATGAGCAGAAGAACTATTAGCC

741 T K A M L K K P V V T E V R T P T N T W
2221 ACCAAAGCGATGTTAAAGAAGCCAGTGGTGACTGAGGTCAGAACACCTACGAATACGTGG

761 S G L G F S K S M P A E T I K E L R R A
2281 AGTGGCCTGGGATTCTCAAAGTCCATGCCGGCAGAAACCATTAAGGAAGTGGAGAGAGCC

¹⁷ ¹⁸
781 N H V S Y K P T M T T A Y E G S S L S L
2341 AACCACGTATCCTATAAGCCCACGATGACCACCGCCTATGAGGGCTCCTCATTGTCCCTC

801 S R S S S R E H L A S G S E S D N W R D
2401 TCAAGGTCCAGCAGTCGTGAGCACCTGGCAAGTGGAAGCGAGTCAGACAAGTGGAGAGAC

821 R N G I G P M G H S E F S A P I G S P K
2461 CGGAATGGAATAGGCCCCATGGGTCACAGTGAATTCTCAGCACCAATCGGCAGCCCCAAG

18 | 19
 841 R K Q N K S R E H Y L S S S N Y M D C I
 2521 CGCAAGCAGAACAATCAAGAGAGCACTATCTAAGCAGCAGCAACTACATGGACTGCATT

SAM DOMAIN
 861 S S L T G S N G C N L N S C F K G S D L
 2581 TCCTCGCTGACGGGAAGCAATGGCTGTAACTGAACAGCTGCTTCAAAGGCTCCGACCTC

19 20
 881 P E L F S K L G L G K Y T D V F Q Q Q E
 2641 CCCGAGCTTTTCAGCAAGCTGGGCCTAGGCAAATACACGGATGTCTTCCAGCAGCAAGAG

901 I D L Q T F L T L T D Q D L K E L G I T
 2701 ATCGATCTTCAGACATTCTCACCCTCACAGATCAGGATCTGAAGGAGCTGGGAATCACA

pET101/FL.7r 20 21
 921 T F G A R R K M L L A I S V C D S V Q I
 2761 ACCTTTGGTGCCCGAAGGAAAATGCTGCTGGCAATCTCAGTTTGTGACTCTGTTTCAGATC

941 R N K I L R A A R I L -
 2821 CGCAACAAGATCCTGAGAGCTGCCAGGATTCTGTGAACCTTGAATGTCAAAGAAAAAAG

21 22
 2883 AGCTAAGTAAAAACCGAAGAAAACCTTTTTGAACCACCAAACGCATCATGCACCTCCTTCC

2941 TGGAAGG▼CGGAGCCAGTGGGAGGCTGCCTCGCCAGTATCATTGAGACATTGCGAGCGTCA
 GC (bpk) insertion

3001 GTGGCCGCTGGTAGCGGTACCTTCTGGACACGCACCTGCTATCTTGCAAAGGTGGACACG

3062 ATCCGTGGACAGTCTTCACTGCACTCGCCTGCCCTTGGCACTCGGAGTGTCTGGTATCAG

3122 GACCAAAGTGTTGATTTTCGTACCTGTACTTCATGGCCAAAAAAAAAAAAAAAAAAAA

BIBLIOGRAPHY

1. **Aberle, H., H. Schwartz, and R. Kemler.** 1996. Cadherin-catenin complex: protein interactions and their implications for cadherin function. *J Cell Biochem* **61**:514-23.
2. **Afzelius, B. A.** 1976. A human syndrome caused by immotile cilia. *Science* **193**:317-9.
3. **Aguiari, G., M. Campanella, E. Manzati, P. Pinton, M. Banzi, S. Moretti, R. Piva, R. Rizzuto, and L. del Senno.** 2003. Expression of polycystin-1 C-terminal fragment enhances the ATP-induced Ca²⁺ release in human kidney cells. *Biochem Biophys Res Commun* **301**:657-64.
4. **Ali, S. M., V. Y. Wong, K. Kikly, T. A. Fredrickson, P. M. Keller, W. E. DeWolf, Jr., D. Lee, and D. P. Brooks.** 2000. Apoptosis in polycystic kidney disease: involvement of caspases. *Am J Physiol Regul Integr Comp Physiol* **278**:R763-9.
5. **Altschul, S. F., W. Gish, W. Miller, E. W. Myers, and D. J. Lipman.** 1990. Basic local alignment search tool. *J Mol Biol* **215**:403-10.
6. **Anderson, G. A., D. Degroot, and R. K. Lawson.** 1993. Polycystic renal disease. *Urology* **42**:358-64.
7. **Ariza, M., V. Alvarez, R. Marin, S. Aguado, C. Lopez-Larrea, J. Alvarez, M. J. Menendez, and E. Coto.** 1997. A family with a milder form of adult dominant polycystic kidney disease not linked to the PKD1 (16p) or PKD2 (4q) genes. *J Med Genet* **34**:587-9.
8. **Atala, A., M. R. Freeman, J. Mandell, and D. R. Beier.** 1993. Juvenile cystic kidneys (jck): a new mouse mutation which causes polycystic kidneys. *Kidney Int* **43**:1081-5.
9. **Aviv, T., Z. Lin, S. Lau, L. M. Rendl, F. Sicheri, and C. A. Smibert.** 2003. The RNA-binding SAM domain of Smaug defines a new family of post-transcriptional regulators. *Nat Struct Biol* **10**:614-21.
10. **Avner, E. D.** 1993. Epithelial polarity and differentiation in polycystic kidney disease. *J Cell Sci Suppl* **17**:217-22.
11. **Avner, E. D.** 1990. Polypeptide growth factors and the kidney: a developmental perspective. *Pediatr Nephrol* **4**:345-53.
12. **Avner, E. D., F. E. Studnicki, M. C. Young, W. E. Sweeney, Jr., N. P. Piesco, D. Ellis, and G. H. Fettermann.** 1987. Congenital murine

polycystic kidney disease. I. The ontogeny of tubular cyst formation. *Pediatr Nephrol* **1**:587-96.

13. **Avner, E. D., W. E. Sweeney, Jr., and W. J. Nelson.** 1992. Abnormal sodium pump distribution during renal tubulogenesis in congenital murine polycystic kidney disease. *Proc Natl Acad Sci U S A* **89**:7447-51.
14. **Barr, M. M., J. DeModena, D. Braun, C. Q. Nguyen, D. H. Hall, and P. W. Sternberg.** 2001. The *Caenorhabditis elegans* autosomal dominant polycystic kidney disease gene homologs *lov-1* and *pkd-2* act in the same pathway. *Curr Biol* **11**:1341-6.
15. **Barr, M. M., and P. W. Sternberg.** 1999. A polycystic kidney-disease gene homologue required for male mating behaviour in *C. elegans*. *Nature* **401**:386-9.
16. **Bergmann, C., J. Senderek, B. Sedlacek, I. Pegiazoglou, P. Puglia, T. Eggermann, S. Rudnik-Schoneborn, L. Furu, L. F. Onuchic, M. De Baca, G. G. Germino, L. Guay-Woodford, S. Somlo, M. Moser, R. Buttner, and K. Zerres.** 2003. Spectrum of mutations in the gene for autosomal recessive polycystic kidney disease (ARPKD/PKHD1). *J Am Soc Nephrol* **14**:76-89.
17. **Bernstein, J.** 1986. Hepatic and renal involvement in malformation syndromes. *Mt Sinai J Med* **53**:421-8.
18. **Bhunja, A. K., K. Piontek, A. Boletta, L. Liu, F. Qian, P. N. Xu, F. J. Germino, and G. G. Germino.** 2002. PKD1 induces p21(waf1) and regulation of the cell cycle via direct activation of the JAK-STAT signaling pathway in a process requiring PKD2. *Cell* **109**:157-68.
19. **Blythe, W. B.** 1971. Severity of established renal disease: criteria for evaluation. *Ann Intern Med* **75**:315.
20. **Boehnke, M.** 1992. Multipoint analysis for radiation hybrid mapping. *Ann Med* **24**:383-6.
21. **Bogdanova, N., A. Markoff, V. Gerke, M. McCluskey, J. Horst, and B. Dworniczak.** 2001. Homologues to the first gene for autosomal dominant polycystic kidney disease are pseudogenes. *Genomics* **74**:333-41.
22. **Bohnenlein, E., K. Chowdhury, and P. Gruss.** 1985. Functional analysis of the regulatory region of polyoma mutant F9-1 DNA. *Nucleic Acids Res* **13**:4789-809.
23. **Boletta, A., and G. G. Germino.** 2003. Role of polycystins in renal tubulogenesis. *Trends Cell Biol* **13**:484-92.

24. **Bouchard, M., A. Souabni, M. Mandler, A. Neubuser, and M. Busslinger.** 2002. Nephric lineage specification by Pax2 and Pax8. *Genes Dev* **16**:2958-70.
25. **Boulter, C., S. Mulroy, S. Webb, S. Fleming, K. Brindle, and R. Sandford.** 2001. Cardiovascular, skeletal, and renal defects in mice with a targeted disruption of the Pkd1 gene. *Proc Natl Acad Sci U S A* **98**:12174-9.
26. **Brown, N. A., and L. Wolpert.** 1990. The development of handedness in left/right asymmetry. *Development* **109**:1-9.
27. **Brueckner, M.** 2001. Cilia propel the embryo in the right direction. *Am J Med Genet* **101**:339-44.
28. **Bryda, E. C., H. Ling, D. E. Rathbun, M. Burmeister, and L. Flaherty.** 1996. Fine genetic map of mouse chromosome 10 around the polycystic kidney disease gene, jcpk, and ankyrin 3. *Genomics* **35**:425-30.
29. **Buckanovich, R. J., and R. B. Darnell.** 1997. The neuronal RNA binding protein Nova-1 recognizes specific RNA targets in vitro and in vivo. *Mol Cell Biol* **17**:3194-201.
30. **Bullions, L. C., and A. J. Levine.** 1998. The role of beta-catenin in cell adhesion, signal transduction, and cancer. *Curr Opin Oncol* **10**:81-7.
31. **Byers, P. H.** 2002. Killing the messenger: new insights into nonsense-mediated mRNA decay. *J Clin Invest* **109**:3-6.
32. **Cai, W. W., J. Reneker, C. W. Chow, M. Vaishnav, and A. Bradley.** 1998. An anchored framework BAC map of mouse chromosome 11 assembled using multiplex oligonucleotide hybridization. *Genomics* **54**:387-97.
33. **Calvet, J. P.** 2003. Ciliary signaling goes down the tubes. *Nat Genet* **33**:113-4.
34. **Calvet, J. P.** 1998. Molecular genetics of polycystic kidney disease. *J Nephrol* **11**:24-34.
35. **Carone, F. A.** 1990. The pathogenesis of polycystic kidney disease. *Contrib Nephrol* **83**:245-9.
36. **Carone, F. A., R. Bacallao, and Y. S. Kanwar.** 1994. Biology of polycystic kidney disease. *Lab Invest* **70**:437-48.

37. **Carone, F. A., S. Nakamura, M. Caputo, R. Bacallao, W. J. Nelson, and Y. S. Kanwar.** 1994. Cell polarity in human renal cystic disease. *Lab Invest* **70**:648-55.
38. **Chalepakis, G., P. Tremblay, and P. Gruss.** 1992. Pax genes, mutants and molecular function. *J Cell Sci Suppl* **16**:61-7.
39. **Chen, T., B. B. Damaj, C. Herrera, P. Lasko, and S. Richard.** 1997. Self-association of the single-KH-domain family members Sam68, GRP33, GLD-1, and Qk1: role of the KH domain. *Mol Cell Biol* **17**:5707-18.
40. **Chittenden, L., X. Lu, N. L. Cacheiro, K. T. Cain, W. Generoso, E. C. Bryda, and L. Stubbs.** 2002. A new mouse model for autosomal recessive polycystic kidney disease. *Genomics* **79**:499-504.
41. **Cogswell, C., S. J. Price, X. Hou, L. M. Guay-Woodford, L. Flaherty, and E. C. Bryda.** 2003. Positional cloning of jcpk/bpk locus of the mouse. *Mamm Genome* **14**:242-9.
42. **Coles, H. S., J. F. Burne, and M. C. Raff.** 1993. Large-scale normal cell death in the developing rat kidney and its reduction by epidermal growth factor. *Development* **118**:777-84.
43. **Cowley, B. D., Jr., S. Gudapaty, A. L. Kraybill, B. D. Barash, M. A. Harding, J. P. Calvet, and V. H. Gattone, 2nd.** 1993. Autosomal-dominant polycystic kidney disease in the rat. *Kidney Int* **43**:522-34.
44. **Cowley, B. D., Jr., and J. C. Rupp.** 1995. Abnormal expression of epidermal growth factor and sulfated glycoprotein SGP-2 messenger RNA in a rat model of autosomal dominant polycystic kidney disease. *J Am Soc Nephrol* **6**:1679-81.
45. **Cox, D. R., M. Burmeister, E. R. Price, S. Kim, and R. M. Myers.** 1990. Radiation hybrid mapping: a somatic cell genetic method for constructing high-resolution maps of mammalian chromosomes. *Science* **250**:245-50.
46. **Crocker, J. F., S. R. Blecher, M. L. Givner, and S. C. McCarthy.** 1987. Polycystic kidney and liver disease and corticosterone changes in the cpk mouse. *Kidney Int* **31**:1088-91.
47. **Culbertson, M. R.** 1999. RNA surveillance. Unforeseen consequences for gene expression, inherited genetic disorders and cancer. *Trends Genet* **15**:74-80.
48. **D'Agata, I. D., M. M. Jonas, A. R. Perez-Atayde, and L. M. Guay-Woodford.** 1994. Combined cystic disease of the liver and kidney. *Semin Liver Dis* **14**:215-28.

49. **Dahanukar, A., J. A. Walker, and R. P. Wharton.** 1999. Smaug, a novel RNA-binding protein that operates a translational switch in *Drosophila*. *Mol Cell* **4**:209-18.
50. **Daoust, M. C., D. M. Reynolds, D. G. Bichet, and S. Somlo.** 1995. Evidence for a third genetic locus for autosomal dominant polycystic kidney disease. *Genomics* **25**:733-6.
51. **de Almeida, S., E. de Almeida, D. Peters, J. R. Pinto, I. Tavora, J. Lavinha, M. Breuning, and M. M. Prata.** 1995. Autosomal dominant polycystic kidney disease: evidence for the existence of a third locus in a Portuguese family. *Hum Genet* **96**:83-8.
52. **Deget, F., S. Rudnik-Schoneborn, and K. Zerres.** 1995. Course of autosomal recessive polycystic kidney disease (ARPKD) in siblings: a clinical comparison of 20 sibships. *Clin Genet* **47**:248-53.
53. **Delmas, P., H. Nomura, X. Li, M. Lakkis, Y. Luo, Y. Segal, J. M. Fernandez-Fernandez, P. Harris, A. M. Frischauf, D. A. Brown, and J. Zhou.** 2002. Constitutive activation of G-proteins by polycystin-1 is antagonized by polycystin-2. *J Biol Chem* **277**:11276-83.
54. **Di Palma, F., R. H. Holme, E. C. Bryda, I. A. Belyantseva, R. Pellegrino, B. Kachar, K. P. Steel, and K. Noben-Trauth.** 2001. Mutations in *Cdh23*, encoding a new type of cadherin, cause stereocilia disorganization in waltzer, the mouse model for Usher syndrome type 1D. *Nat Genet* **27**:103-7.
55. **Dietrich, W., H. Katz, S. E. Lincoln, H. S. Shin, J. Friedman, N. C. Dracopoli, and E. S. Lander.** 1992. A genetic map of the mouse suitable for typing intraspecific crosses. *Genetics* **131**:423-47.
56. **Dipple, K. M., and E. R. McCabe.** 2000. Modifier genes convert "simple" Mendelian disorders to complex traits. *Mol Genet Metab* **71**:43-50.
57. **Donaldson, J. C., R. S. Dise, M. D. Ritchie, and S. K. Hanks.** 2002. Nephrocystin-conserved domains involved in targeting to epithelial cell-cell junctions, interaction with filamins, and establishing cell polarity. *J Biol Chem* **277**:29028-35.
58. **Dressler, G. R.** 1996. Pax-2, kidney development, and oncogenesis. *Med Pediatr Oncol* **27**:440-4.
59. **Dressler, G. R., and E. C. Douglass.** 1992. Pax-2 is a DNA-binding protein expressed in embryonic kidney and Wilms tumor. *Proc Natl Acad Sci U S A* **89**:1179-83.

60. **Dressler, G. R., J. E. Wilkinson, U. W. Rothenpieler, L. T. Patterson, L. Williams-Simons, and H. Westphal.** 1993. Deregulation of Pax-2 expression in transgenic mice generates severe kidney abnormalities. *Nature* **362**:65-7.
61. **Du, J., and P. D. Wilson.** 1995. Abnormal polarization of EGF receptors and autocrine stimulation of cyst epithelial growth in human ADPKD. *Am J Physiol* **269**:C487-95.
62. **Dutcher, S. K.** 2001. Motile organelles: the importance of specific tubulin isoforms. *Curr Biol* **11**:R419-22.
63. **Ebihara, I., P. D. Killen, G. W. Laurie, T. Huang, Y. Yamada, G. R. Martin, and K. S. Brown.** 1988. Altered mRNA expression of basement membrane components in a murine model of polycystic kidney disease. *Lab Invest* **58**:262-9.
64. **Ebihara, I., T. Nakamura, T. Takahashi, M. Yamamoto, Y. Tomino, S. Nagao, H. Takahashi, and H. Koide.** 1995. Altered extracellular matrix component gene expression in murine polycystic kidney. *Ren Physiol Biochem* **18**:73-80.
65. **Eo, H. S., J. G. Lee, C. Ahn, J. T. Cho, D. Y. Hwang, Y. H. Hwang, E. J. Lee, Y. S. Kim, J. S. Han, S. Kim, J. S. Lee, D. I. Jeoung, S. E. Lee, and U. K. Kim.** 2002. Three novel mutations of the PKD1 gene in Korean patients with autosomal dominant polycystic kidney disease. *Clin Genet* **62**:169-74.
66. **Flaherty, L., E. C. Bryda, D. Collins, U. Rudofsky, and J. C. Montgomery.** 1995. New mouse model for polycystic kidney disease with both recessive and dominant gene effects. *Kidney Int* **47**:552-8.
67. **Flaherty, L., A. Messer, L. B. Russell, and E. M. Rinchik.** 1992. Chlorambucil-induced mutations in mice recovered in homozygotes. *Proc Natl Acad Sci U S A* **89**:2859-63.
68. **Flood, P. R., and G. K. Totland.** 1977. Substructure of solitary cilia in mouse kidney. *Cell Tissue Res* **183**:281-90.
69. **Fonck, C., D. Chauveau, M. F. Gagnadoux, Y. Pirson, and J. P. Grunfeld.** 2001. Autosomal recessive polycystic kidney disease in adulthood. *Nephrol Dial Transplant* **16**:1648-52.
70. **Fourney, R. M., K. D. Dietrich, and M. C. Paterson.** 1989. Rapid DNA extraction and sensitive alkaline blotting protocol: application for detection of gene rearrangement and amplification for clinical molecular diagnosis. *Dis Markers* **7**:15-26.

71. **Fowler, K. J., F. Walker, W. Alexander, M. L. Hibbs, E. C. Nice, R. M. Bohmer, G. B. Mann, C. Thumwood, R. Maglitto, J. A. Danks, and et al.** 1995. A mutation in the epidermal growth factor receptor in waved-2 mice has a profound effect on receptor biochemistry that results in impaired lactation. *Proc Natl Acad Sci U S A* **92**:1465-9.
72. **Fry, J. L., Jr., W. E. Koch, J. C. Jennette, E. McFarland, F. A. Fried, and J. Mandell.** 1985. A genetically determined murine model of infantile polycystic kidney disease. *J Urol* **134**:828-33.
73. **Gabow, P. A.** 1993. Autosomal dominant polycystic kidney disease. *Am J Kidney Dis* **22**:511-2.
74. **Gattone, V. H., 2nd, G. K. Andrews, F. W. Niu, L. J. Chadwick, R. M. Klein, and J. P. Calvet.** 1990. Defective epidermal growth factor gene expression in mice with polycystic kidney disease. *Dev Biol* **138**:225-30.
75. **Gattone, V. H., 2nd, J. P. Calvet, B. D. Cowley, Jr., A. P. Evan, T. S. Shaver, K. Helmstadter, and J. J. Grantham.** 1988. Autosomal recessive polycystic kidney disease in a murine model. A gross and microscopic description. *Lab Invest* **59**:231-8.
76. **Gattone, V. H., 2nd, K. A. Kuenstler, G. W. Lindemann, X. Lu, B. D. Cowley, Jr., C. A. Rankin, and J. P. Calvet.** 1996. Renal expression of a transforming growth factor-alpha transgene accelerates the progression of inherited, slowly progressive polycystic kidney disease in the mouse. *J Lab Clin Med* **127**:214-22.
77. **Gattone, V. H., 2nd, D. A. Lowden, and B. D. Cowley, Jr.** 1995. Epidermal growth factor ameliorates autosomal recessive polycystic kidney disease in mice. *Dev Biol* **169**:504-10.
78. **Gattone, V. H., J. L. Ricker, C. M. Trambaugh, and R. M. Klein.** 2002. Multiorgan mRNA misexpression in murine autosomal recessive polycystic kidney disease. *Kidney Int* **62**:1560-9.
79. **Gavis, E. R., and R. Lehmann.** 1992. Localization of nanos RNA controls embryonic polarity. *Cell* **71**:301-13.
80. **Gibson, T. J., P. M. Rice, J. D. Thompson, and J. Heringa.** 1993. KH domains within the FMR1 sequence suggest that fragile X syndrome stems from a defect in RNA metabolism. *Trends Biochem Sci* **18**:331-3.
81. **Gibson, T. J., J. D. Thompson, and J. Heringa.** 1993. The KH domain occurs in a diverse set of RNA-binding proteins that include the antiterminator NusA and is probably involved in binding to nucleic acid. *FEBS Lett* **324**:361-6.

82. **Goebel, M., and M. Yanagida.** 1991. The TPR snap helix: a novel protein repeat motif from mitosis to transcription. *Trends Biochem Sci* **16**:173-7.
83. **Gonzalez-Perret, S., K. Kim, C. Ibarra, A. E. Damiano, E. Zotta, M. Batelli, P. C. Harris, I. L. Reisin, M. A. Arnaout, and H. F. Cantiello.** 2001. Polycystin-2, the protein mutated in autosomal dominant polycystic kidney disease (ADPKD), is a Ca²⁺-permeable nonselective cation channel. *Proc Natl Acad Sci U S A* **98**:1182-7.
84. **Goodyer, P. R., J. Fata, C. G. Goodyer, and H. Guyda.** 1991. Transforming growth factor-alpha and the ontogeny of epidermal growth factor receptors in rat kidney. *Growth Regul* **1**:105-9.
85. **Goodyer, P. R., J. Fata, L. Mulligan, D. Fischer, R. Fagan, H. J. Guyda, and C. G. Goodyer.** 1991. Expression of transforming growth factor-alpha and epidermal growth factor receptor in human fetal kidneys. *Mol Cell Endocrinol* **77**:199-206.
86. **Gretz, N., B. Kranzlin, R. Pey, G. Schieren, J. Bach, N. Obermuller, I. Ceccherini, I. Kloting, P. Rohmeiss, S. Bachmann, and M. Hafner.** 1996. Rat models of autosomal dominant polycystic kidney disease. *Nephrol Dial Transplant* **11 Suppl 6**:46-51.
87. **Grishin, N. V.** 2001. KH domain: one motif, two folds. *Nucleic Acids Res* **29**:638-43.
88. **Gruss, P., and C. Walther.** 1992. Pax in development. *Cell* **69**:719-22.
89. **Guay-Woodford, L. M.** 2003. Murine models of polycystic kidney disease: molecular and therapeutic insights. *Am J Physiol Renal Physiol* **285**:F1034-49.
90. **Guay-Woodford, L. M., E. C. Bryda, B. Christine, J. R. Lindsey, W. R. Collier, E. D. Avner, P. D'Eustachio, and L. Flaherty.** 1996. Evidence that two phenotypically distinct mouse PKD mutations, bpk and jcpk, are allelic. *Kidney Int* **50**:1158-65.
91. **Guay-Woodford, L. M., and R. A. Desmond.** 2003. Autosomal recessive polycystic kidney disease: the clinical experience in North America. *Pediatrics* **111**:1072-80.
92. **Guay-Woodford, L. M., W. J. Green, J. R. Lindsey, and D. R. Beier.** 2000. Germline and somatic loss of function of the mouse cpk gene causes biliary ductal pathology that is genetically modulated. *Hum Mol Genet* **9**:769-78.
93. **Guhaniyogi, J., and G. Brewer.** 2001. Regulation of mRNA stability in mammalian cells. *Gene* **265**:11-23.

94. **Haider, N. B., R. Carmi, H. Shalev, V. C. Sheffield, and D. Landau.** 1998. A Bedouin kindred with infantile nephronophthisis demonstrates linkage to chromosome 9 by homozygosity mapping. *Am J Hum Genet* **63**:1404-10.
95. **Hamada, H., C. Meno, D. Watanabe, and Y. Saijoh.** 2002. Establishment of vertebrate left-right asymmetry. *Nat Rev Genet* **3**:103-13.
96. **Hanaoka, K., F. Qian, A. Boletta, A. K. Bhunia, K. Piontek, L. Tsiokas, V. P. Sukhatme, W. B. Guggino, and G. G. Germino.** 2000. Co-assembly of polycystin-1 and -2 produces unique cation-permeable currents. *Nature* **408**:990-4.
97. **Harris, R. C.** 1991. Potential physiologic roles for epidermal growth factor in the kidney. *Am J Kidney Dis* **17**:627-30.
98. **Hateboer, N., L. P. Lazarou, A. J. Williams, P. Holmans, and D. Ravine.** 1999. Familial phenotype differences in PKD11. *Kidney Int* **56**:34-40.
99. **Haycraft, C. J., P. Swoboda, P. D. Taulman, J. H. Thomas, and B. K. Yoder.** 2001. The *C. elegans* homolog of the murine cystic kidney disease gene *Tg737* functions in a ciliogenic pathway and is disrupted in *osm-5* mutant worms. *Development* **128**:1493-505.
100. **Heasman, J., O. Wessely, R. Langland, E. J. Craig, and D. S. Kessler.** 2001. Vegetal localization of maternal mRNAs is disrupted by *VegT* depletion. *Dev Biol* **240**:377-86.
101. **Herrera, G. A.** 1991. C-erb B-2 amplification in cystic renal disease. *Kidney Int* **40**:509-13.
102. **Herron, B. J., W. Lu, C. Rao, S. Liu, H. Peters, R. T. Bronson, M. J. Justice, J. D. McDonald, and D. R. Beier.** 2002. Efficient generation and mapping of recessive developmental mutations using ENU mutagenesis. *Nat Genet* **30**:185-9.
103. **Hildebrandt, F.** 1995. Genetic renal diseases in children. *Curr Opin Pediatr* **7**:182-91.
104. **Holland, P. M., A. Milne, K. Garka, R. S. Johnson, C. Willis, J. E. Sims, C. T. Rauch, T. A. Bird, and G. D. Virca.** 2002. Purification, cloning, and characterization of *Nek8*, a novel NIMA-related kinase, and its candidate substrate *Bicd2*. *J Biol Chem* **277**:16229-40.
105. **Horikoshi, S., S. Kubota, G. R. Martin, Y. Yamada, and P. E. Klotman.** 1991. Epidermal growth factor (EGF) expression in the congenital polycystic mouse kidney. *Kidney Int* **39**:57-62.

106. **Horster, M., S. Huber, J. Tschop, G. Dittrich, and G. Braun.** 1997. Epithelial nephrogenesis. *Pflugers Arch* **434**:647-60.
107. **Horster, M. F., G. S. Braun, and S. M. Huber.** 1999. Embryonic renal epithelia: induction, nephrogenesis, and cell differentiation. *Physiol Rev* **79**:1157-91.
108. **Hou, X., M. Mrug, B. K. Yoder, E. J. Lefkowitz, G. Kremmidiotis, P. D'Eustachio, D. R. Beier, and L. M. Guay-Woodford.** 2002. Cystin, a novel cilia-associated protein, is disrupted in the cpk mouse model of polycystic kidney disease. *J Clin Invest* **109**:533-40.
109. **Huan, Y., and J. van Adelsberg.** 1999. Polycystin-1, the PKD1 gene product, is in a complex containing E-cadherin and the catenins. *J Clin Invest* **104**:1459-68.
110. **Hubbard, T., D. Barker, E. Birney, G. Cameron, Y. Chen, L. Clark, T. Cox, J. Cuff, V. Curwen, T. Down, R. Durbin, E. Eyras, J. Gilbert, M. Hammond, L. Huminiecki, A. Kasprzyk, H. Lehvaslaiho, P. Lijnzaad, C. Melsopp, E. Mongin, R. Pettett, M. Pocock, S. Potter, A. Rust, E. Schmidt, S. Searle, G. Slater, J. Smith, W. Spooner, A. Stabenau, J. Stalker, E. Stupka, A. Ureta-Vidal, I. Vastrik, and M. Clamp.** 2002. The Ensembl genome database project. *Nucleic Acids Res* **30**:38-41.
111. **Huber, O.** 2003. Structure and function of desmosomal proteins and their role in development and disease. *Cell Mol Life Sci* **60**:1872-90.
112. **Hughes, J., C. J. Ward, B. Peral, R. Aspinwall, K. Clark, J. L. San Millan, V. Gamble, and P. C. Harris.** 1995. The polycystic kidney disease 1 (PKD1) gene encodes a novel protein with multiple cell recognition domains. *Nat Genet* **10**:151-60.
113. **Iakoubova, O., H. Dushkin, L. Pacella, and D. R. Beier.** 1999. Genetic analysis of modifying loci on mouse chromosome 1 that affect disease severity in a model of recessive PKD. *Physiol Genomics* **1**:101-5.
114. **Iakoubova, O. A., H. Dushkin, and D. R. Beier.** 1997. Genetic analysis of a quantitative trait in a mouse model of polycystic kidney disease. *Am J Respir Crit Care Med* **156**:S72-7.
115. **Iakoubova, O. A., H. Dushkin, and D. R. Beier.** 1995. Localization of a murine recessive polycystic kidney disease mutation and modifying loci that affect disease severity. *Genomics* **26**:107-14.
116. **Ibraghimov-Beskrovnya, O., W. R. Dackowski, L. Foggensteiner, N. Coleman, S. Thiru, L. R. Petry, T. C. Burn, T. D. Connors, T. Van Raay, J. Bradley, F. Qian, L. F. Onuchic, T. J. Watnick, K. Piontek, R. M. Hakim, G. M. Landes, G. G. Germino, R. Sandford, and K. W. Klinger.**

1997. Polycystin: in vitro synthesis, in vivo tissue expression, and subcellular localization identifies a large membrane-associated protein. *Proc Natl Acad Sci U S A* **94**:6397-402.
117. **Igarashi, P.** 1994. Transcription factors and apoptosis in kidney development. *Curr Opin Nephrol Hypertens* **3**:308-17.
 118. **Igarashi, P., and S. Somlo.** 2002. Genetics and pathogenesis of polycystic kidney disease. *J Am Soc Nephrol* **13**:2384-98.
 119. **Janaswami, P. M., E. H. Birkenmeier, S. A. Cook, L. B. Rowe, R. T. Bronson, and M. T. Davisson.** 1997. Identification and genetic mapping of a new polycystic kidney disease on mouse chromosome 8. *Genomics* **40**:101-7.
 120. **Joyce, G. F.** 1994. In vitro evolution of nucleic acids. *Curr Opin Struct Biol* **4**:331-6.
 121. **Kamada, S., A. Shimono, Y. Shinto, T. Tsujimura, T. Takahashi, T. Noda, Y. Kitamura, H. Kondoh, and Y. Tsujimoto.** 1995. bcl-2 deficiency in mice leads to pleiotropic abnormalities: accelerated lymphoid cell death in thymus and spleen, polycystic kidney, hair hypopigmentation, and distorted small intestine. *Cancer Res* **55**:354-9.
 122. **Kaplan, B. S., J. Fay, V. Shah, M. J. Dillon, and T. M. Barratt.** 1989. Autosomal recessive polycystic kidney disease. *Pediatr Nephrol* **3**:43-9.
 123. **Kaplan, B. S., I. Rabin, M. B. Nogrady, and K. N. Drummond.** 1977. Autosomal dominant polycystic renal disease in children. *J Pediatr* **90**:782-3.
 124. **Keller, S. A., J. M. Jones, A. Boyle, L. L. Barrow, P. D. Killen, D. G. Green, N. V. Kapousta, P. F. Hitchcock, R. T. Swank, and M. H. Meisler.** 1994. Kidney and retinal defects (Krd), a transgene-induced mutation with a deletion of mouse chromosome 19 that includes the Pax2 locus. *Genomics* **23**:309-20.
 125. **Kim, K., I. Drummond, O. Ibraghimov-Beskrovnaya, K. Klinger, and M. A. Arnaout.** 2000. Polycystin 1 is required for the structural integrity of blood vessels. *Proc Natl Acad Sci U S A* **97**:1731-6.
 126. **Klingel, R., W. Dippold, S. Storkel, K. H. Meyer zum Buschenfelde, and H. Kohler.** 1992. Expression of differentiation antigens and growth-related genes in normal kidney, autosomal dominant polycystic kidney disease, and renal cell carcinoma. *Am J Kidney Dis* **19**:22-30.
 127. **Ko, M. S., J. R. Kitchen, X. Wang, T. A. Threat, A. Hasegawa, T. Sun, M. J. Grahovac, G. J. Kargul, M. K. Lim, Y. Cui, Y. Sano, T. Tanaka, Y.**

- Liang, S. Mason, P. D. Paonessa, A. D. Sauls, G. E. DePalma, R. Sharara, L. B. Rowe, J. Eppig, C. Morrell, and H. Doi.** 2000. Large-scale cDNA analysis reveals phased gene expression patterns during preimplantation mouse development. *Development* **127**:1737-49.
128. **Koch, C. A., D. Anderson, M. F. Moran, C. Ellis, and T. Pawson.** 1991. SH2 and SH3 domains: elements that control interactions of cytoplasmic signaling proteins. *Science* **252**:668-74.
129. **Koptides, M., R. Mean, K. Demetriou, A. Pierides, and C. C. Deltas.** 2000. Genetic evidence for a trans-heterozygous model for cystogenesis in autosomal dominant polycystic kidney disease. *Hum Mol Genet* **9**:447-52.
130. **Koulen, P., Y. Cai, L. Geng, Y. Maeda, S. Nishimura, R. Witzgall, B. E. Ehrlich, and S. Somlo.** 2002. Polycystin-2 is an intracellular calcium release channel. *Nat Cell Biol* **4**:191-7.
131. **Krebs, L. T., N. Iwai, S. Nonaka, I. C. Welsh, Y. Lan, R. Jiang, Y. Saijoh, T. P. O'Brien, H. Hamada, and T. Gridley.** 2003. Notch signaling regulates left-right asymmetry determination by inducing Nodal expression. *Genes Dev* **17**:1207-12.
132. **Krieger, J., and H. Breer.** 1999. Olfactory reception in invertebrates. *Science* **286**:720-3.
133. **Kuida, S., and D. R. Beier.** 2000. Genetic localization of interacting modifiers affecting severity in a murine model of polycystic kidney disease. *Genome Res* **10**:49-54.
134. **Kyte, J., and R. F. Doolittle.** 1982. A simple method for displaying the hydropathic character of a protein. *J Mol Biol* **157**:105-32.
135. **Laird, P. W., A. Zijderveld, K. Linders, M. A. Rudnicki, R. Jaenisch, and A. Berns.** 1991. Simplified mammalian DNA isolation procedure. *Nucleic Acids Res* **19**:4293.
136. **Lee, D. C., K. W. Chan, and S. Y. Chan.** 1998. Expression of transforming growth factor alpha and epidermal growth factor receptor in adult polycystic kidney disease. *J Urol* **159**:291-6.
137. **Lin, F., T. Hiesberger, K. Cordes, A. M. Sinclair, L. S. Goldstein, S. Somlo, and P. Igarashi.** 2003. Kidney-specific inactivation of the KIF3A subunit of kinesin-II inhibits renal ciliogenesis and produces polycystic kidney disease. *Proc Natl Acad Sci U S A* **100**:5286-91.
138. **Liu, S., W. Lu, T. Obara, S. Kuida, J. Lehoczky, K. Dewar, I. A. Drummond, and D. R. Beier.** 2002. A defect in a novel Nek-family kinase

causes cystic kidney disease in the mouse and in zebrafish. *Development* **129**:5839-46.

139. **Lu, W., B. Peissel, H. Babakhanlou, A. Pavlova, L. Geng, X. Fan, C. Larson, G. Brent, and J. Zhou.** 1997. Perinatal lethality with kidney and pancreas defects in mice with a targetted Pkd1 mutation. *Nat Genet* **17**:179-81.
140. **Lu, W., X. Shen, A. Pavlova, M. Lakkis, C. J. Ward, L. Pritchard, P. C. Harris, D. R. Genest, A. R. Perez-Atayde, and J. Zhou.** 2001. Comparison of Pkd1-targeted mutants reveals that loss of polycystin-1 causes cystogenesis and bone defects. *Hum Mol Genet* **10**:2385-96.
141. **Luetkeke, N. C., H. K. Phillips, T. H. Qiu, N. G. Copeland, H. S. Earp, N. A. Jenkins, and D. C. Lee.** 1994. The mouse waved-2 phenotype results from a point mutation in the EGF receptor tyrosine kinase. *Genes Dev* **8**:399-413.
142. **Magistrini, R., P. Manfredini, L. Furci, G. Ligabue, C. Martino, M. Leonelli, C. Scapoli, and A. Albertazzi.** 2003. Epidermal growth factor receptor polymorphism and autosomal dominant polycystic kidney disease. *J Nephrol* **16**:110-5.
143. **Mahone, M., E. E. Saffman, and P. F. Lasko.** 1995. Localized Bicaudal-C RNA encodes a protein containing a KH domain, the RNA binding motif of FMR1. *Embo J* **14**:2043-55.
144. **Mandell, J., W. K. Koch, R. Nidess, G. M. Preminger, and E. McFarland.** 1983. Congenital polycystic kidney disease. Genetically transmitted infantile polycystic kidney disease in C57BL/6J mice. *Am J Pathol* **113**:112-4.
145. **Markowitz, G. S., Y. Cai, L. Li, G. Wu, L. C. Ward, S. Somlo, and V. D. D'Agati.** 1999. Polycystin-2 expression is developmentally regulated. *Am J Physiol* **277**:F17-25.
146. **Marrs, J. A., C. Andersson-Fisone, M. C. Jeong, L. Cohen-Gould, C. Zurzolo, I. R. Nabi, E. Rodriguez-Boulan, and W. J. Nelson.** 1995. Plasticity in epithelial cell phenotype: modulation by expression of different cadherin cell adhesion molecules. *J Cell Biol* **129**:507-19.
147. **Marszalek, J. R., P. Ruiz-Lozano, E. Roberts, K. R. Chien, and L. S. Goldstein.** 1999. Situs inversus and embryonic ciliary morphogenesis defects in mouse mutants lacking the KIF3A subunit of kinesin-II. *Proc Natl Acad Sci U S A* **96**:5043-8.
148. **Martinez, J. R., and J. J. Grantham.** 1995. Polycystic kidney disease: etiology, pathogenesis, and treatment. *Dis Mon* **41**:693-765.

149. **McCarthy, L. C., J. Terrett, M. E. Davis, C. J. Knights, A. L. Smith, R. Critcher, K. Schmitt, J. Hudson, N. K. Spurr, and P. N. Goodfellow.** 1997. A first-generation whole genome-radiation hybrid map spanning the mouse genome. *Genome Res* **7**:1153-61.
150. **McConnell, R. S., D. C. Rubinsztein, T. F. Fannin, C. S. McKinstry, B. Kelly, I. C. Bailey, and A. E. Hughes.** 2001. Autosomal dominant polycystic kidney disease unlinked to the PKD1 and PKD2 loci presenting as familial cerebral aneurysm. *J Med Genet* **38**:238-40.
151. **McQuinn, T. C., D. E. Miga, C. H. Mjaatvedt, A. L. Phelps, and A. Wessels.** 2001. Cardiopulmonary malformations in the inv/inv mouse. *Anat Rec* **263**:62-71.
152. **Mene, P., and A. Amore.** 1998. Apoptosis: potential role in renal diseases. *Nephrol Dial Transplant* **13**:1936-43.
153. **Mercola, M., and M. Levin.** 2001. Left-right asymmetry determination in vertebrates. *Annu Rev Cell Dev Biol* **17**:779-805.
154. **Mochizuki, T., Y. Saijoh, K. Tsuchiya, Y. Shirayoshi, S. Takai, C. Taya, H. Yonekawa, K. Yamada, H. Nihei, N. Nakatsuji, P. A. Overbeek, H. Hamada, and T. Yokoyama.** 1998. Cloning of inv, a gene that controls left/right asymmetry and kidney development. *Nature* **395**:177-81.
155. **Mochizuki, T., G. Wu, T. Hayashi, S. L. Xenophontos, B. Veldhuisen, J. J. Saris, D. M. Reynolds, Y. Cai, P. A. Gabow, A. Pierides, W. J. Kimberling, M. H. Breuning, C. C. Deltas, D. J. Peters, and S. Somlo.** 1996. PKD2, a gene for polycystic kidney disease that encodes an integral membrane protein. *Science* **272**:1339-42.
156. **Mohler, J., and E. F. Wieschaus.** 1986. Dominant maternal-effect mutations of *Drosophila melanogaster* causing the production of double-abdomen embryos. *Genetics* **112**:803-22.
157. **Morgan, D., L. Eley, J. Sayer, T. Strachan, L. M. Yates, A. S. Craighead, and J. A. Goodship.** 2002. Expression analyses and interaction with the anaphase promoting complex protein Apc2 suggest a role for inversin in primary cilia and involvement in the cell cycle. *Hum Mol Genet* **11**:3345-50.
158. **Morgan, D., L. Turnpenny, J. Goodship, W. Dai, K. Majumder, L. Matthews, A. Gardner, G. Schuster, L. Vien, W. Harrison, F. F. Elder, M. Penman-Splitt, P. Overbeek, and T. Strachan.** 1998. Inversin, a novel gene in the vertebrate left-right axis pathway, is partially deleted in the inv mouse. *Nat Genet* **20**:149-56.

159. **Moskowitz, D. W., S. L. Bonar, W. Liu, C. F. Sirgi, M. D. Marcus, and R. V. Clayman.** 1995. Epidermal growth factor precursor is present in a variety of human renal cyst fluids. *J Urol* **153**:578-83.
160. **Moyer, J. H., M. J. Lee-Tischler, H. Y. Kwon, J. J. Schrick, E. D. Avner, W. E. Sweeney, V. L. Godfrey, N. L. Cacheiro, J. E. Wilkinson, and R. P. Woychik.** 1994. Candidate gene associated with a mutation causing recessive polycystic kidney disease in mice. *Science* **264**:1329-33.
161. **Murcia, N. S., W. G. Richards, B. K. Yoder, M. L. Mucenski, J. R. Dunlap, and R. P. Woychik.** 2000. The Oak Ridge Polycystic Kidney (orp^k) disease gene is required for left-right axis determination. *Development* **127**:2347-55.
162. **Murcia, N. S., W. E. Sweeney, Jr., and E. D. Avner.** 1999. New insights into the molecular pathophysiology of polycystic kidney disease. *Kidney Int* **55**:1187-97.
163. **Muto, S., A. Aiba, Y. Saito, K. Nakao, K. Nakamura, K. Tomita, T. Kitamura, M. Kurabayashi, R. Nagai, E. Higashihara, P. C. Harris, M. Katsuki, and S. Horie.** 2002. Pioglitazone improves the phenotype and molecular defects of a targeted Pkd1 mutant. *Hum Mol Genet* **11**:1731-42.
164. **Nagafuchi, A.** 2001. Molecular architecture of adherens junctions. *Curr Opin Cell Biol* **13**:600-3.
165. **Nagao, S., T. Hibino, Y. Koyama, T. Marunouchi, H. Konishi, and H. Takahashi.** 1991. Strain difference in expression of the adult-type polycystic kidney disease gene, pcy, in the mouse. *Jikken Dobutsu* **40**:45-53.
166. **Nagao, S., and H. Takahashi.** 1991. Linkage analysis of two murine polycystic kidney disease genes, pcy and cpk. *Jikken Dobutsu* **40**:557-60.
167. **Nagao, S., T. Watanabe, N. Ogiso, T. Marunouchi, and H. Takahashi.** 1995. Genetic mapping of the polycystic kidney gene, pcy, on mouse chromosome 9. *Biochem Genet* **33**:401-12.
168. **Nagasawa, Y., S. Matthiesen, L. F. Onuchic, X. Hou, C. Bergmann, E. Esquivel, J. Senderek, Z. Ren, R. Zeltner, L. Furu, E. Avner, M. Moser, S. Somlo, L. Guay-Woodford, R. Buttner, K. Zerres, and G. G. Germino.** 2002. Identification and characterization of Pkhd1, the mouse orthologue of the human ARPKD gene. *J Am Soc Nephrol* **13**:2246-58.
169. **Nakanishi, K., V. H. Gattone, 2nd, W. E. Sweeney, and E. D. Avner.** 2001. Renal dysfunction but not cystic change is ameliorated by neonatal epidermal growth factor in bpk mice. *Pediatr Nephrol* **16**:45-50.

170. **Nakanishi, K., W. Sweeney, Jr., and E. D. Avner.** 2001. Segment-specific c-ErbB2 expression in human autosomal recessive polycystic kidney disease. *J Am Soc Nephrol* **12**:379-84.
171. **Nakanishi, K., W. E. Sweeney, Jr., K. Zerres, L. M. Guay-Woodford, and E. D. Avner.** 2000. Proximal tubular cysts in fetal human autosomal recessive polycystic kidney disease. *J Am Soc Nephrol* **11**:760-3.
172. **Nauli, S. M., F. J. Alenghat, Y. Luo, E. Williams, P. Vassilev, X. Li, A. E. Elia, W. Lu, E. M. Brown, S. J. Quinn, D. E. Ingber, and J. Zhou.** 2003. Polycystins 1 and 2 mediate mechanosensation in the primary cilium of kidney cells. *Nat Genet* **33**:129-37.
173. **Nauta, J., Y. Ozawa, W. E. Sweeney, Jr., J. C. Rutledge, and E. D. Avner.** 1993. Renal and biliary abnormalities in a new murine model of autosomal recessive polycystic kidney disease. *Pediatr Nephrol* **7**:163-72.
174. **Nelson, W. J.** 1993. Regulation of cell surface polarity in renal epithelia. *Pediatr Nephrol* **7**:599-604.
175. **Newby, L. J., A. J. Streets, Y. Zhao, P. C. Harris, C. J. Ward, and A. C. Ong.** 2002. Identification, characterization, and localization of a novel kidney polycystin-1-polycystin-2 complex. *J Biol Chem* **277**:20763-73.
176. **Nonaka, S., Y. Tanaka, Y. Okada, S. Takeda, A. Harada, Y. Kanai, M. Kido, and N. Hirokawa.** 1998. Randomization of left-right asymmetry due to loss of nodal cilia generating leftward flow of extraembryonic fluid in mice lacking KIF3B motor protein. *Cell* **95**:829-37.
177. **Norby, S., and M. Schwartz.** 1990. Possible locus for polycystic kidney disease on chromosome 2. *Lancet* **336**:323-4.
178. **Nurnberger, J., R. L. Bacallao, and C. L. Phillips.** 2002. Inversin forms a complex with catenins and N-cadherin in polarized epithelial cells. *Mol Biol Cell* **13**:3096-106.
179. **Okada, Y., S. Nonaka, Y. Tanaka, Y. Saijoh, H. Hamada, and N. Hirokawa.** 1999. Abnormal nodal flow precedes situs inversus in iv and inv mice. *Mol Cell* **4**:459-68.
180. **Omran, H., K. Haffner, S. Burth, C. Fernandez, B. Fargier, A. Villaquiran, H. G. Nothwang, S. Schnittger, H. Lehrach, D. Woo, M. Brandis, R. Sudbrak, and F. Hildebrandt.** 2001. Human adolescent nephronophthisis: gene locus synteny with polycystic kidney disease in pcy mice. *J Am Soc Nephrol* **12**:107-13.
181. **Ong, A. C., and D. N. Wheatley.** 2003. Polycystic kidney disease--the ciliary connection. *Lancet* **361**:774-6.

182. **Onuchic, L. F., L. Furu, Y. Nagasawa, X. Hou, T. Eggermann, Z. Ren, C. Bergmann, J. Senderek, E. Esquivel, R. Zeltner, S. Rudnik-Schoneborn, M. Mrug, W. Sweeney, E. D. Avner, K. Zerres, L. M. Guay-Woodford, S. Somlo, and G. G. Germino.** 2002. PKHD1, the polycystic kidney and hepatic disease 1 gene, encodes a novel large protein containing multiple immunoglobulin-like plexin-transcription-factor domains and parallel beta-helix 1 repeats. *Am J Hum Genet* **70**:1305-17.
183. **Orellana, S. A., and E. D. Avner.** 1995. Cystic maldevelopment of the kidney. *Semin Nephrol* **15**:341-52.
184. **Orellana, S. A., W. E. Sweeney, C. D. Neff, and E. D. Avner.** 1995. Epidermal growth factor receptor expression is abnormal in murine polycystic kidney. *Kidney Int* **47**:490-9.
185. **Ortiz, A., S. G. Cuadrado, C. Lorz, and J. Egido.** 1996. Apoptosis in renal diseases. *Front Biosci* **1**:d30-47.
186. **Ostrom, L., M. J. Tang, P. Gruss, and G. R. Dressler.** 2000. Reduced Pax2 gene dosage increases apoptosis and slows the progression of renal cystic disease. *Dev Biol* **219**:250-8.
187. **Otto, E. A., B. Schermer, T. Obara, J. F. O'Toole, K. S. Hiller, A. M. Mueller, R. G. Ruf, J. Hoefele, F. Beekmann, D. Landau, J. W. Foreman, J. A. Goodship, T. Strachan, A. Kispert, M. T. Wolf, M. F. Gagnadoux, H. Nivet, C. Antignac, G. Walz, I. A. Drummond, T. Benzing, and F. Hildebrandt.** 2003. Mutations in INVS encoding inversin cause nephronophthisis type 2, linking renal cystic disease to the function of primary cilia and left-right axis determination. *Nat Genet* **34**:413-20.
188. **Ozawa, Y., J. Nauta, W. E. Sweeney, and E. D. Avner.** 1993. A new murine model of autosomal recessive polycystic kidney disease. *Nippon Jinzo Gakkai Shi* **35**:349-54.
189. **Parnell, S. C., B. S. Magenheimer, R. L. Maser, C. A. Rankin, A. Smine, T. Okamoto, and J. P. Calvet.** 1998. The polycystic kidney disease-1 protein, polycystin-1, binds and activates heterotrimeric G-proteins in vitro. *Biochem Biophys Res Commun* **251**:625-31.
190. **Parnell, S. C., B. S. Magenheimer, R. L. Maser, C. A. Zien, A. M. Frischauf, and J. P. Calvet.** 2002. Polycystin-1 activation of c-Jun N-terminal kinase and AP-1 is mediated by heterotrimeric G proteins. *J Biol Chem* **277**:19566-72.
191. **Pazour, G. J., B. L. Dickert, Y. Vucica, E. S. Seeley, J. L. Rosenbaum, G. B. Witman, and D. G. Cole.** 2000. Chlamydomonas IFT88 and its mouse homologue, polycystic kidney disease gene tg737, are required for assembly of cilia and flagella. *J Cell Biol* **151**:709-18.

192. **Pazour, G. J., and J. L. Rosenbaum.** 2002. Intraflagellar transport and cilia-dependent diseases. *Trends Cell Biol* **12**:551-5.
193. **Pazour, G. J., J. T. San Agustin, J. A. Follit, J. L. Rosenbaum, and G. B. Witman.** 2002. Polycystin-2 localizes to kidney cilia and the ciliary level is elevated in orpk mice with polycystic kidney disease. *Curr Biol* **12**:R378-80.
194. **Pearson, W. R.** 1990. Rapid and sensitive sequence comparison with FASTP and FASTA. *Methods Enzymol* **183**:63-98.
195. **Pearson, W. R., and D. J. Lipman.** 1988. Improved tools for biological sequence comparison. *Proc Natl Acad Sci U S A* **85**:2444-8.
196. **Pearson, W. R., T. Wood, Z. Zhang, and W. Miller.** 1997. Comparison of DNA sequences with protein sequences. *Genomics* **46**:24-36.
197. **Pennekamp, P., C. Karcher, A. Fischer, A. Schweickert, B. Skryabin, J. Horst, M. Blum, and B. Dworniczak.** 2002. The ion channel polycystin-2 is required for left-right axis determination in mice. *Curr Biol* **12**:938-43.
198. **Peral, B., V. Gamble, C. Strong, A. C. Ong, J. Sloane-Stanley, K. Zerres, C. G. Winearls, and P. C. Harris.** 1997. Identification of mutations in the duplicated region of the polycystic kidney disease 1 gene (PKD1) by a novel approach. *Am J Hum Genet* **60**:1399-410.
199. **Perkins, L. A., E. M. Hedgecock, J. N. Thomson, and J. G. Culotti.** 1986. Mutant sensory cilia in the nematode *Caenorhabditis elegans*. *Dev Biol* **117**:456-87.
200. **Peters, D. J., and L. A. Sandkuijl.** 1992. Genetic heterogeneity of polycystic kidney disease in Europe. *Contrib Nephrol* **97**:128-39.
201. **Plachov, D., K. Chowdhury, C. Walther, D. Simon, J. L. Guenet, and P. Gruss.** 1990. Pax8, a murine paired box gene expressed in the developing excretory system and thyroid gland. *Development* **110**:643-51.
202. **Ponomarenko, J. V., G. V. Orlova, A. S. Frolov, M. S. Gelfand, and M. P. Ponomarenko.** 2002. SELEX_DB: a database on in vitro selected oligomers adapted for recognizing natural sites and for analyzing both SNPs and site-directed mutagenesis data. *Nucleic Acids Res* **30**:195-9.
203. **Praetorius, H. A., and K. R. Spring.** 2001. Bending the MDCK cell primary cilium increases intracellular calcium. *J Membr Biol* **184**:71-9.
204. **Praetorius, H. A., and K. R. Spring.** 2003. The renal cell primary cilium functions as a flow sensor. *Curr Opin Nephrol Hypertens* **12**:517-20.

205. **Preminger, G. M., W. E. Koch, F. A. Fried, E. McFarland, E. D. Murphy, and J. Mandell.** 1982. Murine congenital polycystic kidney disease: a model for studying development of cystic disease. *J Urol* **127**:556-60.
206. **Price, S. J., L. R. Chittenden, L. Flaherty, B. O'Dell, L. M. Guay-Woodford, L. Stubbs, and E. C. Bryda.** 2002. Characterization of the region containing the jcpk PKD gene on mouse Chromosome 10. *Cytogenet Genome Res* **98**:61-6.
207. **Pruess, M., and R. Apweiler.** 2003. Bioinformatics Resources for In Silico Proteome Analysis. *J Biomed Biotechnol* **2003**:231-236.
208. **Pruitt, K. D., K. S. Katz, H. Sicotte, and D. R. Maglott.** 2000. Introducing RefSeq and LocusLink: curated human genome resources at the NCBI. *Trends Genet* **16**:44-7.
209. **Qian, Q., P. C. Harris, and V. E. Torres.** 2001. Treatment prospects for autosomal-dominant polycystic kidney disease. *Kidney Int* **59**:2005-22.
210. **Qin, H., J. L. Rosenbaum, and M. M. Barr.** 2001. An autosomal recessive polycystic kidney disease gene homolog is involved in intraflagellar transport in *C. elegans* ciliated sensory neurons. *Curr Biol* **11**:457-61.
211. **Reed, J. C.** 1998. Bcl-2 family proteins. *Oncogene* **17**:3225-36.
212. **Richards, W. G., W. E. Sweeney, B. K. Yoder, J. E. Wilkinson, R. P. Woychik, and E. D. Avner.** 1998. Epidermal growth factor receptor activity mediates renal cyst formation in polycystic kidney disease. *J Clin Invest* **101**:935-9.
213. **Ricker, J. L., V. H. Gattone, 2nd, J. P. Calvet, and C. A. Rankin.** 2000. Development of autosomal recessive polycystic kidney disease in BALB/c-cpk/cpk mice. *J Am Soc Nephrol* **11**:1837-47.
214. **Rodova, M., M. R. Islam, R. L. Maser, and J. P. Calvet.** 2002. The polycystic kidney disease-1 promoter is a target of the beta-catenin/T-cell factor pathway. *J Biol Chem* **277**:29577-83.
215. **Ronnett, G. V., and S. H. Snyder.** 1992. Molecular messengers of olfaction. *Trends Neurosci* **15**:508-13.
216. **Rossetti, S., S. Burton, L. Strmecki, G. R. Pond, J. L. San Millan, K. Zerres, T. M. Barratt, S. Ozen, V. E. Torres, E. J. Bergstralh, C. G. Winearls, and P. C. Harris.** 2002. The position of the polycystic kidney disease 1 (PKD1) gene mutation correlates with the severity of renal disease. *J Am Soc Nephrol* **13**:1230-7.

217. **Rothenpieler, U. W., and G. R. Dressler.** 1993. Pax-2 is required for mesenchyme-to-epithelium conversion during kidney development. *Development* **119**:711-20.
218. **Rozen, S., and H. Skaletsky.** 2000. Primer3 on the WWW for general users and for biologist programmers. *Methods Mol Biol* **132**:365-86.
219. **Sadowski, I., J. C. Stone, and T. Pawson.** 1986. A noncatalytic domain conserved among cytoplasmic protein-tyrosine kinases modifies the kinase function and transforming activity of Fujinami sarcoma virus P130gag-fps. *Mol Cell Biol* **6**:4396-408.
220. **Saffman, E. E., S. Styhler, K. Rother, W. Li, S. Richard, and P. Lasko.** 1998. Premature translation of oskar in oocytes lacking the RNA-binding protein bicaudal-C. *Mol Cell Biol* **18**:4855-62.
221. **Schalkwyk, L. C., M. Weiher, M. Kirby, B. Cusack, H. Himmelbauer, and H. Lehrach.** 1998. Refined radiation hybrid map of mouse chromosome 17. *Mamm Genome* **9**:807-11.
222. **Schandar, M., K. L. Laugwitz, I. Boekhoff, C. Kroner, T. Gudermann, G. Schultz, and H. Breer.** 1998. Odorants selectively activate distinct G protein subtypes in olfactory cilia. *J Biol Chem* **273**:16669-77.
223. **Schatzmann, F., R. Marlow, and C. H. Streuli.** 2003. Integrin signaling and mammary cell function. *J Mammary Gland Biol Neoplasia* **8**:395-408.
224. **Scheffers, M. S., H. Le, P. van der Bent, W. Leonhard, F. Prins, L. Spruit, M. H. Breuning, E. de Heer, and D. J. Peters.** 2002. Distinct subcellular expression of endogenous polycystin-2 in the plasma membrane and Golgi apparatus of MDCK cells. *Hum Mol Genet* **11**:59-67.
225. **Scheffers, M. S., P. van der Bent, F. Prins, L. Spruit, M. H. Breuning, S. V. Litvinov, E. de Heer, and D. J. Peters.** 2000. Polycystin-1, the product of the polycystic kidney disease 1 gene, co-localizes with desmosomes in MDCK cells. *Hum Mol Genet* **9**:2743-50.
226. **Schell, T., A. E. Kulozik, and M. W. Hentze.** 2002. Integration of splicing, transport and translation to achieve mRNA quality control by the nonsense-mediated decay pathway. *Genome Biol* **3**:REVIEWS1006.
227. **Schieren, G., R. Pey, J. Bach, M. Hafner, and N. Gretz.** 1996. Murine models of polycystic kidney disease. *Nephrol Dial Transplant* **11 Suppl 6**:38-45.
228. **Schild, D., and D. Restrepo.** 1998. Transduction mechanisms in vertebrate olfactory receptor cells. *Physiol Rev* **78**:429-66.

229. **Schlessinger, J.** 1994. SH2/SH3 signaling proteins. *Curr Opin Genet Dev* **4**:25-30.
230. **Schultz, J., C. P. Ponting, K. Hofmann, and P. Bork.** 1997. SAM as a protein interaction domain involved in developmental regulation. *Protein Sci* **6**:249-53.
231. **Sellers, W. R., and D. E. Fisher.** 1999. Apoptosis and cancer drug targeting. *J Clin Invest* **104**:1655-61.
232. **Sessa, A., G. M. Ghiggeri, and A. E. Turco.** 1997. Autosomal dominant polycystic kidney disease: clinical and genetic aspects. *J Nephrol* **10**:295-310.
233. **Sigrist, C. J., L. Cerutti, N. Hulo, A. Gattiker, L. Falquet, M. Pagni, A. Bairoch, and P. Bucher.** 2002. PROSITE: a documented database using patterns and profiles as motif descriptors. *Brief Bioinform* **3**:265-74.
234. **Sikorski, R. S., M. S. Boguski, M. Goebel, and P. Hieter.** 1990. A repeating amino acid motif in CDC23 defines a family of proteins and a new relationship among genes required for mitosis and RNA synthesis. *Cell* **60**:307-17.
235. **Simon, E. A., S. Cook, M. T. Davisson, P. D'Eustachio, and L. M. Guay-Woodford.** 1994. The mouse congenital polycystic kidney (cpk) locus maps within 1.3 cM of the chromosome 12 marker D12Nyu2. *Genomics* **21**:415-8.
236. **Siomi, H., M. J. Matunis, W. M. Michael, and G. Dreyfuss.** 1993. The pre-mRNA binding K protein contains a novel evolutionarily conserved motif. *Nucleic Acids Res* **21**:1193-8.
237. **Siomi, H., M. C. Siomi, R. L. Nussbaum, and G. Dreyfuss.** 1993. The protein product of the fragile X gene, FMR1, has characteristics of an RNA-binding protein. *Cell* **74**:291-8.
238. **Smalla, M., P. Schmieder, M. Kelly, A. Ter Laak, G. Krause, L. Ball, M. Wahl, P. Bork, and H. Oschkinat.** 1999. Solution structure of the receptor tyrosine kinase EphB2 SAM domain and identification of two distinct homotypic interaction sites. *Protein Sci* **8**:1954-61.
239. **Sommardahl, C., M. Cottrell, J. E. Wilkinson, R. P. Woychik, and D. K. Johnson.** 2001. Phenotypic variations of orpk mutation and chromosomal localization of modifiers influencing kidney phenotype. *Physiol Genomics* **7**:127-34.

240. **Sorenson, C. M., B. J. Padanilam, and M. R. Hammerman.** 1996. Abnormal postpartum renal development and cystogenesis in the bcl-2 (-/-) mouse. *Am J Physiol* **271**:F184-93.
241. **Stein, L., L. Kruglayak, D. Slonim, and E. Lander.** 1995. "RHMAPPER", unpublished software, Whitehead Institute/MIT Center for Genome Research.
242. **Stocklin, E., F. Botteri, and B. Groner.** 1993. An activated allele of the c-erbB-2 oncogene impairs kidney and lung function and causes early death of transgenic mice. *J Cell Biol* **122**:199-208.
243. **Strachan, T., and A. P. Read.** 1994. PAX genes. *Curr Opin Genet Dev* **4**:427-38.
244. **Sweeney, W. E., Y. Chen, K. Nakanishi, P. Frost, and E. D. Avner.** 2000. Treatment of polycystic kidney disease with a novel tyrosine kinase inhibitor. *Kidney Int* **57**:33-40.
245. **Sweeney, W. E., Jr., and E. D. Avner.** 1998. Functional activity of epidermal growth factor receptors in autosomal recessive polycystic kidney disease. *Am J Physiol* **275**:F387-94.
246. **Tabin, C. J., and K. J. Vogan.** 2003. A two-cilia model for vertebrate left-right axis specification. *Genes Dev* **17**:1-6.
247. **Takahashi, H., J. P. Calvet, D. Dittmore-Hoover, K. Yoshida, J. J. Grantham, and V. H. Gattone, 2nd.** 1991. A hereditary model of slowly progressive polycystic kidney disease in the mouse. *J Am Soc Nephrol* **1**:980-9.
248. **Takahashi, H., Y. Ueyama, T. Hibino, Y. Kuwahara, S. Suzuki, K. Hioki, and N. Tamaoki.** 1986. A new mouse model of genetically transmitted polycystic kidney disease. *J Urol* **135**:1280-3.
249. **Takeda, S., Y. Yonekawa, Y. Tanaka, Y. Okada, S. Nonaka, and N. Hirokawa.** 1999. Left-right asymmetry and kinesin superfamily protein KIF3A: new insights in determination of laterality and mesoderm induction by kif3A^{-/-} mice analysis. *J Cell Biol* **145**:825-36.
250. **Taub, M., Y. Wang, T. M. Szczesny, and H. K. Kleinman.** 1990. Epidermal growth factor or transforming growth factor alpha is required for kidney tubulogenesis in matrigel cultures in serum-free medium. *Proc Natl Acad Sci U S A* **87**:4002-6.
251. **Taulman, P. D., C. J. Haycraft, D. F. Balkovetz, and B. K. Yoder.** 2001. Polaris, a protein involved in left-right axis patterning, localizes to basal bodies and cilia. *Mol Biol Cell* **12**:589-99.

252. **Thomas, R., R. McConnell, J. Whittaker, P. Kirkpatrick, J. Bradley, and R. Sandford.** 1999. Identification of mutations in the repeated part of the autosomal dominant polycystic kidney disease type 1 gene, PKD1, by long-range PCR. *Am J Hum Genet* **65**:39-49.
253. **Torban, E., and P. Goodyer.** 1998. What PAX genes do in the kidney. *Exp Nephrol* **6**:7-11.
254. **Torra, R., C. Badenas, A. Darnell, C. Nicolau, V. Volpini, L. Revert, and X. Estivill.** 1996. Linkage, clinical features, and prognosis of autosomal dominant polycystic kidney disease types 1 and 2. *J Am Soc Nephrol* **7**:2142-51.
255. **Torres, M., E. Gomez-Pardo, G. R. Dressler, and P. Gruss.** 1995. Pax-2 controls multiple steps of urogenital development. *Development* **121**:4057-65.
256. **Torres, V. E.** 1999. Apoptosis in cystogenesis: hands on or hands off? *Kidney Int* **55**:334-5.
257. **Torres, V. E.** 1998. New insights into polycystic kidney disease and its treatment. *Curr Opin Nephrol Hypertens* **7**:159-69.
258. **Torres, V. E.** 1996. Polycystic kidney disease: guidelines for family physicians. *Am Fam Physician* **53**:847-8, 850.
259. **Troemel, E. R.** 1999. Chemosensory signaling in *C. elegans*. *Bioessays* **21**:1011-20.
260. **Truett, G. E., P. Heeger, R. L. Mynatt, A. A. Truett, J. A. Walker, and M. L. Warman.** 2000. Preparation of PCR-quality mouse genomic DNA with hot sodium hydroxide and tris (HotSHOT). *Biotechniques* **29**:52, 54.
261. **Tsiokas, L., E. Kim, T. Arnould, V. P. Sukhatme, and G. Walz.** 1997. Homo- and heterodimeric interactions between the gene products of PKD1 and PKD2. *Proc Natl Acad Sci U S A* **94**:6965-70.
262. **Upadhyay, P., E. H. Birkenmeier, C. S. Birkenmeier, and J. E. Barker.** 2000. Mutations in a NIMA-related kinase gene, *Nek1*, cause pleiotropic effects including a progressive polycystic kidney disease in mice. *Proc Natl Acad Sci U S A* **97**:217-21.
263. **Upadhyay, P., G. Churchill, E. H. Birkenmeier, J. E. Barker, and W. N. Frankel.** 1999. Genetic modifiers of polycystic kidney disease in intersubspecific KAT2J mutants. *Genomics* **58**:129-37.
264. **Vassilev, P. M., L. Guo, X. Z. Chen, Y. Segal, J. B. Peng, N. Basora, H. Babakhanlou, G. Cruger, M. Kanazirska, C. Ye, E. M. Brown, M. A.**

- Hediger, and J. Zhou.** 2001. Polycystin-2 is a novel cation channel implicated in defective intracellular Ca(2+) homeostasis in polycystic kidney disease. *Biochem Biophys Res Commun* **282**:341-50.
265. **Venables, J. P., M. Ruggiu, and H. J. Cooke.** 2001. The RNA-binding specificity of the mouse Dazl protein. *Nucleic Acids Res* **29**:2479-83.
266. **Viribay, M., T. Hayashi, D. Telleria, T. Mochizuki, D. M. Reynolds, R. Alonso, X. M. Lens, F. Moreno, P. C. Harris, S. Somlo, and J. L. San Millan.** 1997. Novel stop and frameshifting mutations in the autosomal dominant polycystic kidney disease 2 (PKD2) gene. *Hum Genet* **101**:229-34.
267. **Vogler, C., S. Homan, A. Pung, C. Thorpe, J. Barker, E. H. Birkenmeier, and P. Upadhyia.** 1999. Clinical and pathologic findings in two new allelic murine models of polycystic kidney disease. *J Am Soc Nephrol* **10**:2534-9.
268. **Wang, C., and R. Lehmann.** 1991. Nanos is the localized posterior determinant in Drosophila. *Cell* **66**:637-47.
269. **Ward, C. J., M. C. Hogan, S. Rossetti, D. Walker, T. Sneddon, X. Wang, V. Kubly, J. M. Cunningham, R. Bacallao, M. Ishibashi, D. S. Milliner, V. E. Torres, and P. C. Harris.** 2002. The gene mutated in autosomal recessive polycystic kidney disease encodes a large, receptor-like protein. *Nat Genet* **30**:259-69.
270. **Ward, C. J., D. Yuan, T. V. Masyuk, X. Wang, R. Punyashtiti, S. Whelan, R. Bacallao, R. Torra, N. F. LaRusso, V. E. Torres, and P. C. Harris.** 2003. Cellular and subcellular localization of the ARPKD protein; fibrocystin is expressed on primary cilia. *Hum Mol Genet*.
271. **Wessely, O., and E. M. De Robertis.** 2000. The *Xenopus* homologue of Bicaudal-C is a localized maternal mRNA that can induce endoderm formation. *Development* **127**:2053-62.
272. **Wessely, O., U. Tran, L. Zakin, and E. M. De Robertis.** 2001. Identification and expression of the mammalian homologue of Bicaudal-C. *Mech Dev* **101**:267-70.
273. **Wilkins, M. R., I. Lindskog, E. Gasteiger, A. Bairoch, J. C. Sanchez, D. F. Hochstrasser, and R. D. Appel.** 1997. Detailed peptide characterization using PEPTIDEMASS--a World-Wide-Web-accessible tool. *Electrophoresis* **18**:403-8.
274. **Wilson, P. D.** 2004. Polycystic kidney disease. *N Engl J Med* **350**:151-64.

275. **Wilson, P. D., J. Du, and J. T. Norman.** 1993. Autocrine, endocrine and paracrine regulation of growth abnormalities in autosomal dominant polycystic kidney disease. *Eur J Cell Biol* **61**:131-8.
276. **Wilson, P. D., and D. Falkenstein.** 1995. The pathology of human renal cystic disease. *Curr Top Pathol* **88**:1-50.
277. **Woo, D.** 1995. Apoptosis and loss of renal tissue in polycystic kidney diseases. *N Engl J Med* **333**:18-25.
278. **Woo, D. D., D. K. Nguyen, N. Khatibi, and P. Olsen.** 1997. Genetic identification of two major modifier loci of polycystic kidney disease progression in pcy mice. *J Clin Invest* **100**:1934-40.
279. **Woolf, A. S., and P. J. Winyard.** 1998. Advances in the cell biology and genetics of human kidney malformations. *J Am Soc Nephrol* **9**:1114-25.
280. **Wu, G., V. D'Agati, Y. Cai, G. Markowitz, J. H. Park, D. M. Reynolds, Y. Maeda, T. C. Le, H. Hou, Jr., R. Kucherlapati, W. Edelmann, and S. Somlo.** 1998. Somatic inactivation of Pkd2 results in polycystic kidney disease. *Cell* **93**:177-88.
281. **Wu, G., T. Hayashi, J. H. Park, M. Dixit, D. M. Reynolds, L. Li, Y. Maeda, Y. Cai, M. Coca-Prados, and S. Somlo.** 1998. Identification of PKD2L, a human PKD2-related gene: tissue-specific expression and mapping to chromosome 10q25. *Genomics* **54**:564-8.
282. **Wu, G., G. S. Markowitz, L. Li, V. D. D'Agati, S. M. Factor, L. Geng, S. Tibara, J. Tuchman, Y. Cai, J. H. Park, J. van Adelsberg, H. Hou, Jr., R. Kucherlapati, W. Edelmann, and S. Somlo.** 2000. Cardiac defects and renal failure in mice with targeted mutations in Pkd2. *Nat Genet* **24**:75-8.
283. **Xiong, H., Y. Chen, Y. Yi, K. Tsuchiya, G. Moeckel, J. Cheung, D. Liang, K. Tham, X. Xu, X. Z. Chen, Y. Pei, Z. J. Zhao, and G. Wu.** 2002. A novel gene encoding a TIG multiple domain protein is a positional candidate for autosomal recessive polycystic kidney disease. *Genomics* **80**:96-104.
284. **Yoder, B. K., X. Hou, and L. M. Guay-Woodford.** 2002. The polycystic kidney disease proteins, polycystin-1, polycystin-2, polaris, and cystin, are co-localized in renal cilia. *J Am Soc Nephrol* **13**:2508-16.
285. **Yoder, B. K., W. G. Richards, C. Sommardahl, W. E. Sweeney, E. J. Michaud, J. E. Wilkinson, E. D. Avner, and R. P. Woychik.** 1997. Differential rescue of the renal and hepatic disease in an autosomal recessive polycystic kidney disease mouse mutant. A new model to study the liver lesion. *Am J Pathol* **150**:2231-41.

286. **Yoder, B. K., W. G. Richards, W. E. Sweeney, J. E. Wilkinson, E. D. Avenier, and R. P. Woychik.** 1995. Insertional mutagenesis and molecular analysis of a new gene associated with polycystic kidney disease. *Proc Assoc Am Physicians* **107**:314-23.
287. **Yoder, B. K., A. Tousson, L. Millican, J. H. Wu, C. E. Bugg, Jr., J. A. Schafer, and D. F. Balkovetz.** 2002. Polaris, a protein disrupted in orpk mutant mice, is required for assembly of renal cilium. *Am J Physiol Renal Physiol* **282**:F541-52.
288. **Zerres, K., G. Mucher, J. Becker, C. Steinkamm, S. Rudnik-Schoneborn, P. Heikkila, J. Rapola, R. Salonen, G. G. Germino, L. Onuchic, S. Somlo, E. D. Avner, L. A. Harman, J. M. Stockwin, and L. M. Guay-Woodford.** 1998. Prenatal diagnosis of autosomal recessive polycystic kidney disease (ARPKD): molecular genetics, clinical experience, and fetal morphology. *Am J Med Genet* **76**:137-44.
289. **Zerres, K., S. Rudnik-Schoneborn, and G. Mucher.** 1996. Autosomal recessive polycystic kidney disease: clinical features and genetics. *Adv Nephrol Necker Hosp* **25**:147-57.
290. **Zhang, B., K. Fugleholm, L. B. Day, S. Ye, R. O. Weller, and I. N. Day.** 2003. Molecular pathogenesis of subarachnoid haemorrhage. *Int J Biochem Cell Biol* **35**:1341-60.
291. **Zhou, B. P., and M. C. Hung.** 2003. Dysregulation of cellular signaling by HER2/neu in breast cancer. *Semin Oncol* **30**:38-48.

CURRICULUM VITAE

Sarah J. Price

Department of Microbiology, Immunology, and Molecular Genetics
Joan C. Edwards School of Medicine
Marshall University
Huntington, WV 25704-9388

EDUCATION

- Ph.D. Biomedical Sciences
Department of Microbiology, Immunology, and Molecular Genetics
Joan C. Edwards School of Medicine
Marshall University, Huntington, WV
February 1999 - Present
Graduation Date, May 2004
- B.S. Biology (major) and Chemistry (minor), Magna cum laude
Denison University, Granville, OH
1990 -1994

RESEARCH/PROFESSIONAL EXPERIENCE

- Joan C. Edwards School of Medicine, Huntington, WV. (Doctoral Research)
Genetic and Molecular Analysis of the Polycystic Kidney Disease-Causing Gene Bicaudal-C.
Dr. Elizabeth C. Bryda, Dissertation Advisor
Department of Microbiology, Immunology, and Molecular Genetics. 1999-present
- Joan C. Edwards School of Medicine, Huntington, WV. (Research Assistant)
Department of Microbiology, Immunology, and Molecular Genetics. 1996-1999
- West Virginia University School of Medicine, Morgantown, WV. (Research Intern)
Cohort Analysis of a MENIIA Affected Family In Rural West Virginia. Dr. Steven Artz,
Advisor. Department of Endocrinology and Nuclear Medicine, CAMC Medical Center,
Charleston, WV. June-August 1995
- Denison University, Granville, OH. (Baccalaureate Research)
*Interpretation of Stochastic Evolutionary Processes Utilizing the Selectively Neutral
Microsatellite Locus MAF33 In Two Populations of Odocoileus virginianus.* Dr. Charles
Sokolik, Advisor. Departments of Biological Sciences and Chemistry. 1993-1994

Denison University, Granville, OH. (Laboratory Manager)
Department of Biological Sciences
Coordinator for Genetics, Zoology, and Advanced Microbiology. 1991-1994

Duke University, Durham, NC. (Research Intern)
Analysis of Surface to Cell Contacts In Artificial Cardiovascular Surgical Devices.
Department of Biomedical Engineering. 1993

Duke University, Durham, NC. (Research Intern)
Departments of Genetics and Biochemistry
Multidisciplinary Research Rotations. 1992

HONORS AND AWARDS

Graduate Student Travel Award, 17th International Mouse Genome Conference.
November 2003

EpScOR Biomolecular Sciences Trainee Travel Grant. July 2003

Sigma Xi Grants-in-Aid Research Award for *Involvement of the Mouse Bicc1 Gene In Body Plan Asymmetry.* May 2003

Anagene B. Heiner Endowment Award. Outstanding Basic Science Poster Presentation Award. 16th Annual Joan C. Edwards School of Medicine Research Conference, Huntington, WV. March 2003

Lester R. Bryant Research Day Founders Award. Outstanding Basic Science Oral Presentation. 15th Annual Joan C. Edwards School of Medicine Research Conference Huntington, WV. March 2002

Graduate Student Travel Award. 15th International Mouse Genome Conference. November 2001

Anagene B. Heiner Endowment Award. Outstanding Basic Science Poster Presentation. 14th Annual Joan C. Edwards School of Medicine Research Conference, Huntington, WV. March 2001

Sigma Xi Grants-in-Aid Research Award for *Apoptosis and Disease Progression In a Mouse Model for Polycystic Kidney Disease.* January 2001

President, Marshall University Graduate Student Organization. 2000-2002

Graduate Student Travel Award. 13th International Mouse Genome Conference. October 1999

Research Fellow. Department of Biological Sciences, Denison University, Granville, OH. 1992-1994.

PROFESSIONAL SOCIETY MEMBERSHIPS

The American Society of Human Genetics
International Mammalian Genome Society
Sigma Xi
Marshall University Graduate Science Organization

PUBLICATIONS

Cogswell, C*, **Price, S.J.***, Xiaoying, H., Guay-Woodford, L.M, Flaherty, L., and Bryda, E.C. (2003) Positional Cloning of *jcpk/bpk* Locus of the Mouse. *Mammalian Genome*. 14, 242-249. (* **co-authors**)

Price, S.J., Chittenden, L.R, Flaherty, L., O'Dell, B., Guay-Woodford, L.M, Stubbs, L., and Bryda, E.C. (2002) Characterization of the Region Containing the *jcpk* PKD Gene on Mouse Chromosome 10. *Cytogenetic and Genome Research*. 99, 61-66.

Price, S.J. and Sokolik, C. (1994) Interpretation of Stochastic Evolutionary Processes Utilizing the Selectively Neutral Microsatellite Locus MAF33 In Two Populations of *Odocoileus virginianus*. *Denison University Journal of Science*. 28 (2), 53-65.

PRESENTATIONS AND ABSTRACTS

Price, S.J., Davis, K.L., Guay-Woodford, L.M. and Bryda, E.C. *Molecular Characterization of the Polycystic Kidney Disease-Causing Gene Bicc1*. 17th International Mouse Genome Conference, Braunschweig, Germany. November 8-12, 2003

Price, S.J. and Bryda E.C. *Involvement of a Gene for Polycystic Kidney Disease (PKD) In Body Plan Asymmetry and Ciliogenesis*. 12th Annual Sigma Xi Research Conference, Marshall University, Huntington, WV. April 24-25, 2003

Price, S.J. and Bryda E.C. *Involvement of a Gene for Polycystic Kidney Disease (PKD) In Body Plan Asymmetry and Ciliogenesis*. 16th Annual Joan C. Edwards School of Medicine Research Conference, Huntington, WV. March 17-18, 2003

Price, S.J. and Bryda, E.C. *Gene Identification and Molecular Analysis of a Mutation Causing Polycystic Kidney Disease*. 15th Annual Joan C. Edwards School of Medicine Research Conference, Huntington, WV. March 25-26, 2002

Bryda, E.C., **Price, S.J.**, Cogswell, C., Hou, X., and Flaherty, L. *Mutations In the Bicaudal-C Gene on Mouse Chromosome 10 Cause Severe Polycystic Kidney Disease in the Mouse*. 16th International Mouse Genome Conference, San Antonio, Texas. October 2002

Price, S.J. and Bryda, E.C. *Molecular Characterization of a Mouse Model for Polycystic Kidney Disease*. 15th International Mouse Genome Conference, Edinburgh, Scotland. October 21-24, 2001

Cogswell, C., **Price, S.J.**, Flaherty, L., and Bryda E.C. *Positional Cloning of the jcpk Locus*. 15th International Mouse Genome Conference, Edinburgh, Scotland. October 21-24, 2001

Price, S.J. and Bryda, E.C. *Genetic and Molecular Characterization of a Mouse Model for Polycystic Kidney Disease*. 10th Sigma Xi Research Conference, Huntington, WV. April 26-27, 2001

Price, S.J. and Bryda, E.C. *Genetic and Molecular Characterization of a Mouse Model for Polycystic Kidney Disease*. 14th Annual Joan C. Edwards School of Medicine Research Conference, Huntington, WV. March 12-13, 2001

Price, S.J. and Bryda E.C. *Positional Cloning of a Mouse Gene for Polycystic Kidney Disease*. Mouse Molecular Genetics Conference, Cold Spring Harbor, New York. August 30 - September 3, 2000

Price, S.J., Stubbs, L., O'Dell, B., and Bryda, E.C. *Physical Map of the jcpk Region on Mouse Chromosome 10*. 14th International Mouse Genome Conference, Narita, Japan. November 6-10, 2000

Price, S.J. and Bryda, E.C. *Physical Mapping of a Gene for Polycystic Kidney Disease on Mouse Chromosome 10*. 13th Annual Joan C. Edwards School of Medicine Research Conference, Huntington, WV. March 27-28, 2000

Price, S.J., Tartaglia, K.E., Flaherty, L., Bryda, E.C. *Genetic, Radiation Hybrid, and Physical Maps of the Region around the jcpk locus on Mouse Chromosome 10*. 13th International Mouse Genome Conference, Philadelphia, PA. October 31 - November 3, 1999

WORKSHOPS ATTENDED

West Virginia Biomedical Research Infrastructure Network (WV-BRIN) Research Symposium, *Analysis of Multifactorial Genetic Traits and The Future of Genetic Counseling In a Research Environment*. Presented by Dr. Robert Elston and Dr. Nancy Steinberg Warren. Joan C. Edwards School of Medicine, Marshall University, Huntington, WV. August 7, 2003

Write Winning Grants: How to Write Award Winning NIH and NSF Grants. Presented by Stephen Russell, DVM, Ph.D. Joan C. Edwards School of Medicine, Marshall University, Huntington, WV. November 22-23, 2002

WV-BRIN Bioinformatics Workshop, *Introduction to Bioinformatics, Gene Mapping, and Functional Genomics*. Presented by Dr. Cynthia Gibas and Dr. Richard Roman. Joan C. Edwards School of Medicine, Marshall University, Huntington, WV. June 4-6, 2002

Workshop on *Conditional Genetics*. Presented by Richard Behringer and Andras Nagy, Cold Spring Harbor, New York. August 30 - September 3, 2000

TEACHING EXPERIENCE

Medical Histology Instructor. *Polycystic Kidney Disease: Pathogenesis and Treatment*. Joan C. Edwards School of Medicine, Marshall University, Huntington, WV. November 2000

Molecular Cloning Laboratory Instructor . *PCR: Theory and Applications*. Joan C. Edwards School of Medicine, Marshall University, Huntington, WV. February 2000

Research Assistant, Department of Microbiology, Immunology and Molecular Genetics, Joan C. Edwards School of Medicine, Marshall University, Huntington, WV. 1996-1999.

Teaching Assistant (Zoology, Genetics and Advanced Microbiology), Department of Biological Sciences, Denison University, Granville, OH. 1990-1994

SERVICE

Assistant Conference Organizer. Sigma Xi Research Conference, Marshall University, Huntington, WV. April 24-25, 2003.

Judge. 50th Annual West Virginia Jr. Academy of Science West Virginia State Science and Engineering Fair, Marshall University, Huntington, WV. March 28-29, 2003

President, co-founder and member. Marshall University Graduate Science Student Organization. Joan C. Edwards School of Medicine, Huntington, WV. 1999-2004

Rat dissection, anatomical instruction, and mentoring for young students. Fifth Grade Class, Cammack Elementary School, Huntington, WV. April 2003

Graduate Student Mentor and Event Organizer. Joan C. Edwards School of Medicine Graduate Orientation, Huntington, WV. August 2000-2002

Judge. 49th Annual West Virginia Jr. Academy of Science West Virginia State Science and Engineering Fair, Marshall University, Huntington, WV. March 29-30, 2002

Judge, 48th Annual West Virginia Jr. Academy of Science West Virginia State Science and Engineering Fair, Marshall University, Huntington, WV. March 30-31, 2001

Judge. Ohio District Science Fair. March 15, 2000

Volunteer Educator in Biochemistry. West Virginia Women's Conference for Young Women in Science. Parkersburg, WV. June 1999

Editor and contributor, *Denison University Biological Sciences Alumni Newsletter*. Denison University, Granville, OH. 1993-1994